

UNIVERSITY OF SOUTHAMPTON

**Transmission of vibration through backrests and  
apparent mass of the back during whole-body  
fore-and-aft vibration**

Nawal Aswan Abdul Jalil, B.Eng.

A thesis submitted in partial fulfilment for the  
degree of Doctor of Philosophy

FACULTY OF ENGINEERING, SCIENCE AND MATHEMATICS  
INSTITUTE OF SOUND AND VIBRATION RESEARCH

NOVEMBER 2005

**ABSTRACT**

FACULTY OF ENGINEERING, SCIENCE AND MATHEMATICS

INSTITUTE OF SOUND AND VIBRATION RESEARCH

Doctor of Philosophy**TRANSMISSION OF VIBRATION THROUGH BACKRESTS AND APPARENT MASS  
OF THE BACK DURING WHOLE-BODY FORE-AND-AFT VIBRATION**

By Nawal Aswan Abdul Jalil

Knowledge of the transmissibility of seats and the biodynamic responses of a seated person exposed to fore-and-aft vibration are very limited despite extensive research in the vertical direction. This thesis aims to extend understanding of the transmissibility of backrests and the apparent mass of the back during whole-body fore-and-aft excitation.

A series of experiments has measured the transmissibility of backrests and the apparent mass of the back of seated persons exposed to whole-body fore-and-aft vibration. In most experiments, twelve male subjects were exposed to random fore-and-aft vibration in the frequency range 0.25 Hz to 20 Hz at five vibration magnitudes: 0.1, 0.2, 0.4, 0.8 and 1.6  $\text{ms}^{-2}$  r.m.s. The effects of backrest inclination, seat-pan inclination, push force at the feet and fore-and-aft position of the footrest on both the transmissibility of backrests and the apparent mass of the back were investigated. The influence of different foam thickness on the transmissibility of a foam backrest was also investigated.

The transmissibility of a car seat backrest and a foam backrest showed a principal resonance frequency around 5 Hz, which coincides with the principal resonance frequency of the apparent mass of the back. It is suggested that the resonance frequency of the backrest transmissibility is related to the mode of vibration of the body at the principal resonance - a mode of the entire body involving combined bending in the thoracic spine and pitching of the pelvis and the upper body.

The fore-and-aft transmissibility of both backrests varied significantly between 2 and 10 Hz when measured at five vertical locations at the backrest above the seat surface, although the resonance frequencies showed little changed. The variation in the transmissibility may have arisen from relative movement along the spinal column caused by the different modes of vibration the body at the principal resonance during fore-and-aft excitation.

The apparent mass of the back was significantly non-linear with vibration magnitude. The non-linearity of the body is suggested to have greatly influenced the non-linearity in the transmissibility of backrest with vibration magnitude.

Commonly experienced variations in the backrest inclination (up to 20° from vertical) and push force at the feet (from 'no force' to 150 N) had a greater influence on both the fore-and-aft transmissibility of backrests and the apparent mass of the back than variations in the seat-pan inclination (up to 15° from horizontal) and variation in the fore-and-aft footrest position. In addition, increasing foam thicknesses (from 25 mm to 200 mm) decreased the resonance frequency of the transmissibility of the foam backrest.

Four alternative multi-degree-of-freedom linear lumped parameter models were developed to represent the human-body and showed good predictions of the apparent mass of the back between 0.25 and 10 Hz. The dynamic impedance of the backrest cushions of the two seats were measured using an indenter and the backrest cushions were represented by a model consisting of a spring and a damper. A seat-person model was developed (i.e. human-body model combined with the backrest cushion model) to predict the transmissibility of both backrests. It was found that a seat-person model with rotational capability provide encouraging predictions of the transmissibility of both backrests, although further development is required.

# Contents

<b>List of Symbols</b>	<b>vii</b>
<b>Acknowledgements</b>	<b>ix</b>
<b>Chapter 1 Introduction .....</b>	<b>1</b>
1.1    General objective .....	2
1.2    Principal assumption.....	2
1.3    Thesis overview.....	3
<b>Chapter 2 Literature review .....</b>	<b>5</b>
2.1    Introduction .....	5
2.2    Dynamic responses of a sitting person exposed vertical and horizontal (fore-and-aft and lateral) vibration .....	7
2.2.1        Introduction.....	7
2.2.2        Mechanical impedance of seated person exposed to whole-body vertical vibration .....	8
2.2.3        Factors affecting body impedance of seated persons exposed to whole-body vertical vibration.....	13
2.2.3.1        Effect of posture and muscle tension .....	13
2.2.3.2        Effect of footrest.....	21
2.2.3.3        Effect of backrest, backrest and seat angles.....	25
2.2.3.4        Effect of vibration magnitude.....	30
2.2.4        Mechanical impedance of seated persons exposed to whole-body horizontal vibration (fore-and-aft or lateral) .....	35
2.2.5        Factors affecting body impedance of seated persons exposed to whole-body horizontal vibration (fore-and-aft or lateral) .....	39
2.2.5.1        Effect of posture and backrest .....	39
2.2.5.2        Effect of vibration magnitude.....	42
2.2.6        Conclusions.....	46
2.3    Seating dynamics .....	47
2.3.1        Introduction.....	47
2.3.2        Methods of evaluating seating dynamics .....	47
2.3.3        Measurement devices for vibration on seats .....	47

---

2.3.4	Transmissibility of seats (conventional and suspension) in the vertical direction .....	50
2.3.5	Factors affecting seat transmissibility in the vertical direction.....	53
2.3.5.1	Effect of sitting posture.....	53
2.3.5.2	Effect of footrest.....	55
2.3.5.3	Effect of backrest, backrest inclination and seat pan inclination.....	55
2.3.5.4	Effect of subject characteristics .....	59
2.3.5.5	Effect of different material properties.....	60
2.3.5.6	Effect of vibration magnitude.....	62
2.3.6	Transmissibility of seats in horizontal directions.....	64
2.3.6.1	Fore-and-aft direction .....	64
2.3.6.2	Lateral direction.....	67
2.3.7	Factors affecting seat transmissibility in the horizontal direction.....	67
2.3.7.1	Effect of vibration magnitude.....	67
2.3.8	Conclusions .....	69
2.4	Biodynamic modelling of the seated person .....	69
2.4.1	Introduction.....	69
2.4.2	Lumped parameter modelling in the vertical direction .....	70
2.4.2.1	Linear models.....	70
2.4.2.2	Non-linear models.....	79
2.4.3	Lumped parameter modelling in the horizontal vibrations (fore-and-aft and lateral) .....	81
2.4.4	Conclusions .....	82
2.5	Measuring seat transmissibility without subjects.....	83
2.5.1	Introduction.....	83
2.5.2	Testing seat with rigid mass .....	84
2.5.3	Testing seat with antropodynamic dummy .....	85
2.5.4	Methods of predicting seat transmissibility .....	88
2.5.5	Conclusions .....	93
2.6	General conclusions.....	94
2.7	Motivation of research .....	96
<b>Chapter 3</b>	<b>Experimental apparatus and data analysis .....</b>	<b>99</b>
3.1	Introduction .....	99
3.2	Apparatus .....	99
3.2.1	Vibrators .....	99
3.2.1.1	Electro-hydraulic vibrator .....	99
3.2.1.2	Electro-magnetic vibrator.....	100
3.2.2	Transducers .....	101
3.2.2.1	Accelerometers .....	101

---

3.2.2.2	Force transducers .....	104
3.3	Data acquisition .....	106
3.3.1	<i>HVLab</i> Data Acquisition and Analysis System (version 3.81) .....	106
3.4	Data analysis: frequency response functions .....	108
3.4.1	Transmissibility .....	108
3.4.2	Apparent mass .....	108
3.4.2.1	Mass cancellation .....	109
3.4.3	Dynamic properties of the backrest cushion .....	110
3.5	Data analysis: statistical tests .....	111
3.5.1	Friedman two-way analysis of variance .....	111
3.5.2	Wilcoxon matched-pairs signed ranks test .....	112
3.5.3	Spearman rank order correlation coefficient .....	112
<b>Chapter 4 Fore-and-aft transmissibility of backrests .....</b>		<b>113</b>
4.1	Introduction .....	113
4.2	Method .....	114
4.3	Analysis .....	118
4.4	Results .....	119
4.4.1	Inter-subject variability .....	119
4.4.2	Variation in backrest transmissibility .....	121
4.4.3	Effect of vibration magnitude .....	129
4.5	Discussion .....	132
4.6	Conclusions .....	135
<b>Chapter 5 Factors affecting transmissibility of backrests .....</b>		<b>136</b>
5.1	Introduction .....	136
5.2	Effect of foam thickness and vibration magnitude .....	136
5.2.1	Introduction .....	136
5.2.2	Method .....	138
5.2.3	Analysis .....	140
5.2.4	Results .....	140
5.2.4.1	Inter-subject variability .....	140
5.2.4.2	Effect of foam thickness .....	141
5.2.4.3	Effect of vibration magnitude .....	142
5.2.5	Discussion .....	143
5.2.6	Conclusions .....	145
5.3	Effect of backrest inclination and seat-pan inclination .....	145
5.3.1	Introduction .....	145
5.3.2	Method .....	147
5.3.3	Analysis .....	150
5.3.4	Results .....	151

---

5.3.4.1	Effect of backrest inclination .....	151
5.3.4.2	Effect of seat-pan inclination .....	154
5.3.5	Discussion .....	158
5.3.5.1	Effect of backrest inclination .....	158
5.3.5.2	Effect of seat-pan inclination .....	160
5.3.6	Conclusions .....	161
5.4	Effect of the push force at the feet and the horizontal position of the footrest .....	161
5.4.1	Introduction .....	161
5.4.2	Method .....	162
5.4.3	Analysis .....	164
5.4.4	Results .....	165
5.4.4.1	Effect of the fore-and-aft push force at the feet .....	165
5.4.4.2	Effect of the horizontal position of the footrest .....	166
5.4.5	Discussion .....	167
5.4.5.1	Effect of the fore-and-aft push force at the feet .....	167
5.4.5.2	Effect of the horizontal position of the footrest .....	168
5.4.6	Conclusion .....	168
<b>Chapter 6</b>	<b>Fore-and-aft apparent mass of the back .....</b>	<b>169</b>
6.1	Introduction .....	169
6.2	Method .....	171
6.3	Results .....	175
6.3.1	Apparent mass of the back at five locations above the seat surface .....	175
6.3.1.1	Effect of vibration magnitude .....	180
6.3.2	Apparent mass of the entire back .....	182
6.3.2.1	Effect of vibration magnitude .....	183
6.3.3	Comparison of the apparent mass of the back measured at five locations and with the entire back .....	184
6.4	Discussion .....	185
6.4.1	Modes of vibration of the body .....	185
6.4.2	Biodynamic responses at low frequency (i.e. near 0 Hz) .....	187
6.4.3	Variation in apparent mass of the back .....	188
6.4.4	Non-linearity of the body with vibration magnitude .....	189
6.4.5	Biodynamic model .....	190
6.5	Conclusions .....	190
<b>Chapter 7</b>	<b>Factors affecting apparent mass of the back .....</b>	<b>192</b>
7.1	Introduction .....	192
7.2	Effect of backrest inclination and seat-pan inclination .....	192
7.2.1	Introduction .....	192
7.2.2	Method .....	194

7.2.3	Analysis .....	197
7.2.4	Results .....	199
7.2.4.1	Effect of backrest inclination .....	199
7.2.4.1.1	'Fore-and-aft' apparent mass .....	199
7.2.4.1.2	'Cross-axis vertical' apparent mass .....	201
7.2.4.2	Effect of seat pan inclination .....	202
7.2.4.2.1	'Fore-and-aft' apparent mass .....	202
7.2.4.2.2	'Cross-axis vertical' apparent mass .....	204
7.2.5	Discussion .....	205
7.2.5.1	Effect of analysis method .....	205
7.2.5.2	Effect of backrest inclination .....	207
7.2.5.2.1	'Fore-and-aft' apparent mass .....	207
7.2.5.2.2	'Cross-axis vertical' apparent mass .....	209
7.2.5.3	Effect of seat-pan inclination .....	210
7.2.5.3.1	'Fore-and-aft' apparent mass .....	210
7.2.5.3.2	'Cross-axis vertical' apparent mass .....	210
7.2.6	Conclusion .....	211
7.3	Effect of the push force at the feet and the horizontal position of the footrest .....	211
7.3.1	Introduction .....	211
7.3.2	Method .....	212
7.3.3	Analysis .....	213
7.3.4	Results .....	214
7.3.4.1	Effect of the push force at the feet .....	214
7.3.4.2	Effect of horizontal footrest position .....	216
7.3.5	Discussion .....	218
7.3.5.1	Effect of the fore-and-aft push force at the feet .....	218
7.3.5.2	Effect of the horizontal position of the footrest .....	219
7.3.6	Conclusion .....	220
<b>Chapter 8 Predicting fore-and-aft backrest transmissibility .....</b>		<b>221</b>
8.1	Introduction .....	221
8.2	Modelling apparent mass of the back .....	222
8.2.1	Introduction .....	222
8.2.2	Lumped parameter model .....	223
8.2.3	Fitting with experimental data .....	225
8.2.3.1	Discussion and concluding remarks .....	228
8.2.4	Sensitivity analysis .....	229
8.3	Measurement of seat mechanical impedance with an indenter .....	230
8.3.1	Introduction .....	230
8.3.2	Method and analysis .....	231

---

8.3.3	Results and Discussion.....	233
8.3.4	Backrest cushion model.....	235
8.3.5	Conclusions.....	238
8.4	Predicting backrest transmissibility .....	238
8.4.1	Mathematical equation of the transmissibility model .....	239
8.4.2	Results and discussion .....	240
8.5	Alternative models for predicting backrest transmissibility .....	241
8.5.1	Alternative models of the apparent mass of the back.....	241
8.5.1.1	Fitting with experimental data.....	243
8.5.1.2	Sensitivity analysis.....	248
8.5.1.3	Predicting backrest transmissibility.....	250
8.5.1.4	Discussion and concluding remarks .....	253
8.5.2	Alternative dynamic impedance of the backrest .....	253
8.5.2.1	Predicting backrest transmissibility.....	254
8.5.2.2	Discussion and concluding remarks .....	257
8.6	Discussion .....	257
8.7	Conclusions.....	259
<b>Chapter 9 General discussion .....</b>	<b>260</b>	
9.1	Introduction.....	260
9.2	Validity of using linear method.....	260
9.3	General discussion.....	262
9.3.1	Mode of vibration of the body.....	262
9.3.2	Variation in the transmissibility of backrests .....	263
9.3.3	Non-linearity.....	265
9.3.4	Factors affecting transmissibility of backrests .....	266
9.3.5	Biodynamic responses at low frequency (i.e. near 0 Hz) .....	267
9.3.6	Conceptual model .....	268
<b>Chapter 10 General conclusions and future work .....</b>	<b>271</b>	
10.1	General conclusions.....	271
10.2	Future work.....	272
<b>Appendix A Fore-and-aft transmissibility of backrests: individual data.....</b>	<b>275</b>	
<b>Appendix B Effect of foam thickness: individual data .....</b>	<b>289</b>	
<b>Appendix C Apparent mass of the back: individual data .....</b>	<b>296</b>	
<b>Appendix D Derivation of equations of motion (EOM) using <i>Lagrange's</i> method.....</b>	<b>304</b>	
<b>REFERENCES .....</b>	<b>307</b>	

# List of Symbols

$a(f)$	Acceleration ( $\text{ms}^{-2}$ )
$a_f(f)$	Fore-and-aft acceleration ( $\text{ms}^{-2}$ )
$a_{ii}(\omega)$	Power spectral density (PSD) input acceleration
$d(f)$	Displacement (m)
$F_{DP}(f)$	Frequency response of the force measured at the driving-point
$F(f)$	Force (N)
$F_L(f)$	Force load on the foam block (N)
$F_{io}(f)$	Cross spectral density (CSD) of force and acceleration
$F_{oo}(f)$	PSD of measured force
$F_T(f)$	Total force acting on the subject (N)
$F_p(f)$	Force of the force-platform (N)
$F_F(\omega)$	'Fore-and-aft' force (measured normal to the force platform)
$F_V(\omega)$	'Cross-axis vertical' force (measured parallel to the force platform)
$g$	Gravity ( $\text{ms}^{-2}$ )
$G_{io}(f)$	Cross-spectral density of the input and output acceleration
$G_{ii}(f)$	Power-spectral density of input acceleration
$G_{oo}(f)$	Power-spectral density of output acceleration
$H(f)$	Transmissibility
$ H $	Modulus of $H(f)$
Hz	Hertz
Im	Imaginary number
k	kilo
kg	Kilogram
m	Metre
mm	millimetre
mV	milliVolts
$M(f)$	Apparent mass
$M_B(f)$	Apparent mass of the back
$M_{BF}(f)$	'Fore-and-aft' apparent mass of the back (i.e. normal to the force platform)
$M_{BV}(f)$	'Cross-axis vertical' apparent mass of the back (i.e. parallel to the force platform)

---

$M_T(f)$	Apparent mass of the subject and force platform
$M_P(f)$	Apparent mass of the force platform
N	Newton
Re	Real number
r.m.s	Root mean square
$S(f)$	Dynamics stiffness (N/m)
$T_{DP}(f)$	Driving-point mechanical impedance frequency response
$T_T(f)$	Driving-point transmissibility frequency response
$v(f)$	Velocity (ms <sup>-1</sup> )
W	Watts
$x$	Displacement
$\dot{x}$	Velocity
$\ddot{x}$	Acceleration
$X_{DP}(f)$	Frequency response of the resultant movements (acceleration, velocity or displacement)
$X_{\%p}(f)$	Frequency response of the output acceleration
$X_{\%p}(f)$	Frequency response of the input acceleration
$Z(f)$	Mechanical impedance (N/ms <sup>-1</sup> )
$\gamma_{io}^2(f)$	Coherency
$\theta$	Phase of $H(f)$
$\theta_{M_B}$	Phase of $M_B(\omega)$
$\omega$	Omega
°	Degree

## Acknowledgements

First and foremost, I would like to express my utmost gratitude to God, the Almighty, for blessing me with many good things in my life, and guiding me in the right path.

My special gratitude and appreciation goes to my supervisor, Professor M.J. Griffin, for his skilful guidance, consistent encouragement and motivation, and excellent support throughout my PhD study.

Special thanks to Universiti Putra Malaysia and the Malaysian Government for giving me the opportunity and financial support to pursue my PhD study.

My research was also made easier with the help of my research colleagues within the HFRU. Special thanks to Dr Miyuki Morioka for her statistical knowledge, Dr Thomas Gunston and Dr Naser Nawayseh for their help in Matlab, and Gary and Peter for their consistent help during my experimental work. My thanks also go to all member of the HFRU unit. It has been a real pleasure being part of this research group.

Thanks also to all of my friends, in which I appreciated their help, in particular, Patleey, Abu, Abang Pauzi and his family, Junaidi, Abang Sallehuddin and wife, Ober, Ucop, Amp and many more which are too numerous to mention. Special thanks also to Abang Nizar and Kak Ani, and Abang Yusairi and Kak Lin for keeping me 'healthy' for the past years.

My special thanks to my family for their unconditional love, support, motivation, encouragement and all the beautiful things that they have done for me. To mak and ayah (my parents), I will always be in debt with you with all the love that you gave to me and raised me as a man I am today and for that, I thank you.

To my one special friend, my soul mate, my other half, my beloved wife, Gee, there is no word that can describe how much I appreciate all your support, encouragement, criticism, help and many more. Thank you for always being there for me. Most importantly, thank you for your unconditional love to me. As the saying goes, behind every successful man is a wonderful woman, and that woman is you!

*To my parents*

*and*

*my beloved wife...*

# Chapter 1

## Introduction

People are exposed to vibration almost everyday. The exposure comes in many different forms, directions and magnitudes. The vibration exposure of the human body occurs in vehicles, through seating, or when standing, or through vibrating-tools transmitting vibration to the body through hands.

In vehicles, for example a car, much of the vibration exposure of a driver is through the seat, but part of the vibration may be transmitted to the body through the steering wheel and the pedals, via the hands and legs respectively. This vibration exposure to the whole-body inevitably leads to discomfort when sitting for a period of time and may also disturb activities.

An understanding of the biodynamic responses of the body to vibration, together with the dynamic performance of seats has become increasingly important so as to improve the comfort and performance, and to reduce any adverse effects of vibration on the health of drivers and passengers. This is because the dynamic performance of seats is largely affected by the dynamic response of the occupant.

Previous studies have shown that the body has a major resonance around 5 Hz during vertical excitation. The vertical transmissibility of seats also shows a principal resonance around 5 Hz. There are many factors that can affect the biodynamic responses of the body and the transmissibility of seats. These findings are often obtained from the experimental studies involving human subjects. However, the experimental work is labour intensive, time consuming and involves inherent risks to the exposed subjects.

Some researchers have developed mathematical model that can adequately represent the biodynamic responses of the body when exposed to vibration. Subsequently, the human body model can be used to predict the seat transmissibility when it is combined with a seat cushion model. This method is useful to assess seating dynamic for different seats without having to use human subjects. However, most of the research conducted has focused on

vertical vibration. Only a few studies have been conducted with vibration exposure in other directions.

## 1.1 General objective

The general objective of this thesis is to improve understanding of the biodynamic responses of seated persons and the dynamic performance of seats with fore-and-aft vibration. In addition, this research continues the idea of predicting the backrest transmissibility based on the seat-person model (i.e. combined biodynamic human body model that can adequately approximate the apparent mass of the back with the backrest cushion model). This includes quantifying the apparent mass of the back, the transmissibility of backrests and the impedance of the backrest cushion. The factors that can affect both the impedance of the back and the backrest transmissibility were also investigated.

## 1.2 Principal assumption

In this thesis, all studies were conducted with an assumption that the vibration on the seat had little effect on the vibration at the back-backrest interface - any motion of the pelvic girdle is de-coupled from motion of subjects' spine and upper body. As the backrest transmissibility is mostly, if not totally, dependent on the impedance of the back, and therefore, there could be only small effect of the vibration on the seat to the vibration at the backrest. This is based on a previous study by Fairley and Griffin (1984), which the authors reported that the horizontal transmissibility (i.e. fore-and-aft seat transmissibility) in the fore-and-aft direction is near unity. The assumption simplifies the estimations of the dynamic properties of the back and backrest by rendering unnecessary any calculations that would otherwise involve the seat as a correlated input."

Likewise, it is also assumed that the effect of vibration on the seat is small to interface the general responses of the impedance at the back at the back-backrest. The knowledge of the influence of the vibration on the seat to the apparent mass of the back was only recently uncovered (Nawayseh and Griffin, 2004a). Notwithstanding the mechanism involved, the results of that study showed that high forces were measured between the thigh and the seat surface. These high forces can be assumed to cause small relative movement (i.e. forward and backward) of the body and seat surface, which may have little effect on the biodynamic responses at the back-backrest interface.

The main advantage of specifying the principal assumption is that it simplifies the estimations of the dynamic properties of the back and the backrest by rendering any unnecessary calculations that would otherwise involve the seat as a correlated input.

### 1.3 Thesis overview

The research approach in this study is simplified as in Figure 1.1. The apparent mass data leads to a development of a linear lumped parameter model representing the human back in the fore-and-aft direction. The human-back model is combined with the experimental data of the dynamic stiffness of backrest cushions (to form a back-backrest model) so as to predict the transmission of vibration through backrest of a seated subject during fore-and-aft excitation. Experimental measurements of transmissibility are compared with the theoretical predictions. Refinements are made to both the human-back model and the back-backrest model to improve the predictions of the backrest transmissibility. In addition, the effect of input location at the backrest, backrest inclination, seat-pan inclination, push force at the feet, footrest position and foam thickness (for transmissibility measurement only) are studied as an aid to further understand the biodynamic responses of the back and the dynamics of the back-backrest system during exposure to fore-and-aft vibration.

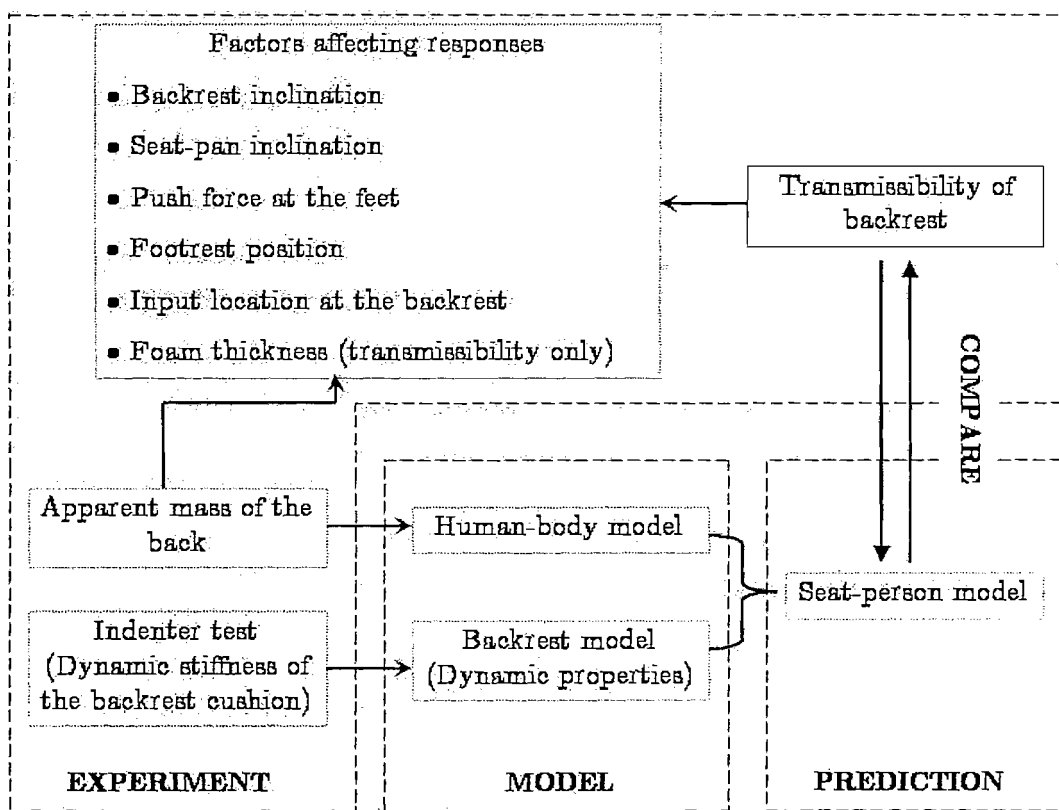


Figure 1.1: Simplified diagram showing the research methodology employed in this study.

This thesis is organised into ten chapters (including this introductory chapter).

**Chapter 2** reviews the principal literature on the dynamic responses of the human body in the seated position and the dynamic performance of seats. Experimental studies and mathematical models representing the experimental findings are discussed. Methods of predicting the transmissibility of seats are also mentioned briefly.

**Chapter 3** summarises the experimental equipment used. Methods of data analysis are also discussed.

**Chapter 4** reports the experimental findings on the transmission of vibration through backrests with seated persons. The influence of the vertical position of the accelerometer on the backrest and the effect of vibration magnitude are investigated.

**Chapter 5** explores the factors that can affect the transmission of vibration through backrests. The influence of foam thickness, backrest inclination, seat-pan inclination, push force at the feet and horizontal position of the footrest are investigated.

**Chapter 6** documents measurements of the apparent mass of the back. The non-linear response of the body with vibration magnitude was investigated. The influence of input location at the back on the apparent mass of the back is also discussed.

**Chapter 7** investigates the influence of backrest inclination, seat-pan inclination, push force at the feet and horizontal footrest position on the apparent mass of the back.

**Chapter 8** predicts the backrest transmissibility from the measured apparent mass of the back and the dynamic stiffness of the backrest cushion. Mathematical models representing seated person based on the results of Chapter 6 were developed. The measurement of the dynamic properties of backrest cushions is also discussed.

**Chapter 9** presents a general discussion of the work in this thesis.

**Chapter 10** offers the conclusions of this thesis and suggests some recommendations for future work.

# Chapter 2

## Literature review

### 2.1 Introduction

Human responses to whole-body vibration are very complex phenomena. Over several decades, researchers and scientists have conducted studies, either laboratory work, field measurements or questionnaire surveys to understand the complex responses of the body to vibration. Most of these studies have been written in scientific papers, reports and other documents. This chapter cites the scientific work relevant to this research.

Dynamic responses of the human body exposed to whole-body vibration are usually represented by transfer functions of the frequency response. The transfer functions are calculated based on spectral analysis. A minimum of two measurements is required to calculate a frequency response function. These measurements may be at the same point or at different points. The results express the relation between two signals and allow both the relative magnitude and the relative phase to be determined. These frequency responses may therefore be expressed either in a single complex number or in two numbers consisting of magnitude and phase.

In the case of calculating the frequency response from two measurements at the same point, the transfer functions are normally obtained from the ratio of the driving-point force of the seat-person interface to the resultant movements:

$$T_{DP}(f) = \frac{F_{DP}(f)}{X_{DP}(f)} \quad (2.1)$$

where  $T_{DP}(f)$  is the transfer function of the frequency response of the 'driving-point mechanical impedance',  $F_{DP}(f)$ , is the frequency response of the force measured at the driving-point seat-person interface and  $X_{DP}(f)$ , is the measured frequency response of the resultant movements (acceleration, velocity or displacement).

The term ‘mechanical impedance’ is a generic term for all relations between the driving-point force of a system at a particular frequency and the resultant movements at that frequency. However, it also has a specific meaning as the ratio between the force and the velocity measured at the same point.

In measurements of the ‘dynamic-point mechanical impedance’, the input motion can be acceleration, velocity or displacement and the output motion is the force measured at the seat-person interface. *Apparent mass*, *mechanical impedance* and *dynamic stiffness* are some of the common dynamic responses of seated subjects to vibration.

The term apparent mass,  $M(f)$ , can be defined as the complex ratio of the driving force,  $F(f)$ , at the driving-point to the resulting acceleration,  $a(f)$ , at the same point:

$$M(f) = \frac{F(f)}{a(f)} \quad (2.2)$$

Likewise, the terms mechanical impedance,  $Z(f)$ , and dynamic stiffness,  $S(f)$ , are defined as the ratios of the driving force,  $F(f)$ , at the driving-point acting on a system to the resulting velocity,  $v(f)$ , and displacement,  $d(f)$ , at the same point, respectively:

$$Z(f) = \frac{F(f)}{v(f)} \quad (2.3)$$

$$S(f) = \frac{F(f)}{d(f)} \quad (2.4)$$

Table 2.1 summarises some of the common measures of dynamic response used in biodynamics.

In the case of calculating the transfer function between two different measurement points, the common term for this response function is known as ‘transmissibility’. The transmissibility is a measure of ratio between the motion at the output and the motion at the input:

$$T_T(f) = \frac{X_{o/p}(f)}{X_{i/p}(f)} \quad (2.5)$$

where  $T_T(f)$  is the transmissibility,  $X_{i/p}(f)$  and  $X_{o/p}(f)$  are the input and output motions respectively. Transmissibility frequency responses may also be expressed in terms of magnitude and phase. For instance, the magnitude of the seat-to-head transmissibility may indicate the ratio of the magnitude of head motion to the magnitude of the seat

motion at a particular frequency. The corresponding phase of the seat-to-head transmissibility may be considered to represent the time delay between the two motions.

Both the ‘driving-point mechanical impedance’ and the ‘transmissibility’ frequency responses are important to understand the manner in which vibration is transmitted to and through the body. These functions can also be used to represent the dynamic responses of the body in response to vibration, which may influence the human comfort, performance and health.

**Table 2.1** Some common measures of dynamic response.

Terms	Ratio	Terms	Ratio
Apparent mass	Force/acceleration	Accelerance	Acceleration/force
Impedance	Force/velocity	Mobility	Velocity/force
Dynamic stiffness	Force/displacement	Receptance	Displacement/force

## 2.2 Dynamic responses of a sitting person exposed vertical and horizontal (fore-and-aft and lateral) vibration

### 2.2.1 Introduction

Some knowledge of mechanical impedance and apparent mass of the body is essential for an understanding the dynamic responses of the body in response to vibration. It gives the relation between the force and the movement, which is indicated by the magnitude and phase. The relation depends on the dynamic characteristics of the body to which the force is applied.

Previously, researchers measured mechanical impedance or apparent mass of the seated body mainly in the vertical direction (e.g. Coermann, 1962; Miwa, 1975; Mertens, 1978; Hinz and Seidel, 1987; Fairley and Griffin, 1989; Matsumoto and Griffin, 1998; Mansfield and Griffin, 2000 and Nawayseh and Griffin, 2003). Only a few published studies have concerned vibration in the horizontal direction (e.g. Fairley and Griffin, 1990; Holmlund and Lundström, 1998; Mansfield and Lundström, 1999a).

In this section, most of the documented studies regarding the impedance of the body (vertical and horizontal) will be presented briefly so as to acknowledge and understand previous findings.

### **2.2.2 Mechanical impedance of seated person exposed to whole-body vertical vibration**

Most of the studies measuring mechanical impedance of a seated subject were conducted in laboratories on mechanical, electrodynamic or hydraulic vibrators. These studies involved human subjects exposed to vertical vibration. There are many published studies in this area (e.g. Coermann, 1962; Suggs *et al.*, 1969; Miwa, 1975; Sandover, 1978; Donati and Bonthoux, 1983; Boileau and Rakheja, 1998; Kitazaki and Griffin, 1998; Fairley and Griffin, 1989; Mansfield and Griffin, 2000; Rakheja *et al.*, 2002; Matsumoto and Griffin, 2002 and Nawayseh and Griffin, 2003). However, there is one study of mechanical impedance of seated subjects performed in a field test (Holmlund and Lundström, 2001).

The results of all previous studies suggest that the body has a major resonance at approximately 5 Hz. However, some researchers found evidence of a second resonance at approximately 10 Hz (e.g. Coermann, 1962; Holmlund and Lundström, 2001; Rakheja *et al.*, 2002 and Mansfield and Griffin, 2002). The second resonance was found to be more pronounced when the back was supported on an inclined backrest coupled with hands on the steering-wheel (Wang *et al.*, 2004). There was an idea that a third resonance exists at about 50 Hz (e.g. Miwa, 1975, Holmlund and Lundström, 2001), but the third resonance peak is small and not clear, and the effect of it is also small.

Figure 2.1 illustrates an example on the moduli of the apparent mass 60 people (24 men, 24 women and 12 children) on a rigid seat with no backrest when all subjects were exposed to  $1.0 \text{ ms}^{-2}$  r.m.s. random vertical vibration (Fairley and Griffin, 1989).

The results showed that the apparent mass of every subject had a main resonance at about 5 Hz. A second mode was also evident in most subjects in the region of 10 Hz. The large scatter of the data at frequency near 0 Hz is mainly due to the differences in the static masses. However, this can be accounted by dividing the apparent mass of each subject with its own static weight on the platform and is also known as 'normalisation'. The normalised apparent mass showed small variability between subjects (Figure 2.2). The normalised biodynamic responses of the men, women and children showed similar responses.

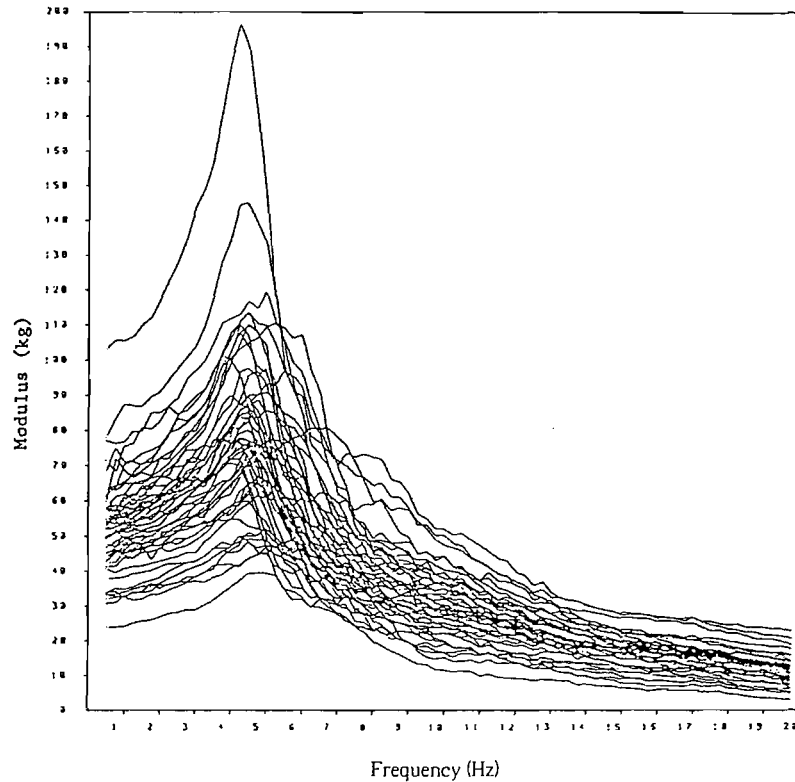


Figure 2.1: Apparent masses of sixty subjects in the vertical direction. Data from Fairley (1989).

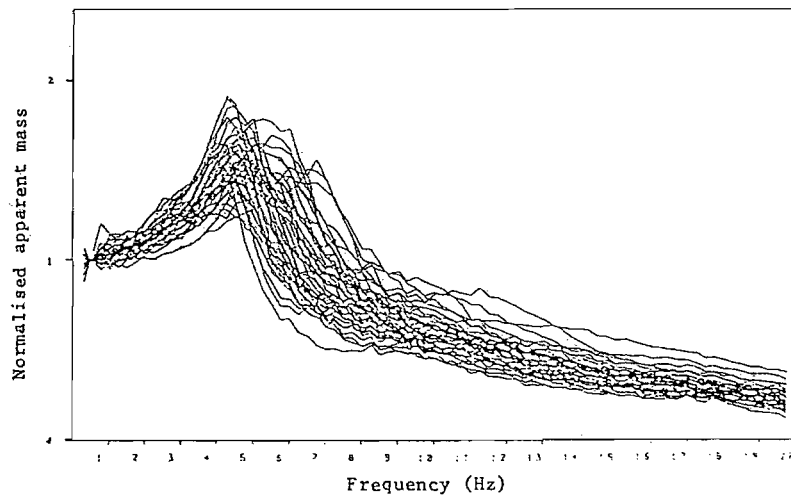
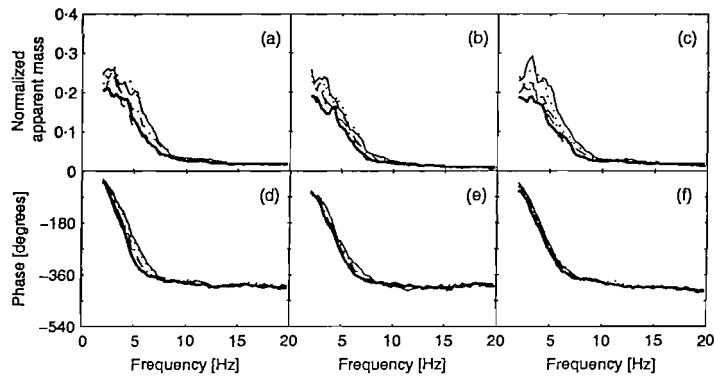


Figure 2.2: Normalised apparent masses of the same results as in Figure 2.1.

Almost all studies of the point impedance (mechanical impedance or apparent mass) of the body have been restricted to responses in the direction of the applied vibration. As the human response to vibration is a complex phenomenon and involves complex mechanisms, it is possible that the body would respond in another directions other than the direction of the excitation. This can be known as a 'cross-axis' response. Using sinusoidal vertical vibration at five frequencies and random vertical vibration, the 'cross-axis' fore-and-aft apparent mass of seated person was first measured by Matsumoto and Griffin (2002). With eight subjects, the authors found that, generally, the 'cross-axis' fore-and-aft apparent mass during vertical excitation tended to decrease with increasing frequency (Figure 2.3). A resonance around 5 Hz was evident in some of the individual results. In that study, the 'cross-axis' responses were statistically non-linear with vibration magnitude.



**Figure 2.3:** Median 'cross-axis' fore-and-aft apparent masses and phases of eight subjects measured with sinusoidal vibration. (a and d) Condition 1, (b and e) Condition 2 and (c and f) Condition 3. Data taken from Matsumoto and Griffin (2002).

Recently, Nawayseh and Griffin (2003) further investigated the response of the seated person in directions other than the direction of excitation (i.e. 'cross-axis' responses). The authors hypothesized that there would be appreciable forces on the seat in the fore-and-aft and lateral directions when subjects were exposed to vertical excitation. The apparent masses of twelve subjects in the vertical, fore-and-aft and lateral directions were calculated by means of comparing the measured forces on the seat in each direction (vertical, fore-and-aft, and lateral) with the applied vertical acceleration. There was a clear resonance around 5 Hz in the vertical apparent mass of the body (Figure 2.4), similar to previous findings. Appreciable forces on the seat were measured in the fore-and-aft direction and the 'cross-axis' fore-and-aft apparent mass of the body also showed a principal resonance in the vicinity of 5 Hz (Figure 2.5). Forces in the lateral direction, however, were relatively low, and a clear peak was difficult to see (Figure 2.6). The vertical and 'cross-axis' fore-and-aft

apparent masses of the body were non-linearly with vibration magnitude, but no clear effect of the vibration magnitude was observed in the lateral direction.

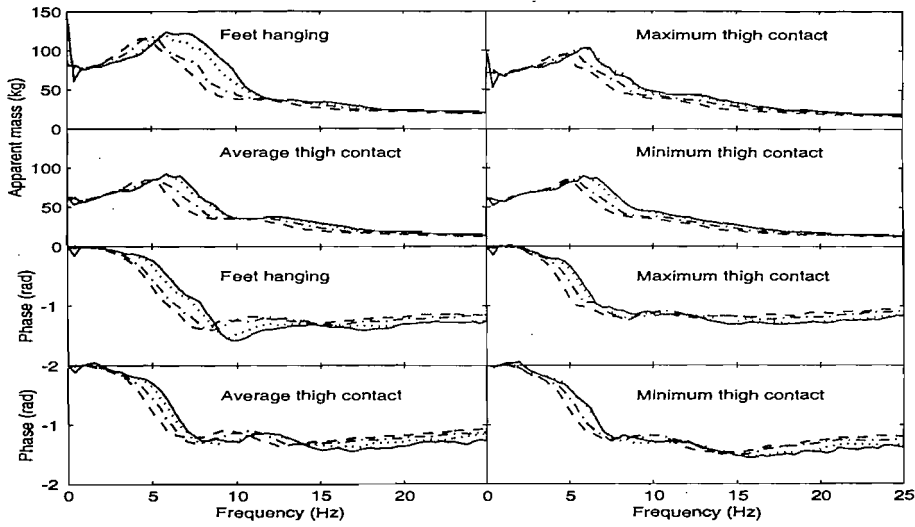


Figure 2.4: Median vertical apparent mass and phase of twelve subjects on the seat and at four sitting postures at four magnitudes. Data taken from Nawayseh and Griffin (2003).

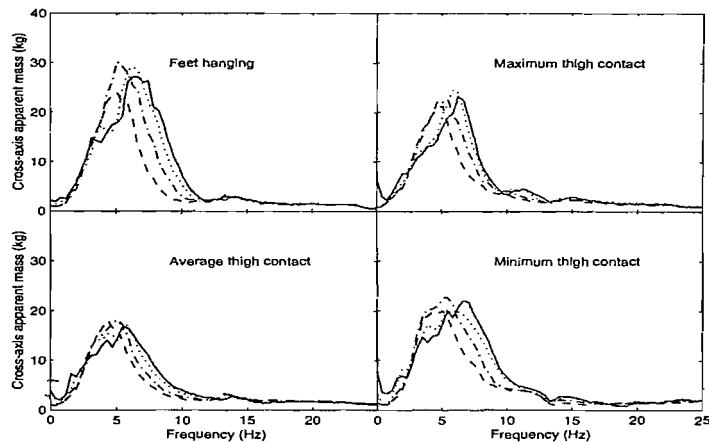
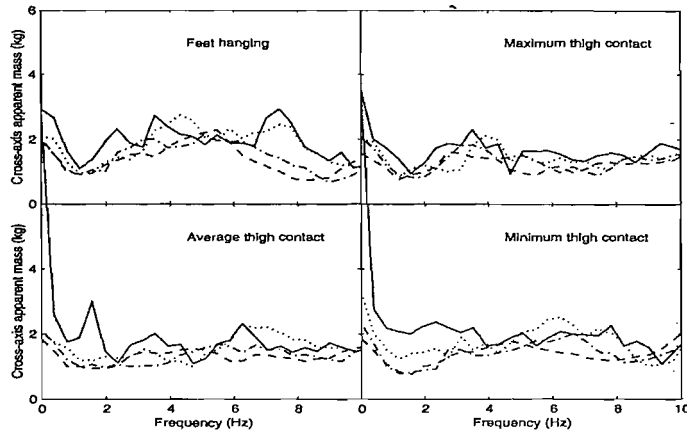
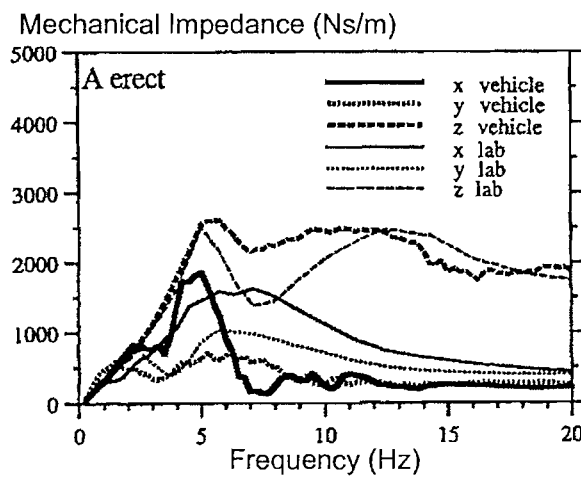


Figure 2.5: Median 'cross-axis' fore-and-aft apparent mass of twelve subjects on the seat and at four sitting postures at four magnitudes. Data taken from Nawayseh and Griffin (2003).



**Figure 2.6:** Median 'cross-axis' lateral apparent mass of twelve subjects on the seat and at four sitting postures at four magnitudes. Data taken from Nawayseh and Griffin (2003).

Previously, studies that documented the mechanical impedance and apparent mass of seated person have been conducted with laboratory measurements. Only recently, one field study has been carried out by Holmlund and Lundström (2001) to measure the mechanical impedance of seated person when subjects experienced a *real-life* vibration exposure and compare the results with the results obtained in single-axis laboratory measurements. The authors tried to argue the relevancy of the data in the International Standard, ISO/FDIS 5982 (2001) for applications in the field or road tests such that the data in the International Standard, ISO/FDIS 5982 (2001) were obtained from laboratory studies (i.e. single axis vibration). Based on this argument, the authors conducted a comparison of mechanical impedance of seated person in the vertical direction obtained in the laboratory (with thirty subjects; 15 males and 15 females) and road measurements (with three subjects and all subjects participated in the laboratory study). In the vehicle measurements, subjects were asked to adopt erect sitting posture while a minibus was driven over a gravel road, covered in snow and the speed was maintain at approximately  $50 \text{ kmh}^{-1}$ . In the laboratory measurements, all subjects were exposed to four vibration magnitudes (0.5, 0.7, 1.0 and  $1.4 \text{ ms}^{-2}$  r.m.s.) in the vertical direction (Figure 2.7). The results showed that although some differences are evident, the vertical mechanical impedance of the body in vehicle measurements showed, in general, good agreement with the laboratory results. Likewise, the impedance in the lateral mechanical impedance of the body in both vehicle measurements and laboratory results showed similar trend and showed magnitudes in the same range. Conversely, clear differences were observed between the laboratory studies and vehicle measurements in the fore-and-aft direction.



**Figure 2.7:** Comparison of vertical, fore-and-aft and lateral mechanical impedance of the body obtained from in vehicle and laboratory measurements. Thick lines indicate in vehicle measurements. Data taken from Holmlund and Lundström (2001).

### 2.2.3 Factors affecting body impedance of seated persons exposed to whole-body vertical vibration

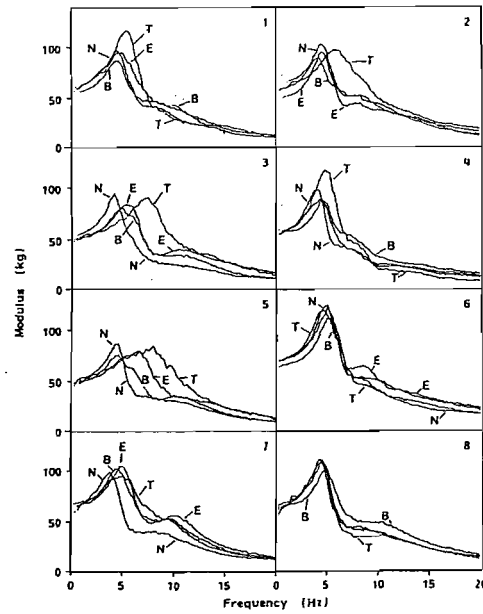
Biodynamic responses to vibration are complex and involve complex mechanisms. It can be said that previous researchers fundamentally agreed and have shown that the body has major resonance around 5 Hz. However, the biodynamic responses are influenced by various factors. This section will cover some of the factors that can influence the responses of the human body to vertical vibration.

#### 2.2.3.1 Effect of posture and muscle tension

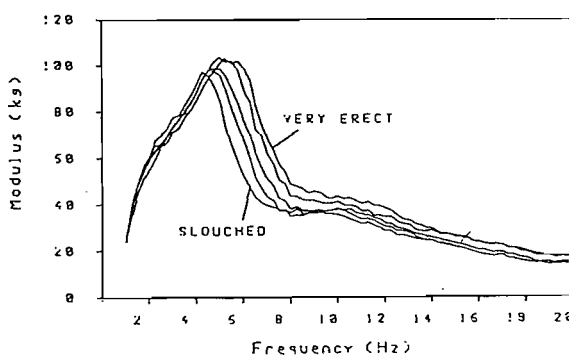
Coermann (1962) suggested that the resonance frequency would increase by about 1 Hz when an 'erect' posture was adopted instead of a 'relaxed' posture, although Miwa (1975) did not find the similar findings. However, in none of these studies was the effect of the muscle tension (e.g. 'tense' and 'relaxed') investigated separately from posture (e.g. 'erect' or 'slouched').

Fairley and Griffin (1989) investigated the effect of posture and muscle tension using eight subjects. The authors studied the effect of 'normal', 'erect', 'tense' and 'backrest' conditions and compared their apparent masses. There appeared to be a general trend for the resonance frequencies and the apparent masses at resonance to both be greater with

'erect', 'tense' and 'backrest' conditions compared to a 'normal' condition (Figure 2.8a). As would be expected, increasing muscle tension increases the body stiffness and so increases the resonance frequency. The authors further investigated the effect of an 'erect' to 'very erect' sitting posture with one subject and found the resonance frequency increased and the resonance peak became broader as the posture became more erect (Figure 2.8b).



(a)



(b)

Figure 2.8: Effect of the posture and muscle tension on (a) the apparent masses of the body of eight people. N = 'normal'; B = 'backrest'; T = 'tense'; E = 'erect', and (b) from 'slouched' to 'very erect'. Data taken from Fairley and Griffin (1989).

Similarly, Kitazaki and Griffin (1998) found that the principal resonance frequency of the apparent mass of the body increased from 4.4 to 5.2 Hz when the subjects changed posture from 'slouched' to 'erect' (Figure 2.9a). In that study, the authors also showed that the principal mode in 'slouched' posture was separated into the entire body mode and the combination of the visceral and bending mode of the upper spine (Figure 2.9b). They also found that the shear deformation of buttocks tissue in the entire body mode decreased from the 'slouched' posture to the 'erect' posture.

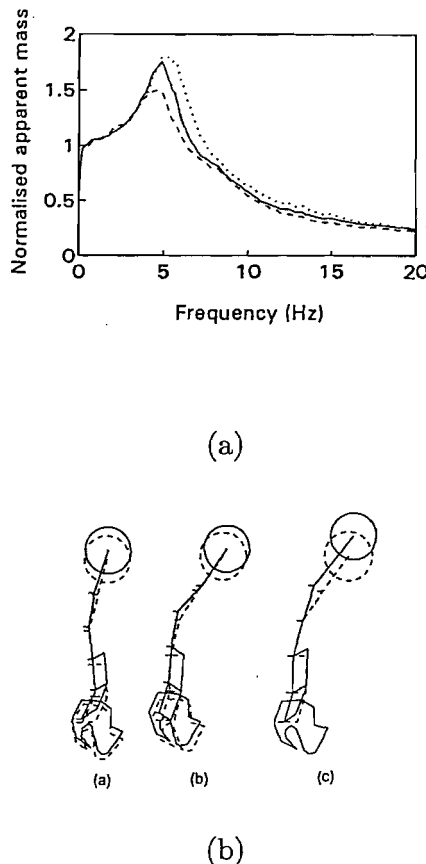


**Figure 2.9:** (a) Effect of the posture on the apparent masses of the body of eight people in the 'erect' posture (dotted), 'normal' posture (line) and 'slouched' posture (dashed). (b) Vibration mode shape for the principal resonance of the apparent mass (line) and the initial posture (dashed) at 5.2 Hz in the 'erect' posture (a), mode at 4 Hz in the 'slouched' posture (b) and mode at 4.9 Hz in the 'slouched' posture (c). Data taken from Kitazaki and Griffin (1998).

Increasing in the resonance frequency when the upper-body adopted a stiffer sitting posture (i.e. from 'slouched' to 'erect') was also evident in a study by Boileau and Rakheja (1998). In that study, the influence of a backrest support while subjects adopted an 'erect' sitting posture was also investigated (Figure 2.10). The authors found that the backrest support decreased the forces measured on the seat surface at frequencies less than 6 Hz

compared to when subjects maintaining 'erect' posture without a backrest. However, the backrest was found to increase the forces on the seat at frequencies higher than 6 Hz. The effect of posture on the impedance magnitude was not noticeable at frequencies below 4 Hz. The authors suggested that the effect of posture on the impedance magnitude in the resonance frequency region may be partly attributed to variations in the vertical component of the seated mass associated with the three postures. This was supported by other the results of the same study (not shown here) in which heavier subjects (around 57 kg of sitting mass) showed higher mechanical impedance at resonance than light subjects (approximately 40 kg of sitting mass). However, since the variation in the vertical load was less than 10% for different postures, the differences observed in the mechanical impedance of the body in different postures cannot be entirely attributed to the changes in the seated mass.

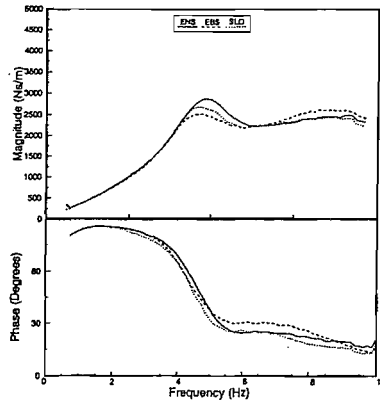
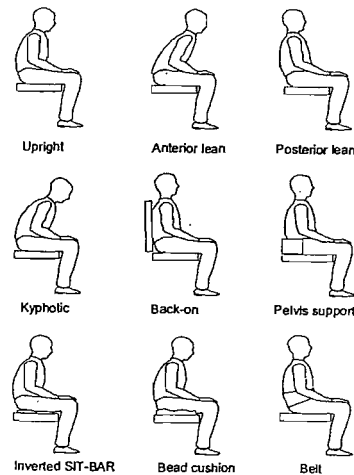


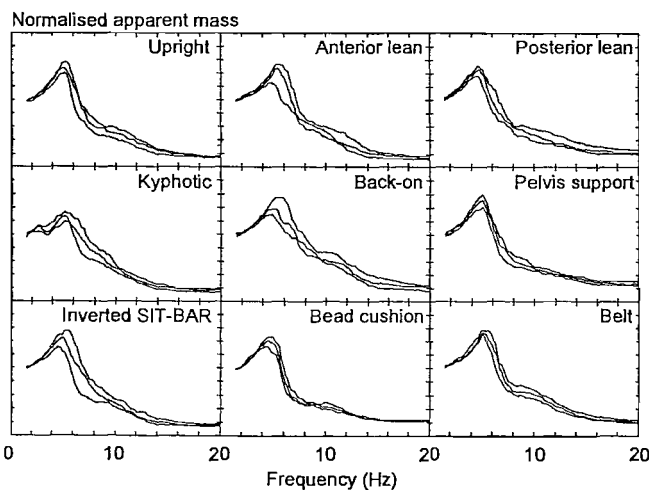
**Figure 2.10:** Effect of the backrest support on 'erect' sitting posture (ENS: erect no backrest support; EBS: erect with backrest support and SLO: slouched). Data taken from Boileau and Rakheja (1998).

The apparent masses of seated subjects adopting nine different postures ('upright', 'anterior lean', 'posterior lean', 'kyphotic', 'back-on', 'pelvis support', 'inverted SIT-BAR' (increased pressure beneath ischial tuberosities), 'bead cushion' (decreased pressure beneath ischial tuberosities), and 'belt' (wearing an elastic belt); Figure 2.11a) were investigated by Mansfield and Griffin (2002). Although the apparent mass was found to have small changes with posture, the 'kyphotic' posture had significantly lower apparent mass at resonance than that the 'upright' posture (Figure 2.11b). It was suggested that this posture increased the damping of the biodynamic system. The authors suggested that some of the postures used in this study were chosen in response to previously suggested mechanisms that might influences the primary peak in the apparent mass of the body. For instance, the 'pelvis support' posture was intended to alter the natural pelvis pitching

motion that was found to be associated to the some of the body modes during resonance (Kitazaki and Griffin, 1998). Likewise, the ‘belt’ condition was meant to restrict the visceral movement, the ‘ anterior’ and posterior’ lean conditions were designed to depict the whole-body bending and ‘inverted SIT-BAR’ and ‘cushion’ conditions were oriented to observe the influence of the tissue beneath the ischial tuberosities and the effect of increasing the loading area, respectively. However, they concluded that the results of this study gave no consistent support of the previously suggested mechanisms that might influence the frequency of the primary peak in the apparent mass.



(a)



(b)

Figure 2.11: Effect of the nine sitting posture (a) on the normalised apparent mass of the body (b). Data taken from Mansfield and Griffin (2002).

Most of the laboratory studies reported on the mechanical impedance and the apparent mass of seated persons were conducted while subjects adopted sitting posture, such as recommended in the International Standard ISO/FDIS 5982 (2001). The standard presented the idealised values to characterise seated-body biodynamic response under vertical vibration for subjects seated on a flat rigid platform, with feet supported and vibrated, and maintaining an 'erect' posture without backrest support.

Rakheja *et al.* (2002) argued that in the automotive applications, the drivers, for instance, would adopt different postures than the passengers. This sitting posture is different from that recommended by ISO/FDIS 5982 (2001). To see the implication of having a 'driving' posture (i.e. hands-on-steering wheel) compared to subjects adopted a 'passenger' posture (i.e. hands on the laps) on the apparent mass of the body, the authors conducted an experiment using twenty-four subjects (12 males and 12 females). In both sitting postures, subjects were supported with an inclined backrest ( $24^\circ$  from vertical) and inclined seat-pan ( $13^\circ$  from horizontal) and were exposed to random vertical vibration in the frequency range 0.5 to 40 Hz. The results showed that when subjects adopted the 'passenger' posture, the median apparent mass of the bodies of 24 subjects was found to show a resonance in the frequency range of 6.5 to 8.6 Hz, which is higher than that in most previous studies (approximately 5 Hz; e.g. Fairley and Griffin, 1989; Mansfield and Griffin, 2000; Matsumoto and Griffin, 2002 and Nawayseh and Griffin, 2003) with an upright posture, hands on the laps and mostly with no backrest (Figure 2.12). In the 'driving' posture, two peaks were evident in the region of 5.1 – 8.25 Hz and 8 – 12 Hz. The differences in the apparent masses in both sitting postures were suggested to be partly attributed to differences in the body masses supported on the seat-pan. From the figure, the low apparent mass at resonance for the 'driving' posture suggested that the body showed a well-damped behaviour compared to the 'passenger' posture. The authors suggested that resting the hands on the steering-wheel may partially influence the biodynamic responses, although previous study suggested the distinct influence of hands position has not been clearly identified (Donati and Bonthoux, 1983).

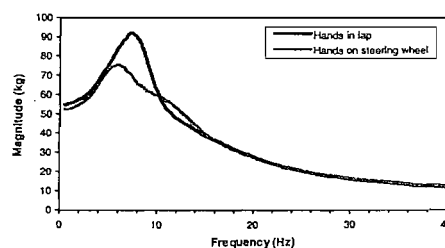


Figure 2.12: Apparent mass of seated subject in 'driving' (i.e. hands on steering-wheel) and 'passenger' (i.e. hands in lap) sitting posture. Data taken from Rakheja *et al.* (2002).

Wang *et al.* (2004) further investigated the effect of 'driving' and 'passenger' sitting postures with different seating conditions. The apparent masses of the body of twenty-seven subjects (13 males and 14 females) were measured in both sitting postures while subjects seated on: (i) flat seat pan with no backrest support (NVF), (ii) flat seat-pan and vertical backrest (BVF) and (iii) flat seat-pan with inclined backrest support (BIF). The results showed that the effect of hands position becomes more relevant only for postures involving back support conditions (Figure 2.13). The resonance frequency of the apparent mass in a 'passenger' posture was higher than that of the 'driving' posture when the back was supported, but showed minimal change with no backrest, similar to that found by Rakheja *et al.* (2002).

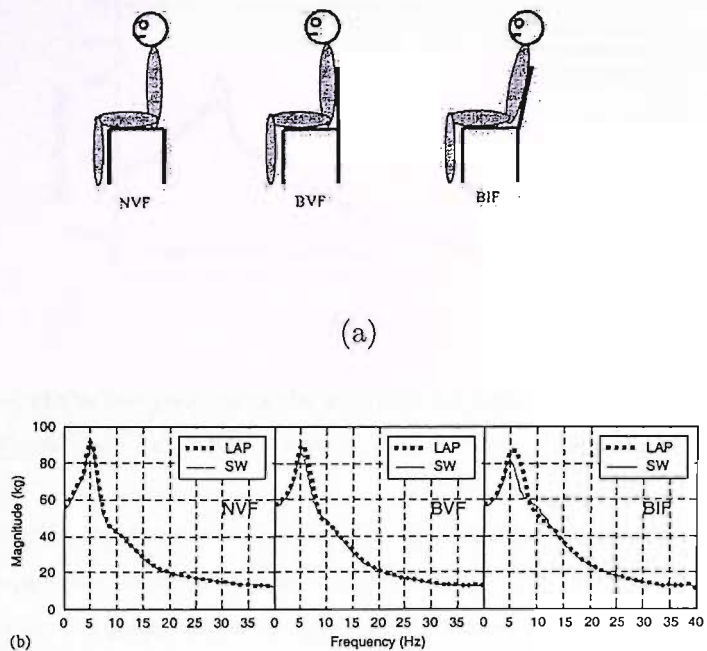
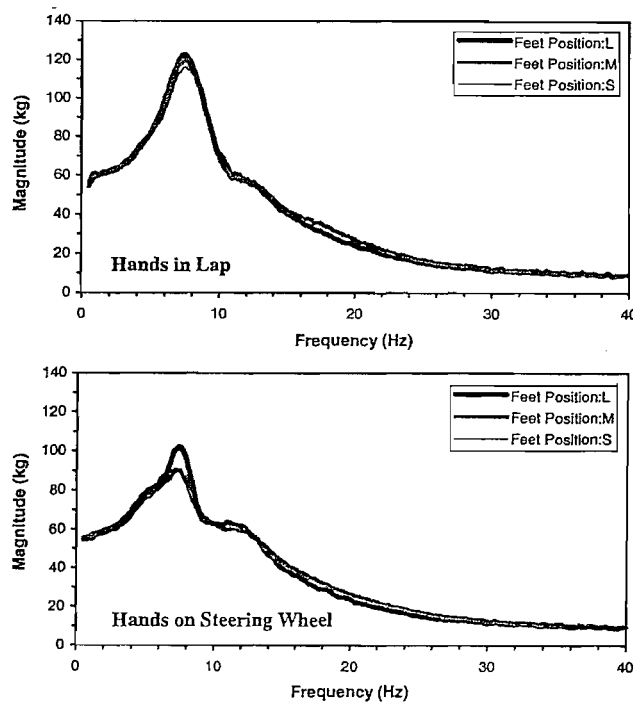


Figure 2.13: Effect of the backrest support on hand positions (i.e. 'driving' or 'passenger' sitting postures). Data taken from Wang *et al.* (2004).

The effect of foot position on the apparent mass of the body was investigated by Rakheja *et al.* (2002). In that study and in both 'passenger' and 'driving' postures, the apparent mass of the body was measured during random vertical vibration while subjects adopted leg postures such that: (i) 'normal' posture (i.e. the subjects selected themselves the feet position when seated on an inclined seat-pan and inclined backrest as their felt comfortable and stable, referred as 'M'), (ii) the feet was positioned 0.075 m ahead of the 'M' position (referred as 'L'), and (iii) the feet was positioned 0.075 m behind of the 'M' position (referred as 'S'). The results showed little influence of the foot position in both postures, except that with furthest location of the feet (i.e. 'L' position) yielded higher apparent

mass at resonance in both the 'driving' and 'passenger' postures (Figure 2.14). The authors concluded that the effect of foot position was negligible in either posture.



**Figure 2.14:** Effect of the feet position of the apparent mass of seated subjects in both 'passenger' and 'driving' postures. Data taken from Rakheja *et al.* (2002).

In a different study, Matsumoto and Griffin (2002) investigated the effect of muscle tension on the apparent mass of seated subjects exposed to vertical whole-body vertical vibration. All eight subjects were asked to adopt three sitting postures: (i) comfortable, upright posture with normal muscle tension (Condition 1), (ii) with the muscles of the buttock tensed, or stiffen as much as possible (Condition 2) and (iii) with the abdominal muscles tensed as much as possible (i.e. minimise the volume of the abdomen; Condition 3). While adopting all these three sitting conditions, subjects were exposed to sinusoidal and random vibration from 2 Hz and up to 20 Hz and at five vibration magnitudes (0.35, 0.5, 0.7, 1.0 and  $1.4 \text{ ms}^{-2}$  r.m.s.). The authors chosen the specified conditions, in particular for Condition 2 and Condition 3 because these parts of the body appeared to be responsible for the principal resonance of the apparent mass of the body, such as reported by Kitazaki and Griffin (1997) and Matsumoto and Griffin (2001). The results of study of Matsumoto and Griffin (2002) showed that the resonance frequency of the apparent mass of the body increased significantly when the buttock muscle was tensed (i.e. Condition 2) compared to sitting in normal muscle tension (i.e. Condition 1). This was evident at all vibration magnitudes tested (Figure 2.15). However, when subjects tensioned the

abdominal muscles (i.e. Condition 3), the influence was small at lower magnitude, but showed differences at higher magnitudes, in which the resonance frequency of the body was higher when the volume of the abdomen was minimised compared to when subjects sat in normal muscle tension.

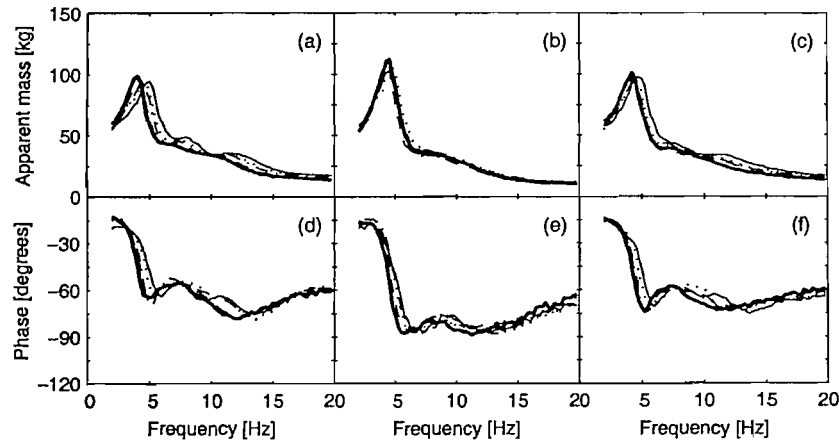


**Figure 2.15:** Effect of the muscle tension on the apparent mass and phases of the body at Condition 1 (a and d), Condition 2 (b and e) and Condition 3 (c and f). Data taken from Matsumoto and Griffin (2002).

### 2.2.3.2

#### *Effect of footrest*

When the apparent mass of one subject was measured with no footrest support so that the feet would hang freely, the apparent mass of the body increased at frequencies below 8 Hz (Fairley and Griffin, 1989). However, when the feet were supported with a stationary footrest, the apparent mass of the body decreased, most obvious at frequencies less than 8 Hz (Figure 2.16). The authors further investigated the effect of the height of stationary footrest on the apparent mass of the body and discovered that with increasing in height of the stationary footrest, the apparent mass increased at low frequencies (less than 2 Hz). Then, the authors measured the apparent masses of eight subjects with a moving footrest (position at 0.46 m below the top surface of the seat surface) and found that the effect of the height of the moving footrest was small compared to the effect of the height of stationary footrest. The apparent mass of the body above 10 Hz and the static weight on the platform both increased slightly when the height of the moving footrest was reduced. The authors suggested the differences in the apparent mass found with either different heights of a stationary footrest, or, different heights of a moving footrest to some extent depended upon the stiffness between the thigh and the seat surface. A higher footrest will tend to make less contact between the thighs and the seat surface, and vice-versa. This, in

part, would affect the load supported on the seat pan, which can influence the apparent mass on the seat surface.

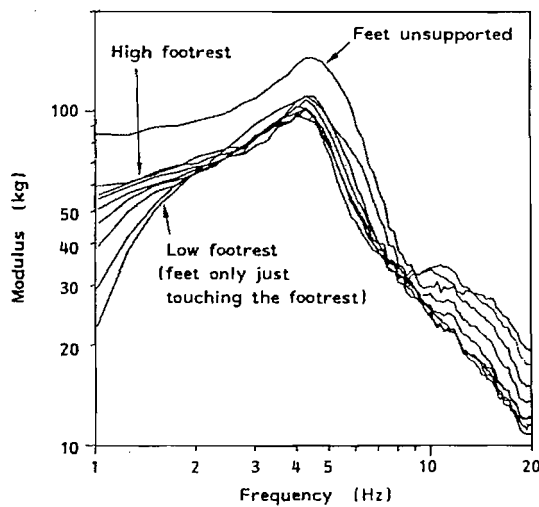


**Figure 2.16:** Effect of the footrest position on the apparent mass of a seated person of one subject. Data from Fairley and Griffin (1989).

Nawayseh and Griffin (2003) further investigated the effect of moving footrest position on the apparent mass of the body on the seat with no backrest in the vertical, fore-and-aft and lateral directions during exposure to vertical excitation. In that study, four footrest positions were designed so as to give: (i) a 'feet hanging' posture (with no foot support), (ii) a 'maximum thigh contact' posture, in which the feet was supported such that the heel just in contact with the footrest, (iii) an 'average thigh contact' posture (where the upper and lower legs were horizontal and vertical, respectively, and supported on the footrest) and (iv) a 'minimum thigh contact' posture, in which the footrest was positioned 0.16 m above the position with 'average thigh contact' posture for each subject. Twelve subjects participated in that study and all subjects were exposed to four vibration magnitudes (0.125, 0.25, 0.625 and 1.25  $\text{ms}^{-2}$  r.m.s) in the frequency range 0.25 to 25 Hz. The results showed that the vertical apparent mass of the body decreased over the frequency range tested when the thigh contact was reduced (i.e. from 'feet hanging' to 'minimum thigh contact'; Figure 2.17). The trend was evident at all magnitudes. The authors suggested that an increase in the footrest height partially, if not totally, reduced the load bearing supported on the seat surface and increased the mass supported on the footrest, but also changed the stiffness of the thighs during vibration. Both changes in mass distribution on the seat surface and footrest and changes in the thigh's stiffness may have maintained the same proportional contribution to the resonance frequency in the four postures, although

varying the thigh contact had little influence on the resonance frequency of the apparent mass of the body in the vertical direction.

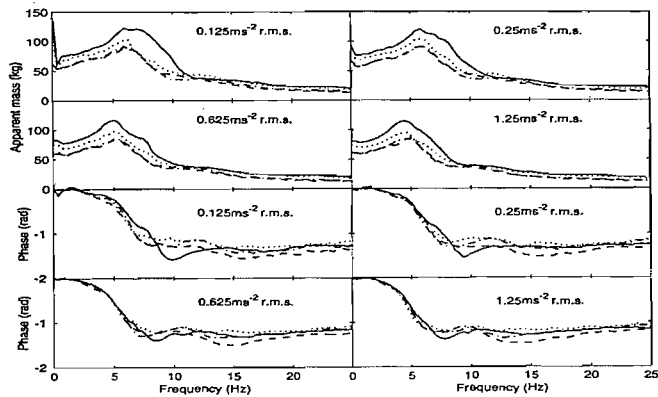
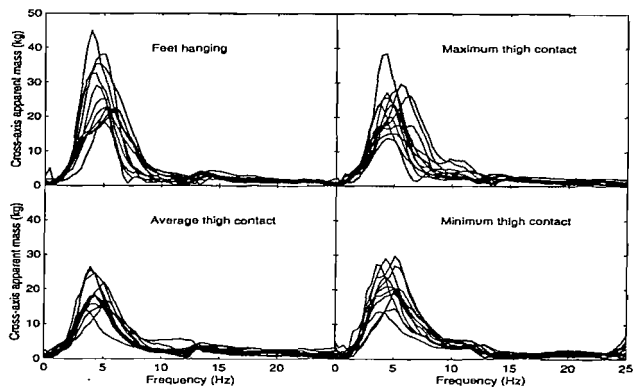


**Figure 2.17:** Effect of the thigh contact on the vertical apparent mass of subject during vertical excitation. Data from Nawayseh and Griffin (2003).

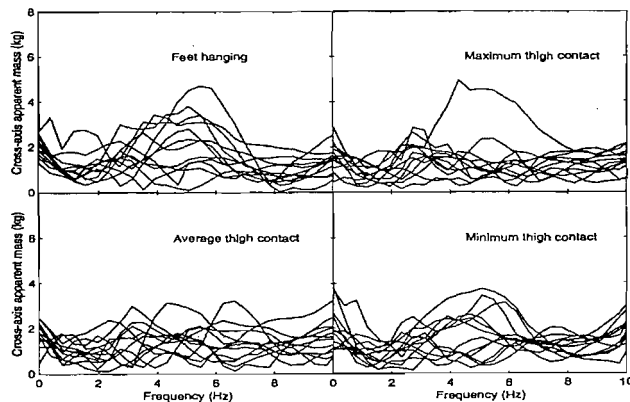
In a similar study (i.e. Nawayseh and Griffin, 2003), the ‘cross-axis’ fore-and-aft and lateral apparent masses of the subjects with similar thigh conditions were also calculated (by comparing the fore-and-aft or lateral forces measured on the seat with the applied vertical acceleration). The results showed that, in all sitting conditions, there were appreciable fore-and-aft forces on the seat, while the lateral forces on the seat were relatively low (Figures 2.18a to 2.18b). The ‘cross-axis’ fore-and-aft apparent mass of the body was also influenced by the thigh contact. With increasing thigh contact (i.e. from ‘average thigh contact’ to ‘feet hanging’), the ‘cross-axis’ fore-and-aft apparent mass increased, with an exception in the ‘minimum thigh contact’ where the forces were more than those with ‘average thigh contact’ and slightly less, similar, or more than those with ‘maximum thigh contact’, depending on the frequency. And in all postures, the ‘cross-axis’ fore-and-aft apparent mass of the body showed a principal resonance around 5 Hz, similar to that for the vertical apparent mass. However, it was difficult to notice the resonance frequency of the ‘cross-axis’ lateral apparent mass.

Nawayseh and Griffin (2004) further investigated the effect of thigh contact on the apparent masses of seated persons, but with vertical backrest support. The design and the other conditions (i.e. number of subjects, stimuli type and direction and frequency range) in this study were almost identical to the study of Nawayseh and Griffin (2003). In this study, the forces on the seat and backrest in the vertical, fore-and-aft and lateral directions were measured with subjects exposed to vertical vibration and subjects adopted similar sitting conditions (i.e. ‘feet hanging’, ‘minimum thigh contact’, ‘average thigh contact’ and ‘maximum thigh contact’). When the authors compared the results of the study with their

previous findings (i.e. with no backrest; Nawayseh and Griffin, 2003), they found that: (i) the effect of the sitting conditions on the vertical apparent mass of the body were more pronounced when the thigh had less contact with the seat (i.e. from 'feet hanging' to 'minimum thigh contact'), (ii) only with greater thigh contact was the effect of posture was significant on the 'cross-axis' fore-and-aft apparent mass of the body, and (iii) no obvious effect of the sitting posture were shown on the 'cross-axis' lateral apparent mass of the body, even when the backrest was used. The authors also found that changing the thigh contact with the seat-pan had little influence on the forces measured at the backrest in the vertical, fore-and-aft and lateral direction.



(a)



(b)

Figure 2.18: Effect of thigh contact on the (a) 'cross-axis' fore-and-aft apparent mass of the body and (b) 'cross-axis' lateral apparent mass of the body. Data taken from Nawayseh and Griffin (2003).

### 2.2.3.3 Effect of backrest, backrest and seat angles

When subjects adopted a ‘normal’ sitting posture (i.e. comfortable, upright posture with normal muscle tension) and sat on a rigid seat, with the body leaning against a vertical backrest, the apparent mass of the body was reduced at frequencies less than the resonance frequency (around 5 Hz), but increased at frequencies higher than the resonance compared to when subjects seated in the same posture but without a backrest (Fairley and Griffin, 1989; see Figure 2.8a). Mansfield and Griffin (2002) also found similar findings: the vertical apparent mass of the body increased at frequencies higher than the resonance frequency compared to when subjects seated in ‘upright’ posture (Figure 2.19). It seems that the backrest may increase the vibration to the body, in particular, to the back at higher frequencies. The authors also compared the results of subjects adopting different sitting posture without a backrest and with vertical backrest.

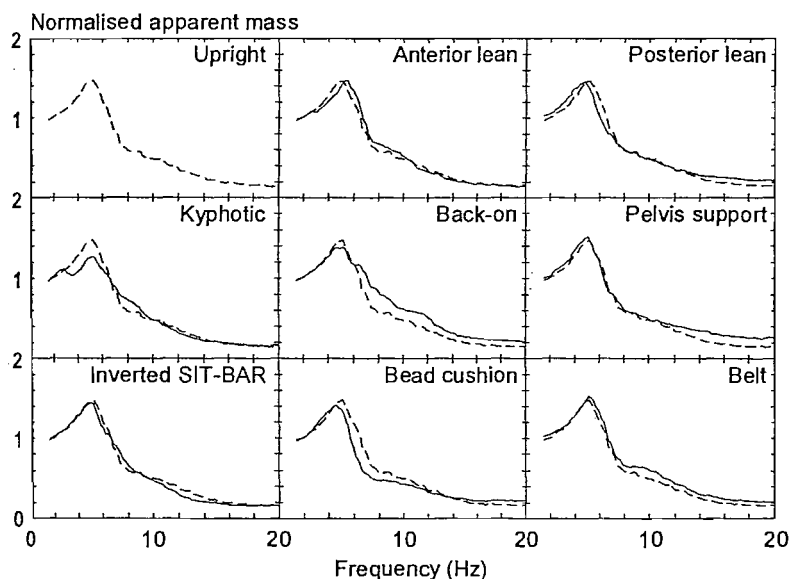
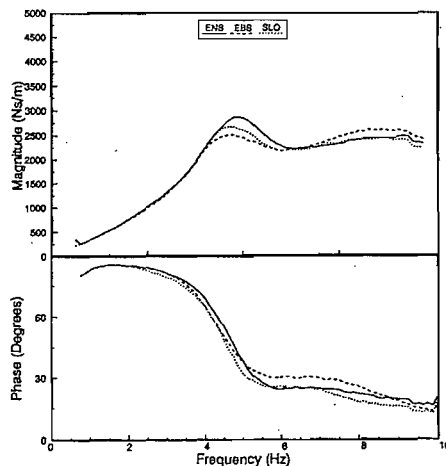


Figure 2.19: Effect of the backrest on the apparent mass of the body. Data from Mansfield (1998).

Boileau and Rakheja (1998) found the impedance of the body was higher around the region of the resonance frequency (between 4 and 6 Hz) when subjects seated in ‘erect’ posture, compared to when subjects sat in the same posture but with a backrest (Figure 2.20). At higher frequencies, however, the impedance of the body was similar to previous studies: the forces on the seat were higher with the backrest than without the backrest. The differences found in this study, compared with the findings of Fairley and Griffin (1989) and Mansfield and Griffin (2002), were probably due to the different hand position between the studies. In the Fairley and Griffin (1989) and Mansfield and Griffin (2002) studies, subjects

rested their hands on the laps ('passenger' posture), while in the study of Boileau and Rakheja (1998), subjects were asked to rest the hands on a steering-wheel as when 'driving'. Wang *et al.* (2004) also reported that the apparent mass of the body increased at frequencies higher than the resonance frequency, and suggested that the hand position becomes relevant only for postures involving back support conditions.



**Figure 2.20:** Effect of the backrest on the driving-point mechanical impedance of seated subjects with 'driver' position (ENS: erect with no backrest support; EBS: erect with backrest support and SLO: slouched). Data from Boileau and Rakheja (1998).

Nawayseh and Griffin (2004) investigated the effect of a vertical backrest on the apparent mass of the body in the vertical, fore-and-aft and lateral directions. In that study, subjects were exposed to only vertical excitation and forces on the seat and backrest in all three directions were measured while adopting four sitting postures ('feet hanging', 'minimum thigh contact', 'average thigh contact' and 'maximum thigh contact'). The apparent masses of the body on the seat were compared with their previous findings when no backrest was used (Nawayseh and Griffin, 2003). They found that: (i) the use of the vertical backrest modified the vertical forces on the seat - the backrest increased the vertical forces on the seat at frequencies higher than the resonance frequency in all sitting postures (Figure 2.21a) (ii) the backrest has significant influence on the 'cross-axis' fore-and-aft apparent mass of the body only with greater thigh contact (i.e. 'feet hanging' and 'maximum thigh contact' postures) – the fore-and-aft forces on the seat were reduced at frequencies less than around 8 Hz in these two postures, and they suggested that the presence of the backrest restrained the upper body and helped reduce the pitching motion that was difficult to reduce when there was no backrest (Figure 2.21b), and (iii) there was only a small effect of the backrest on the 'cross-axis' lateral apparent mass of the body in all sitting postures (Figure 2.21c).

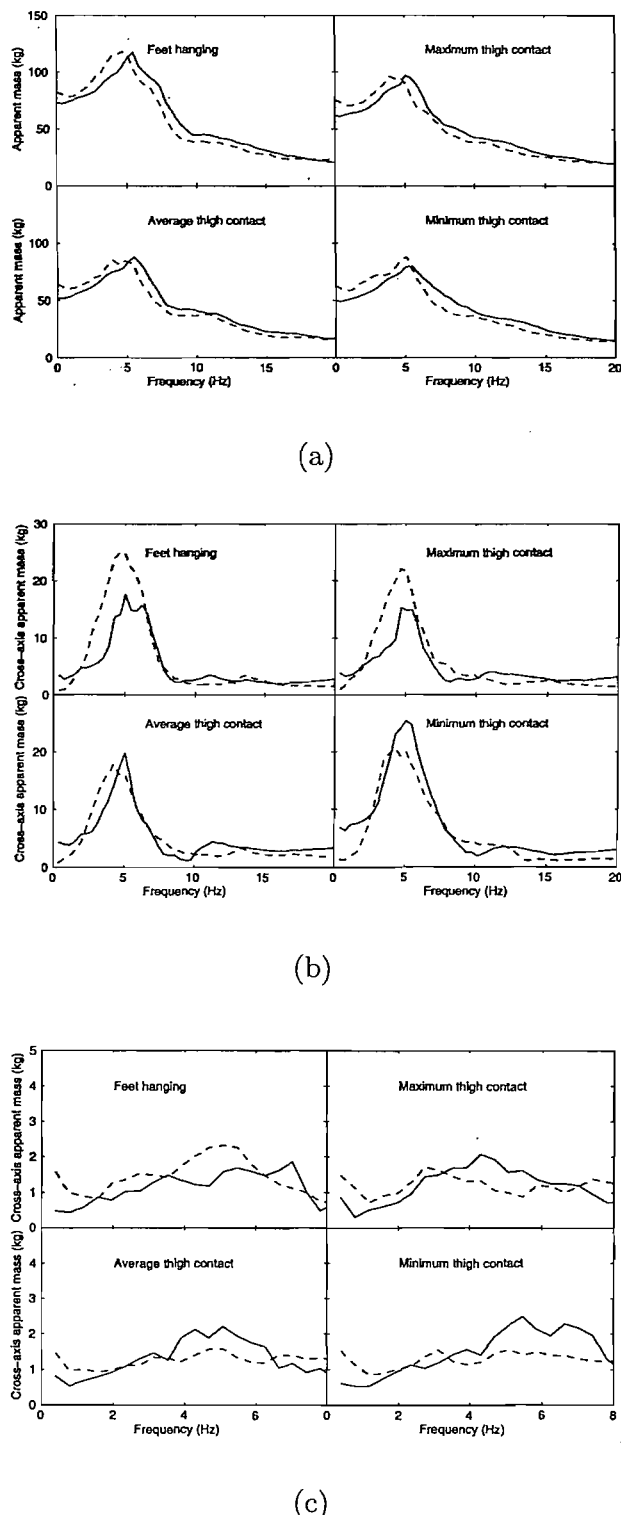


**Figure 2.21:** Effect of backrest on the (a) vertical apparent mass of the body, (b) 'cross-axis' fore-and-aft apparent mass of the body and (c) 'cross-axis' lateral apparent mass of the body. Data taken from Nawayseh and Griffin (2004).

The effect of the either backrest inclination or seat-pan inclination on the apparent mass of the body has been studied by Wei and Griffin (1998a and 1999), Wang *et al.* (2004) and Nawayseh and Griffin (2005c). The former authors found the resonance frequency of the apparent mass of the body increased with increasing backrest inclination from 0° to 20° (measured from vertical; Figure 2.22), but the apparent mass at resonance remained unchanged. In the same study, similar findings were also found when the foam in the backrest changed from soft to hard: the resonance frequency increased, but the apparent mass at resonance remained unchanged. Wang *et al.* (2004) found that the second resonance of the apparent mass of the body (around 10 Hz) was found to be more pronounced with an inclined backrest (i.e. from 0° to 12°, measured from vertical). Increasing backrest inclination also tended to increase the biodynamic damping of the body (i.e. the apparent mass at resonance decreased with increasing backrest inclination).

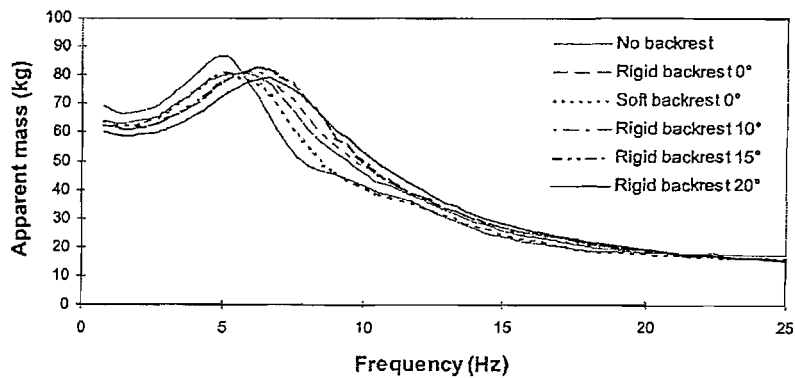


**Figure 2.22:** Effect of the backrest inclination and backrest condition on the apparent mass of the body. Data from Wei and Griffin (1999).

There was only a small influence of increasing seat-pan inclination on the apparent mass of the body without a backrest during vertical excitation (Wei and Griffin, 1998a). The differences in the apparent mass of the body when the seat pan changed from 0° to 20° (measured from horizontal) were only significant around the resonance frequency (Figure 2.23). Similar findings were also found by Wang *et al.* (2004) and Nawayseh and Griffin (2005c): there was negligible effect of seat-pan inclination on the apparent mass of the body with, and without a backrest, irrespective of the hand position (either hands on laps, or hands on steering-wheel).

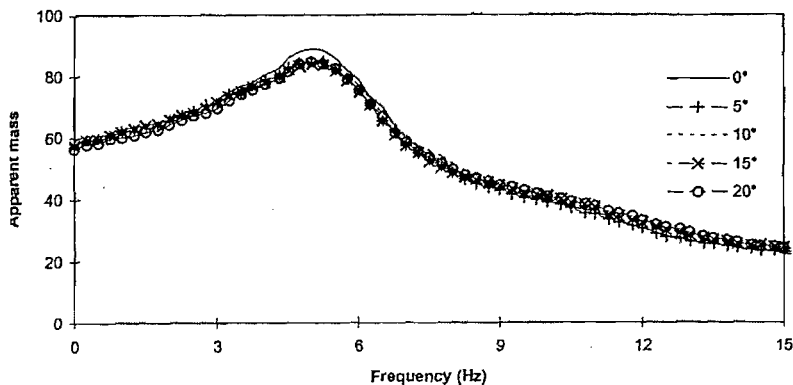


**Figure 2.23:** Effect of the seat-pan inclination the apparent mass of the body. Data from Wei and Griffin (1998a).

Nawayseh and Griffin (2005c) also measured the 'cross-axis' fore-and-aft apparent mass of the body, with and without a backrest with increasing seat-pan inclination from 0° to 15°. The authors found that the 'fore-and-aft' forces on the seat (i.e. the forces parallel with the seat-surface) generally increased with increasing seat-pan inclination at all four magnitudes tested (0.125, 0.25, 0.625 and 1.25 ms<sup>-2</sup> r.m.s.; Figure 2.24). The 'cross-axis fore-and-aft' apparent mass of the body (calculated by comparing the parallel forces measured on the seat surface with the applied vertical acceleration) with no backrest was highest with greatest seat-pan inclination (i.e. 15°.) although no significant change in the resonance frequency was observed. When a vertical backrest was used, there were statistical differences in the magnitude of the 'cross-axis fore-and-aft' apparent mass measured with and without backrest only at frequencies less than 6 Hz. There was a trend on the biodynamic damping of the body to increase with increasing seat-pan inclination when the backrest was used – the apparent mass at resonance decreased with a more inclined seat-pan. The authors suggested that the considerable 'fore-and-aft' forces found with increasing seat-pan inclination, in particular, at low frequencies, was caused mostly, if not totally, by an increase in the component of the mass in the 'fore-and-aft' direction (i.e. parallel to the seat surface).

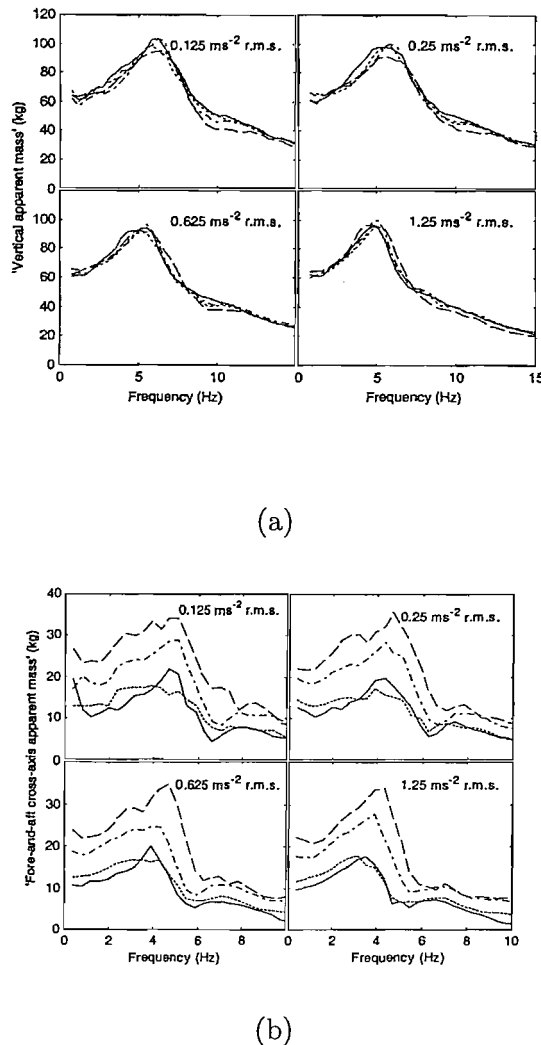


Figure 2.24: Effect of the seat-pan inclination the (a) 'vertical' and (b) 'cross-axis fore-and-aft' apparent mass of the body without backrest. Data from Nawayseh and Griffin (2005c).

#### 2.2.3.4 Effect of vibration magnitude

An early study by Coermann (1962) concluded that the body behaves like a linear system when exposed to vibration. Pradko *et al.* (1966) and Sandover (1978) reached the same conclusion, although the conditions in their experiments were different (i.e. with and without the presence of a backrest).

Other studies (e.g. Wittman and Phillips, 1969 and Hinz and Seidel, 1987) produced evidence that the impedance of the human body may be modified by changes in the magnitude of the applied vibration. These studies suggested that the human body responds to vibration in a non-linear manner.

Fairley and Griffin (1989) further investigated the non-linear characteristic of the body when exposed to different vibration magnitudes. Using eight subjects, they conducted an experiment to compare apparent masses of the seated person when subjects were exposed to four different vibration magnitudes (0.25, 0.5, 1.0 and 2.0  $\text{ms}^{-2}$  r.m.s.). With increasing magnitude of vibration, there was a 'softening' of the system, in which the lowest resonance frequency consistently decreased with increasing vibration magnitude for every subject (Figure 2.25).

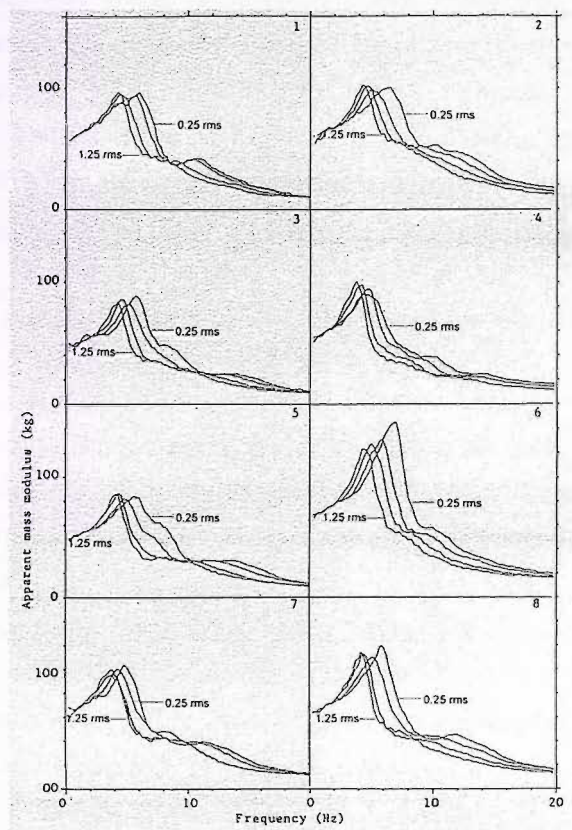


Figure 2.25: Effect of the vibration magnitude on the apparent masses of eight subjects. Principal resonance frequency of the body decreased with increasing vibration magnitude. Data from Fairley and Griffin (1989).

The non-linearity behaviour of the body in response to different vibration magnitude, in particular, reduction in resonance frequency of the body with increasing vibration magnitude has also been obtained by Mansfield and Griffin (2000 and 2002), Mansfield and Griffin (2002), Matsumoto and Griffin (2002), Rakheja *et al.* (2002), Wang *et al.* (2004) and Nawayseh and Griffin (2003, 2004 and 2005c).

The 'softening' effect was observed in all nine postures (see Figure 2.11a), including the reduction in the second resonance of the body (around 10 Hz) that was evident in most of the postures (Mansfield and Griffin, 2002). The non-linearity of the body in response to different vibration magnitudes was not significantly affected when subjects were asked to control muscle tension, either around the buttocks, or the abdomen (Matsumoto and Griffin, 2002). In that study, the authors suggested that involuntary muscles changes in muscle tension may be partly responsible for the non-linearity of the body.

Rakheja *et al.*, (2002) and Wang *et al.* (2004), both found that the non-linearity of the body was more sensitive when subjects adopted 'passenger' posture (i.e. hands on the laps and with a back support) than in a 'driving' posture (i.e. hands on the steering-wheel and with back support). The latter study, however, found that the 'softening' effect tended to be more pronounced when the upper body was not supported – the principal resonance frequency reduced by 0.5 or 0.6 Hz with increasing vibration magnitude from 0.5 to 1.0 ms<sup>2</sup> r.m.s., irrespective of the hand position (i.e. 'passenger' or 'driving'), compared to only 0.3 Hz when the back was supported, either with vertical or inclined backrests.

The non-linearity of the body on the seat and at the backrest when subjects were exposed to vertical vibration was further investigated by Nawayseh and Griffin (2003 and 2004). Twelve subjects participated in both studies and were exposed to four vibration magnitudes (0.125, 0.25, 0.625 and 1.25 ms<sup>2</sup> r.m.s.), while adopting four sitting postures ('feet hanging', 'maximum thigh contact', 'average thigh contact' and 'minimum thigh contact') in each magnitude. In the first study (Nawayseh and Griffin, 2003), the authors measured forces on the seat in the vertical, fore-and-aft and lateral directions, while the latter study (Nawayseh and Griffin, 2004), both forces on the seat and at the backrest in all three directions were measured. The results of the earlier study showed that the vertical apparent mass of the body and the 'cross-axis' fore-and-aft apparent mass of the body showed clear reductions in the resonance frequencies with increasing vibration magnitude in all sitting postures (Figure 2.26a to 2.26b). In addition, the body posture affected the sizes of differences in the resonance frequencies of the vertical apparent mass of the body only at the two higher vibration magnitudes, but not at the two lower vibration magnitudes. However, no clear effect of the vibration magnitude on the 'cross-axis' lateral apparent mass of the body was observed in any sitting posture (Figure 2.26c).

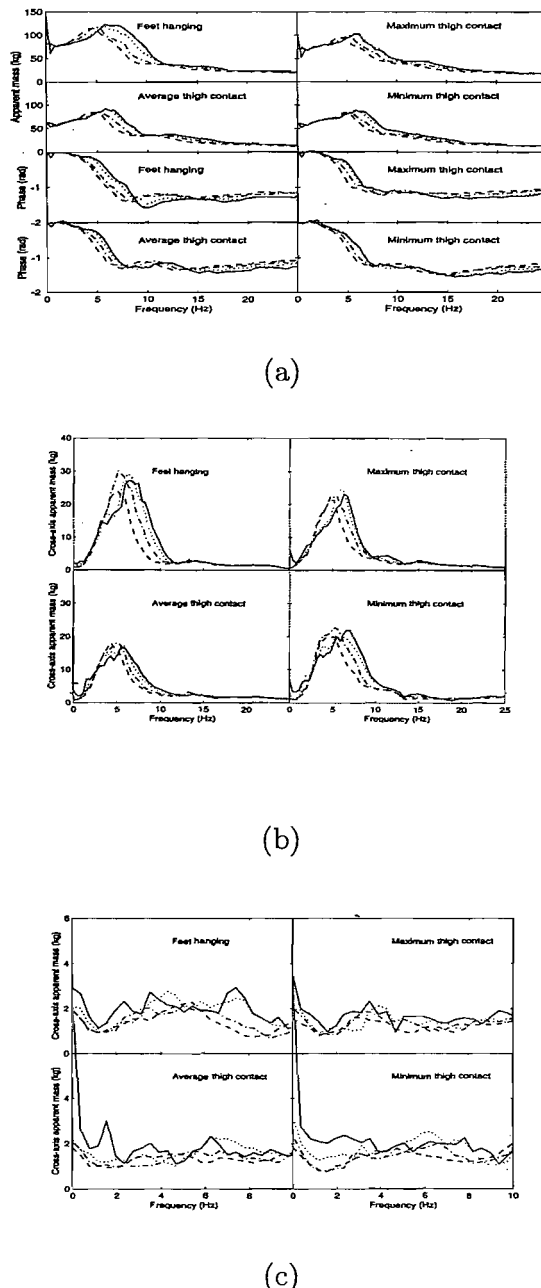
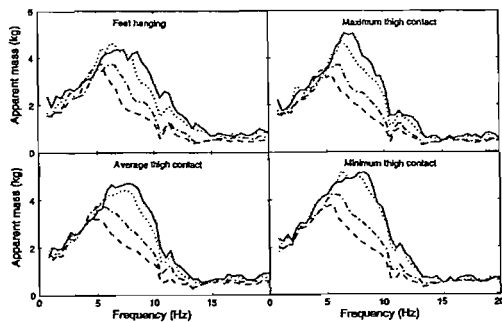


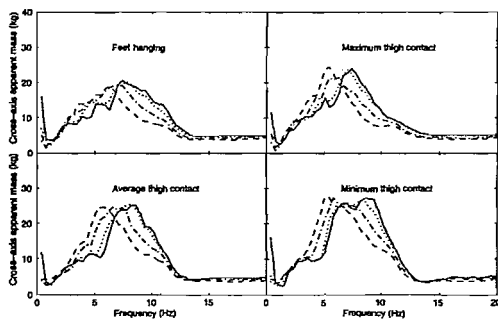
**Figure 2.26:** Effect of vibration magnitude on the (a) vertical apparent mass of the body, (b) 'cross-axis' fore-and-aft apparent mass of the body and (c) 'cross-axis' lateral apparent mass of the body. Data taken from Nawayseh and Griffin (2003).

In the later study (i.e. Nawayseh and Griffin, 2004), the authors found similar non-linearity characteristic on the seat in the vertical and fore-and-aft directions, although a less clear effect of vibration magnitude in the lateral direction was noticed. The authors also found that, while fore-and-aft forces at the backrest were appreciable, the vertical forces at the backrest were relatively low, with forces at the backrest in the lateral

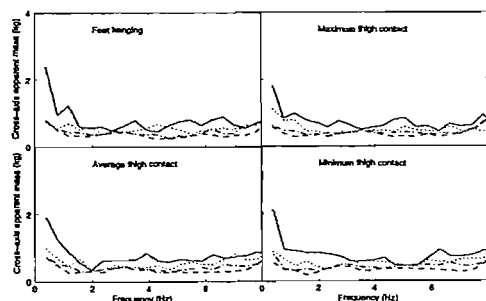
direction the lowest. The vertical apparent mass of the back, and the 'cross-axis' fore-and-aft apparent mass of the back showed a principal resonance frequency around 5 Hz, in which the frequency decreased with increasing vibration magnitude in all sitting postures (Figure 2.27a to 2.27b). The 'cross-axis' lateral apparent mass of the back, however, showed little change with vibration magnitude (Figure 2.27c).



(a)



(b)



(c)

**Figure 2.27:** Effect of vibration magnitude on the (a) vertical apparent mass of the back, (b) 'cross-axis' fore-and-aft apparent mass of the back and (c) 'cross-axis' lateral apparent mass of the back. Data taken from Nawayseh and Griffin (2004).

## 2.2.4 Mechanical impedance of seated persons exposed to whole-body horizontal vibration (fore-and-aft or lateral)

One of the earliest studies the apparent mass of seated person during either fore-and-aft or lateral vibration was reported by Fairley and Griffin (1990). During fore-and-aft vibration, the apparent masses of eight subjects without a backrest showed two resonances, at about 0.7 and in the region of 2.5 Hz (Figure 2.28a). Similarly, the apparent mass of the body during lateral excitation also showed two resonance frequencies: around 0.7 Hz and 2 Hz (Figure 2.28b). However, there appeared to be only one mode of vibration when motion of the upper body was restrained by a backrest, with a resonance in the region of 3.5 Hz for the fore-and-aft direction and at about 1.5 Hz for the lateral direction.

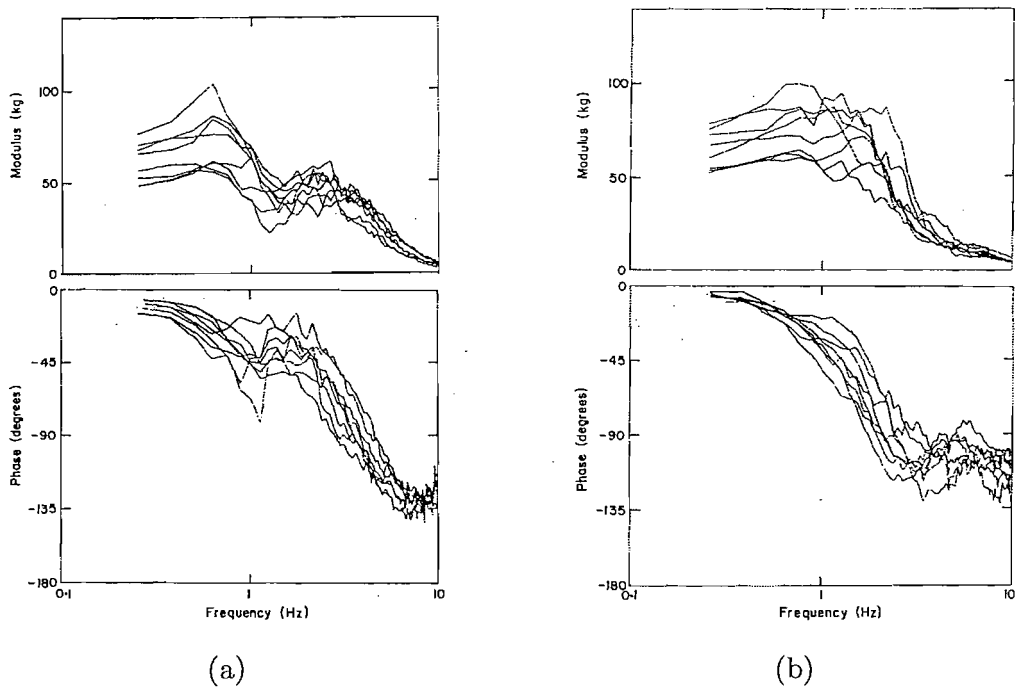
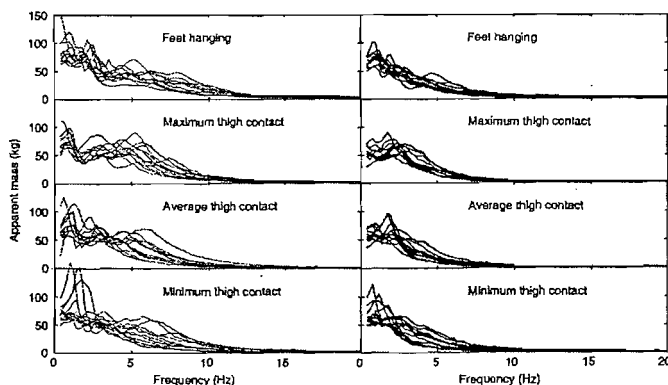


Figure 2.28: Apparent masses of eight subjects during (a) fore-and-aft vibration and (b) lateral vibration, both with no backrest. Data taken from Fairley and Griffin (1990).

Holmlund and Lundström (1998) reported that the mechanical impedance of the body in the fore-and-aft direction without backrest support showed only one principal resonance frequency between 3 and 5 Hz, and found two body modes during lateral excitation – around 2 and 6 Hz. Similar resonance frequencies of the body in both directions (i.e. around 3 Hz for the first peak and around 6 Hz for the second peak) were also reported by Mansfield and Lundström (1999a). However, these resonances (in both directions) were slightly higher than the resonances reported by Fairley and Griffin, (1990). A possible

cause for the differences is that in the earlier study, the subjects' feet were supported on a moving footrest, but the latter studies, the body was excited by vibration at the feet supported on a stationary footrest.

Nawayseh and Griffin (2005a and 2005b) conducted a series of studies to investigate the biodynamic responses of the body during exposure to fore-and-aft vibration. In both studies, the forces on the seat were measured in vertical, fore-and-aft and lateral directions, while the earlier study also included the forces at the backrest in all three directions. In both studies, twelve subjects were exposed to random fore-and-aft vibration, with four vibration magnitudes (0.125, 0.25, 0.625 and 1.25  $\text{ms}^{-2}$  r.m.s.) in the frequency range 0.25 to 10 Hz. With no backrest, Nawayseh and Griffin (2005b) found that the fore-and-aft apparent mass of the body showed three vibration modes: around 1 Hz, between 1 and 3 Hz and between 3 and 5 Hz (Figure 2.29). These modes were observed in all sitting postures used in the study (i.e. 'feet hanging', 'maximum thigh contact', 'average thigh contact' and 'minimum thigh contact'). Considerable vertical forces on the seat were also measured, although the lateral forces on the seat were relatively small compared to the vertical forces (Figures 2.30a to 2.30b). The 'cross-axis' vertical apparent mass on the seat (calculated by comparing the vertical forces on the seat with the applied fore-and-aft acceleration) showed evidence of three resonance frequencies: around 1 Hz, around 3 Hz and between 4 and 7 Hz, particularly when subjects adopted 'maximum thigh contact' posture. The vertical forces on the seat increased at frequencies less than 5 Hz with increasing feet support (i.e. from 'feet hanging' to 'minimum thigh contact').



**Figure 2.29:** Fore-and-aft apparent mass at the seat for each posture for twelve subjects at 0.125  $\text{ms}^{-2}$  r.m.s. (left column) and 1.25  $\text{ms}^{-2}$  r.m.s. (right column). Data taken from Nawayseh and Griffin (2005b).

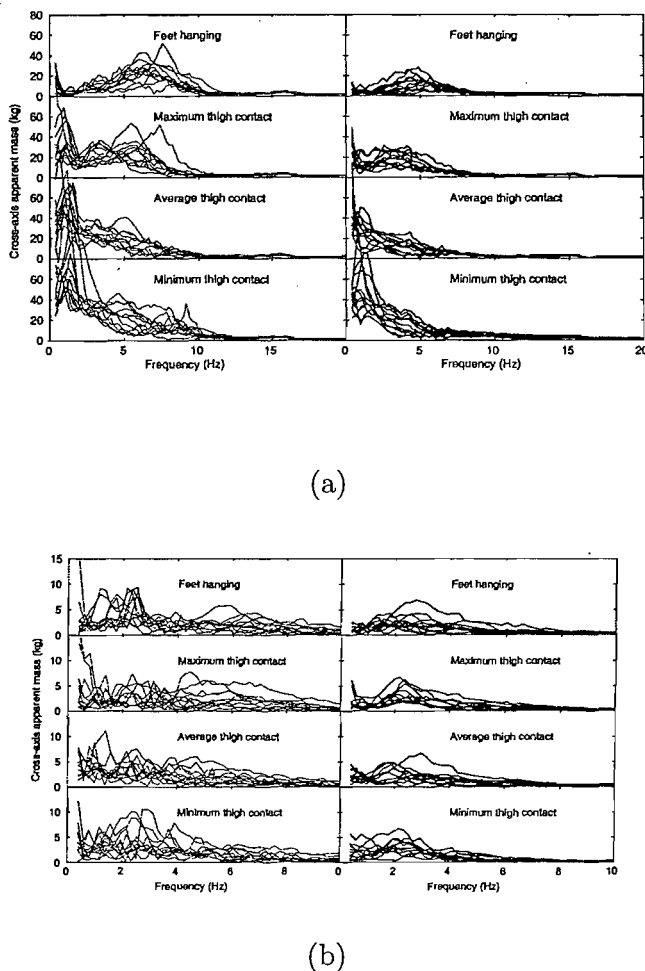


**Figure 2.30:** 'Cross-axis' (a) fore-and-aft, and (b) lateral, apparent masses at the seat for each posture for twelve subjects at  $0.125 \text{ ms}^{-2}$  r.m.s. (left column) and  $1.25 \text{ ms}^{-2}$  r.m.s. (right column). Data taken from Nawayseh and Griffin (2005b).

When a vertical backrest was used (i.e. Nawayseh and Griffin, 2005a), the fore-and-aft apparent mass on the seat only showed one principal resonance in the range of 2 to 6 Hz in all postures (depending on subject and vibration magnitude), except with 'feet hanging' posture, in which additional peak was visible around 1 to 2 Hz (Figure 2.31). The findings of this study resemble the findings of Fairley and Griffin (1990), in which the backrest restrained the body from pitching and reduced the body resonance to only one peak. This study was also the first study to measure forces at the backrest during fore-and-aft excitation. The fore-and-aft apparent mass at the backrest showed three peaks: less than 2 Hz, between 3 and 5 Hz, and a broad third peak in the frequency range 4 to 7 Hz (Figure 2.32). The authors reported that the first and the third peaks were clearer at low vibration magnitudes than at high vibration magnitudes. The vertical forces at the backrest was low and that 'cross-axis' vertical apparent mass at the backrest of one subject showed a

principal resonance between 5 and 7 Hz, depending on the vibration magnitude (Figure 2.33a). However, lateral forces at the backrest were relatively low (Figure 2.33b).

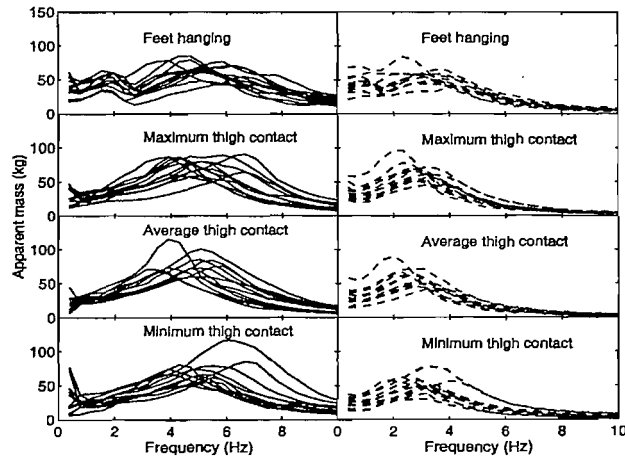


**Figure 2.31:** Fore-and-aft apparent mass on the seat for four sitting postures with a vertical backrest at  $0.125 \text{ ms}^{-2}$  (left column) and  $1.25 \text{ ms}^{-2}$  (right column). Data taken from Nawayseh and Griffin (2005a).

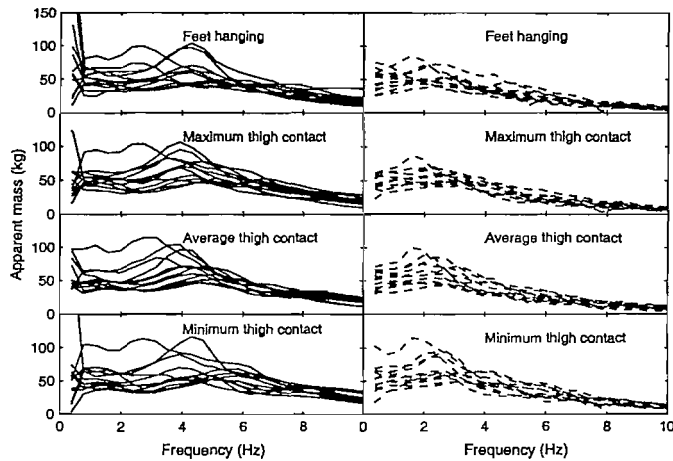


**Figure 2.32:** Fore-and-aft apparent masses of the body at the backrest at four sitting postures at  $0.125 \text{ ms}^{-2}$  (left column) and  $1.25 \text{ ms}^{-2}$  (right column). Data taken from Nawayseh and Griffin (2005a).

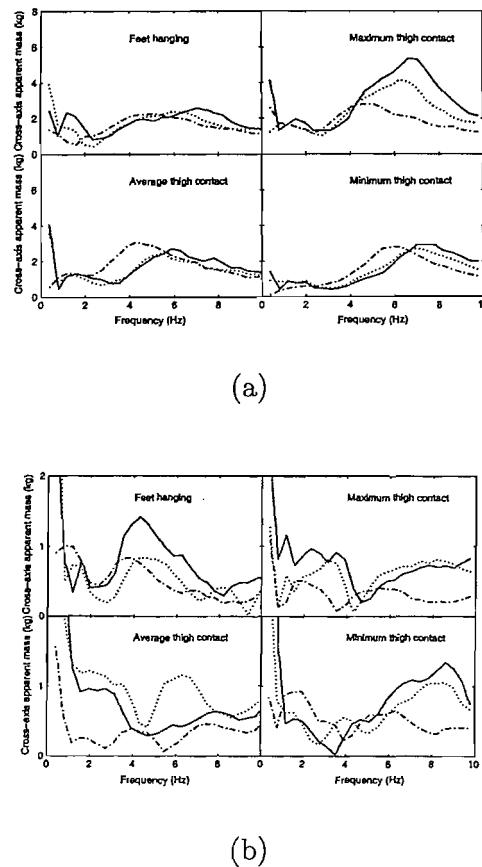


**Figure 2.33:** Apparent mass of the back of one subject at four sitting postures at  $0.125 \text{ ms}^{-2}$  (left column) and  $1.25 \text{ ms}^{-2}$  (right column) in the (a) 'cross-axis' vertical and (b) 'cross-axis' lateral directions. Data taken from Nawayseh and Griffin (2005a).

## 2.2.5 Factors affecting body impedance of seated persons exposed to whole-body horizontal vibration (fore-and-aft or lateral)

There is little knowledge of the factors that affect the biodynamic responses of the body during fore-and-aft or lateral excitation.

### 2.2.5.1 Effect of posture and backrest

When the feet of the subjects were supported on a footrest, and moved together with the seat (with no backrest) during either fore-and-aft, or lateral vibration, the first resonance frequency of the apparent mass of the body was exhibited at frequency around 1 Hz

(Fairley and Griffin, 1990 and Nawayseh and Griffin, 2005b). However, when the feet were rested on a stationary footrest, while the subjects were exposed to either fore-and-aft, or lateral vibration, the frequency of the first peak was observed at higher frequency – around 3 Hz (Holmlund and Lundström, 1998 and Mansfield and Lundström, 1999). The relative movement between feet and the seat might have some influences on the responses of the body in either direction. It is reasonable to expect different forces on the seat with a moving footrest and a stationary footrest due to different phases between the seat and the feet.

The effect of backrest on the apparent mass of the body in fore-and-aft and lateral directions was studied by Fairley and Griffin (1990). The authors found that the forces on the seat in the fore-and-aft and lateral directions were increased at frequencies above 0.8 Hz – more pronounced in the fore-and-aft direction (Figure 2.34).

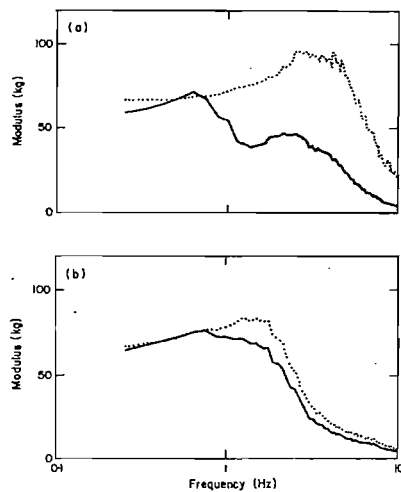
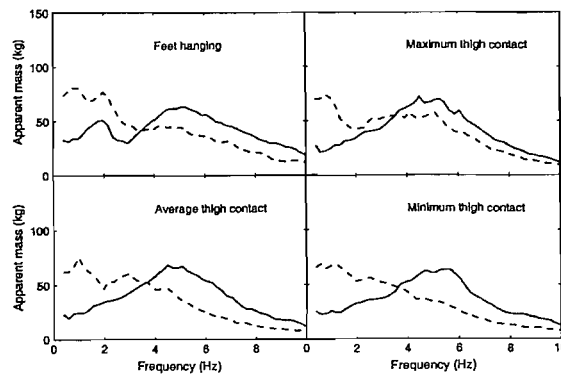
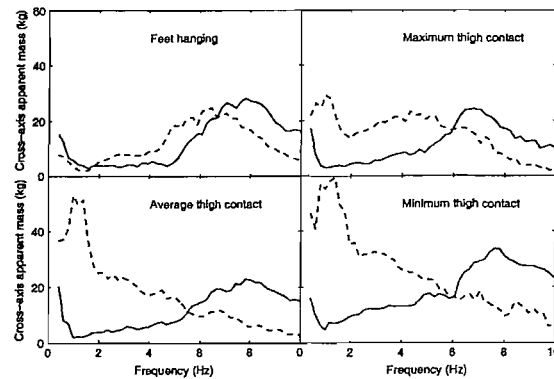


**Figure 2.34:** Effect of backrest on the apparent mass of the body. (dotted) - no backrest; (solid) - with backrest. Data taken from Fairley and Griffin (1990).

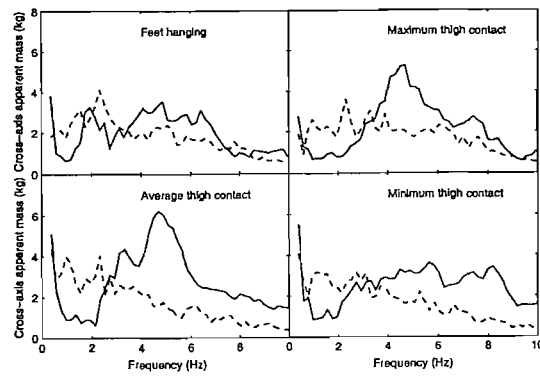
Similar findings were also observed by Nawayseh and Griffin (2005a): the fore-and-aft forces on the seat were at frequencies higher than 4 Hz (Figure 2.35a). In addition, the authors also reported that with a vertical backrest, the 'cross-axis' vertical and lateral forces on the seat were increased at frequencies higher than 6 and 3 Hz, respectively (Figures 2.35b to 2.35c).



(a)



(b)



(c)

**Figure 2.35:** Effect of backrest on the (a) fore-and-aft apparent mass of the body, (b) 'cross-axis' vertical apparent mass of the body and (c) 'cross-axis' lateral apparent mass of the body, during fore-and-aft excitation. Data taken from Nawayseh and Griffin (2005a).

In both studies (Fairley and Griffin, 1990 and Nawayseh and Griffin, 2005a), the backrest reduced the mode of the body from two modes in both directions to only one mode. The later study also showed that when the feet were not supported, two peaks were evident: between 1 and 2 Hz and in the frequency range 2 to 6 Hz (depending on the subject and vibration magnitude), while when the feet was supported on a moving footrest, only one resonance was exhibited.

### 2.2.5.2 Effect of vibration magnitude

Fairley and Griffin (1990) investigated the non-linear response of seated persons in both the fore-and-aft and lateral directions. Eight subjects were exposed to either fore-and-aft or lateral vibration in the frequency range 0.25 to 20 Hz with three magnitudes (0.5, 1.0 and  $2.0 \text{ ms}^{-2}$  r.m.s) and with no backrest. There appeared to be no effect of the vibration magnitude on the first resonance frequency of the apparent mass of the body in either direction, but the second resonance in both directions decreased with increasing vibration magnitude. The changes appeared to be of the order of 1 or 2 Hz (Figures 2.36). Similarly, Holmlund and Lundström (1998) and Mansfield and Lundström (1999a) also observed the non-linear response of seated persons to vibration magnitude in the fore-and-aft and lateral directions – the principal resonance frequency in either fore-and-aft or lateral direction decreased with increasing vibration magnitude.

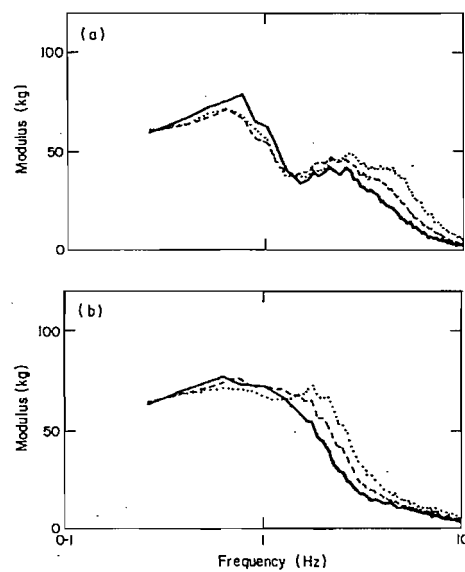


**Figure 2.36:** Effect of vibration magnitude on the apparent mass of the body. Top graph: fore-and-aft direction; bottom graph: lateral direction. (dotted) –  $0.5 \text{ ms}^{-2}$  r.m.s.; (dashed) –  $1.0 \text{ ms}^{-2}$  r.m.s.; (solid) –  $2.0 \text{ ms}^{-2}$  r.m.s.. Data taken from Fairley and Griffin (1990).

Nawayseh and Griffin (2005a and 2005b) also studied the non-linearity of the body in the vertical, fore-and-aft and lateral directions during fore-and-aft excitation. Without a backrest, the fore-and-aft apparent mass of the body was non-linear with vibration magnitude at frequencies higher than 6 Hz (Nawayseh and Griffin, 2005b). With a backrest, the resonance frequency and apparent mass at resonance reduced significantly with increasing vibration magnitude (Nawayseh and Griffin, 2005a). The 'cross -axis' vertical and lateral apparent masses of the body (with or without backrest) also tended to decrease with increasing vibration magnitude (Figures 2.37a to 2.37c). In addition, the earlier study (i.e. Nawayseh and Griffin, 2005a) also reported non-linearity in the apparent mass of the body at the backrest in all three directions. With a change in vibration magnitude, there were significant differences in the resonance frequency of the fore-and-aft apparent mass at the backrest (Figures 2.38a). The resonance frequency and, generally, the 'cross-axis' vertical apparent mass at the backrest also decreased with increasing vibration magnitude (Figures 2.38b). Although the lateral forces at the back were relatively low, compared to vertical forces, the non-linear trend was also observed – the 'cross-axis' lateral apparent mass at the backrest tended to decrease with increasing vibration magnitude (Figures 2.38c).

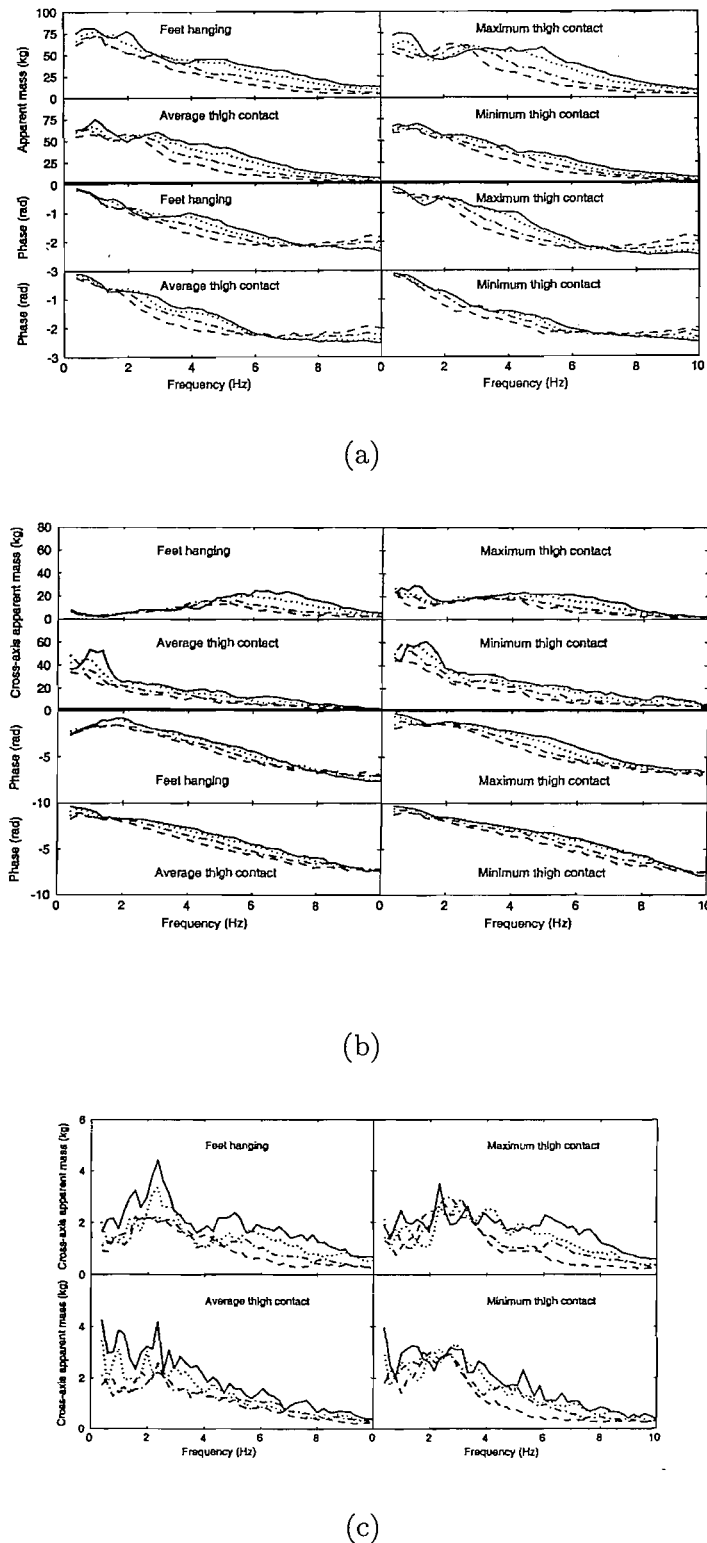


**Figure 2.37:** Effect of vibration magnitude on the (a) fore-and-aft apparent mass , (b) 'cross-axis' vertical apparent mass of the body and (c) 'cross-axis' lateral apparent mass of the body, on the seat during fore-and-aft excitation (with backrest). Data taken from Nawayseh and Griffin (2005a).

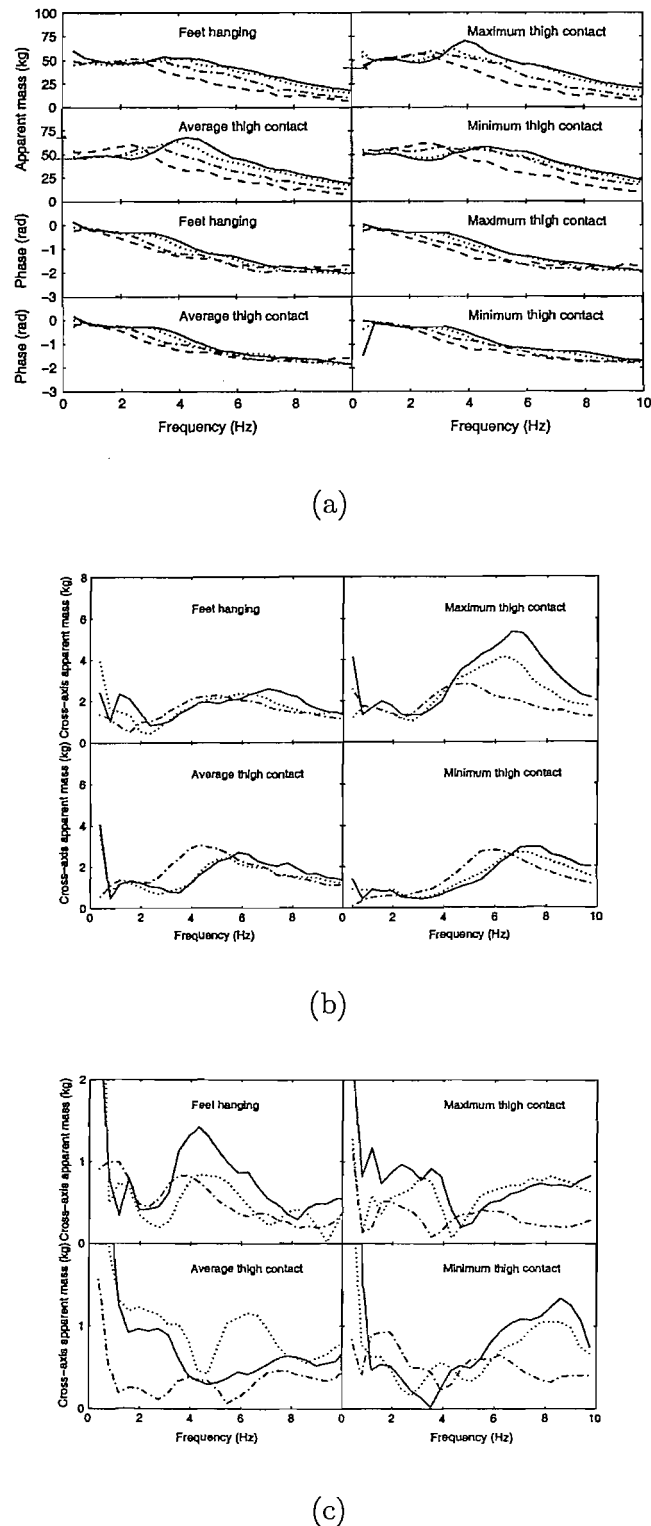


**Figure 2.38:** Effect of vibration magnitude on the (a) fore-and-aft apparent mass, (b) 'cross-axis' vertical apparent mass of the body and (c) 'cross-axis' lateral apparent mass of the body, at the backrest during fore-and-aft excitation. Data taken from Nawayseh and Griffin (2005a).

### 2.2.6 Conclusions

Studies have shown that the body has three vertical resonances during vertical excitation: a major resonance was found around 5 Hz while the second and third resonances at approximately 10 Hz and 50 Hz. Equivalent responses in the fore-and-aft and lateral directions depended on the feet and upper body support. Without a backrest and with feet supported and moved together with the seat, the body showed three resonances in the fore-and-aft direction (around 1 Hz, between 1 and 3 Hz, and between 3 and 5 Hz) and two resonances in the lateral direction (around 0.7 Hz and 2 Hz), while when the feet were supported on a stationary footrest, the frequency of the resonances were slightly higher (between 3 and 5 Hz in the fore-and-aft direction and around 2 Hz and 6 Hz in the lateral direction). When the upper body leaned against a backrest, there appeared to be only one principal resonance frequency of the body in either direction (3 Hz in the fore-and-aft direction and 1.5 Hz in the lateral direction).

During either vertical or fore-and-aft excitation, recent studies have shown that the body gives rise to 'cross-axis' response on the seat and at the backrest. During vertical excitation, there was a resonance of the 'cross-axis' fore-and-aft apparent mass of the body around 5 Hz on both the seat and at the backrest. Likewise, during fore-and-aft excitation, the 'cross-axis' vertical apparent mass of the body on the seat showed three resonances without a backrest, but only one resonance was evident with a backrest. The 'cross-axis' vertical apparent mass of the body at the backrest showed resonance around 6 Hz. In either direction of vibration excitation, the 'cross-axis' lateral apparent masses on both the seat and at the backrest were relatively low.

The apparent mass of the seated persons during either vertical or fore-and-aft excitation was found to be non-linear with vibration magnitude: the principal resonance frequency of the body decreased with increasing vibration magnitude. The 'cross-axis' responses of the body, either on the seat, or at the backrest, during either vertical, or fore-and-aft vibration was also non-linear - the magnitude of the 'cross-axis' responses reduced with increasing vibration magnitude.

Various factors have been found to affect the vertical apparent mass of the body during vertical excitation. However, further study is needed in the horizontal directions. The presence of a vertical backrest has been found to greatly influence the biodynamic responses on of the body on the seat during either vertical or fore-and-aft excitation.

## 2.3 Seating dynamics

### 2.3.1 Introduction

Seats play an important role in vehicles. For instance, they give support to the body when using a vehicle and may be needed to attenuate high vibration magnitudes in the case of agricultural vehicles. A seated person in a car will be exposed to different types and directions of vibrations. The vibration can be either translational or rotational or both and it can be in vertical or horizontal directions. It is an important aspect to consider the seat dynamics in order to understand the responses of seated subjects exposed to vibration in vehicle.

### 2.3.2 Methods of evaluating seating dynamics

A common method that has been widely used to evaluate the seating dynamics is transmissibility measurements. Seat transmissibility can be defined as the amount of vibration transmitted through the seat to the body. This amount can be described in the form of a transfer function between the input and the output accelerations of the system (see Section 3.4.1 for the methods of calculation). For instance, the vertical transmissibility of a seat is the ratio of the acceleration at the buttock-seat cushion interface (normally beneath the ischial tuberosities) to the acceleration at the seat base. For backrest transmissibility, a similar method applies (in this case, the human back and the backrest can be regarded as the output point).

The transmissibility of seats can be either measured in vehicles (for field tests), or in laboratory measurements. In either case, suitable transducers (i.e. accelerometers) can be mounted at the base of a seat, or on the floor of a vibrator platform so as to measure the input accelerations, and at the human-seat interface (e.g. beneath ischial tuberosities, or between the human back and the backrest cushion).

### 2.3.3 Measurement devices for vibration on seats

Measuring seat transmissibility requires accelerometers to be placed close to the interface point between the body and the seat. The transducers must offer little resistance to the movement of the body-seat system as moving together with the interface point.

In early studies of seat transmissibility, there were few methods employed by the researchers to measure the acceleration at the seat-person interface point. For example, Radke (1956) used accelerometers fixed to a belt worn by the subjects to measure the vertical transmissibility of a cushion seat. However, this method has a potential of giving an inaccurate results, as the vibration was not measured at the point of interface between the seat and the buttocks. Matthews (1964) measured the vertical seat transmissibility of a tractor seat during field tests in which the accelerometer was attached by a leather harness to the subject's back. This method is also prone to give inaccurate reading of the acceleration at the seat-person interface as the acceleration may be affected by pitching movement of the upper-body. In a later study, Matthews (1966) used a different approach to measure the seat transmissibility in both field and the laboratory studies so as to assess the ride quality of an agricultural tractor seat. The acceleration on the seat-person interface was monitored by attaching the accelerometer to a wooden board approximately 130 in<sup>2</sup> (equivalent to 0.0834 m<sup>2</sup>) area, which was placed on the cushion or seat pan beneath the subject. The author suggested that the area of the board was chosen to be similar to that area of cushion, which is normally depressed by the operator, although he argued that this was only approximated to the natural conditions, since the board was both rigid and flat. In a different study, Miwa and Yonekawa (1971) used a 'box-type' accelerometer mounting to measure the acceleration between subject and the seat cushion. In that study, three types of box with different measurements and weight were examined: i) 230 by 180 by 45 mm<sup>3</sup> weighted 1.3 kg, ii) 280 by 240 by 45 mm<sup>3</sup> weighted 2.2 kg and iii) 300 by 300 by 30 mm<sup>3</sup> weighted 1.3 kg. The authors found that box iii) can be used to measure the seat transmissibility, in particular, in the field tests in the frequency range 2 to 100 Hz. However, in both studies (i.e. Matthews, 1966, and Miwa and Yonekawa, 1971), either the flat and rigid board, or the 'box type' accelerometer, did not 'allow' the natural compression of the buttock on the seat cushion and that pressure distribution is not accurate. In addition, the size and weight of the later accelerometer mountings were big and heavy.

Recognising the importance of having a more suitable device that can be used to measure the acceleration at the seat-person interface point without altering the measurements, the Society of Automobile Engineers (SAE) defined a mount to measure the acceleration at the point of interface (SAE, 1974). The recommended device is a 'semi-rigid' interface, known as an SAE pad, or SIT-pad (SIT – Seat Interface Transducer). The primary requirement for the pad has been specified to '*provide a suitable mounting for the accelerometers, not disturb the operator comfort, and not significantly distort the buttock-cushion load distribution*'. The pad is a circular pad with thin edges but thickens towards the centre to provide a central cavity for miniature accelerometers. The pad is recommended to be

placed on the seat so that the accelerometer is midway between the ischial tuberosities. Figure 2.39 shows the device with the appropriate dimensions.

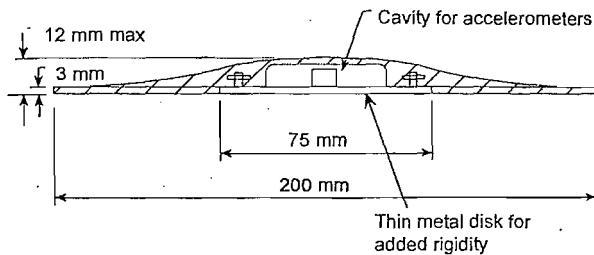


Figure 2.39: SAE pad, or SIT-pad. From the Society of Automotive Engineers (1974).

Whitham and Griffin (1977) investigated the difference between three accelerometer-mounting methods to measure the vibration on foam. The first mounting was a simple aluminium bar (290 by 45 by 20 mm), which contained an accelerometer oriented to respond to vertical vibration. The second mounting was a SAE pad, which was similar to that in SAE (1974). The third mounting was a 'Seat Interface for Transducers indicating Body Acceleration Received' or SIT-BAR (Figure 2.40). The SIT-BAR had a hard and flat upper surface to provide a rigid contact with the ischial tuberosities while the lower surface imitate the shape of the portion of the human buttocks normally in contact with a seat. The authors found that the design of the SIT-BAR meets the principle requirements for measuring vibration on soft seat and gave good agreements with the results obtained using SAE-pad in the range of 2 to 32 Hz.

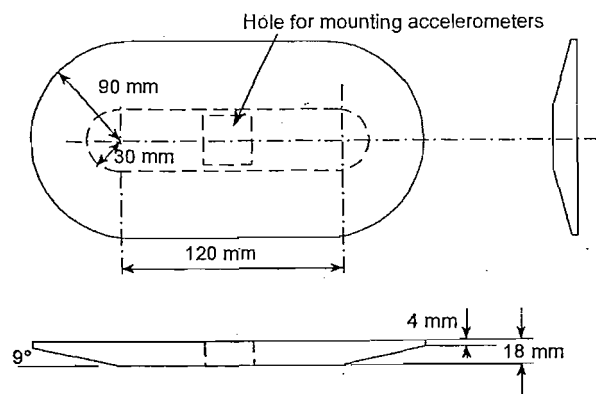


Figure 2.40: SIT-BAR. From Whitham and Griffin (1977).

When measuring acceleration on a backrest, the principal requirement of placing the accelerometer near to the interface point sill applies. As specified in the International Standard ISO 10326-1 (1992), such that *if measurements are made on the backrest, the accelerometers shall be (horizontally) located in the vertical longitudinal plane through the center-line of the seat*. The interface device is, generally, sandwiched against the backrest and the back.

### **2.3.4 Transmissibility of seats (conventional and suspension) in the vertical direction**

The vertical transmissibilities of seats have been extensively studied in both the field and the laboratory. Radke (1956) conducted both field and laboratory measurements and found that the vertical transmissibility of cushion seats showed a resonance around 3 Hz, while a suspension seat showed a peak around 1 Hz. However, the transmissibilities were measured from the floor to around the waist of the subjects (since the accelerometer were attached at the subject's belt), and possibly this may have included the pitching motion of the body. The resonance frequencies of vertical transmissibility of the tractor seats were found around 3.5 Hz (with rigid seat-pan and foam cushion), but the peak frequency reduced around 2.5 Hz for suspension seats (Matthews, 1966). In this study the accelerometer was attached on a flat wooden board (approximately 130 in<sup>2</sup>) and placed between the seat cushion and the subject. Leatherwood (1975) studied the dynamic characteristics of three typical transport vehicle seats: i) first class aircraft seat, ii) aircraft tourist class seats and iii) city rapid-transit bus seats. All seat types contained foam cushion. The results showed that between 1 to 9 Hz, the bus seats showed the least transmissibility. The resonance frequencies of all three seats were found around 4 Hz. In this study, the accelerometer at the seat-person interface (i.e. between the buttock and the seat cushion) was installed inside the foam cushion and around the middle part of the seat cushion. The accelerometer was protected with metal box, in which the top box was a disk plate with 0.1524 cm in diameter. Although there was no systematic technique of positioning the accelerometer between the buttock and the seat cushion in all three studies, the results showed agreement in the resonance frequency of the transmissibility of conventional seats.

Whitham and Griffin (1977) measured the transmissibility of a 100 mm foam cushion with three types of accelerometer mountings; (i) aluminium bar (290 by 45 by 20 mm), (ii) SAE pad (as suggested in the SAE, 1974) and (iii) SIT-PAD. The authors developed the later mount such that: i) it met the requirements as suggested in the SAE (1974), and that the accelerometer can be mounted near the center of the disc, and beneath the ischial tuberosities, and ii) the mount can provide a firm platform in which rotational

accelerometer can be mounted. The results showed the cushion transmissibility showed resonance at approximately 3 Hz for the aluminium bar and at 5 Hz for both the SAE pad and the SIT-BAR (Figure 2.41). The authors concluded that the design of the SIT-BAR could be used for measuring vibration on soft seats. A resonance around 4 to 5 Hz of conventional seats was also found by Corbridge *et al.* (1989), Fairley and Griffin (1989), Ebe and Griffin (1995), Lewis and Griffin (1996), Mansfield and Griffin (1996) and Wei and Griffin (1998c).

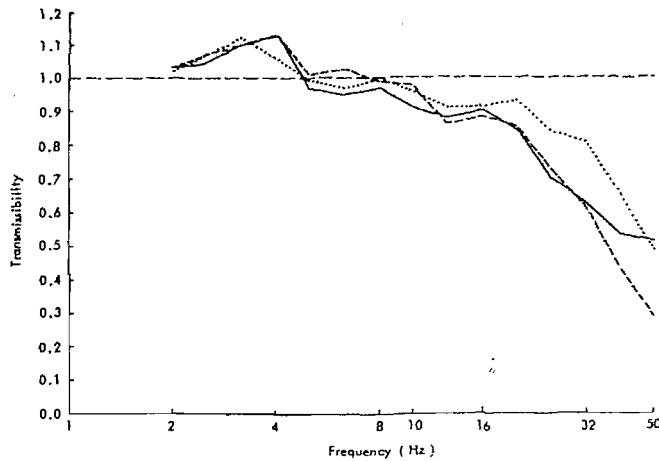


**Figure 2.41:** Transmissibility of foam measured with one subject using an aluminium bar (dotted line), the SIT-BAR (dashed line) and the SAE pad (solid line). Data taken from Whitham and Griffin (1977).

A study by Lewis and Griffin (1996) showed that the vertical transmissibilities from the floor to a fixed backrest showed a principal resonance around 4 Hz. In that study, the authors also measured the vertical backrest transmissibility with a moving backrest. As it was suggested that low-back pain can be caused by the strain imposed on the lumbar spine from differential motion occurring between the seat and the back. By allowing the backrest to move vertically (i.e. not attached to the seat-pan), the lumbar strain might be reduced so as to allow the motion of the back and reduced the imposed strain. With the moving backrest, although the vertical transmissibility to the lumbar 2 was reduced between 6 and 40 Hz compared to the fixed backrest, the transmissibility at resonance with the moving backrest was much higher than the fixed backrest (Figure 2.42). The vertical transmissibility to the moving backrest, however, also showed a resonance around 4 Hz. Houghton (2003) also measured the vertical transmissibility to the seat and backrest during vertical excitation. The author found that the vertical transmissibility to the seat and backrest, both showed a resonance around 4 Hz. In that study, the 'cross-axis' fore-and-aft transmissibility to the seat and to the backrest was also measured (by comparing

the fore-and-aft acceleration measured on the seat and at the backrest with the applied vertical acceleration at the floor). Several resonances were observed in the 'fore-and-aft' transmissibility of the seat (at 4 to 5 Hz, 17 to 18 Hz and 34 to 39 Hz), while the 'fore-and-aft' transmissibility of the seat showed a resonance around 5 Hz.

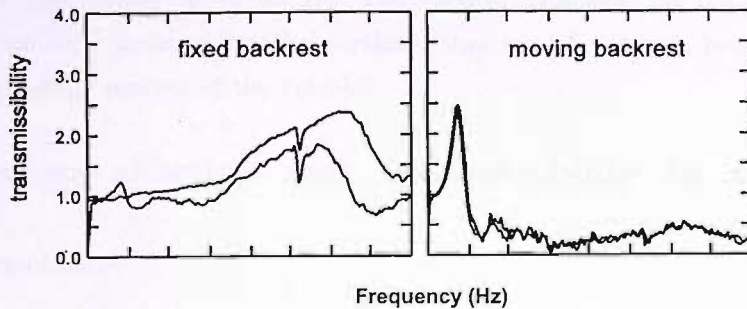


Figure 2.42: Transmissibility from the seat to the back (at lumbar 2). Data from Lewis and Griffin (1996).

A suspension mechanism, which can be mounted below a seat cushion can attenuate the vibration to the body through the seat and reduce the resonance frequency of the seat transmissibility. This can be achieved by including a low stiffness spring in the additional suspension mechanism. Figure 2.43 shows an example of a comparison between the transmissibility of a conventional seat and a suspension seat (Griffin, 1990). It can be seen that with the suspension mechanism, the transmissibility was greatly reduced and the resonance frequency reduced from around 4 Hz with conventional seat to around 2 Hz with the suspension seat.

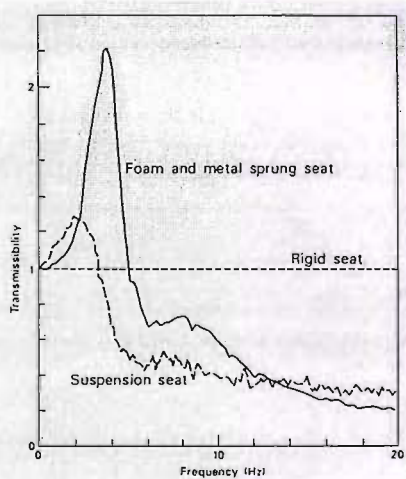


Figure 2.43: Comparison of the transmissibilities of a rigid seat, foam and metal sprung car seat and a truck suspension seat. Data from Griffin (1990).

Almost all the previous studies reported on the vertical seat transmissibility, or the vertical floor-to-backrest transmissibility was conducted in laboratory measurements and the vibration was confined only to vertical excitation. A recent study by Qiu and Griffin (2003) showed that in a field test, the power spectral density of the time history acceleration measured on the seat and at the backrest in the vertical and fore-and-aft directions were distributed up to 60 Hz. The vertical vibration on the seat, or at the backrest was not only induced by the vertical vibration of the car, but also it can be caused by the pitching motion of the vehicle.

### 2.3.5 Factors affecting seat transmissibility in the vertical direction

Knowledge of the factors that may affect seat transmissibility is useful when designing a seat, or when trying to identify the cause of discomfort, which may come from vibration transmitted to a seat. The seat transmissibility may be changed if, for instance, the properties of the seat are changed in order to improve the dynamic performance of the seat. It is hence important to study and observe the factors that can affect the seat transmissibility.

#### 2.3.5.1 *Effect of sitting posture*

Radke (1956) studied the effect of driver's arm and leg effort on the seat transmissibility with both conventional and suspension seats. For a conventional seat, the transmissibility was greatly reduced between 1 to 6 Hz when the subjects pushed against the footrest and the steering-wheel, compared to when subjects adopted normal sitting posture (i.e. without applying additional forces on the steering-wheel, or footrest). However, the resonance frequency of the seat transmissibility remained unchanged. For the suspension seat, the authors found that when subjects pushed against a footrest and a steering-wheel, the transmissibility was reduced between 1 and 3 Hz, but increased at frequencies higher than 3 Hz compared to normal sitting posture. The author also found that when pushing against the footrest and the steering-wheel, the resonance frequency of the vertical transmissibility of a suspension seat was increased. It seems that when pushing the footrest and the steering wheel, possibly, the body stiffness and the dynamic stiffness of the suspension seat increase, hence the resonance frequency increased.

The effect of the upper and lower body posture on the seat transmissibility of a seat cushion was investigated by Corbridge *et al.* (1989). The effect of lower body posture was investigated when thirty subjects were asked to sit in a 'normal' sitting posture (hands on

laps and seated against the backrest) and adopted three leg positions: i) feet flat on the floor in line with the front of the seat cushion, ii) feet flat on the floor 200 mm from the front of the seat and iii) feet resting on heels, legs fully extended. The effect of the upper body posture was investigated when subjects sat with their feet flat on the floor, approximately 200 mm from the front of the seat cushion, while the upper body adopted: i) 'normal' sitting posture, ii) 'arms on armrests', in which it was similar with the 'normal' posture, except that the subjects were required to rest their lower arms and hands on the armrests, which were in a fixed position on either side of the seat, and iii) 'back off' posture, in which subjects leaned forward so that the back was not in contact with the backrest, and the hands rested on their laps. The authors found that changes in the position of the upper body had a more pronounced effect on the seat transmissibility than changes in the leg position. Extending the legs further from the seat cushion had little influence on the seat transmissibility – the transmissibility increased slightly between 1 and 4 Hz, and a slight decrease in the transmissibility between 5 and 15 Hz and between 22 and 25 Hz. However, there was a significant effect of the upper body posture on the seat transmissibility. The resonance frequency of the seat transmissibility in 'back off' posture was lower than 'normal' and 'arms on armrests', and less vibration was transmitted between 4 and 8 Hz (Figure 2.44). The 'arms on armrests' produced the highest resonance frequency and transmitted more vibration through the seat between 4 and 8 Hz. The 'normal' sitting posture had the highest transmissibility at resonance than the other two upper body postures.

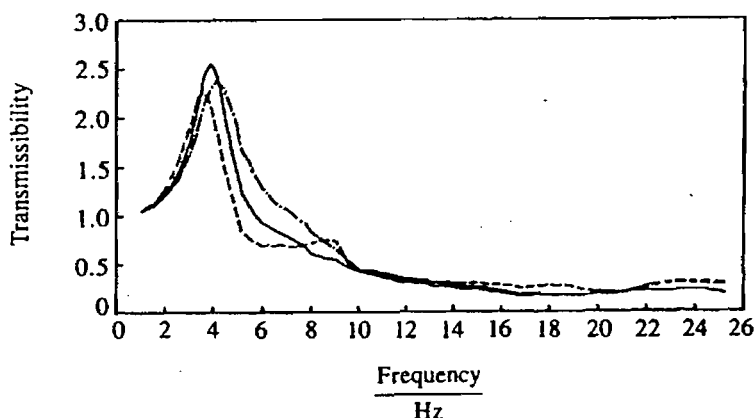
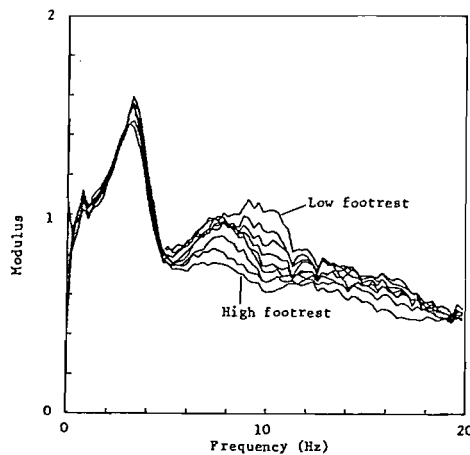


Figure 2.44: Effect of the upper body posture: (solid) 'normal', (dashed-dot) 'arms on armrests' and (dashed) 'back off' on the seat transmissibility. Data from Corbridge *et al.* (1989).

### 2.3.5.2 *Effect of footrest*

Fairley (1986) investigated the effect of the footrest height on the seat transmissibility using one subject. Eight heights of footrest positions were studied. The highest position was described as giving minimum contact between the thighs and the seat. The footrest was then lowered by a total of 0.32 m in 0.04 m steps. The seat transmissibility showed a resonance around 3.5 Hz, and that changes in the footrest height had minimal influence on the resonance frequency and transmissibility at resonance (Figure 2.45). At frequencies higher than 4 Hz, the transmissibility tended to decrease with increasing height of the footrest.



**Figure 2.45:** Effect of the footrest height on the seat transmissibility. Data from Fairley (1986).

### 2.3.5.3 *Effect of backrest, backrest inclination and seat pan inclination*

The vertical seat transmissibility of four subjects seated on a cushion seat with no backrest showed a resonance around 4 Hz (Fairley, 1986). With a backrest (in which subjects made full contact with the backrest), the resonance frequency increased slightly compared to when no backrest was used. The transmissibility was also greater than with no backrest at frequencies higher than the resonance frequency up to 20 Hz. However, when only the lumbar was supported, the resonance frequency was higher than with the no backrest condition, but lower than when the back was in full contact with the backrest. At

frequencies higher than around 8 Hz, the transmissibility of the seat was highest with only the lumbar was supported.

Cogger (1979) reported that the backrest inclination showed little effect on the seat transmissibility of a foam seat cushion. With twelve subjects involved in the study, the results showed that as the backrest inclination was increased from 16° to 32°, there was no change in the resonance frequency of the seat transmissibility and there was only slight increased in the transmissibility at resonance. Similarly, Fairley (1986) also found that with increasing backrest inclination from a vertical backrest (i.e. 90°) to 150° of backrest inclination (measured from horizontal), the effect was small on the resonance frequency of the seat transmissibility (Figure 2.46). Between 5 and 10 Hz, the transmissible of the seat increased with increasing backrest inclination. Corbridge *et al.* (1989) found a similar trend for the effect of the backrest angle: with increasing backrest inclination from 95° to 115° (both measured from horizontal), no change in the resonance frequency of the seat transmissibility was reported and only slight increased in the transmissibility at resonance was observed. The transmissibility between 6 and 9 Hz was increased with increasing backrest inclination, but the magnitude of this effect was small. The small influence of the backrest inclination with a rigid backrest was also reported by Toward (2001).

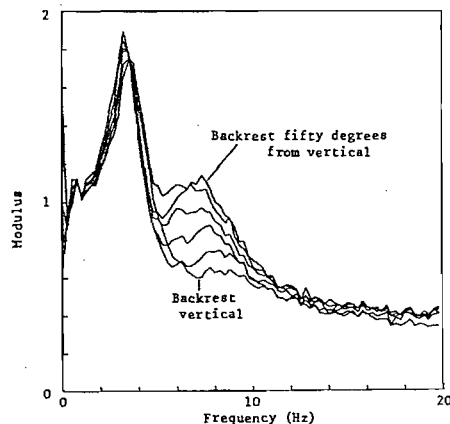


**Figure 2.46:** Effect of the backrest inclination on the seat transmissibility. Data from Fairley (1986).

Houghton (2003) also reported that increasing the backrest inclination from 90° to 120° (measured from horizontal) increased the transmissibility at resonance, and the transmissibility between 5 and 10 Hz was highest with more inclined backrest. The author, however, reported that the resonance frequency of the vertical seat transmissibility increased with increasing backrest angle, although previous studies (e.g. Cogger, 1979,

Fairley, 1986, Corbridge *et al.*, 1989 and Toward, 2001) suggested that increasing backrest inclination had a small effect on the resonance frequency of the seat transmissibility. The author suggested that the increase in the resonance frequency of the vertical seat transmissibility can be explained by the change in the distribution of mass between the seat and the backrest, with the backrest supporting more of the upper-body weight when the backrest was inclined. A study by Wei and Griffin (1999) reported that the resonance frequency of the apparent mass of the body increased with increasing backrest inclination – in part, or not, totally, due to less body mass supported on the seat surface.

Houghton (2003) also reported that with increasing backrest inclination, the small effect was reported on the resonance frequency and transmissibility at resonance of vertical vibration at floor to the vertical vibration on the backrest, and the magnitude of the transmissibility was relatively lower than that on the seat. The author also reported that considerable fore-and-aft vibration was induced by the vertical excitation of the seat. The 'fore-and-aft' transmissibilities at the seat pan and at the backrest, both showed a principal resonance around 5 Hz, and that frequency was significantly increased with increasing backrest inclination. The transmissibilities at resonance of both the 'fore-and-aft' transmissibilities of the seat and the backrest increased significantly with increasing backrest inclination (Figure 2.47a and 2.47b). Between 0.25 and 8 Hz, the 'fore-and-aft' transmissibilities at the seat pan and at the backrest increased with increasing backrest inclination.

Wei and Griffin (1998a) investigated the influence of seat cushion inclination on the seat transmissibility with five cushion inclinations ( $0^\circ$ ,  $5^\circ$ ,  $10^\circ$ ,  $15^\circ$  and  $20^\circ$ ). Twelve subjects participated in the study and all the subjects were exposed to a vibration magnitude at  $1.5 \text{ ms}^{-2}$  r.m.s. over the frequency range of 0.2 to 25 Hz. The subjects were asked to adopt upright postures, with their backs not touching the backrest. The results showed that the seat transmissibility appeared to decrease at frequencies below 6 Hz and increased above 6 Hz with increasing seat-pan inclination (Figure 2.48). However, there was small effect of the seat pan inclination on the resonance frequency of the seat transmissibility. The transmissibility at resonance was found to decrease with increasing seat pan inclination. It seems that changing in the lower body posture has small effect on the vertical seat transmissibility.

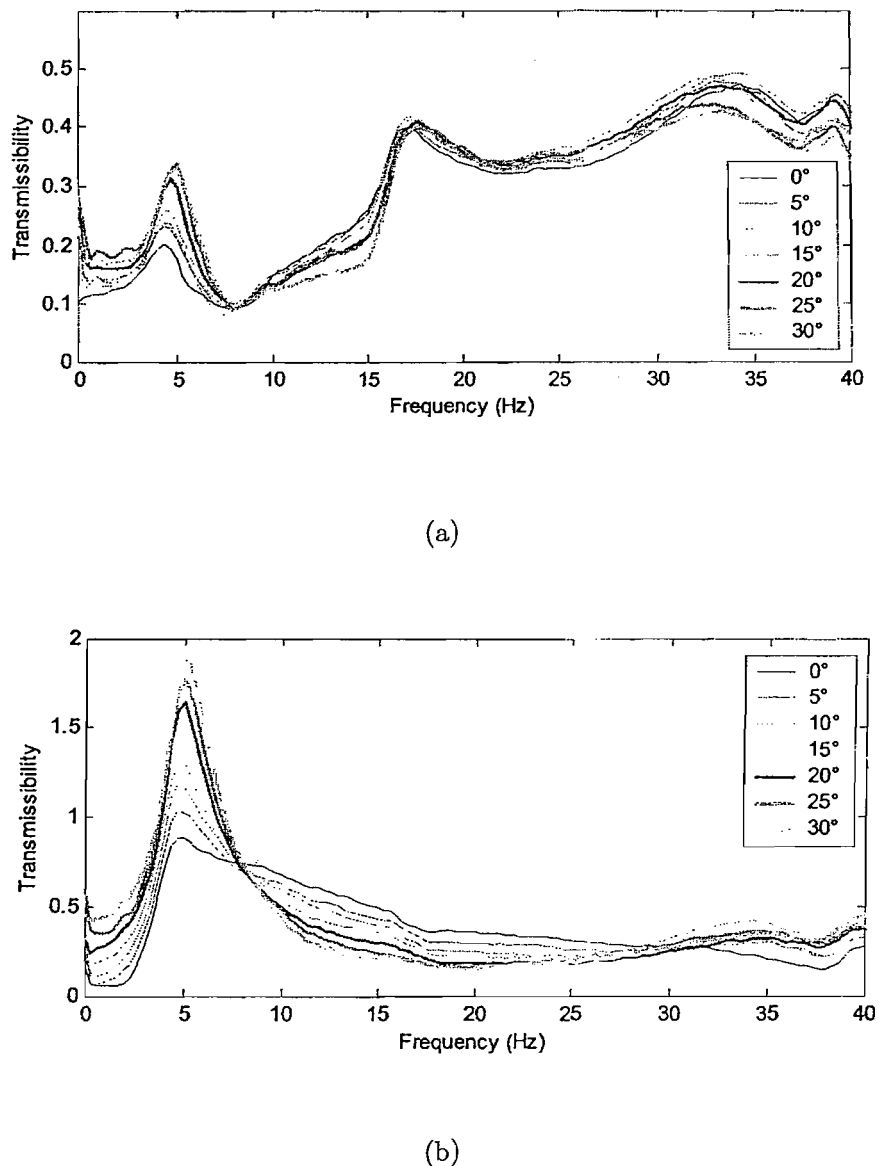
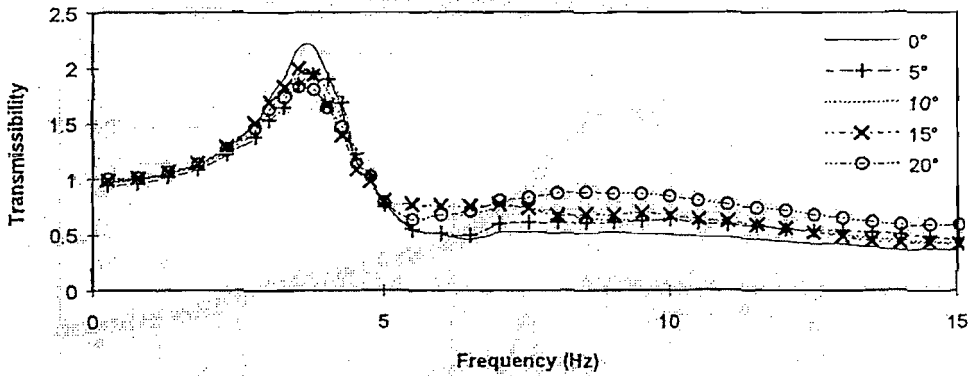


Figure 2.47: Effect of backrest inclination on 'fore-and-aft' transmissibilities at the (a) seat-pan and (b) backrest, during vertical excitation of the seat. Data taken from Houghton (2003).



**Figure 2.48:** Effect of seat-pan inclination on seat transmissibility. Data taken from Wei and Griffin (1998a).

#### 2.3.5.4 *Effect of subject characteristics*

Mathews (1967) reported that the transmissibility of a suspension seat showed better isolation for heavier subjects than that the lighter subjects. Similar findings were also documented by Stayner and Bean (1971) – the seat transmissibility decreased for heavier subjects. However, Corbridge (1981) found that subject weight had relatively little effect on the performance of the seat.

In the case of conventional seat, Fairley (1986) found that prediction of the seat transmissibility showed increased transmissibility at resonance when the mass of the person was increased (i.e. with increasing pre-load from 300 N to 900 N). The resonance frequency decreased with increasing pre-load on the seat cushion. A similar finding was also reported by Wei and Griffin (2000): with increasing pre-load of the seat cushion (greater pre-load associated with heavier subject's weight), the predicted foam transmissibility showed lower resonance frequency with heavier subject.

Corbridge (1981) studied the effect of two subjective variables, age and gender, on suspension seat performance. Two seating conditions were used. The first condition was that the suspension system of the seat was fully wound up in order to lock the mechanism. In the second condition, the seat was adjusted to the subject's weight. The subject variables were found to have relatively little effect on the performance of the seat. Richard (1996) also found that the effect of gender on the seat transmissibility of a car seat was small.

### 2.3.5.5 *Effect of different material properties*

Ebe (1993 and 1994) and Griffin (1995) conducted a series of studies to investigate the effect of: i) the composition, ii) the density and iii) the foam pad construction of polyurethane foam on transmissibility of an automotive seat. Eight subjects participated in the first two studies, while the later study involved twelve subjects. In the first study, four different types of seats with different composition were investigated. All four seat types (either foam blocks or real automotive seats) consisted of polyurethane and were described as: i) low density type, or type 'A', ii) standard type, or type 'B', iii) long durability type, or type 'C', and iv) soft feeling type, or type S. The results showed that the composition of polyurethane foam of the seat does affect the seat transmissibility by affecting the resonance frequency. The type 'A' foam attenuated more vibration at the resonance frequency than the other foams, but had the highest resonance frequency of the seat transmissibility for both the foam blocks and the real automotive seats (Figure 2.49a). In the second study, the authors found that the seat transmissibility of five different densities of a same composition (i.e. type 'C', or long durability type) did not have significant effect on the seat transmissibility (Figure 2.49b). In the later study, the authors investigated the effect of foam pad construction on the seat transmissibility. Using twelve subjects, the seat transmissibilities were measured on a bumpy road and on a motorway. The authors found that the foam pad construction had significant effect on the transmissibility at resonance for both the bumpy and motorway roads, but showed no significant effect on the resonance frequency of the seat transmissibility (Figure 2.49c).

Toward (2001) studied the effect of backrest interaction on seat cushion transmissibility. The effect of backrest bulk properties (i.e. soft, hard and rigid backrests), backrest's surface conditions (i.e. lubricated backrest, soft-foam backrest, 'stuck' to rigid backrest and no backrest) were investigated. The transmissibility from the seat base to the seat surface cushion appeared to be unaffected by the bulk properties of the seat backrest.

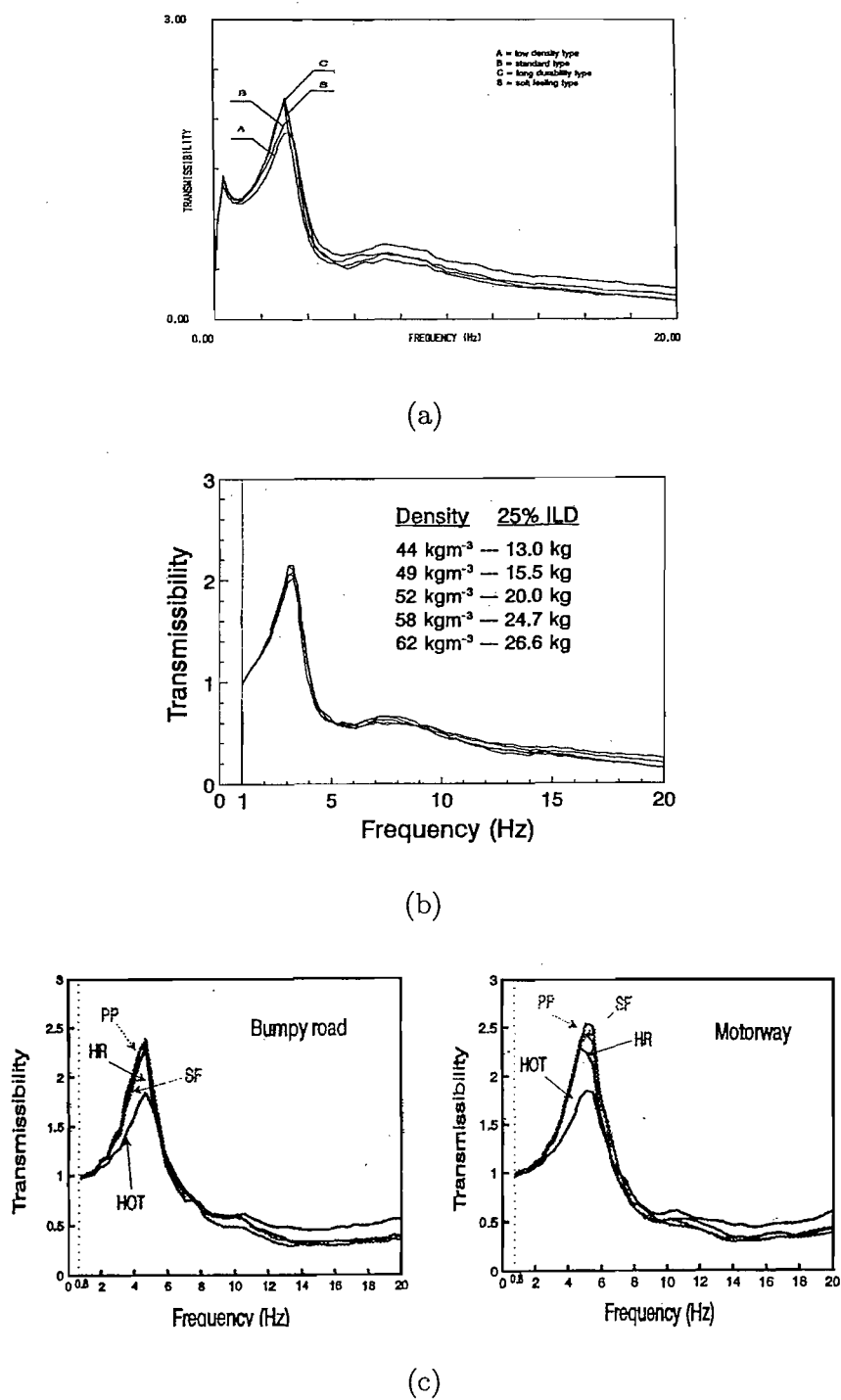


Figure 2.49: Effect of (a) composition, (b) density and (c) foam pad construction of polyurethane foam on the seat transmissibility. Data taken from Ebe (1993, 1994) and Griffin (1995).

### 2.3.5.6 *Effect of vibration magnitude*

The effect of the vibration magnitude on seat transmissibility has been studied by many researchers to give better understanding of the seat dynamics of suspension seats (e.g. Ashley, 1976 and Wu and Griffin, 1996) and conventional seats (e.g. Leatherwood, 1975; Fairley, 1983; Corbridge *et al.*, 1989; Toward, 2001 and Houghton, 2003).

Wu and Griffin (1996) demonstrated that the transmissibility of four suspension seats was affected by the vibration magnitude. The suspension seat system consisted of the seat cushion and the suspension system. Only one subject was involved in the study. The subject was exposed to five vibration magnitudes ( $0.35, 0.7, 1.05, 1.4$  and  $1.75 \text{ ms}^{-2}$  r.m.s.). The authors found that when the input magnitude increased, both the resonance frequency and transmissibility at resonance of the seat cushion decreased (Figure 2.50a). The resonance frequency of the suspension mechanism tended to decrease with increasing vibration magnitude at lower magnitudes, although at high vibration magnitudes, there appeared to be no change in resonance frequency. Transmissibility at resonance of the suspension system at higher magnitudes was higher than at low magnitudes (Figure 2.50b). Between 2 and 20 Hz, transmissibility decreased with increasing vibration magnitude of the whole seat-suspension cushion system. At lowest magnitude, the suspension mechanism showed no effect on attenuating the vibration, but the effect of suspension mechanism was more pronounced on attenuating vibration at higher magnitudes.

Fairley (1986) studied the effect of vibration input characteristics on the seat transmissibility. Only one seat was used and the seat comprised of conventional foam and spring construction without a backrest. Different subjects were used and subjects were exposed to magnitudes of  $0.25, 0.5, 1.0$  and  $2.0 \text{ ms}^{-2}$  r.m.s. in the frequency range of 0.25 to 20 Hz. The author found that the resonance frequency decreased by about 1 Hz when the magnitudes were increased from  $0.25$  to  $2.0 \text{ ms}^{-2}$  r.m.s. (Figure 2.51). The transmissibility at resonance also decreased with increasing vibration magnitude. The author suggested that the results found reflected the non-linearities in the seat, or the seated person, or both. Non-linearity response of the seat transmissibility with vibration magnitude were also reported by Corbridge *et al.* (1989), Toward (2001) and Houghton (2003).

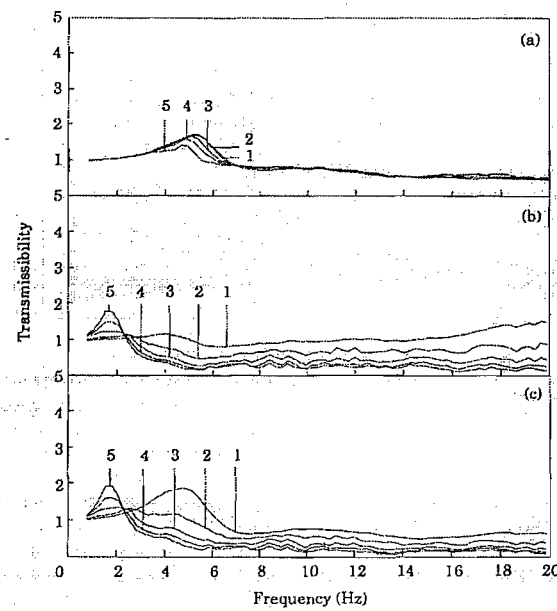


**Figure 2.50:** Transmissibilities of the seat cushion (a), the suspension (b) and the whole seat (suspension and seat cushion; c) at five vibration magnitudes with 75 kg of human subject. Five magnitudes of vibration input: 1 ( $0.35 \text{ ms}^2$  r.m.s.); 2 ( $0.70 \text{ ms}^2$  r.m.s.); 3 ( $1.05 \text{ ms}^2$  r.m.s.); 4 ( $1.40 \text{ ms}^2$  r.m.s.) and 5 ( $1.75 \text{ ms}^2$  r.m.s.). Data taken from Wu and Griffin (1996).

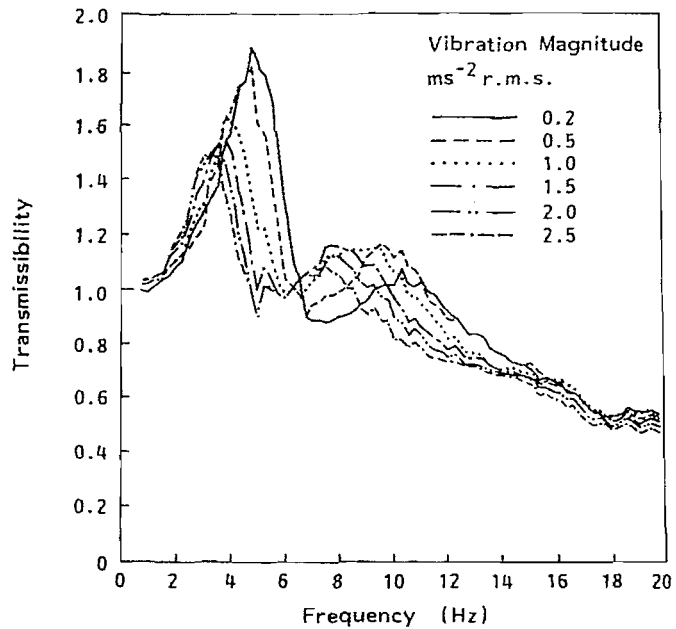


**Figure 2.51:** Mean seat transmissibility of a seat measured with eight subjects at six different vibration magnitudes. Resonance frequency decreased with increasing vibration magnitude. Data taken from Fairley (1986).

### 2.3.6 Transmissibility of seats in horizontal directions

Most of the documented studies of seat transmissibility have concerned vibration in the vertical direction. Only a few studies have been reported in the horizontal directions (i.e. fore-and-aft and lateral).

#### 2.3.6.1 *Fore-and-aft direction*

When one subject was exposed to random fore-and-aft vibration at a vibration magnitude of  $1.0 \text{ ms}^{-2}$  r.m.s. and in the frequency range of 1 to 20 Hz, the vibration transmission from the floor to the seat cushion of a suspension seat in the fore-and-aft direction showed a resonance around 3.5 Hz (Fairley and Griffin, 1984). The transmissibility, however, showed a magnitude near unity. When the seat was loaded with rigid mass, the results showed that the resonance frequency and the transmissibility at resonance were increased compared to when a human subject was used. Likewise, six suspension seats showed principal resonance of the fore-and-aft transmissibility between 1 and 2 Hz, with transmissibility at resonance of 1.5 to 2.5 (Corbridge, 1984).

With a conventional seat, Mansfield and Griffin (1996) measured the vehicle seat transmissibility in vertical, fore-and-aft and lateral directions in with anthropometric dummy and human subjects in a field study. Twelve subjects were involved in the experiment and all subjects were driven on a motorway, two minor country roads, two major urban roads and a minor urban road. The results showed that with human subjects, the fore-and-aft seat transmissibility exhibited resonances at 1 to 2 Hz and 4 to 5 Hz. The dummy data gave similar results at frequencies below 10 Hz.

Recently, Qiu and Griffin (2003) conducted field and laboratory studies to measure the fore-and-aft transmissibility from the seat base to the seat surface and to the backrest. In the car tests measurement, only two subjects were involved in the study and the car was driven over two different roads with a constant speed of 40 m.p.h. In the laboratory test, the authors used twelve subjects. All subjects were exposed to three vibration magnitudes ( $0.498$ ,  $1.015$  and  $1.951 \text{ ms}^{-2}$  r.m.s.) in the frequency range of 0.4 to 60 Hz. The laboratory test results showed that the transmissibility from the floor to the seat exhibited three resonance frequencies at about 5 Hz, 28 Hz and 48 Hz (Figure 2.52a). Similar resonance frequencies were also obtained for the transmissibility from the floor to the backrest but with better visibility and more pronounced than that on the seat (Figure 2.52b). Likewise, similar resonances were also obtained on both the seat and the backrest in the car test measurements. However, due to lower coherency and the multi-input vibrations, the peaks

were less visible compared to the laboratory study. In the field test results, the fore-and-aft transmissibility to the backrest tended to be higher than the fore-and-aft transmissibility to the seat. The author suggested that this may be due to the effect of pitch and roll motions on the seat pan were not as significant as on the backrest. In addition, the contribution of the vertical input to the seat pan is relatively small compared to the backrest due to smaller inclined angle of the seat pan. While the results from the field test may incorporate the multi-axis vibration input and that the subject may adopt the real sitting posture in vehicles, the laboratory tests provided a much better coherency for the transmissibility and the vibration input spectra can be controlled and manipulated, especially when it is not possible to measure the response in the appropriate vehicle. Figure 2.52c shows the comparison of the results of the fore-and-aft transmissibility to the seat and backrest measured in field and laboratory tests.

Qiu and Griffin (2004 and 2005) evaluated the vibration to the backrest of car seat measured in their earlier study (Qiu and Griffin, 2003) with multi-input models to determine the vibration input at the seat base can induce the fore-and-aft vibration at the backrest. The authors found that the fore-and-aft vibration and the vertical vibration, but not the lateral vibration at the four corners of the seat base contributed to the fore-and-aft vibration (Qiu and Griffin, 2004). This result was found when they investigated the transmission of vibration from the seat base to the backrest using a single-input and multi-input models. They concluded that a single-input model is not sufficient to study the transmission of vibration to the seat back in the horizontal directions. In the later study (Qiu and Griffin, 2005), the authors used the same single-input and multi-input models as in their previous study (Qiu and Griffin, 2004) and found that the pitch and roll vibration, together with the translational vibration at the seat base, made significant contributions to the fore-and-aft backrest vibration. They also found that a translational model comprising the fore-and-aft and vertical inputs, and a combined rotational and translational model consisting of pitch, vertical and fore-and-aft vibration input appeared to give equally good prediction of fore-and-aft backrest transmissibility.

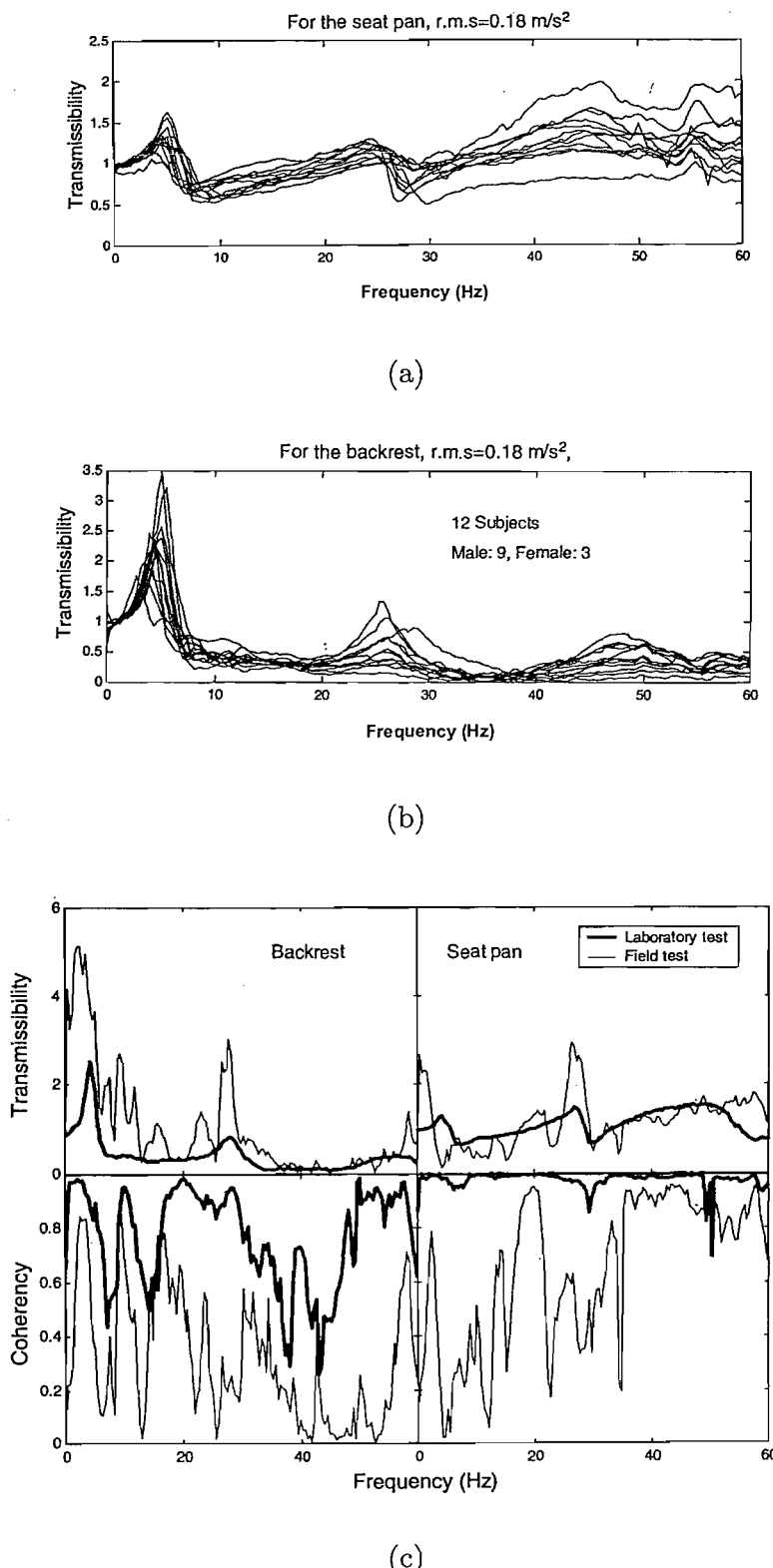


Figure 2.52: Fore-and-aft transmissibility from the floor to the: (a) seat and (b) backrest, and (c) the comparison of the transmissibility from the floor to the seat pan and to the backrest measured in field tests and laboratory measurements. Data from Qiu and Griffin (2003).

### 2.3.6.2 *Lateral direction*

Leatherwood (1975) measured the lateral vibration characteristics on two aircraft seats and one bus seat. A total of ninety-two subjects participated in the experiment. The subjects were tested in groups of four and six, depending on the seat type. Each group of subjects was exposed to sinusoidal vibration over the frequency range of 1 to 30 Hz at three vibration magnitudes (approximately at 0.49, 0.98 and 1.47  $\text{ms}^{-2}$  r.m.s.). The results showed that lateral seat transmissibility had a resonance frequency at 1 to 2 Hz. A similar finding was also reported by Smith and Kwak (1978) when the authors measured the lateral seat transmissibility of a bench-type automotive front seat. However, Mansfield and Griffin (1996) found that the lateral seat transmissibility on a road test did not show a clear resonance with twelve subjects but showed two resonances at 4 Hz and 15 Hz when an anthropometric dummy was used.

## 2.3.7 Factors affecting seat transmissibility in the horizontal direction

There is very limited knowledge of the factors that can affect the seat transmissibility in the horizontal vibration. The only factor that some researchers have investigated is the effect of vibration magnitude.

### 2.3.7.1 *Effect of vibration magnitude*

Seat transmissibility has been found to show a non-linear response with vibration magnitude in the vertical direction - the resonance frequency decreased with increasing vibration magnitude. One study showed evidence that the vibration magnitude has little effect on the resonance frequency of the fore-and-aft seat transmissibility (e.g. Corbridge, 1984). A recent study conducted by Qiu and Griffin (2003) found that the fore-and-aft seat transmissibility is non-linear with vibration magnitude - both the first and second resonance frequency decreased with increasing vibration magnitude from 0.498 to 1.951  $\text{ms}^{-2}$  r.m.s. (Figure 2.53). In the same study, a similar non-linear characteristic was found for the fore-and-aft backrest transmissibility. Although the effect of the vibration magnitude on the first peak of the fore-and-aft backrest transmissibility was marginally statistically significant, the second resonance frequency reduced significantly with increasing vibration magnitude (Figure 2.54). The transmissibility at resonances of both peaks tended to decrease with increasing vibration magnitude, but only the changes in the first peak was

found to be statistically significant. The non-linearity of the body with vibration magnitude during fore-and-aft vibration (as previously shown, e.g. Nawayseh and Griffin, 2005a) may largely caused the non-linearity in the fore-and-aft seat transmissibility.

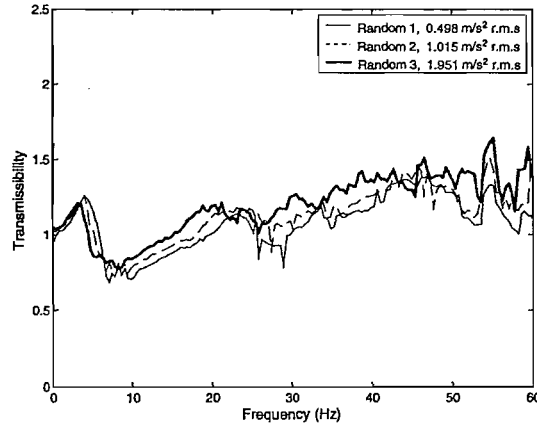
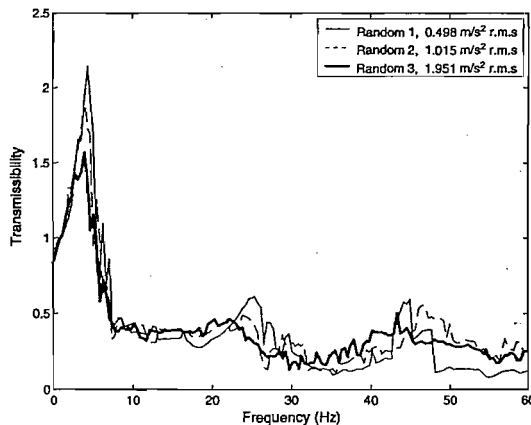


**Figure 2.53:** Effect of the vibration magnitude on the fore-and-aft transmissibility from the floor to the seat. Data taken from Qiu and Griffin (2003).



(b)

**Figure 2.54:** Effect of the vibration magnitude on the fore-and-aft transmissibility from the floor to the backrest. Data taken from Qiu and Griffin (2003).

In the case of lateral vibration, Leatherwood (1975) found that the resonance frequency did not change with increased vibration magnitudes but there was evidence that the transmissibility at resonance increased with higher magnitudes.

### 2.3.8 Conclusions

The vibration transmitted through a seat cushion, or a backrest can be measured using accelerometers (e.g. mounted in a SAE-pad, or SIT-BAR). The accelerometers are usually positioned at the principal load bearing on the seat-person interface (e.g. under beneath the ischial tuberosities). The common analysis to quantify the vibration transmitted through seats is the transmissibility method: a method of comparing the output acceleration to the input acceleration.

The transmissibility of conventional seat was found to have resonance frequency in the range of 3 to 5 Hz. In the case of a suspension seat, the resonances were found to reduce to 1 to 2 Hz. With few studies, fore-and-aft seat transmissibility has been found to have resonances at 1 to 2 Hz, 4 to 5 Hz, 28 Hz and 48 Hz, while the fore-and-aft backrest transmissibility exhibited resonances at 4 Hz, 28 Hz and 48 Hz. In the lateral direction, the seat transmissibility showed resonance at about 1 to 2 Hz with magnitude near unity.

Various factors have been found to influence the vertical seat transmissibility, such as sitting posture, variation in footrest height, backrest inclination, seat pan inclination and different material properties of the foam cushion. Studies have also shown that the vertical seat transmissibility is non-linear with vibration magnitude: the resonance frequency tends to decrease with increasing vibration magnitude. Likewise, the fore-and-aft transmissibility of seats on the cushion and at the backrest is also non-linear with vibration magnitude. No study has reported on the non-linearity of the seat transmissibility in the lateral direction.

## 2.4 Biodynamic modelling of the seated person

### 2.4.1 Introduction

'The prediction of the forces and movements in the body is only the first step towards predicting the effects of vibration on comfort, performance and health' (Griffin, 1990). A mechanical analogue with masses, dampers and spring, can therefore, act as simple steps of modeling the biodynamic responses of human to vibration. The author also states seven principal applications of biodynamic models as listed in Table 2.2.

**Table 2.2** Some application of the biodynamic models (from Griffin, 1990).

To represent understanding of the nature of body movements
To predict the influence of variables affecting biodynamic response
To provide a convenient method of summarising average experimental biodynamic data
To predict movements or forces caused by situations too numerous and varied for experimental determination
To predict movements or forces caused by situations too hazardous for an experimental determination
To provide information necessary for the optimisation of isolation systems (and other systems) coupled to the body
To determine standard impedance conditions for the vibration testing of systems used by man

The biodynamic responses of the human body exposed to whole-body vibration can be represented by means several different types of model (Griffin, 2001). The author suggested that the models can be categorized into three main groups: i) 'mechanistic models', ii) 'quantitative models' and iii) 'effect models'. The first may reflect the mechanism involved in the biodynamic responses of the human body and qualitatively described how the body moves. The degree of complexity of such models would probably be higher than with the two later types of model. The second type represents the input-output relationships without claiming to represent the mechanism involved between the input and the output. This may include prediction of one or more of the responses of the body to force or motion. The third type of model may attempt to predict the effects of motion on human health, comfort or performance. Currently, most biodynamic models fall into the second type, in which lumped-parameter models (single degree-of-freedom, or multi degree-of-freedom consisting masses, springs and dampers) were developed and fitted to the responses obtained from the experimental studies.

This section will show some examples of the biodynamic models that had been developed.

#### 2.4.2 Lumped parameter modelling in the vertical direction

##### 2.4.2.1 *Linear models*

Coermann (1962) suggested one of the earliest and simplest model of the seated-human body, consisted of one mass, one spring and one damper (Figure 2.556). The model was

intended to represent the mechanical impedance of seated subjects subjected to vertical excitation in the frequency range 1 to 20 Hz. The model, however, did not fit well with the measurements data of the mechanical impedance of the body at frequencies higher than 5 Hz for obvious reason – the mechanical impedance of the body showed two resonances, around 5 Hz and 11 Hz. In addition, the author also measured i) the seat-to-pelvis transmissibility, relative to seat excitation, ii) pelvis-to neck transmissibility, relative to seat excitation and iii) pelvis-to-neck transmissibility relative to pelvis excitation. The results of i) and ii) showed two resonances around 5 Hz and 9 Hz, while iii) only showed one resonance around 5 Hz. The author suggested that, the oversimplified one degree-of-freedom human model cannot be considered to represent the body transmissibility since the model also did not show good fit with the measured transmissibility data. Vogt *et al.* (1968) also showed that the single degree-of-freedom model was oversimplified to represent the mechanical impedance of sitting person under vertical excitation. Although a single degree-of-freedom model can be oversimplified, Payne (1969) used such a model to calculate the dynamic response index (DRI), as a measure of determining the peak stress in the vertebral column for a given force, representing the dynamic response of the body exposed to the forces of an aircraft ejector seat. The mass corresponded to the mass of the upper torso and head, supported on the spring stiffness of the spine. The model showed reasonable agreement with the experimental measurements, and the author suggested the model could be improved by inclusion of the mass corresponded to lower pelvis.

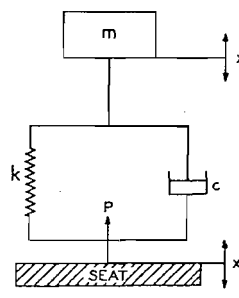


Figure 2.55: One degree-of-freedom model by Coermann (1962).

A two degree-of-freedom model consisted of masses, springs and dampers were developed so as to approximate the human body response, in which the model can be used for testing vehicle seats (Suggs *et al.*, 1969). Two uncoupled masses, suspended from the same frame formed the main construction of the model (Figure 2.56). The larger lower mass than that the upper mass represents the 'pelvis and abdomen', while the other mass represents the 'head and the chest'. The 'spinal column' was represented by the relatively rigid frame. The model parameters were identified by comparing the average response of the mechanical impedance of seated subject obtained with eleven subjects earlier by the

authors. The results showed a close fit and good agreement between the model and the subject data, with a resonance clearly shown at 4.5 Hz. When the model was used to simulate the transmissibility of seats, it showed good agreement with the transmissibility measured with a 77 kg subject. The authors concluded that model was sufficient to represent the dynamic response of seated person exposed to vertical excitation in the frequencies below 10 Hz.

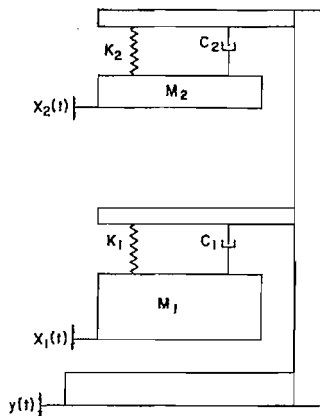


Figure 2.56: Two degree-of-freedom model by Suggs *et al.* (1969).

Payne and Band (1971) expanded a single-degree-of freedom model used to calculate the Dynamic Response Index (DRI) to a four degree-of-freedom lumped parameter model for the same purpose (Figure 2.57). The authors found necessary to include the 'pelvis mass' at the bottom of the 'spine spring' and a buttock resiliency beneath the pelvis mass. The 'pelvis mass' and 'buttock spring' represented the 'buttock mode' because the authors found that this mode has the greatest influence on impedance measurements of seated person based on previous study reported by Vogt *et al.* (1968). The main body parts that the model represented were the 'buttock and pelvis mass', the 'viscera', 'the spine and upper thorax' and the 'head and neck'. The parameters of the model were obtained from various previous experimental data. The authors conducted a parametric study, whereby the parameters of the model were varied and thus compared the driving point impedance with those measured in experimental studies (e.g. Dieckmann, 1957, Lantham, 1957, Vogt *et al.*, 1968). The results of the model showed good agreement with the experimental data at frequencies up to about 8 Hz. The author further developed the final model by using the non-linear spine and buttock spring constants based on previous experimental studies (e.g. Vogt *et al.*, 1968). Although the authors expected similar results of the model with non-linear properties and with that the experimental measurements, however, due to insufficient time at that present time, the comparison data was not presented in the paper.

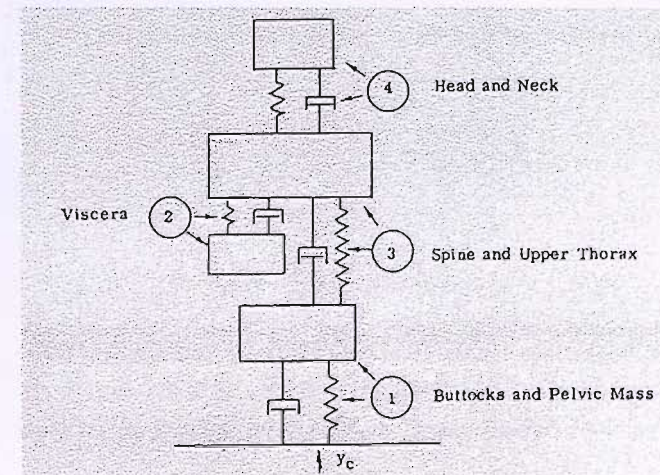


Figure 2.57: Four degree-of-freedom by Payne and Band (1971).

Mertens and Vogt (1978) developed a five degree-of-freedom lumped parameter model of the seated body so as to represent the dynamic response of the body under high magnitude of vertical impact or pulse (Figure 2.58). The model consisted of five masses. These masses were intended to represent the main body parts of a sitting subject. The represented body parts were the 'legs' ( $m_1$ ), the 'buttocks' ( $m_2$ ), the 'abdominal system' ( $m_4$ ), the 'chest system' ( $m_6$ ) and the 'head' ( $m_7$ ). The 'spinal column' was represented by the springs ( $k_3$ ,  $k_5$  and  $k_7$ ) and dampers ( $c_3$ ,  $c_5$  and  $c_7$ ). The values of the masses in the model were obtained from the anthropometric measurements, such as reported by Clause *et al.* (1969). At first, the values of the springs and dampers were derived by fitting the magnitude and phase of the response from the model with the measured mechanical impedance of the body and seat-to-head transmissibility under vertical vibration at a vibration magnitude around 0.3 G. However, the parameters of the model only valid for low level of vibration magnitude. For higher vibration magnitude (up to +4 Gz), the authors suggested that the body may respond non-linearly, thus values of the stiffness and damping of the body will be shifted to different region. To obtain the stiffness and damping values of the model under high level of vibration magnitude, the parameters of the model were derived by fitting the model response with the measured impedance and seat-to-head transmissibility from the measurements carried out earlier by Mertens (1978). The authors then made comparison of the Dynamic Response Index (DRI) of model with linear parameters and with the same model with the non-linear parameters. They found that the model with non-linear parameters will tend to give higher index value than the model with linear parameters.

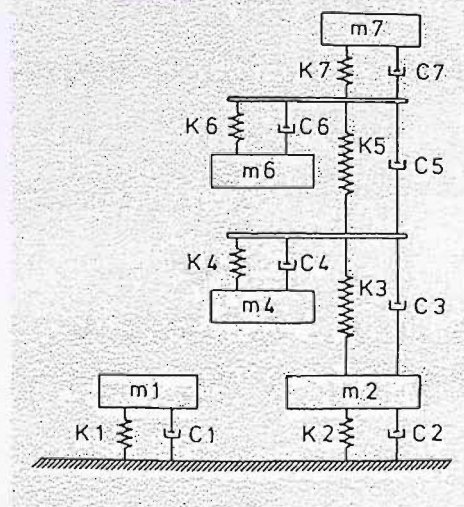
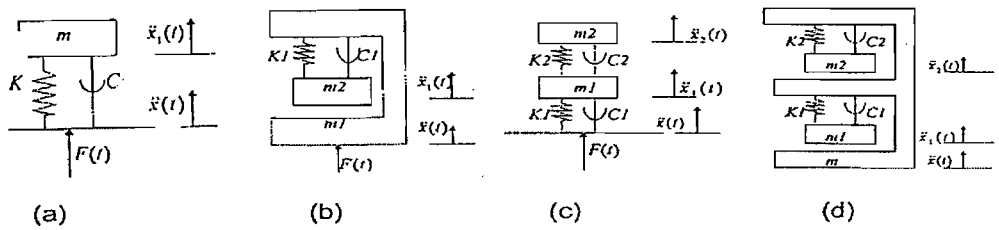


Figure 2.58: Five degree-of-freedom model by Mertens and Vogt (1978).

While some of the models described earlier were developed to calculate the DRI, others were developed so that it can be used for testing seats (e.g. Suggs *et al.*, 1969). A recent study reported by Wei and Griffin (1998b), in which the authors developed four lumped-parameter models seated people so as to represent the apparent mass of seated person exposed to vertical vibration in the frequency range 0.25 to 20 Hz. Subsequently the models were combined with cushion model (comprises of spring and damper only, connected to the model at the base) used to predict vertical transmissibility of seats. Figure 2.59 shows all the four models. The authors modelled two single degree-of-freedom models and a couple of two degree-of-freedom models. The parameters of each model were derived from fitting the magnitude and phase of the mean measured apparent masses of sixty subjects, which had been reported by Fairley and Griffin (1989). The models were not intended to propose the mechanism of the body during excitation but to provide similar apparent mass response of the body with that of human subjects. All models showed good fitting with the modulus and phases of the measured apparent masses data in the frequency range 0.25 to 20 Hz. The authors concluded that the two degree-of-freedom models appeared to compute a better fit to the magnitude and phase than the single degree-of-freedom model. In addition, the two degree-of-freedom models also showed better fit near the principal resonance frequency at 5 Hz.



**Figure 2.59:** Single degree-of-freedom models (a and b) and two degree-of-freedom models (c and d) by Wei and Griffin (1998b).

The lumped parameter model of human body can also be developed to explain the mechanisms involved in the biodynamic responses of the body to vibration. An example of such application of the lumped parameter model has been reported by Matsumoto and Griffin (2001). The authors constructed two lumped parameter models with multi degree-of-freedom (more than two) to simulate the dynamic mechanisms of the body associated with the principal resonance of the seated human body exposed to vertical vibration (Figure 2.60). Both models incorporated translational and rotational degrees of freedom. The first model consisted of four masses, which correspond to the 'whole legs (1)', the 'pelvis (2)', the 'viscera (4)' and the 'upper-body (3)' (see Figure 2.60a), while the second model incorporated five masses (Figure 2.60b), representing similar body parts with that in the model 1, except that in this model, the 'upper-body' was represented by two masses (3 and 5). Although previous study has shown that the body is non-linear, for simplicity, the authors neglected the non-linear properties of the body components. The masses and the geometric parameters of the models were determined from the model parameters available from literature (e.g. Liu and Wickstrom, 1973; Belytschko and Privitzer, 1978; National Aeronautics and Space Administration, 1978 and Kitazaki and Griffin, 1997). The stiffness and damping values of the both models were determined by fitting the response of the models with the magnitude and phase of the apparent mass of the body and the transmissibility of the body from the seat to several location along the spine (i.e. pelvis, thoracic 5 and 1, lumbar 1), which was measured earlier by the same authors (Matsumoto and Griffin, 1998). The models showed good fitting with measured apparent mass, and generally, showed similar trends with the measured body transmissibility. After the parameters of the models were obtained, the authors performed modal analyses so as to

observe the mode that correspond with the resonance of the body (Figure 2.61). Four vibration modes in the frequency range below 20 Hz were found for both models. The authors concluded that the principal resonance of the apparent mass of the body during vertical excitation (which is around 5 Hz) is attributed to a vibration mode consisting of vertical motion of the pelvis and legs and pitch motion of the pelvis, both of which cause vertical motion of the upper-body, bending of the spine and vertical motion of the viscera.

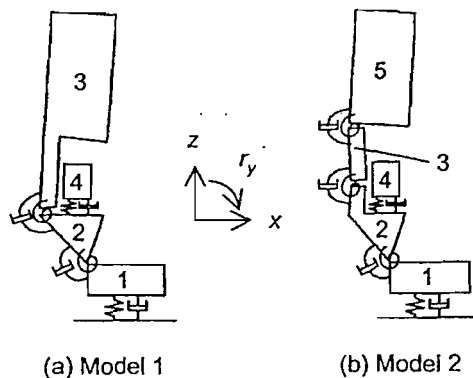


**Figure 2.60:** Four degree-of-freedom model (model 1) and five degree-of-freedom model (model 2) developed to propose the dynamic mechanism of seated body at resonance frequency. Models developed by Matsumoto and Griffin (2001).

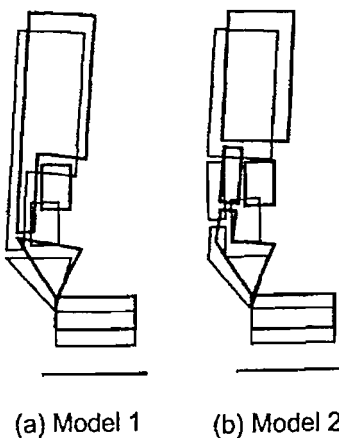


**Figure 2.61:** Vibration mode shapes corresponding to the principal resonance pf the apparent mass of both for Model 1 and for Model 2. Taken from Matsumoto and Griffin (2001).

Recent studies have shown that the response of the body in other directions than that the direction of excitation has a great importance in the biodynamic responses of the seated person (e.g. Matsumoto and Griffin, 1998 and Nawayseh and Griffin, 2003, 2004 and 2005a and 2005b). However, models that can predict the responses in other direction than that the directions of excitation and still limited. Nawayseh (2002) developed a two degree-of-

freedom model that can predict the vertical and fore-and-aft forces on the seat of a seated subject during vertical vibration. Although the model was a simple model, the author tried to suggest the 'crude' mechanisms of the body in responses to vertical vibration. The model consisted of two masses, a linear translational spring and damper and a linear rotational spring and damper (Figure 2.62). The masses represented the upper legs carried by the seat (mass 1) and the total mass of the upper body, including the pelvis (mass 2). The stiffness and damping of the thighs and tissue under the ischial tuberosities were represented by a translational spring and damper, while the rotational motions of the upper-body were represented by a rotational spring and damper. While the value of mass 1 was fixed, in which it was obtained from the literature (e.g. National Aeronautics and Space Administration, 1978), the value of mass 2 was varied so as to observe the effect of different thigh contact on the seat on the model. The model parameters (except mass 1) were obtained by optimising the squared error for both the magnitude and phase of the vertical apparent mass and equivalent 'cross-axis' fore-and-aft apparent mass of the measured data and the predicted data. The model showed good fitting with the magnitude of both the vertical and 'cross-axis' fore-and-aft apparent masses in the frequency range 0.25 to 25 Hz, but only fitted well with the phases up to 8 Hz. The author suggested that the results may be improved by adding more degrees-of-freedom. In addition, the author suggested that the resonance frequency of the body (around 5 Hz) could be due to the vertical deformation of the tissue beneath the pelvis (from  $k_1$  and  $c_1$ ). The pitching motion of the upper-body (i.e. pitching of mass 2) seemed to make a minor contribution to the resonance of the vertical apparent mass. The author also suggested that the non-linearity of the body with vibration magnitude was attributed by the stiffness of the tissue beneath the pelvis, which corresponded with the  $k_1$  and  $c_1$  in the model.

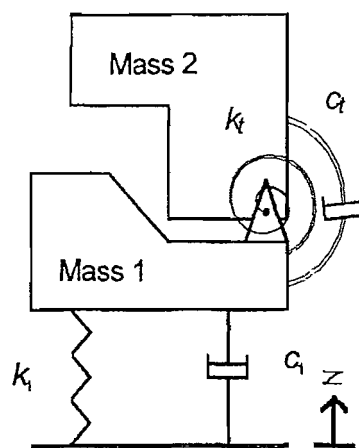
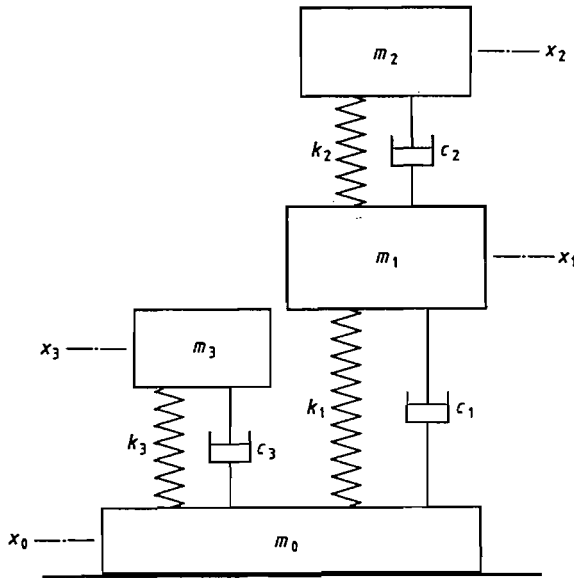


Figure 2.62: Two degree-of-freedom model by Nawayseh (2002) that can predict the responses in other direction than that the direction of excitation.

The International Organization for Standardization published an International Standard for the range of idealised values to characterise seated-body biodynamic response under vertical vibration, in which a three degree-of-freedom model was defined so as to represent the seated human body (ISO/FDIS 5982, 2001; Figure 2.63). The models consisted masses, spring and dampers, which do not correspond to physiological structures within the body. The model parameters were derived by fitting the predicted response of the model with the measured mechanical impedance, apparent mass of the body and seat-to-head transmissibility reported previously. When using the model to predict the seat-to-head transmissibility, mass  $m_2$ , however, may be taken to represent the head. The organization recognised that the feet and back support, sitting posture, excitation amplitude and subject mass could have significant influence on the biodynamic responses to vertical vibration, and thus the model was determined under a well-defined and restricted range of condition. Therefore, the idealised parameters values of the model presented in the ISO/FDIS 5982 (2001) only valid for seated-person exposed to sinusoidal or broad-band random vertical vibration with unweighted r.m.s acceleration lower or equals to  $5 \text{ ms}^{-2}$  in the frequency range 0.5 to 20 Hz while the feet were supported on the vibrating platform with the back is unsupported, and the individual body masses are within 49 kg to 93 kg.



**Figure 2.63:** Three degree-of-freedom model defined by International Standard of Organization, ISO/FDIS 5982 (2001) to represent the seated human body.

## 2.4.2.2

## Non-linear models

Hopkins (1971) modelled a non-linear lumped parameter model of the dynamic response of the human body to low frequency vertical vibration. The author developed two non-linear models of human body and each model consisted of three masses with two degrees-of-freedom (Figure 2.64). The three masses represented some of the body parts such as the 'lower torso', the 'visceral' and the 'upper torso'. The 'vertebral column' was represented by a linear spring and damper in both models. In the first model, the author considered the non-linearity geometry of the visceral mass motion to account the non-linearity of the human response and the characteristic was represented by linear springs, which were not rigidly attached to the visceral mass (Figure 2.64a). The author found that the model gave a close fit of the mechanical impedance data obtained in the experimental study reported earlier by Coerman (1962). In the second model, the author considered the non-linearity effect of the lungs as the contribution to the non-linear response of the body and modelled the component by 'a piston in a cylinder with an orifice' (Figure 2.64b). The author concluded that the non-linear response of the body can be accounted from the non-linear mechanics of the lungs.

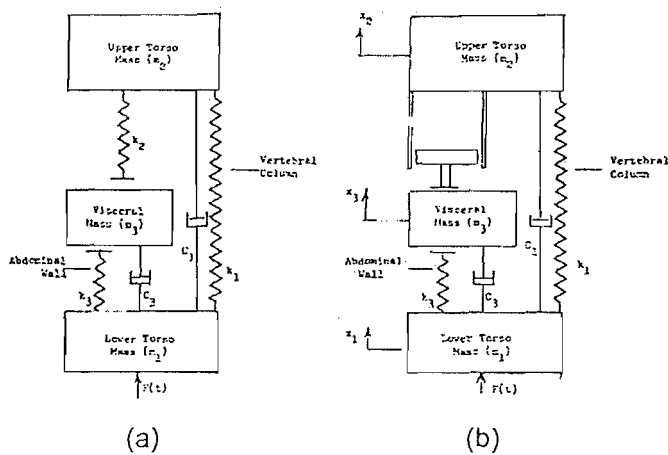


Figure 2.64: Non-linear models of seated person by Hopkins (1971).

A multi-degree-of-freedom lumped-parameter model of seated body incorporating some non-linear components was developed by Muksian and Nash (1974). The authors claimed that the model described the anatomical path between the pelvis and head (i.e. spinal column and viscera), which also include active forces within the body and both non-linear and passive elements (Figure 2.65). Eight masses were defined in the model to represent the 'pelvis and legs', 'abdomen', 'diaphragm', 'thorax', 'torso', 'back' and 'head' of a

seated person. The model, however, was limited to only vertical sinusoidal excitation. The non-linearity of the body was presented by the non-linear springs and dampers supporting the 'torso', 'thorax', 'diaphragm' and 'abdomen', exception to the spring supporting the 'back' and 'head' which was considered as linear springs and dampers. The authors predicted: i) seat-to-head transmissibility, ii) seat-to-back transmissibility, iii) seat-to-torso transmissibility, iv) seat-to-thorax transmissibility, v) seat-to-diaphragm and vii) seat-to-abdomen transmissibility and compared with the measurements from literature (e.g. Goldman and von Gierke, 1960; Coermann *et al.*, 1960 and Pradko *et al.*, 1966). The response of the model showed agreement with the experimental results, and the authors concluded that the model can represent the non-linearity response of seated person exposed to vertical vibration within acceptable tolerances.

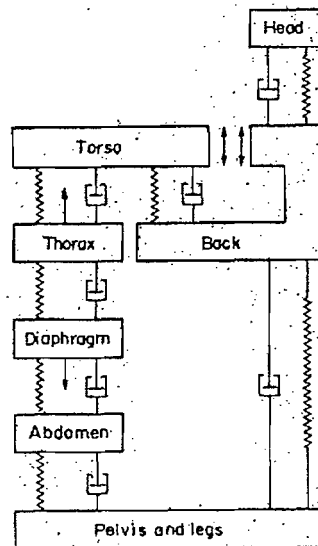
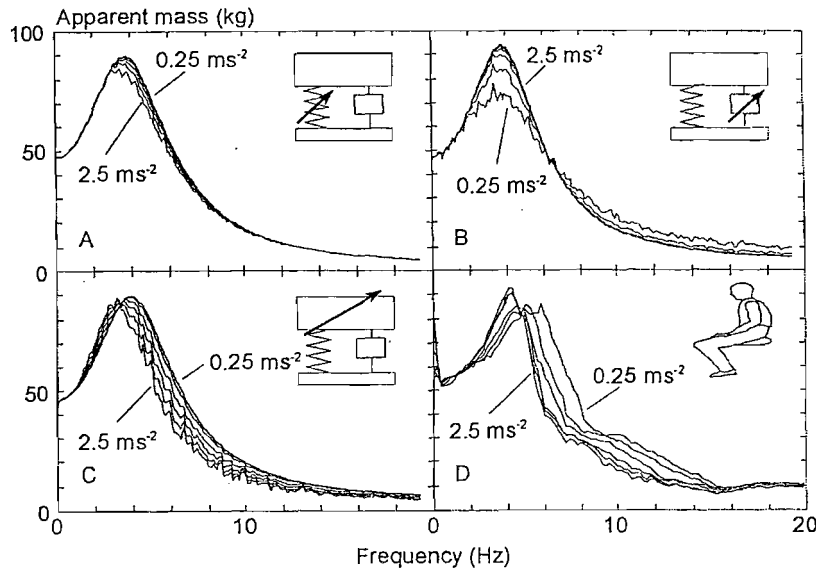


Figure 2.65: Non-linear models of seated person by Muksian and Nash (1974).

Mansfield (1998) developed a simple form of a quasi-static non-linear lumped parameter model of the apparent mass of a seated person which consisted only two masses with one degree-of-freedom (Figure 2.66). Unlike some of the previous studies mentioned earlier (e.g. Hopkins, 1971 and Muksian and Nash, 1974), the mass in the model did not intend to represent any body parts of the human body. In addition, the model of Mansfield (1998) was intended to predict the apparent mass of the body exposed to vertical vibration at six different vibration magnitudes (0.25, 0.5, 1.0, 1.5, 2.0 and 2.5  $\text{ms}^{-2}$  r.m.s.) so as to include the non-linear response the body with increasing vibration magnitude. The model parameters were derived fitting the model response with experimental data obtained by the author earlier (Mansfield, 1994). By adding the non-linear component in the stiffness and

damping values, the model predicted better approximations of the apparent mass of seated person at all six vibration magnitudes than that the linear model can predict. The author concluded that models with non-linear masses and non-linear stiffness showed better results than that the models with non-linear damping.



**Figure 2.66:** The predicted apparent mass of the seated person using one degree-of-freedom of non-linear. Data taken from Mansfield (1998).

### 2.4.3 Lumped parameter modelling in the horizontal vibrations (fore-and-aft and lateral)

Recent studies have shown that the apparent mass on the body on the seat showed evidence of three resonances: around 1 Hz, 3 Hz and between 4 and 7 Hz when exposed to fore-and-aft vibration (e.g. Fairley and Griffin, 1990; Mansfield and Lundström, 1999 and Nawayseh and Griffin, 2003). The lateral apparent mass of the body also showed evidence of two peaks (e.g. Fairley and Griffin, 1990 and Holmlund and Lundström, 1998). However, models representing biodynamic responses in the horizontal directions is limited.

Based on previous findings that the body showed three resonances when exposed to either fore-and-aft or lateral vibration, Mansfield and Lundström (1999b) developed several lumped parameter models, in which each model consisted three degree-of-freedom to allow for the resonance frequencies to be depicted by the models. Each model consisted of three one-degree-of-freedom mass-spring-damper systems arranged either in parallel, or in series,

or in combination of both (Figure 2.67). The models did not represent any part of the body, but rather arbitrary chosen to fit with the measured data. The parameters for each model were derived by comparing the models responses with the synthesised responses (target responses). The synthesised target responses were obtained by combining the measured responses of the apparent mass of the body in either fore-and-aft or lateral directions at two magnitudes of vibration (0.5 and 1.0 ms<sup>-2</sup> r.m.s.) reported by Fairley and Griffin (1990) and Mansfield and Lundström (1999a). The authors found that these models provided good agreements in the magnitude of the apparent masses between the prediction and the target response in the frequency below 10 Hz. The predicted phases only showed good fit with the target response at frequencies less than 4 Hz. The three one-degree-of-freedom mass-spring-damper systems arranged in parallel, with a rigid mass in contact at the driving point was found to produce the best prediction. The authors suggested that the 'softening' effect (i.e. resonance frequency reduced with increasing vibration magnitude) was also observed with some manipulations of the stiffness of the spring of the models.

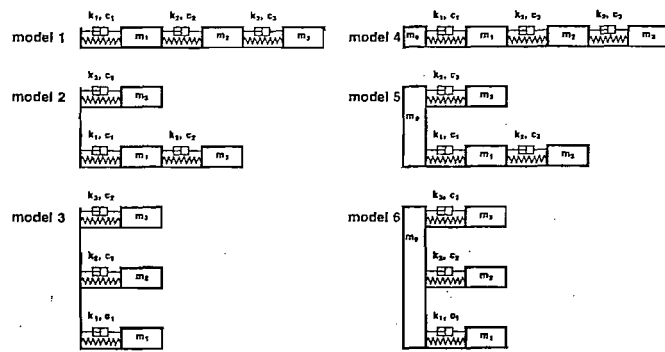


Figure 2.67: Six three degree-of-freedom models by Mansfield and Lundström (1999b).

#### 2.4.4 Conclusions

The biodynamic responses of the body can be represented by means of mathematical models, which can be derived from the experimental measurements. Previous researchers have developed two types of biodynamic models: i) 'quantitative model, in which the model described the relation between the input and output, and ii) the 'mechanistic' model, in which some of the 'crude' mechanisms of the body involved in response to vibration are described.

The vertical impedance of the body exposed to vertical excitation can be, in the simplest form, presented by a one degree-of-freedom lumped parameter model (i.e. mass-spring-damper system). The parameters of the model can be achieved by comparing the response of the model with the measurements data. Some of the application of using lumped parameter models are i) to calculate the Dynamic Response Index (DRI), or ii) to calculate seat-to-head transmissibility, or iii) for seat testing. Only one study reported few multi-degree-of-freedom models that can predict the apparent mass of the body with no backrest in fore-and-aft and lateral direction.

Few researchers have shown that it is possible to improve the predicted response of the one-degree-of-freedom model by including more degree-of-freedom, but it comes with more complexity to derive the mathematical equation.

All the models that have been developed (either single or multi degree-of-freedom) were limited to specific vibration magnitude, and in a specific frequency range. However, there were few models have been developed to cope with the non-linearity of the body during vibrations, such as inclusions of non-linear spring and damping characteristics.

## 2.5 Measuring seat transmissibility without subjects

### 2.5.1 Introduction

Previously, the vibrations transmitted to the seated person through seats were measured with human subjects. Consequently, it needs careful consideration, for example the safety and ethical issues regarding exposing human subjects to vibration. In addition, when using human subjects as the main testing object, it is prone to some limitations, whether the subjects are 'safe' to the exposed stimuli.

This limitation can be overcome by substituting the human subject with alternative analogue, such as rigid masses or a sandbag. With more experiments being carried, generating more data on the impedance of the body and transmissibility of seats, a standardised method for predicting the seat transmissibility from mathematical models of seat-seated person system. This section will show some of the studies that have been performed on vehicle seat testing using masses and dummies.

### 2.5.2 Testing seat with rigid mass

Matthews (1966) tested two tractor seats using rigid masses to calculate and compare the seat transmissibility measured with the human subjects. The two tractors seats were: i) rigid seat-pan with foam cushion (seat A) and ii) suspension seat with rubber suspension (seat D). The author used a dead weight equivalent with 75% of the total body weight of the tractor operator. The percentage was obtained from the approximation proportion of an operator's weight taken by a seat in a static condition. The results showed that with seat A, the seat transmissibility with rigid masses tended to be higher than with the subject occupant at low frequencies (less than 3 Hz), but subsequently, the transmissibility was reduced significantly (Figure 2.68). With the suspension seat, the seat transmissibility showed similar trend when loaded with either the masses or occupied with human subject. Despite showing similar trend, the transmissibility with rigid masses tended to have a higher magnitude between 1 and 5.5 Hz, and higher transmissibility at resonance than that occupied with human subject. Similar findings of overshooting the transmissibility at resonance when using a rigid mass on suspension seat was also observed Ashley (1976) and Toward (2000). Toward (2000) also found the when a foam cushion car seat was loaded with rigid masses (approximately 53.2 kg, which approximately 75 % of the means weight of subjects of 68.7 kg), the resonance of the seat transmissibility occurred at higher frequency, and with much greater amplification, than that with the subjects. The rigid masses showed resonance around 7 Hz, while with human subjects, the resonance frequency of the seat transmissibility showed resonance around 4 Hz. The transmissibility at resonance was approximately doubled with the masses than with the subjects.

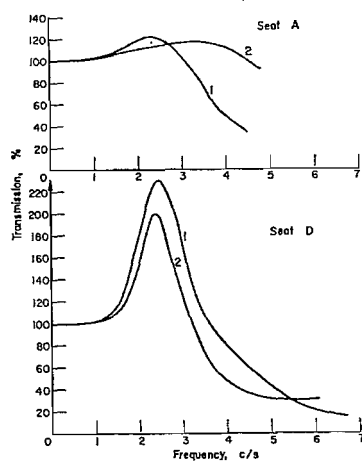
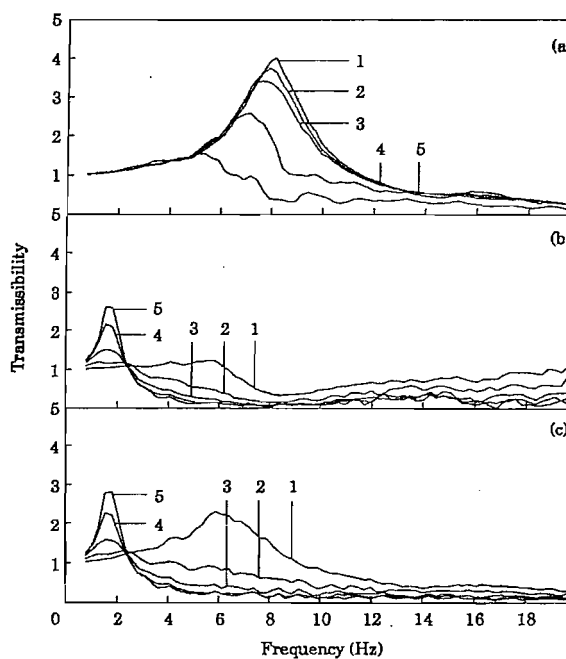


Figure 2.68: Transmissibilities of suspension seat and foam cushion seat with rigid masses (1) and human subject (2). Data taken from Matthews (1966).

Wu and Griffin (1996) used a sandbag of 56 kg (i.e. 75% of the mass of a 75 kg human subject participated in the study) as the load on a suspension seat to simulate the weight of a sitting subject when measuring the transmissibility of a suspension seat. The transmissibility of the suspension seat with the sand-bag is shown in Figure 2.69. The authors then compared the results obtained with the sandbag with that with the human subject data and found that resonance frequency of the transmissibilities of the suspension alone and of the whole-seat are the same with a human subject or a bag of sand. However, the transmissibilities with the sand bag were much higher than the human subject. The authors suggested that with the use of sand bag was sufficient to measure the resonance frequency of a suspension seat, but not to measure the transmissibility of the seat.



**Figure 2.69:** Transmissibilities of (a) the seat cushion, (b), the suspension (b) and (c) the whole seat (suspension and seat cushion) at five vibration magnitude with a 56 kg mass (sandbag). Five magnitudes of vibration input: 1 ( $0.35 \text{ ms}^{-2}$  r.m.s.); 2 ( $0.70 \text{ ms}^{-2}$  r.m.s.); 3 ( $1.05 \text{ ms}^{-2}$  r.m.s.); 4 ( $1.40 \text{ ms}^{-2}$  r.m.s.) and 5 ( $1.75 \text{ ms}^{-2}$  r.m.s.). Data taken from Wu and Griffin (1996).

### 2.5.3 Testing seat with antropodynamic dummy

Matthews (1967) used an antropodynamic dummy for testing suspension seats. The antropodynamic dummy was analogous to the seated human body, and had similar dynamic impedance of the human subjects. The base of the dummy simulated the

buttocks shaped and size so as to give the similar contact with the seat cushion as human subjects. The principal of the impedance simulation of the dummy was based on the work reported by Coermann (1959), which suggested that the seated body can be presented by a single degree-of-freedom system with a 5 Hz of natural frequency and with relatively high damping. The simulation of the dummy was fairly accurate in the frequency range 0.5 to 10 Hz. The authors found that the dummy fitted well the resonance frequency of the seat transmissibility (around 2 Hz) and gave fairly good results of the transmissibility of a suspension seat across the frequency range compared to that with human subjects when the friction in the suspension was low. However, when greater friction in the suspension was present, the dummy tended to increase the transmissibility at frequencies higher than the resonance frequency.

Mansfield and Griffin (1996) used a passive anthropodynamic dummy to measure the dynamic characteristics of a car seat traveling over six different road surfaces (Figure 2.70). As described by the authors, the anthropodynamic dummy 'consisted of a pair of steel precision shafts on which a 46 kg mass could move vertically. A single 739 Ns/m low friction damper was fitted between the mass and an aluminium shaft at the top of the dummy. Compression springs were fitted between each of the four corners of the moving mass and an aluminium base plate. The combined stiffnesses were 50176 N/m. The mass included a pair of steel plates which ran on ball bushings vertically constrained by the shafts. Between these were a central set of steel masses which made up the complete moving mass of the dummy. The dynamic response of the dummy was based on the single degree-of-freedom model of the body developed from measurements of the vertical apparent mass of human subjects (Fairley and Griffin, 1989). A SIT-BAR (Whittham and Griffin, 1977) was fitted to the base and back of the dummy to provide indentors for the seat on which the dummy was placed. The rigid mass of the frame was 6 kg. The static friction measured for the movement of the assembled dummy was 14.2 N'. The authors measured the transmissibilities of the seat cushion in vertical, fore-and-aft and lateral direction, and the cross-axis' fore-and-aft backrest transmissibility (by comparing fore-and-aft vibration measured at the backrest with the vertical acceleration measured at the seat base) with twelve subjects. The six traveling roads consisted of i) a motorway, ii) two minor country roads, iii) two major urban roads and iv) a minor urban road. The results of transmissibilities of the seat using the dummy and human subjects are shown in Figure 2.71. The vertical seat transmissibilities showed similar results with both the human subjects and the dummy, both showed resonance around 4 Hz. However, differences in the transmissibilities were obvious at frequencies higher than 15 Hz. Similarly, the dummy showed similar results with the subjects in the fore-and-aft seat transmissibilities, with both showed resonances around 2 and 4 Hz, and the trend was similar at frequencies below 10 Hz. While the lateral seat transmissibilities with the subjects were near unity, the

dummy showed two resonances around 4 Hz and 15 Hz, and the dummy did not show similar trend with the subjects. The 'cross-axis' fore-and-aft backrest transmissibilities of both measured using dummy and the human subjects showed good similarity: both the dummy and the subjects showed resonances around 2 Hz and 4 Hz, and the trend was generally good at frequencies less than 10 Hz. The authors suggested the dummy can be used to replace subjects for measuring seat dynamics and gave representatives measures of the vertical dynamics response of the seat at resonance.

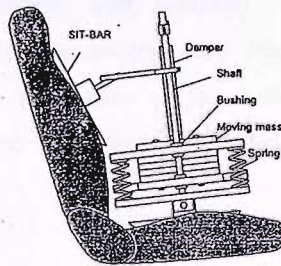


Figure 2.70: Seat testing using passive antropodynamic dummy (Mansfield and Griffin, 1996).

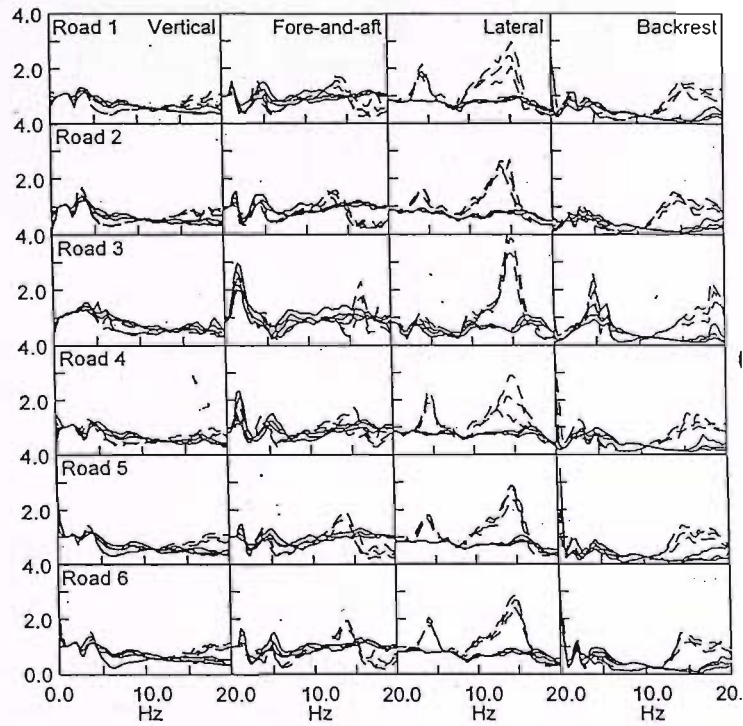


Figure 2.71: Transmissibility of a car seat measured on six roads. Median and inter-quartile for 12 subjects (solid line) and anthropodynamic dummy test (dashed line). Data taken from Mansfield and Griffin (1996).

The passive anthropodynamic dummy studies mentioned above are limited to low excitation magnitudes by the non-linear phenomena, such as friction in the mechanical components that provide damping. Some researchers have tried to overcome this limitation by developing an active dummy. Lewis and Griffin (2002) designed an active vibration dummy to simulate the dynamic behaviour of sitting man expressed in terms of apparent mass, which employed an active control system. The active control system consisted an electrodynamic actuator that can generate damping forces, and is controlled by the feedback from the acceleration and force transducers, which allow the dummy to comply with the adjustment of parameters, and adapted to different prescribed vibration characteristics (Figure 2.72). By comparing the seat transmissibility measurements obtained with nine subjects and with that of the active dummy, the transmissibilities measured using the dummy showed high correlations with the median measurements from the nine human subjects.

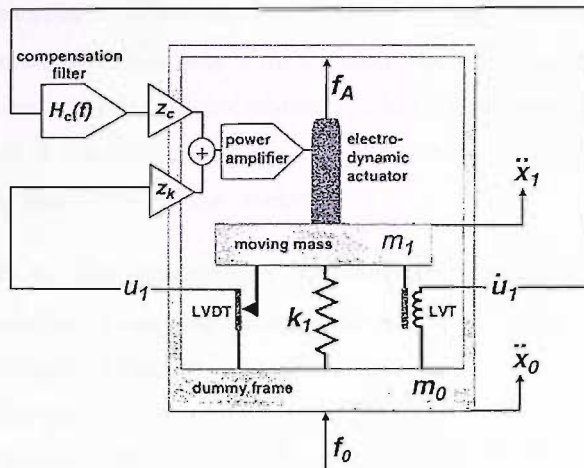


Figure 2.72: Schematic diagram of the active control used in an antropodynamic dummy (Lewis and Griffin, 2002).

#### 2.5.4 Methods of predicting seat transmissibility

One method of predicting transmissibility of seats without using human subjects is to replace the human body with either rigid masses, or sand bags or anthropodynamic dummies. However, all these alternatives had difficulties, for example dead masses tended to over-shoot the response near resonance, and it is difficult to maintain the calibration of a dummy. An alternative method of predicting seat transmissibility is to use mathematical models representing seat-seated person system. This method is based on separate

measurements of the impedance of the seat and the impedance of the human body, which was shown to give useful predictions (Fairley and Griffin, 1986). In that study, the seated human model was derived from the measured apparent mass of seated subjects with no backrest, as part of their study. The cushion dynamic characteristics were obtained from an indenter test. In the indenter test, the seat cushion (which was supported on a vibrator plate) was forced with an indenter, with a shaped and contoured like a SIT-BAR (Whitham and Griffin, 1977). The forces on the indenter and the accelerations at the seat base were measured with different pre-loads (300 N to 900 N), and consequently the dynamic characteristics (stiffness and damping) of the seat cushion were calculated (the equivalent dynamic stiffness and damping were obtained from the real and imaginary part of the dynamic stiffness frequency function). The transmissibility of a seat with eight subjects and eight seats with one subject were compared with that obtained from the prediction method. The authors showed that the model predicted well the transmissibilities of the seats (with no contact with the backrest), but the predictions tended to show higher transmissibilities at resonance. When the back was in contact with the backrest, although the trend of the transmissibilities was similar with both the prediction model and the human subject, the predicted transmissibilities tended to increase the transmissibility at frequencies higher than 5 Hz (Figure 2.73). The authors suggested that this was possibly due to the effect of the contact with the backrest.

Wei and Griffin (1997) further investigated the indenter test method (i.e. for determining the dynamic characteristics of the foam/seat cushion), in which they studied the effect of contact area of the indenter, vibration magnitude and static force on the dynamic stiffness of foam cushion. In this study, the authors found that the dynamic stiffness and damping of the foam cushion increased with increasing pre-load from 300 N to 700 N. The vibration magnitude, however, had little influence on the stiffness or the damping of the foam. The effect of the contact area on the dynamic stiffness of the foam did not show a consistent trend, although the authors suggested that it is possible to select the reasonable shape of the indenter for predicting the seat transmissibility. The shape of the indenter that had been investigated were i) SIT-BAR (similar to Whitham and Griffin, 1977), ii) three metal discs with different diameters (150 mm, 200 mm and 250 mm) and iii) a similar shape to buttock shape, moulded from a HYBRID III Exterior (General Motor, 1978).

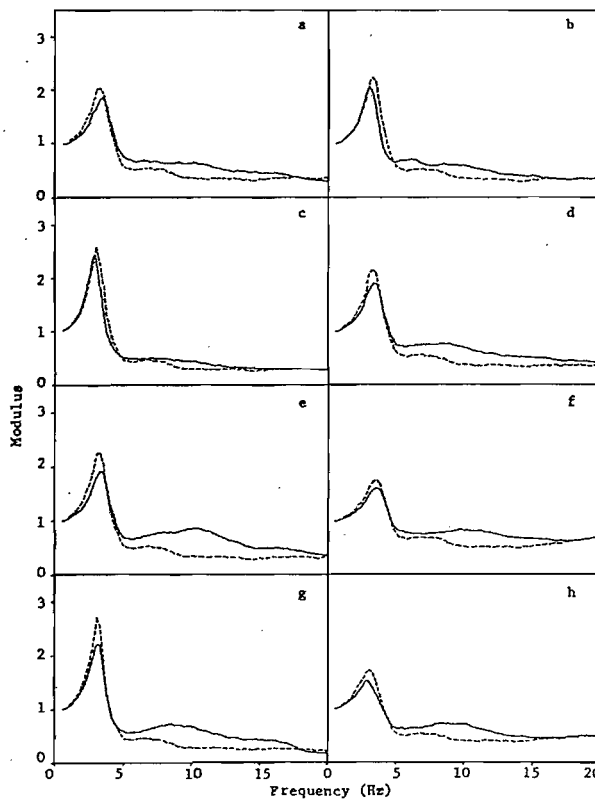
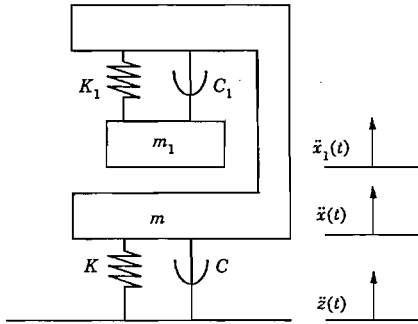
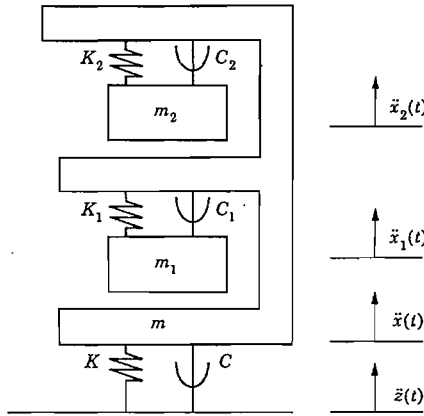


Figure 2.73: Comparison of measured (solid line) and predicted (dotted line) transmissibilities from eight different seats with one subject. Data from Fairley (1986).

The authors later employed the method of predicting seat transmissibility, which was proposed by Fairley and Griffin (1986) to predict the foam and seat transmissibility in the vertical direction (Wei and Griffin, 1998c). In that study, the authors used two lumped parameter seated person models, which they developed earlier (Wei and Griffin, 1998b) and combined them with the cushion model, obtained from the indenter test. The combined seat-seated person models are shown in Figures 2.74 to 2.75, one consisting of one degree-of-freedom model of human body (Figure 2.74), the other used two degree-of-freedom model of human body (Figure 2.75). The models parameters were obtained by fitting the models response with apparent mass of sixty subjects, measured by Fairley and Griffin (1986).



**Figure 2.74:** Seat-seated person lumped parameter model consisting of one degree-of-freedom model of human body to predict transmissibility of seats in the vertical direction. Data taken from Wei and Griffin (1998c).



**Figure 2.75:** Seat-seated person lumped parameter model consisting of two degree-of-freedom model of human body to predict transmissibility of seats in the vertical direction. Data taken from Wei and Griffin (1998c).

Wei and Griffin (1998c) later compared the predicted transmissibilities of foam and seat cushion with the measured transmissibilities using eight subjects. The results showed that the model incorporating the single-degree-of-freedom seated human model was able to depict the first resonance frequency (around 4 Hz) of seat transmissibility, but failed to predict the second resonance around 7 Hz, which was apparent for most subjects (Figure 2.76). The model, however, only fitted well the phases with the measured response up to the frequencies of the first resonance frequency. When using two-degree-of-freedom seated human model, the predicted transmissibility was improved in which the model was able to predict both resonance frequencies of the transmissibility of the seats (Figure 2.77). The latter model also improved the predicted phase response. The authors concluded that, although the single-degree-of-freedom model can adequately predict the transmissibility of seat in the vertical direction at low frequencies and can be used to predict the principal resonance of the seat transmissibility (around 5 Hz), the two degree-of-freedom showed

better predictions. The latter model can predict the second resonance of the seat transmissibility, and, may give useful prediction of the seat transmissibility at frequencies up to 25 Hz. Nevertheless, these models are limited to subjects exposed to vertical vibration and seated with no contact with the backrest.

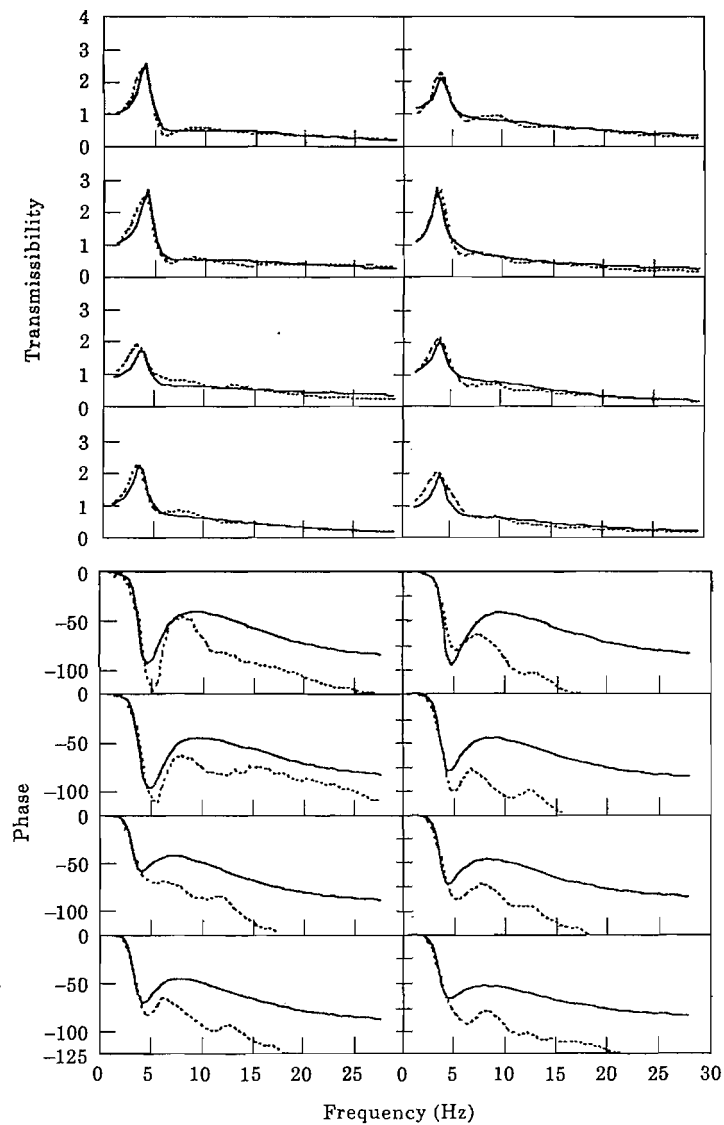


**Figure 2.76:** Comparison of measured (dashed) and predicted (solid) transmissibility and phase of seat cushion using single-degree-of-freedom model for eight subjects. Data taken from Wei and Griffin (1998c).

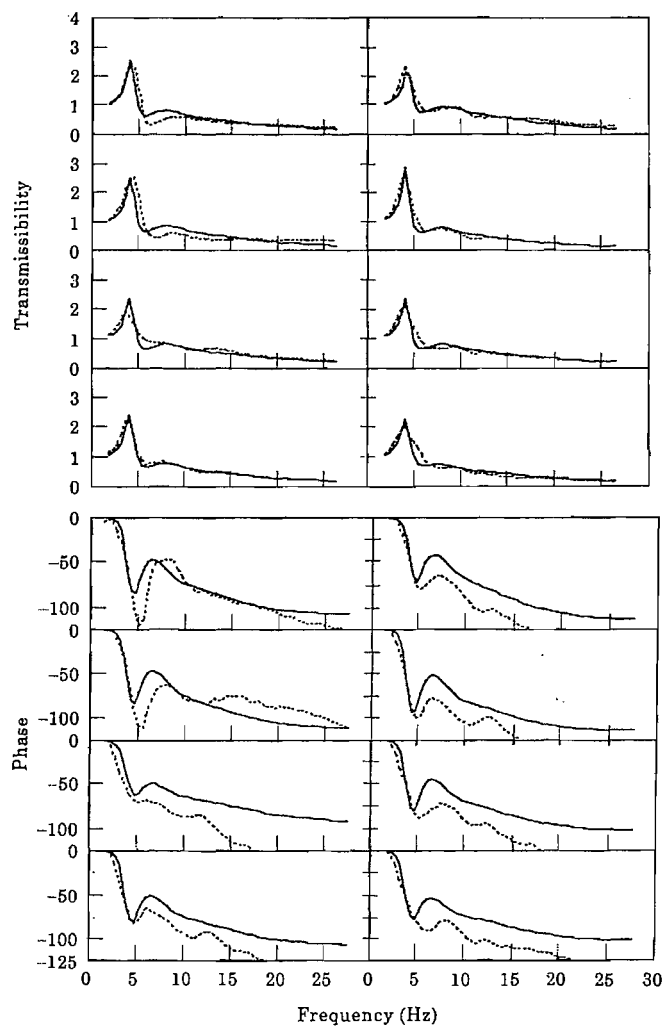


**Figure 2.77:** Comparison of measured (dashed) and predicted (solid) transmissibility and phase of seat cushion using two-degree-of-freedom model for eight subjects. Data taken from Wei and Griffin (1998c).

### 2.5.5 Conclusions

The transmissibility of seats can be predicted by using either rigid masses, or sand-bags loaded on the seat so as to produce similar loading on the seat cushion when seated with human subjects. While both can be used to predict the resonance frequency of the seat, neither would produce similar transmissibility as human subjects. Using anthropodynamic

dummy can give useful results. The dummy had similar impedance response with seated subjects.

Alternatively, the transmissibility of a seat can be predicted from the impedance of the body and the impedance of the seat from separate measurements. A seated human model can be developed from the impedance measurements of the body, while the dynamic stiffness of the seat cushion can be obtained from indenter test. Subsequently, the human and seat cushion model can be combined to give seat-seated person model. This method can give useful prediction of seat transmissibilities up to frequencies of 25 Hz.

## 2.6 General conclusions

Biodynamic responses of the body to vibrations can be represented by frequency responses functions. While the mechanical impedance represents the response of the driving-point force with the resulting movements (acceleration, velocity or displacement), the transmissibility method represent the vibration transmitted though a system (either the seat or body).

When exposed to vertical whole-body vibration, the body shows principal resonance around 5 Hz. This resonance of the body has been associated with the pitching movement of the pelvis and the upper-body, combined with the bending mode of the spine. A second and third resonance frequency of the body has also been reported around 10 Hz and 50 Hz. The body also showed several resonances when exposed to horizontal vibrations. During fore-and-aft excitation, the body showed three peaks: around 1 Hz, between 1 and 3 Hz and between 3 and 5 Hz while resonances around 0.7 Hz and 2 Hz were observed during lateral excitation.

The apparent mass of the body was found to be greatly affected when a vertical backrest was used. During vertical excitation, the backrest tended to transmit more vibration to the body at higher frequencies: the apparent mass of the body was increased at frequencies higher than 5 Hz when the vertical backrest was used. With a vertical backrest, the body only showed one principal resonance around 3 Hz on the seat during fore-and-aft vibration and around 1.5 Hz during the lateral excitation. During fore-and-aft excitation, the back showed resonances around 2 Hz, 3 to 5 Hz and a broad peak in the frequency range 4 to 7 Hz.

Exposure of seated persons to either vertical or fore-and-aft vibration give rise to responses in the directions other than the direction of excitation, also known as 'cross-axis' responses. The 'cross-axis' fore-and-aft apparent mass of the body during vertical vibration showed principal resonance around 5 Hz, while when the body is exposed to fore-and-aft excitation,

the body shows resonances around 1 Hz, 3 Hz and between 4 and 7 Hz in the 'cross-axis' vertical direction. In both vibration excitations, the responses in the 'cross-axis' lateral direction shows small effect.

The body is non-linear when exposed to different vibration magnitudes. During either vertical or fore-and-aft excitation, the resonance frequency of the body in the direction of excitation tends to decrease with increasing vibration magnitude, suggesting a 'softening' effect. The 'cross-axis' responses are also non-linear with vibration magnitude during either excitation, but the extent is less visible in the 'cross-axis' lateral direction. The effect of stiffening the body posture resembles the reverse effect of vibration magnitude on the body: the resonance frequency of the body increased with stiffer sitting posture (i.e. from 'slouched' to 'erect') during vertical excitation. Various factors have been found to affect the vertical apparent mass of the body during vertical excitation. Variation in footrest height and backrest inclination showed more effect on the biodynamic responses of the body during vertical excitation than common changes in the seat pan inclination. However, equivalent study in the horizontal direction is still limited.

The biodynamic responses of the body to vibration can be represented using lumped parameter models, consisting from one degree-of-freedom, up to several degrees-of-freedom. The parameters of the model can be obtained by comparing the model response with the experimental data. However, most of the models are restricted to specific vibration conditions. Non-linear models have been developed to cope with the non-linearity of the body in response to vibration. A single degree-of-freedom with non-linear spring and damping characteristics can adequately represent the apparent mass of the body with different vibration. A mechanistic model has been developed to depict the 'crude' mechanism of movement of the body at the resonance frequency. The modal analysis showed that a vibration mode consisting of vertical motion of the pelvis and leg and pitch motion of the pelvis, both of which cause vertical motion of the upper-body, bending of the spine and vertical motion of the viscera contribute to the movement of the body at resonance frequency.

When subjects are seated on compliant seats, the vibration transmitted through the seat to the body can be measured using accelerometers positioned at the floor and at the seat-person interface. Subsequently, the transmissibility analysis can be calculated (i.e. transfer function between the input acceleration and the output acceleration).

The transmissibility of conventional seat has been found to show a resonance in the range of 3 to 5 Hz, in which the frequency is reduced to 1 to 2 Hz when a suspension mechanism was placed beneath the seat cushion. With few studies, fore-and-aft seat transmissibility showed resonances at 1 to 2 Hz, 4 to 5 Hz, 28 Hz and 48 Hz, while the fore-and-aft

backrest transmissibility exhibited resonances at 4 Hz, 28 Hz and 48 Hz. The vertical, pitch and roll vibration make a significant contribution to the fore-and-aft vibration at the backrest besides the fore-and-aft vibration at the backrest. In the lateral direction, the seat transmissibility showed resonance at about 1 to 2 Hz with magnitude near unity.

An effect of vibration magnitude on seat transmissibility with either vertical or fore-and-aft vibration is apparent: the resonance frequency tends to decrease with increasing vibration magnitude. The non-linearity found in the seat transmissibility is in part, or totally, influenced by the non-linearity of the body at different vibration magnitudes since a study showed that vibration magnitude had little influence on the stiffness and damping of seat cushion. Changes in the upper body posture were found to have more influence on the transmissibility of seats than variation in lower body posture. Variations in the footrest height and backrest inclination tended to have more influence on the seat transmissibility, in particular at frequencies higher than the resonance frequency than other factors such as the subjects' characteristics (e.g. age and sex), seat-pan inclination and foam cushion physical properties (e.g. density, composition and foam pad construction). Equivalent study in the fore-and-aft direction is still limited.

The transmissibility of seats can be predicted by using either rigid masses, or sand-bags loaded on the seat so as to produce similar loading on the seat cushion when seated with human subjects. Although either rigid masses or sand-bags could predict the resonance frequency of seats, but neither would produce similar trend of the transmissibility with the human subjects. Using an anthropodynamic dummy, which had similar impedance response with seated subjects, could give useful results and predict similar trend of the transmissibility of seats with that measured with human subjects. Alternatively, the transmissibility of seat can be predicted from mathematical models of seat-seated person system. The models can be derived from the impedance of the body and the impedance of the seat in separate measurements. While the dynamic stiffness of the seat cushion can be obtained from indenter test, the models of seated person could be derived from the measurements data with human subjects. Subsequently, the human and seat cushion model can be combined to give seat-seated person model, this method can give useful prediction of seat transmissibilities up to frequencies of 25 Hz.

## 2.7 Motivation of research

The literature review reveals that the knowledge of the biodynamic responses of seated human body and seating dynamics (vibration transmitted to the body through seats) is very limited. Only one study reported on the fore-and-aft apparent mass of the back during exposure to whole-body fore-and-aft vibration (see Section 2.2.4) and one study

reported on the fore-and-aft backrest transmissibility during fore-and-aft excitation (see Section 2.3.6). In contrast, there have been many studies conducted to study the apparent mass of the body (see Section 2.2.2) and the seat transmissibility (see Section 2.3.4) during vertical excitation. Therefore, the principal motivation of this research is to expand the knowledge (as well as reporting the *measurement data*) on both the apparent mass of the back and the backrest transmissibility during exposure to fore-and-aft vibration.

Previous studies have shown that during vertical excitation, the principal area of the interface between the seat and the body for the seat transmissibility measurement is beneath the ischial tuberosities (see Section 2.3.3). For backrest transmissibility, it is hypothesised that the interface between the back and the backrest is more complex than one principal area. No known studies have investigated the variation of the vibration transmitted through the backrest. Therefore, one of the motivations of this research is to investigate the variation of the transmissibility across the height of the backrest from the seat surface (reported in Chapter 4). As the backrest transmissibility greatly depends on the apparent mass of the back, it would also be interesting to investigate the variation of the apparent mass of the back (reported in Chapter 6).

Previous studies also shown that there are many factors that can influence the apparent mass of the body (see Section 2.2.3) and the seat transmissibility (see Section 2.3.5) during whole-body vertical excitation. One of the distinct findings is that both the body and seat transmissibility is non-linear with vibration magnitude (see Sections 2.2.3.4 and 2.3.5.6). However, only Nawayseh and Griffin (2005a) have investigated the non-linearity of the body with vibration magnitude during whole-body fore-and-aft excitation and Qiu and Griffin (2003) investigating the similar effect of vibration magnitude on the backrest transmissibility. But, both studies only investigated the effect of the vibration magnitude at the middle part of the interface between the back and the backrest. This research aims to further investigate the non-linearity of the body and the backrest transmissibility with vertical location on the backrest.

As there is only little study investigating the factors that can affect the fore-and-aft apparent mass of the back (see Section 2.2.5) and the fore-and-aft backrest transmissibility (see Section 2.3.7), this research also aims to expand the knowledge. The factors that are commonly experienced by seated subject in vehicles, such as varying backrest inclination and seat-pan inclination on both the apparent mass of the back and fore-and-aft backrest transmissibility would be studied (which are reported in Chapter 5 and Chapter 7).

The loading on the backrest is hypothesised to have an important influence on the backrest transmissibility, based on the analogy of that the seat transmissibility depends on the loading on the seat cushion and the impedance of the occupant (Griffin, 1990). A study

investigating the effect of push force on the feet (which subsequently increases the load on the backrest) on both the apparent mass of the back and the backrest transmissibility would be studied. In addition, previous study also showed that varying the leg posture (from variation in footrest) can affect both the vertical apparent mass of the body (see Section 2.2.3.2) and the vertical seat transmissibility (see Section 2.3.5.2). Hence, similar factors would be investigated in this research on both the apparent mass of the back and the backrest transmissibility.

Previous study also showed that vertical seat transmissibility could be measured without using human subjects (see Section 2.5). Fairley and Griffin (1986) showed that it is also possible to predict the transmissibility of seat during vertical vibration by using a seat-person mathematical model. This model comprises a human body model and a seat cushion model. Wei and Griffin (1998c) developed further the idea of predicting the seat transmissibility based on the impedance of the body and the impedance of the seat cushion which they proposed a standardised method of predicting vertical seat transmissibility. In both studies, the human body was represented with a simple linear lumped parameter model that can adequately estimate the apparent mass of the body without showing the mechanism of the biodynamic responses involved. Wei and Griffin (1998c) showed that a simple linear lumped parameter model representing a seated human body can be used to predict the vertical seat transmissibility when combined with a seat cushion model, which was represented by a simple model consisting only of a spring and a damper. As part of the objective of this research is to predict the backrest transmissibility from the apparent mass of the back and the impedance of the backrest cushion, the idea of Fairley and Griffin (1986) and Wei and Griffin (1998b and 1998c) would be applied in this research. A seat-person model is developed in this research based on the apparent mass of the back and the impedance of the backrest cushion. The prediction of the backrest transmissibility using the seat-person model is then compared with the backrest transmissibility, measured with human subjects so as to observe the accuracy of the prediction.

# Chapter 3

## Experimental apparatus and data analysis

### 3.1 Introduction

The core data of this research were obtained from five experiments, involving human subjects exposed to vibration so as to study the human responses during whole-body fore-and-aft vibration. All experiments were conducted in the laboratory of the Human Response Research Unit (HFRU), Institute of Sound and Vibration Research (ISVR), University of Southampton and using appropriate apparatus. This chapter describes briefly the apparatus used in all of the experiments and the analysis methods applied to the experimental data. Some of the statistical analyses used to support the results are also mentioned.

### 3.2 Apparatus

#### 3.2.1 Vibrators

##### 3.2.1.1 *Electro-hydraulic vibrator*

All the experiments involving human subjects were carried out using an electro-hydraulic vibrator, capable of producing 1 metre peak-to-peak displacement of suitable stimuli to humans (Figure 3.1). The vibrator consisted of a servo-hydraulic actuator, a vibration platform, electronic control equipment and hydraulic power supply. The seats and footrests in all experiments were mounted on the vibrator platform (an aluminium plate) with the

dimensions 1.5 by 1 by 0.22 m attached to the upper carriage frame, which in turn is driven by a servo-hydraulic actuator. The performance of the vibrator is in accordance with BS 7085 (1989): British Standard Guide to Safety aspects of experiments in which people are exposed to mechanical vibration and shock. The manual for the vibrator (Human Factors Research Unit 1-metre stroke hydraulic vibrator safety manual, HFRU 03/63) is available for further information, which incorporates the user protocol, general description of the vibrator and the safety aspects.

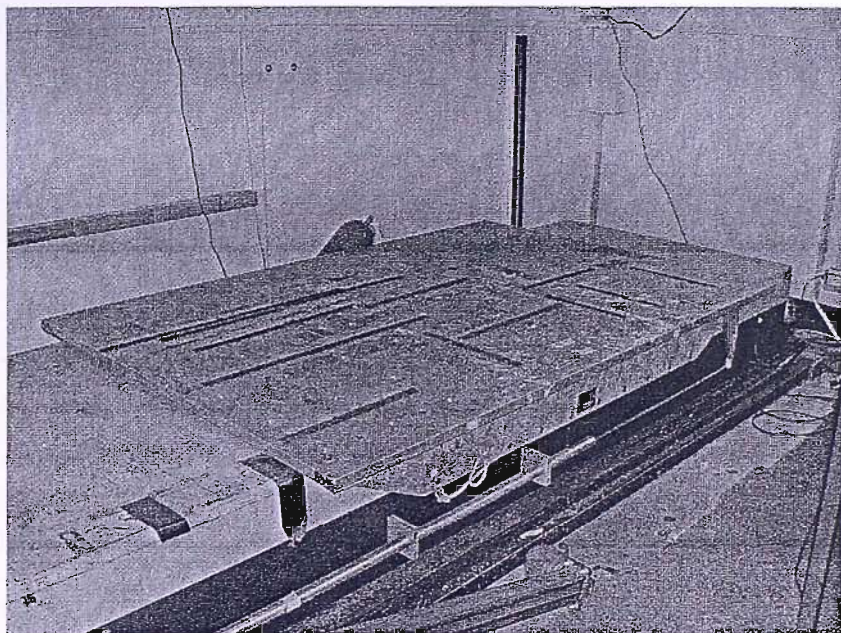


Figure 3.1: 1-metre peak-to-peak horizontal hydraulic vibrator.

### 3.2.1.2 *Electro-magnetic vibrator*

An electro-magnetic vibrator, Derritron VP 85 - 6LA (Figure 3.2) was used in the dynamic stiffness testing of the backrest and foam block. The vibrator was powered by a 1000 W Derritron amplifier and was capable of producing a maximum peak-to-peak displacement of 25.4 mm and a maximum force of 3.3 kN in the frequency range 1.5 to 5 kHz. The vibrator was used to produce vertical vibration in indenter test of the backrest cushion with the horizontal backrest cushion.

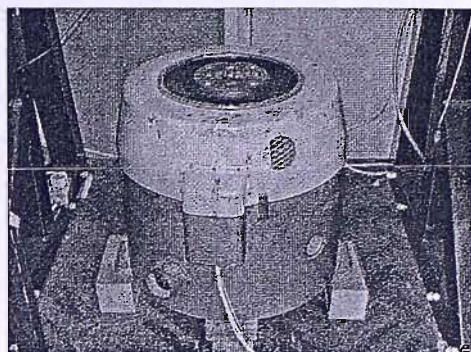


Figure 3.2: Electro-magnetic vibrator, VP 180 6LA, used in the dynamic stiffness tests.

### 3.2.2 Transducers

#### 3.2.2.1 Accelerometers

In most the experiments, the input motion to the subjects was measured and monitored using a piezo-resistive accelerometer, i.e. an Entran EGCS-Y 24-10-D (Figure 3.3). The accelerometer had a sensitivity of approximately 13 mV/g with an operating range of  $\pm 10$  g.

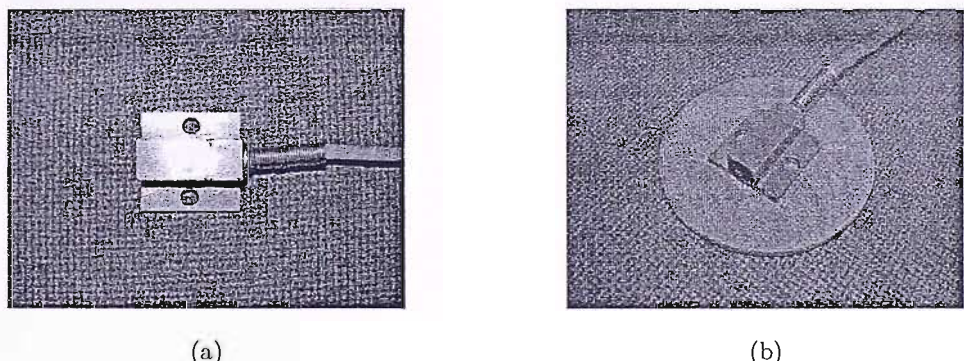
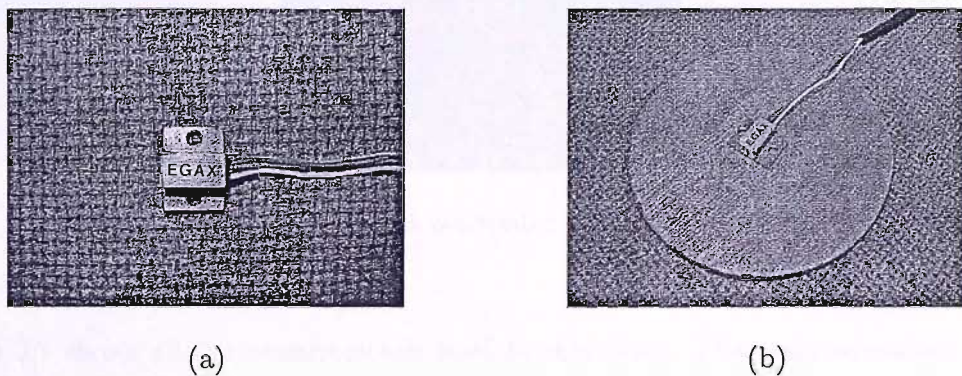
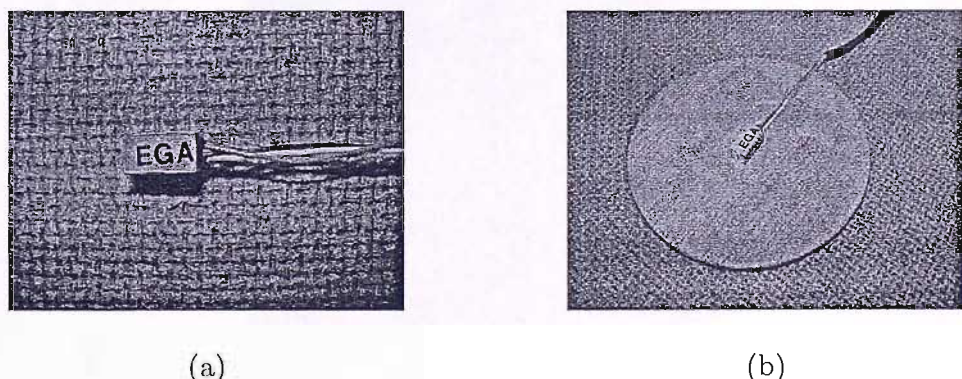


Figure 3.3: An Entran EGCS-Y 24-10-D. (a) top view of the accelerometer; (b) attachment of the accelerometer with a wooden plate of 50 mm diameter and 2 mm thickness used in some of the experiments (also known as 'mini SIT-pad').

Measurements of accelerations at the back-backrest interface at several vertical heights on the backrest from the seat surface were measured by using either EGCS-Y 24-10-D (Figure 3.3) or miniature piezo-resistive accelerometers, such as Entran EGAX-F-5 (Figure 3.4) or EGA-125F\*-10-D (Figure 3.5). The Entran EGAX-F-5 had a sensitivity of approximately 5 mV/g with an operating range  $\pm 5g$  while the Entran EGA-125F\*-10-D had a sensitivity of approximately 8 mV/g with an operating range of  $\pm 10g$ . Each of the accelerometer was attached to circular wooden plates, and is referred as 'mini SIT-pad' (see Figure 3.3(b) to Figure 3.5(b)).



**Figure 3.4:** An Entran EGAX-F-5 accelerometer. (a) Top view of the accelerometer; (b) attachment of the accelerometer with a wooden plate of 50 mm diameter and 2 mm thickness used in part of the experiment.



**Figure 3.5:** An Entran EGA-125F\*-10-D accelerometer. (a) Top view of the accelerometer; (b) attachment of the accelerometer with a wooden plate of 50 mm diameter and 2 mm thickness used in part of the experiment.

In a study, which investigated the effect of foam thickness and vibration magnitude on the fore-and-aft backrest transmissibility during fore-and-aft vibration, the acceleration at the back-backrest interface was measured using an SAE-pad (Figure 3.6), containing an Entran EGCS-Y-240D-10 accelerometer, which had a sensitivity of 13 mV/g with an operating range of  $\pm 10$  g. The SAE-pad follows the specification in the ISO 10326-1 (1992).

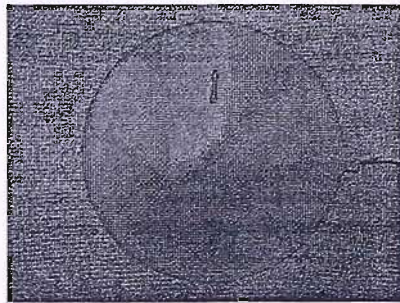


Figure 3.6: The SAE-pad, conforming the ISO 10326-1 (1992).

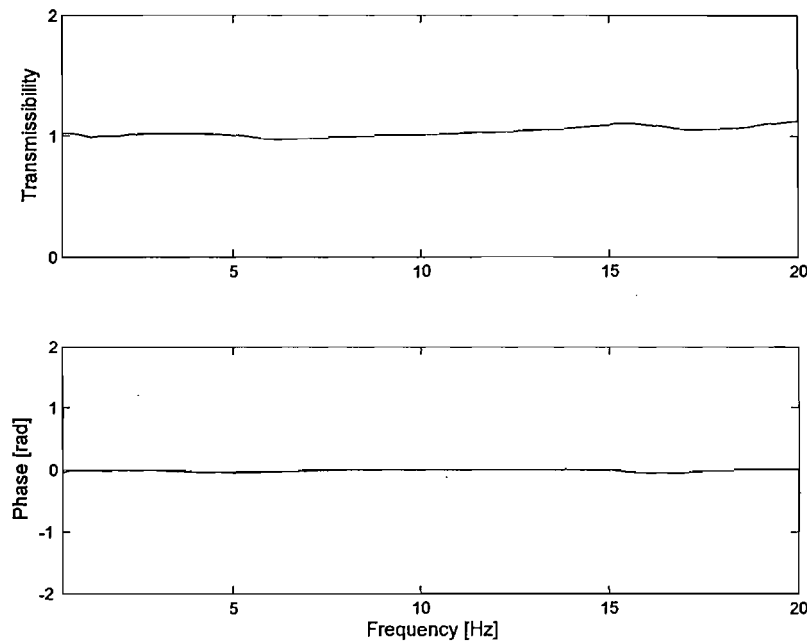
Figure 3.7 shows all the accelerometers used in this study. The main advantage of the 'mini SIT-pads' (all three from right) compared to the SAE-pad is that they were sufficiently small to allow several 'mini SIT-pads' to be placed at different locations on the backrest and measure transmissibilities at different locations at the same time.



Figure 3.7: Accelerometers used in all of the transmissibility studies. (Left: SAE-pad; all three from right: 'mini SIT-pads').

All the accelerometers were calibrated prior each experiment and checked before and after each test with subject. A d.c. calibration procedure was used, such that each accelerometer gave zero reading when it was attached to a vertical surface and  $+1$  g when it was placed on a horizontal surface and  $-1$  g when it was inverted. Ideally, with calibrated

accelerometers, the transmissibility of a rigid backrest will give a unity value. An example of a transmissibility of a rigid backrest with calibrated accelerometers is shown Figure 3.8.



**Figure 3.8:** Transmissibility and phase angle of a rigid backrest between two calibrated accelerometers with  $0.4 \text{ ms}^{-2}$  r.m.s.

### 3.2.2.2 Force transducers

The force at the back-backrest interface was measured with a force platform, either Kistler 9281 B (Figure 3.9 (a)) or Kistler 9421 A11 (Figure 3.9 (b)). Both of the force platforms consisted of four quartz piezo-electric forces transducers mounted at the corners of a rectangular welded steel frame. The former is capable of measuring forces in the  $x$ ,  $y$  and  $z$  directions, while the latter is only capable of measuring force in the direction normal to its surface. An aluminium alloy plate was bolted on each of the force platform (0.6 by 0.4 by 0.02 on the Kistler 9281 B and 0.6 by 0.4 by 0.047 m on the Kistler 9421 A11). All the force transducers had closely matched sensitivity and the signals from each of the force transducers were summed and conditioned to give the total output using Kistler 5007 charge amplifier.

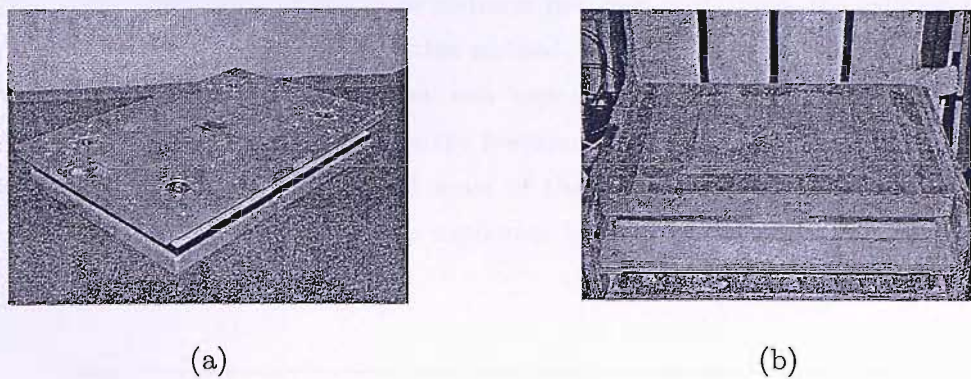


Figure 3.9: Force platforms. (a) Kistler 9281 B; (b) Kistler 9421 A11.

The total force of the back measured during fore-and-aft excitation was influenced by the mass of the top plate of force platform (i.e. the aluminium plate). When using either force platform, the effect of the mass of the plate (approximately 15 kg for Kistler 9281 B and 22.5 kg for Kistler 9421 A11) was subtracted from the measured forces with subjects in the time-domain analysis so as to obtain solely the force acting on the subjects. This is also known as '*mass cancellation*' (see Section 3.4.2.1)

The force platforms were calibrated statically and dynamically. Figure 3.10 shows an example of the static calibration of the force performed on the Kistler 9281 B. In this process, four masses with approximately 5 kg for each mass were loaded and unloaded on the force platform for 100 s and the output forces were recorded.

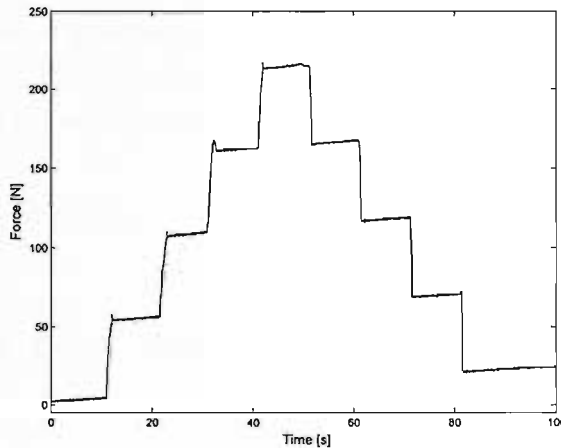


Figure 3.10: Statically calibrated force platform (Kistler 9281 B) using four masses with approximately 5 kg for each mass.

When the static calibration of the force platform has been performed, the calibrated force platform was checked dynamically. In this method, the force platform was attached to a rigid vertical backrest and the system was exposed to fore-and-aft vibration with a vibration magnitude of  $0.4 \text{ ms}^{-2}$  r.m.s. in the frequency range 0.25 to 10 Hz. Ideally, with a calibrated force platform, the apparent mass of the force platform should read 15 kg – which is the mass of the aluminum plate supported ‘above’ the force cells (Figure 3.11).

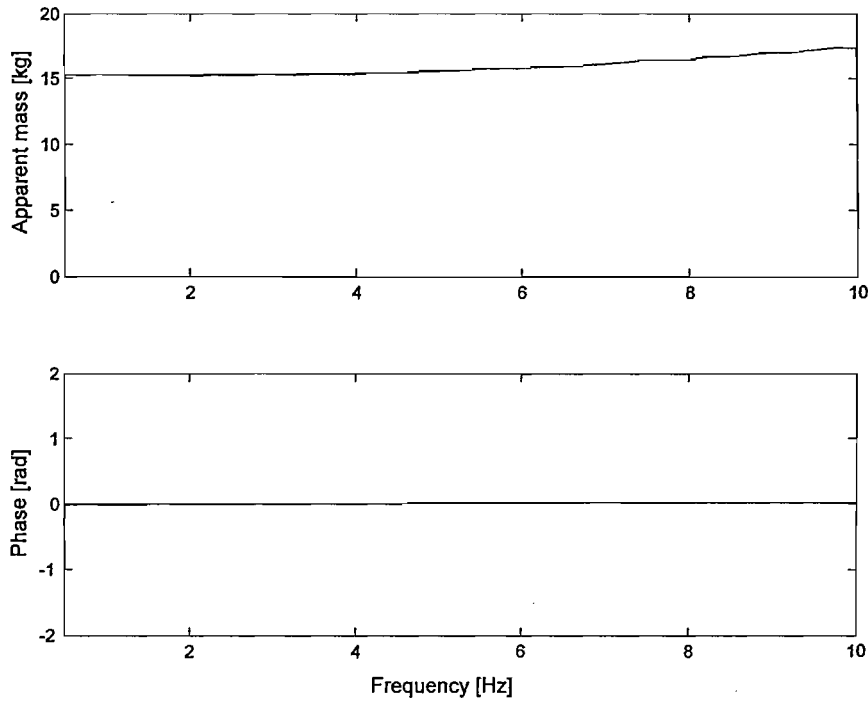


Figure 3.11: An example of measured apparent mass and phase of the force platform, giving an approximately of 15 kg in the frequency range 0.25 to 10 Hz, indicating the mass of the aluminum plate (i.e. 15 kg) supported ‘above’ the force cells.

### 3.3 Data acquisition

#### 3.3.1 *HVLab* Data Acquisition and Analysis System (version 3.81)

The input Gaussian random vibration signal in each experiment was generated using an *HVLab* Data Acquisition and Analysis system (version 3.81), which was developed at the Human Factors Research Unit. This system can acquire and analyse up to 16 channels of

time-varying analogue signals, which used an Advantech PCL-818 data acquisition card and Techfilter TF-16 anti-aliasing card. Figure 3.12 illustrates a schematic diagram of the experimental set-up used to generate the stimuli and to acquire the signals. All the input signals were low-pass filtered after which they were fed through the oscilloscope, and then to the vibrator. The vibrator can be controlled using the vibrator controller. The acceleration signals from the accelerometers and the force signals from the force platform were acquired using the same *HVLab* system through the 16-channel box. The sampling rate, duration and the magnitude of the vibration stimuli were specified in the software.

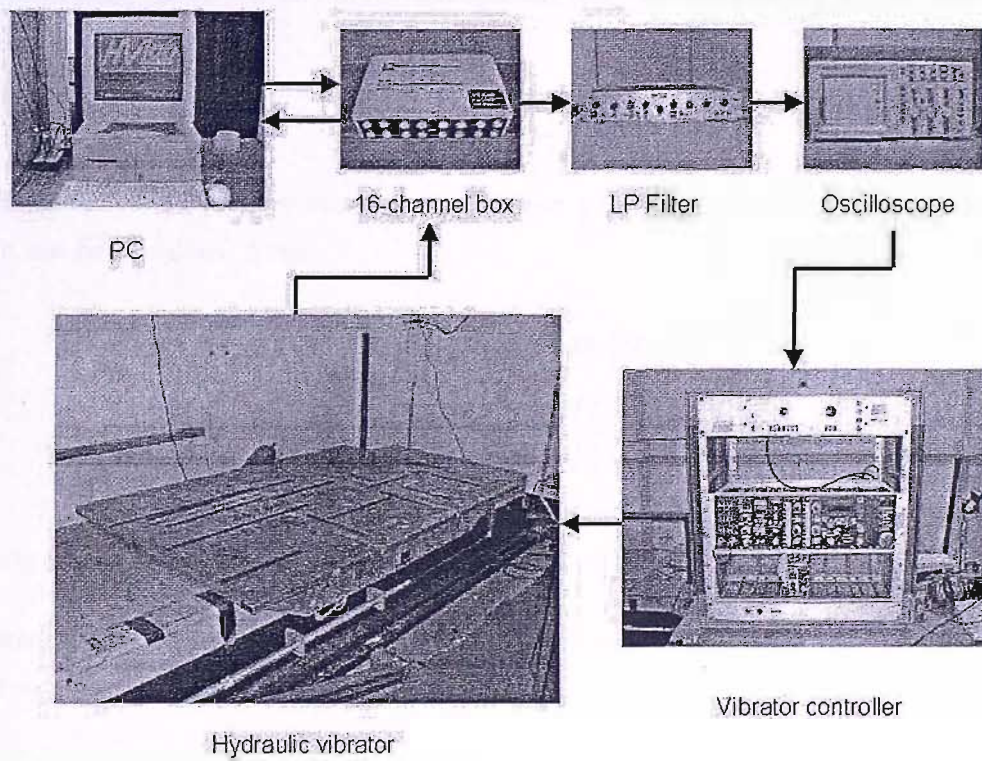


Figure 3.12: Schematic diagram of the experimental set-up to drive and acquire the output signals.

## 3.4 Data analysis: frequency response functions

### 3.4.1 Transmissibility

The vibration transmitted through the backrest during fore-and-aft excitation (i.e. the backrest transmissibility),  $H(f)$ , was calculated using a ‘cross-spectral density’ (CSD) method. The  $H(f)$  was calculated as the ratio of CSD of the input and output acceleration (i.e. the acceleration at the back-backrest interface),  $G_{io}(f)$ , to the power spectral density (PSD) of the input acceleration (i.e. the acceleration at the base of the backrest),  $G_{ii}(f)$ :

$$H(f) = \frac{G_{io}(f)}{G_{ii}(f)} \quad (3.1)$$

This function is a complex function, and it can generate modulus,  $|H|$  and phase,  $\theta$ , which can be calculated from:

$$|H(f)| = \left[ (Re[H(f)])^2 + (Im[H(f)])^2 \right]^{\frac{1}{2}} \quad (3.2)$$

$$\theta(f) = \tan^{-1} \left\{ \frac{Im[H(f)]}{Re[H(f)]} \right\} \quad (3.3)$$

where  $Re[H(f)]$  and  $Im[H(f)]$  are the real and imaginary parts of the complex transfer function  $H(f)$ , respectively.

Coherency,  $\gamma_{io}^2(f)$ , was used to inspect the linearity of the calculated transmissibility. The coherency can be calculated from:

$$\gamma_{io}^2(f) = \frac{|G_{io}(f)|^2}{G_{ii}(f)G_{oo}(f)} \quad (3.4)$$

where  $G_{oo}(f)$  is the PSD of the output and the values of  $\gamma_{io}^2(f)$  always lie in the range 0 – 1. For an ideal system with no noise interference, the coherency is unity, which indicates that the entire output is linearly correlated to the entire input.

### 3.4.2 Apparent mass

The forces at the back during fore-and-aft vibration were presented by the apparent mass function,  $M_B(f)$ , which is a transfer function of two measures (i.e. the force and the

applied acceleration) measured at the same point. The apparent mass of the back were also calculated using the CSD method:

$$M_B(f) = \frac{F_{io}(f)}{a_{ii}(f)} \quad (3.5)$$

where  $F_{io}(f)$  is the CSD of the force and acceleration and  $a_{ii}(\omega)$ , is the PSD of the input acceleration. It is also possible to calculate the apparent mass of the back using the PSD:

$$|M_B(f)|^2 = \frac{F_{oo}(f)}{a_{ii}(f)} \quad (3.6)$$

where  $F_{oo}(f)$  is the PSD of the measured force of the back.

The former method is a complex function and is capable of giving modulus,  $|M_B(f)|$  and phase,  $\theta_{M_B}$ . In contrary, the later only generate the modulus,  $|M_B(f)|$ , and includes all signals, correlated or uncorrelated (including noise).

With the CSD method, the modulus of the apparent mass of the back,  $|M_B(f)|$ , and the phase,  $\theta_{M_B}$ , were calculated:

$$|M_B(f)| = \left[ (Re[M_B(f)])^2 + (Im[M_B(f)])^2 \right]^{\frac{1}{2}} \quad (3.7)$$

$$\theta_{M_B}(f) = \tan^{-1} \left\{ \frac{Im[M_B(f)]}{Re[M_B(f)]} \right\} \quad (3.8)$$

where  $Re[M_B(f)]$  and  $Im[M_B(f)]$  are the real and imaginary parts of the complex transfer function  $M_B(f)$ , respectively. The coherency of the function can also be calculated, using Equation 3.4 to observe the linearity of the system within the frequency range of interest.

### 3.4.2.1 Mass cancellation

The measured fore-and-aft forces at the back were influenced by the apparent mass of the subject and the mass of the force plate supported on the force transducers (Section 3.2.2.2). Hence, ‘mass cancellation’ was applied to subtract the mass ‘above’ the force transducers. This mass cancellation can be applied in two methods: in a time domain or in a frequency-domain.

Rather than real time subtraction, a frequency domain technique was adopted as the measured force influenced by the mass of the plate. The plate mass was subtracted from the total measured force acting on the combined subject and force plate, such that:

$$M_B(f) = \frac{F_T(f) - F_P(f)}{a(f)} \quad (3.9)$$

where  $F_T(f)$  is the total measured force acting on the subject and the force plate,  $a(f)$  is the input fore-and-aft acceleration and  $F_P(f)$  is the force of the plate.

An alternative frequency domain method is where the real and the imaginary parts of the apparent mass of the force plate (without subject) was calculated and subtracted from the real and imaginary part of the apparent mass of the subject and the plate.

$$M_B(f) = M_T(f) - M_P(f) \quad (3.10)$$

where  $M_T(f)$  is the apparent mass of the subject and the plate, and  $M_P(f)$  is the measured apparent mass of force platform only. In practice,  $M_P(f)$  is a real quantity in the frequency range of interest, i.e. acting as a rigid mass like body.

### 3.4.3 Dynamic properties of the backrest cushion

The dynamic properties of the backrest cushion and foam backrest (i.e. the stiffness and damping) were obtained from the indenter test measurement. A schematic representation of the indenter test is shown in Figure 3.13.

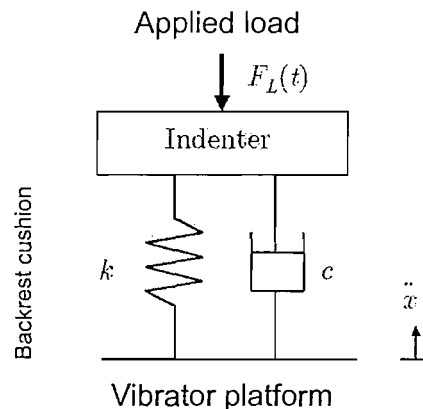


**Figure 3.13:** Schematic diagram of the backrest cushion and the indenter to obtain the dynamic properties of the backrest cushion.

The frequency response of the backrest cushion or foam when a load was applied can be written as:

$$F(t) = kx + c\dot{x} \quad (3.11)$$

where  $F(\omega)$  is the equivalent force from the platform to the force applied on the backrest/foam,  $k$  is the stiffness and  $c$  is the damping of the backrest/foam. The

displacement,  $x$ , and the velocity,  $\dot{x}$ , can be obtained by double and single integration of the measured the acceleration,  $\ddot{x}$ , respectively. Using *Laplace Transform* on the assumption that  $x(0) = 0$  and  $\dot{x}(0) = 0$  and replacing the *Laplace Transform* variable  $s$  with the angular frequency  $\omega$  based on the relation of  $s = i\omega$ , the Equation 3.11 can be written as:

$$F_L(w) = (k + cs) X(s) \quad (3.12)$$

The dynamic stiffness of the backrest cushion/foam was:

$$\frac{F_L(\omega)}{X(\omega)} = S(\omega) = k + c\omega i \quad (3.13)$$

From Equation 3.13, the stiffness,  $k$  and damping,  $c$ , of the backrests are the real and imaginary of the dynamic stiffness of the backrest/foam,  $S(\omega)$ , respectively.

## 3.5 Data analysis: statistical tests

Statistical analyses were performed to compare results between different conditions used and to test for correlations between different variables. Non-parametric statistical techniques or *distribution free tests* were used to perform the statistical tasks. This technique avoids making assumptions about the underlying distribution of the population, in particular all the subjects used in each experiment were drawn from an unknown population and the results from all subjects in each experiment were not necessarily distributed in a particular form. The statistical analyses were performed in the SPSS statistical software (version 12.0). In the course of the studies, the statistical tests were performed: i) to make comparisons between repeated measured within samples (Friedman) or between two variables or conditions (Wilcoxon), and ii) to determine whether there is a clear relation between two variables or not (Spearman) (see Siegel and Castellan (1988), or Barlow (1989), or Clegg (1990) for further information).

### 3.5.1 Friedman two-way analysis of variance

The Friedman two-way analysis of variance tests the null hypothesis of the measurements, in which the measures of  $k$  dependent samples come from the same population. It is based on the rationale that if the groups do not differ on the criterion variable, then the rankings of each subject will be random and there will be no difference in mean ranks between groups on the criterion variable.

The Friedman test can be seen as a two-way analysis of variance with one observation per cell. It can also be seen as a repeated measures analysis of variance for one group.

### 3.5.2 Wilcoxon matched-pairs signed ranks test

The Wilcoxon matched-paired signed rank test is used to test the null hypothesis that the population median of the paired differences of the two samples is zero. It is also used to test whether the mean values of two sets of data are compatible or not, given that both sets have the same number of measurements. This test uses the magnitudes as well as the signs within pairs of the two samples under investigation.

### 3.5.3 Spearman rank order correlation coefficient

The Spearman rank order correlation coefficient can be used to determine correlation between two sequences of variables. For example, this test was used to investigate whether there was a relation between the physical characteristics of the subjects (e.g. body mass, stature) and the resonance frequency of the backrest of the apparent mass of the back during fore-and-aft vibration.

A correlation coefficient is a number between -1 and 1, which measures the degree to which two variables (for example subject mass and resonance frequency of the apparent mass of the back) are linearly related. If there is perfect relationship with positive slope between the two variables, a correlation coefficient of 1 will be obtained (positive correlation). If there is a perfect relationship with negative slope between the two variables, a correlation coefficient of -1 will be obtained (negative correlation). A correlation coefficient of zero indicates that there is no relationship between the variables.

# Chapter 4

## Fore-and-aft transmissibility of backrests

### 4.1 Introduction

The vibration discomfort of seated persons in vehicles is often dominated by vertical vibration and so many studies have investigated the vertical transmissibility of seats (e.g. Whitham and Griffin, 1977; Fairley and Griffin, 1986; Corbridge *et al.*, 1989 and Wei and Griffin, 1998c). However, fore-and-aft vibration is also present on the seats of vehicles and may contribute to discomfort (Qiu and Griffin, 2003). An understanding of the transmission of fore-and-aft vibration through seats to the backrest may assist the reduction in discomfort caused by such vibration.

According to the frequency weightings in current standards, if a seat is rigid, fore-and-aft vibration at the backrest will cause more discomfort than fore-and-aft vibration on the seat at frequencies greater than about 3.15 Hz (e.g. British Standard BS 6841, 1987). The frequency weightings show a human sensitivity to fore-and-aft acceleration that falls in inverse proportion to the vibration frequency at frequencies greater than 2 Hz on the seat and at frequencies greater than 8 Hz on the backrest. Consequently, fore-and-aft backrest vibration needs to be only half the magnitude of seat vibration at 4 Hz and only a quarter of the magnitude of seat vibration at 8 Hz to cause similar discomfort to fore-and-aft seat vibration. In practice, seats are not rigid and so, at these frequencies, there is often a greater magnitude of fore-and-aft vibration on the backrest than on the supporting seat surface.

The fore-and-aft vibration on backrests has been measured in some laboratory studies with single-axis excitation and, in a few field studies, with multiple axis excitation. When

excited with vertical vibration, a pronounced peak at 4 to 5 Hz has been reported in the fore-and-aft motion of a car seat backrest (Houghton, 2003). A car seat with seated subjects showed three resonances (4 to 5 Hz, 25 to 30 Hz and 45 to 50 Hz) when exposed to fore-and-aft vibration in the laboratory study (e.g. Qiu and Griffin, 2003).

In previous studies, the backrest vibration has been measured using an accelerometer contained within a mount (i.e. a seat interface transducer pad, 'SIT-pad') positioned near the middle of the backrest, although the location has differed between studies (Qiu and Griffin, 2003 and 2004, and Houghton, 2003). International Standard ISO 10326-2 (2001) specifies that the vibration on the backrest should be measured by positioning the transducer '*in the area of principal support for the body*', although it is not clear how this position is to be found. British Standard 6841 (1987) says that measurements at the backrest '*should be made at the position with the greatest effective vibration in contact with the body*'. This gives recognition to the potential for the vibration to vary with location on a backrest, but there are no known studies investigating how the position of measurement affects the vibration on backrests.

Recent studies have found that the transmission of vibration through backrests is non-linear, showing a reduction in the resonance frequency with an increase in vibration magnitude (Qiu and Griffin, 2003). This is due, at least in part, to the non-linearity in the apparent mass of the back when subjects are exposed to fore-and-aft vibration (Nawayseh and Griffin, 2005a).

This chapter describes a study to measure the transmission of vibration through backrests of a car seat and a block of foam supported on a rigid flat frame. In addition, the variation in the transmissibility of both backrest with vertical position was investigated. It was hypothesised that the transmission of vibration through the backrests would vary with vertical position on both backrests. It was also hypothesized that, because the impedance of the human body is non-linear in the fore-and-aft direction, the fore-and-aft transmissibility would be non-linear with vibration magnitude.

## 4.2 Method

### 4.2.1 Subjects

Twelve male subjects participated in the study. All subjects were healthy and without disorders of the musculoskeletal system. Table 4.1 lists the medians and ranges of age, weight, stature, and seat-to-shoulder height of the subjects. The experiment was approved

by the Human Experimentation, Safety and Ethics Committee of the Institute of Sound and Vibration Research (ISVR), University of Southampton.

**Table 4.1** Subject age, stature, weight and seat-to-shoulder height.

	Age (yrs)	Stature (m)	Weight (kg)	Seat-to-shoulder height (m)
Minimum	20	1.65	58	0.58
Maximum	39	1.86	99	0.69
Median	24.5	1.75	72.3	0.62

#### 4.2.2 Apparatus

##### 4.2.2.1 *Vibration generation*

The experiment was conducted using a 1-metre stroke horizontal electro-hydraulic vibrator in the Human Factors Research Unit at the ISVR, University of Southampton (see Figure 3.1, Section 3.2.1.1). The vibrator was designed to reproduce motions suitable and safe for the study of human responses to vibration.

##### 4.2.2.2 *Seat description*

Two types of seat were used in the experiment: a car seat (from a popular current family car) and a rigid seat with a backrest containing of a block of foam.

The car seat weighed 19.3 kg and was constructed from a steel frame in which the backrest was connected to the seat-pan frame via a connecting-plate (Figure 4.1). The connecting-plate between the seat-pan and the backrest were screwed together to form the pivot for the backrest. The contoured cloth covers of the seat cushion and backrest contained moulded foam supported by springs. The inclination of the seat-pan was adjusted by a rotating lever located beneath the seat pan. The inclination of the backrest was adjusted by rotating a knob at the left side of the seat. The adjustments were set using a SAE H-point manikin (ISO 5353, 1978) so that the backrest was 17° from the vertical and the seat pan was 10° from the horizontal.

For measurements with the block of foam, subjects sat on a seat with a rigid frame and flat rigid horizontal and vertical wooden surfaces on the seat and backrest (Figure 4.1). The rectangular block of polyurethane foam (540 mm by 355 mm by 100 mm) had flat surfaces and was attached to the vertical backrest using Velcro. The lower edge of the

foam block was 30 mm above the horizontal surface of the flat rigid seat. There was no cushion beneath the subjects.

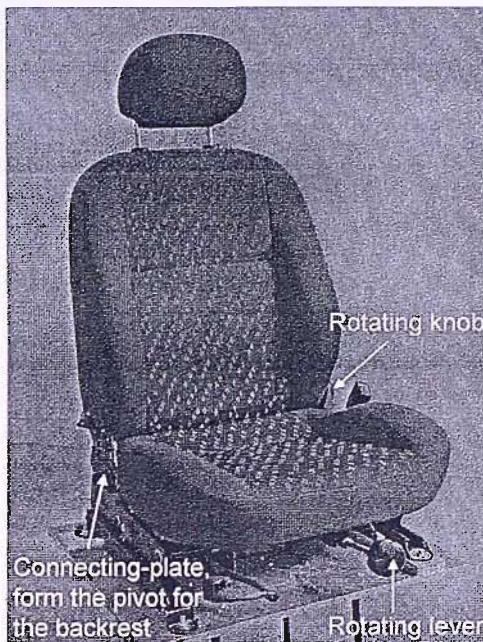


Figure 4.1: Car seat.

#### 4.2.2.3

#### *Accelerometers*

Vibration was measured using six Entran EGCS-Y 24-10-D accelerometers. Five accelerometers were attached to circular wooden plates of 50 mm diameter and 2 mm thickness (see Figure 3.3 (b), Chapter 3). Each combined accelerometer and wooden plate weighed 14 grams and is referred to as a 'mini SIT-pad'. These 'mini SIT-pads' were mounted to the surfaces of the backrests at five heights above the seat surface using Velcro. The flat surfaces of the plates faced the back of the body with the accelerometer on the side adjacent to the seat surfaces.

One Entran EGCS-Y 24-10-D accelerometer was attached to the vibrator platform beneath the seats to measure the fore-and-aft excitation.

The five locations of the 'mini SIT-pads' on the backrests were obtained by dividing the 50<sup>th</sup> percentile seat-to-shoulder height of the British male population aged 19 to 45 years

(approximately 595 mm; Pheasant, 1996) into five equal bands of 120 mm, with an accelerometer at the centre of each band. For the car seat, the location of the central 'mini SIT-pad' was assumed to be 340 mm above the seat cushion surface, after the addition of 40 mm to compensate for seat compression (Pheasant, 1996). For the foam backrest, the central 'mini SIT-pad' was 300 mm above the flat seat surface. Table 4.2 shows the height of each of the accelerometers above the supporting seat surface for both backrest types. Location 1 was nearest to the seat surface and location 5 was nearest to the top of the backrest (i.e. shoulder area). For both the car seat and the foam backrests, the accelerations were measured normal to the backrest cushion. The contoured surface of the car seat backrest cushion is assumed to have small effect on the measured acceleration.

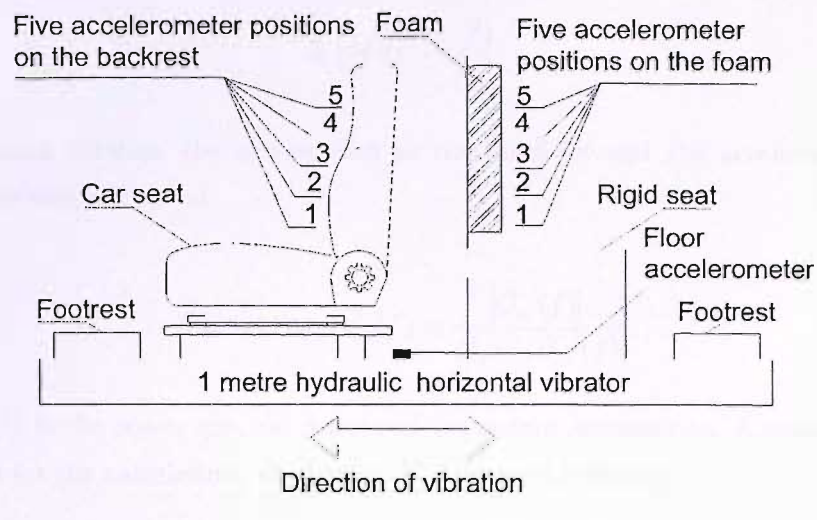
The arrangement of the experimental equipment is shown in Figure 4.2.

**Table 4.2** Locations of the accelerometers on the surfaces of the backrests and the corresponding height above the seat surface.

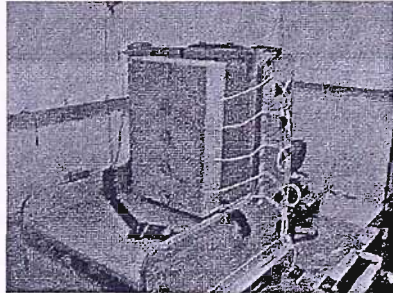
Location	Vertical distance from the seat surface (mm)	
	On foam secured to the rigid seat	On car seat (after the addition of 40 mm compensation)
1	60	100
2	180	220
3	300	340
4	420	460
5	600	640

#### 4.2.2.4 Signal generation

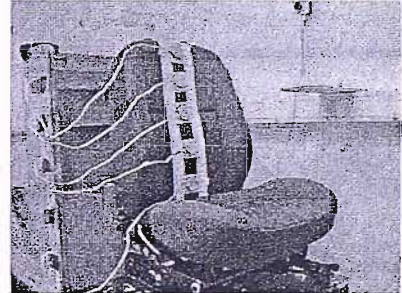
A Gaussian random signal having a duration of 60 s and a nominally flat constant-bandwidth acceleration power spectrum over the frequency range 0.25 to 20 Hz was generated using an *HVL*ab Data Acquisition and Analysis system (version 3.81). Subjects were exposed to five vibration magnitudes (0.1, 0.2, 0.4, 0.8, 1.6 ms<sup>-2</sup> r.m.s.) in independent random orders. All acceleration signals were conditioned and acquired directly into the *HVL*ab Data Acquisition and Analysis system at 512 samples per second via 170 Hz anti-aliasing filters.



(a)



(b)



(c)

Figure 4.2: Experimental set-up (a). Accelerometers attachment on the foam backrest with rigid seat (b) and on the car seat backrest (c).

### 4.3 Analysis

The acquired acceleration data were normalised to remove any d.c. offsets before they were used to calculate the modulus, phase and coherency of the backrest transmissibility for each location. The transfer functions between the floor and all five accelerometers on the backrest surface were calculated using the cross-spectral density method.

The transfer function,  $H(f)$ , was determined as the ratio of cross-spectral density of the input and output acceleration,  $G_{io}(f)$ , to the power spectral density of the input acceleration,  $G_{ii}(f)$ :

$$H(f) = \frac{G_{io}(f)}{G_{ii}(f)} \quad (4.1)$$

The coherencies between the acceleration at the platform and the accelerations on the backrest were also calculated:

$$\text{Coherency, } \gamma_{io}^2(f) = \frac{|G_{io}(f)|}{G_{ii}(f)G_{oo}(f)} \quad (4.2)$$

where  $G_{oo}(f)$  is the power spectral density of the output acceleration. A resolution of 0.25 Hz was used for the calculation, which gave 60 degrees-of-freedom.

## 4.4 Results

### 4.4.1 Inter-subject variability

Individual results show high inter-subject variability in the fore-and-aft backrest transmissibilities at each height above the seat surface with both the car seat and the foam backrest (Figure 4.3). The car seat showed resonances between 2.4 and 7.2 Hz, while the foam backrest showed resonances between 1.4 and 7.1 Hz. The resonance frequency was defined, as the frequency at which there is a peak in magnitude of the transmissibility. High coherencies (more than 0.9) were obtained at each height for all subjects and at all vibration magnitudes with both backrests.

Inspection of individual data showed that with the car seat, four subjects exhibited only one resonance frequency (in the range 2.5 to 5.7 Hz) at each height for all vibration magnitudes. Two resonances were visible for eight subjects (in the range 2.4 to 7.2 Hz): two resonance did not occur at all measurement locations – they were most visible at the middle part of the backrest. The lowest of the two resonance frequencies was in the frequency range 2.4 to 5.3 Hz, while the second resonance was evident in the range 3.3 to 7.2 Hz. For six subjects, the transmissibility at the first resonance was greater than the second resonance, while two subjects had a greater transmissibilities at the second resonance.

With the foam backrest, a single resonance (in the frequency range 1.5 to 6.1 Hz) was clearly visible for eight subjects at all vibration magnitudes. Four subjects showed two resonances in the range 1.4 to 7.1 Hz, but again not at all locations and most visible at the

middle part of the backrest. For these four subjects, the first and the second resonance frequencies were in the range 1.4 to 3.9 Hz and 3.9 to 7.1 Hz, respectively. For two subjects the transmissibility at the first resonance was greater than at the second resonance, while the other two subjects gave the opposite response.

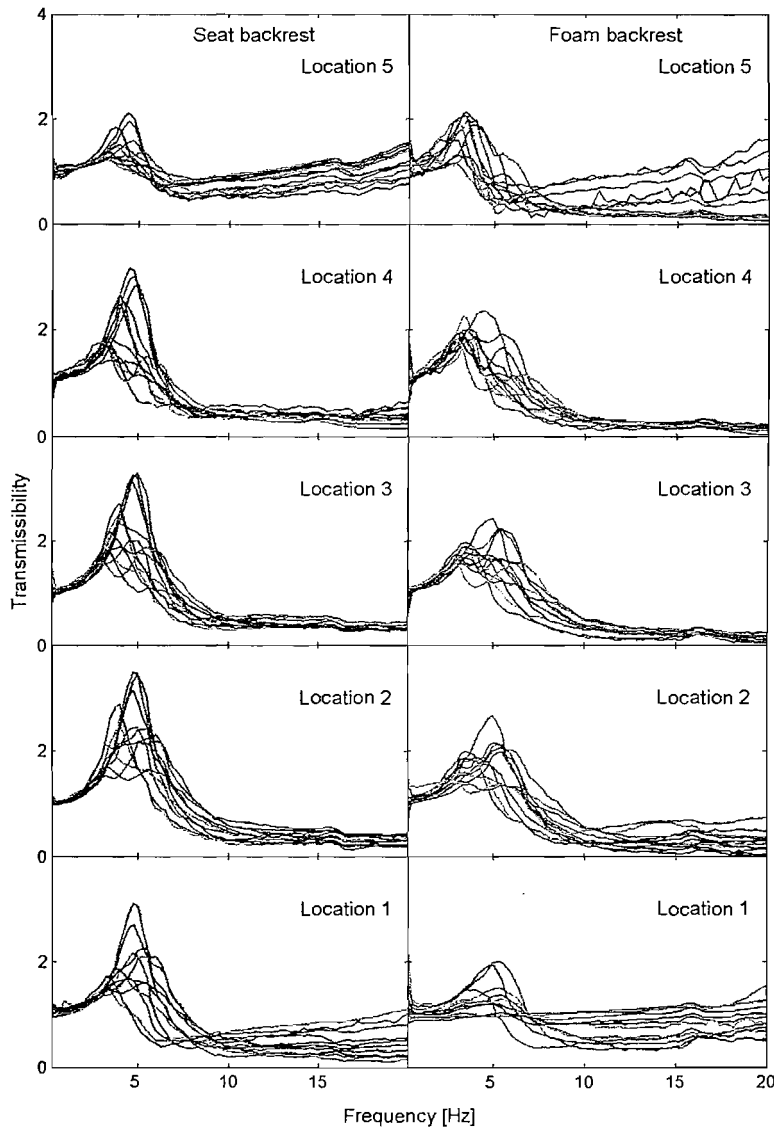


**Figure 4.3:** Inter-subject variability in the fore-and-aft transmissibilities of a car backrest and foam backrest with 12 subjects at a vibration magnitude of  $0.4 \text{ ms}^{-2}$  r.m.s. The figure shows transmissibilities at five locations (see Figure 4.2).

In general, the fore-and-aft vibration at the back-backrest interface was amplified relative to the vibrator platform at frequencies less than 7 Hz for both the car seat and the foam backrest. At frequencies greater than 7 Hz, the transmissibilities were progressively attenuated up to around 10 Hz, and remained less than 1.0 at frequencies between 10 Hz and 20 Hz.

#### 4.4.2 Variation in backrest transmissibility

Prior to calculating the median results, an artefact in an individual result with the foam backrest (in subject 6) was removed. The 'mini SIT-pad' was 'detached' from its location by the belt of the subject. Five transmissibilities at all locations (at  $0.1 \text{ ms}^{-2}$  r.m.s. with foam backrest) were excluded from the median calculations (the artefact data are not shown in the figures or tables).

The median fore-and-aft backrest transmissibilities showed resonances in the range 4 to 5 Hz for the car seat, and in the range 3 to 6 Hz for the foam backrest (Figure 4.4). With neither backrest was a second resonance evident in the median data as its influence was 'smeared' across the frequency range.

With all twelve subjects and both backrests, the fore-and-aft transmissibilities from the floor to the backrest show differences between measurement locations (Figure 4.5 to Figure 4.6; see Appendix A for all individual results). For both the car seat and the foam backrest, the transmissibilities differed significantly over the five measurement locations at the centre frequency of each preferred 1/3-octave from 2 Hz to 10 Hz at all vibration magnitudes ( $p<0.05$ ; Friedman).

A Wilcoxon matched-pairs signed ranks test was performed on the transmissibilities between measurement locations with both backrests (Tables 4.3 to 4.4). A total of 40 pairs were tested at each preferred 1/3-octave centre frequency from 2 Hz to 10 Hz and at all magnitudes (Table 4.5). With the car seat, the total number of significant differences (i.e.  $p<0.05$ , Wilcoxon) between location 1 and location 4, between location 2 and location 3, between location 2 and location 4, and between location 3 and location 4 was less than 50% of the possible differences. For other paired-locations, at least 65% of the transmissibilities differed significantly, with the transmissibilities between location 2 and location 5 having the greatest number of significant differences (90%). With the foam backrest, the number of significant differences in transmissibilities between location 2 and location 3, and between location 2 and location 5, was less than 50% of the possible differences. Between location 3 and location 5, and between location 4 and location 5, the number of statistically significant differences was 50% to 55%. For other paired-locations,

at least 65% of the transmissibilities differed significantly, with the transmissibilities between location 3 and location 4 having the greatest number of significant differences (83%).

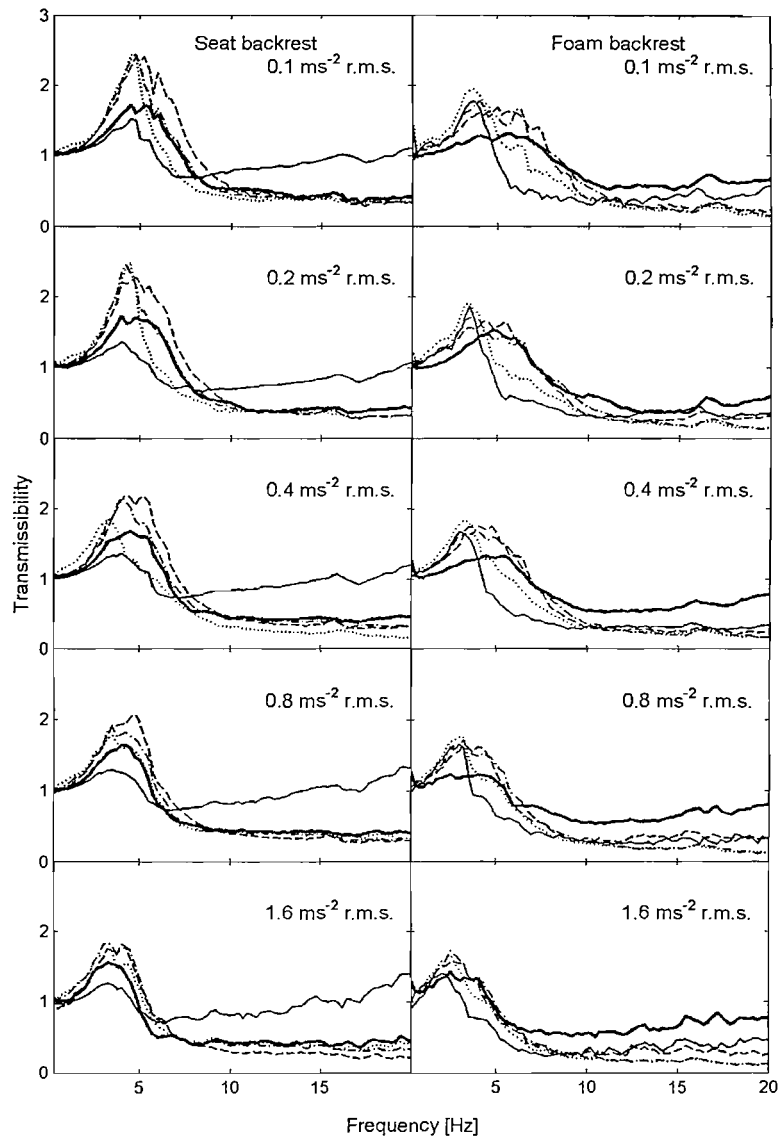


**Figure 4.4:** Median fore-and-aft backrest transmissibilities with twelve subjects for both the car backrest and the foam backrest at five magnitudes. Location 1 (—); Location 2 (---); Location 3 (----); Location 4 (.....); Location 5 (—).

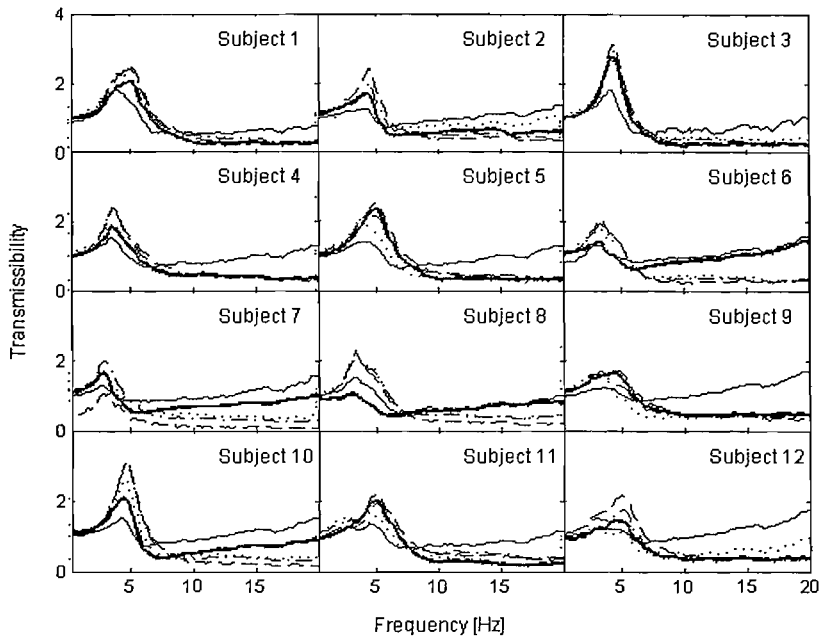


**Figure 4.5:** Variation in car seat backrest transmissibility with location for twelve subjects at a vibration magnitude of  $0.4 \text{ ms}^{-2}$  r.m.s.. Key: Location 1 (—); Location 2 (---); Location 3 (-·-·-); Location 4 (····); Location 5 (—).

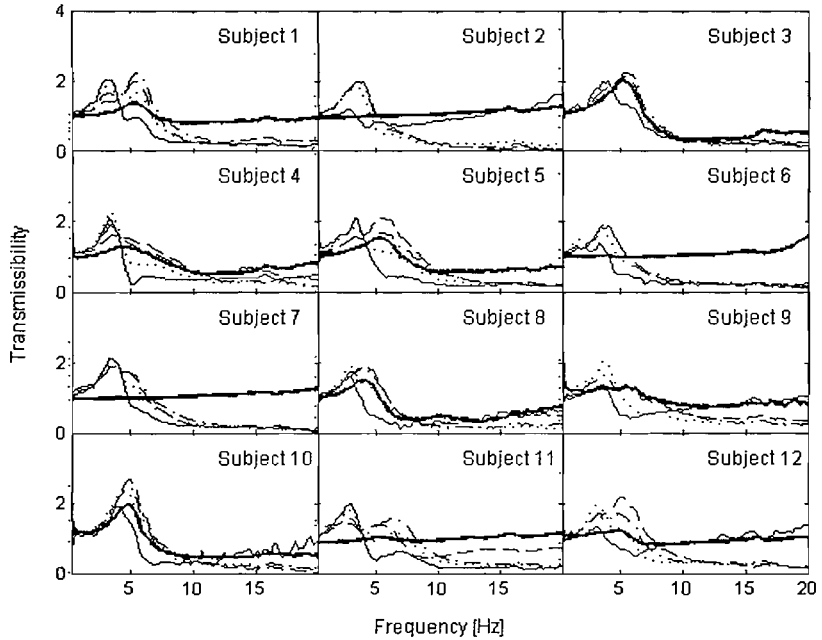


**Figure 4.6:** Variation in foam backrest transmissibility with location for twelve subjects at a vibration magnitude of  $0.4 \text{ ms}^{-2}$  r.m.s.. Key: Location 1 (—); Location 2 (---); Location 3 (-·-·-); Location 4 (····); Location 5 (—).

For both the car seat and the foam backrest, variations in the vertical position of the measurement location had little effect of the resonance frequencies shown in the median data, although the transmissibilities at resonance varied with measurement location.

With both the car seat and the foam backrest, the median transmissibilities were greater at the middle part (i.e. locations 2 to 4) than at the top (location 5) or bottom (location 1) of the backrest. The least transmissibility was measured at the top of the car seat (location 5), but at the bottom of the foam backrest (location 1). For six subjects, the transmissibilities of the foam backrest at location 1 sometimes showed 'unity transmissibility' with no evidence of a resonance (see Figure 4.6). This may have arisen from these subjects having little or no contact between the back and the backrest at this location.

**Table 4.3** Wilcoxon matched-pairs signed ranks test between backrest transmissibilities at five locations (L = location; 1, 2...5 = location position) with car seat backrest. (- =  $p > 0.05$ ; \* =  $p < 0.05$ ; † =  $p < 0.01$ ).

Vib. mag.	Freq	L1-	L1-	L1-	L1-	L2-	L2-	L3-	L3-	L4-
		L2	L3	L4	L5	L3	L4	L5	L4	L5
0.1	2	†	†	†	-	-	-	†	-	†
	2.5	†	†	*	*	-	-	†	-	†
	3.15	†	†	†	*	-	-	†	-	†
	4	†	†	†	*	-	-	†	-	†
	5	†	*	-	†	-	-	†	-	†
	6.3	†	-	-	†	†	†	†	†	-
	8	†	-	*	-	†	†	*	†	-
	10	-	-	*	*	*	*	-	-	†
0.2	2	†	†	†	-	†	*	†	-	†
	2.5	†	†	†	-	-	-	†	-	†
	3.15	*	†	†	-	-	-	†	-	†
	4	†	†	†	*	-	-	†	-	†
	5	†	*	-	*	-	-	†	-	†
	6.3	†	-	-	*	†	†	†	†	-
	8	*	-	*	-	†	†	-	*	-
	10	-	-	-	*	*	-	-	-	†

continue...

Vib. mag.	Freq	L1-	L1-	L1-	L1-	L2-	L2-	L2-	L3-	L3-	L4-
		L2	L3	L4	L5	L3	L4	L5	L4	L5	L5
0.4	2	*	<i>t</i>	<i>t</i>	-	-	<i>t</i>	*	*	<i>t</i>	<i>t</i>
	2.5	*	<i>t</i>	<i>t</i>	*	-	-	*	-	<i>t</i>	<i>t</i>
	3.15	*	<i>t</i>	<i>t</i>	-	-	-	<i>t</i>	-	<i>t</i>	<i>t</i>
	4	<i>t</i>	<i>t</i>	-	*	-	-	<i>t</i>	-	<i>t</i>	<i>t</i>
	5	<i>t</i>	-	-	<i>t</i>	*	<i>t</i>	<i>t</i>	<i>t</i>	<i>t</i>	*
	6.3	<i>t</i>	-	-	*	<i>t</i>	<i>t</i>	<i>t</i>	<i>t</i>	<i>t</i>	-
	8	*	-	*	-	<i>t</i>	<i>t</i>	-	<i>t</i>	-	<i>t</i>
	10	-	-	-	<i>t</i>	-	*	<i>t</i>	-	<i>t</i>	<i>t</i>
	2	-	<i>t</i>	*	-	-	-	<i>t</i>	-	<i>t</i>	<i>t</i>
0.8	2.5	*	<i>t</i>	*	-	-	-	<i>t</i>	-	<i>t</i>	<i>t</i>
	3.15	<i>t</i>		*	*	-	-	<i>t</i>	-	<i>t</i>	<i>t</i>
	4	<i>t</i>	*	-	*	*	<i>t</i>	<i>t</i>	<i>t</i>	<i>t</i>	*
	5	<i>t</i>	<i>t</i>	-	*	*	<i>t</i>	<i>t</i>	<i>t</i>	<i>t</i>	<i>t</i>
	6.3	<i>t</i>	*	-	-	<i>t</i>	<i>t</i>	*	*	*	-
	8	-	-	-	<i>t</i>	*	-	*	-	<i>t</i>	<i>t</i>
	10	-	-	-	<i>t</i>	-	-	<i>t</i>	-	<i>t</i>	<i>t</i>
	2	-	*	-	-	<i>t</i>	<i>t</i>	*	-	<i>t</i>	<i>t</i>
1.6	2.5	-	<i>t</i>	-	*	<i>t</i>	-	<i>t</i>	-	<i>t</i>	<i>t</i>
	3.15	<i>t</i>	<i>t</i>	-	*	-	-	<i>t</i>	<i>t</i>	<i>t</i>	<i>t</i>
	4	<i>t</i>	<i>t</i>	-	*	-	*	<i>t</i>	<i>t</i>	<i>t</i>	<i>t</i>
	5	<i>t</i>	<i>t</i>	-	-	-	*	<i>t</i>	<i>t</i>	<i>t</i>	<i>t</i>
	6.3	<i>t</i>	*	-	*	-	*	-	<i>t</i>	-	-
	8	-	-	-	*	-	-	<i>t</i>	-	<i>t</i>	<i>t</i>
	10	-	-	-	*	*	-	<i>t</i>	-	<i>t</i>	<i>t</i>

**Table 4.4** Wilcoxon matched-pairs signed ranks test between backrest transmissibilities at five locations (L = location; 1, 2...5 = location position) with foam backrest. (- =  $p > 0.05$ ; \* =  $p < 0.05$ ; † =  $p < 0.01$ ).

Vib. mag.	Freq	L1-	L1-	L1-	L1-	L2-	L2-	L2-	L3-	L3-	L4-
		L2	L3	L4	L5	L3	L4	L5	L4	L5	L5
0.1	2	<i>t</i>	<i>t</i>	<i>t</i>	*	-	<i>t</i>	-	*	-	-
	2.5	<i>t</i>	<i>t</i>	<i>t</i>	*	-	*	-	<i>t</i>	-	*
	3.15	<i>t</i>	<i>t</i>	<i>t</i>	<i>t</i>	<i>t</i>	<i>t</i>	-	<i>t</i>	-	-
	4	<i>t</i>	<i>t</i>	<i>t</i>	*	-	*	-	*	-	-
	5	<i>t</i>	*	-	*	<i>t</i>	<i>t</i>	<i>t</i>	<i>t</i>	<i>t</i>	<i>t</i>
	6.3	<i>t</i>	*	-	<i>t</i>	-	<i>t</i>	<i>t</i>	<i>t</i>	<i>t</i>	<i>t</i>
	8	-	-	*	<i>t</i>	-	*	<i>t</i>	<i>t</i>	<i>t</i>	*
	10	-	-	<i>t</i>	*	-	*	-	*	-	-
	2	<i>t</i>	<i>t</i>	<i>t</i>	<i>t</i>	-	<i>t</i>	-	<i>t</i>	-	<i>t</i>
0.2	2.5	<i>t</i>	<i>t</i>	<i>t</i>	*	-	*	-	<i>t</i>	-	<i>t</i>
	3.15	<i>t</i>	<i>t</i>	-	*	*	*	-	*	-	*
	4	<i>t</i>	<i>t</i>	*	-	-	-	-	*	*	*
	5	-	-	<i>t</i>	<i>t</i>	-	<i>t</i>	*	<i>t</i>	<i>t</i>	-
	6.3	-	-	<i>t</i>	<i>t</i>	-	<i>t</i>	*	<i>t</i>	*	-
	8	-	-	<i>t</i>	<i>t</i>	-	*	-	<i>t</i>	-	-
	10	<i>t</i>	<i>t</i>	<i>t</i>	-	-	<i>t</i>	-	*	-	-
0.4	2	<i>t</i>	<i>t</i>	<i>t</i>	*	-	<i>t</i>	-	<i>t</i>	-	*
	2.5	<i>t</i>	<i>t</i>	<i>t</i>	<i>t</i>	<i>t</i>	<i>t</i>	-	<i>t</i>	-	-
	3.15	<i>t</i>	<i>t</i>	<i>t</i>	<i>t</i>	<i>t</i>	<i>t</i>	-	*	-	-
	4	<i>t</i>	<i>t</i>	<i>t</i>	-	-	<i>t</i>	*	-	<i>t</i>	*
	5	<i>t</i>	<i>t</i>	<i>t</i>	<i>t</i>	*	-	<i>t</i>	<i>t</i>	<i>t</i>	<i>t</i>
	6.3	-	-	-	<i>t</i>	-	<i>t</i>	<i>t</i>	<i>t</i>	<i>t</i>	<i>t</i>
	8	-	-	-	<i>t</i>	-	*	*	<i>t</i>	*	-
	10	<i>t</i>	<i>t</i>	<i>t</i>	<i>t</i>	-	-	-	*	-	-

continue...

Vib. mag.	Freq	L1-	L1-	L1-	L1-	L2-	L2-	L3-	L3-	L4-	
		L2	L3	L4	L5	L3	L4	L5	L4	L5	
0.8	2	†	†	†	-	-	-	-	†	-	*
	2.5	†	†	†	-	-	-	-	-	-	*
	3.15	†	†	-	-	-	-	-	*	*	*
	4	†	†	-	*	-	†	-	†	†	†
	5	-	*	*	†	-	†	*	†	†	*
	6.3	-	-	†	†	-	-	-	†	-	-
	8	†	†	*	*	-	*	-	†	-	-
	10	†	†	-	*	*	†	-	-	*	-
1.6	2	*	†	†	*	-	-	-	-	*	†
	2.5	*	†	†	-	-	-	*	-	†	†
	3.15	†	†	†	-	-	-	†	†	†	†
	4	*	†	-	†	-	-	†	†	†	†
	5	-	-	-	†	-	-	*	†	*	-
	6.3	*	-	†	†	-	-	-	†	-	-
	8	†	†	†	†	-	-	-	*	-	-
	10	†	†	†	†	*	†	-	-	*	*

**Table 4.5** Total number of statistically significant differences (i.e.  $p < 0.05$ , Wilcoxon) between the transmissibilities at pairs of locations for all vibration magnitudes at  $1/3$ -octave centre frequencies between 2 Hz and 10 Hz.

Paired-location	Number of statically significant differences
a) Car seat	
L1 – L2	30/40
L1 – L3	26/40
L1 – L4	19/40
L1 – L5	27/40
L2 – L3	17/40
L2 – L4	18/40
L2 – L5	35/40
L3 – L4	15/40
L3 – L5	36/40
L4 – L5	33/40
b) Foam backrest	
L1 – L2	30/40
L1 – L3	30/40
L1 – L4	30/40
L1 – L5	32/40
L2 – L3	8/40
L2 – L4	26/40
L2 – L5	15/40
L3 – L4	33/40
L3 – L5	20/40
L4 – L5	22/40

There were no statistically significant correlations between subject characteristics (seat-to-shoulder measurements, stature, mass) and either the principal resonance frequencies or transmissibilities at resonance at any measurement location on either backrest ( $p > 0.05$ , Spearman).

#### 4.4.3 Effect of vibration magnitude

The effect of the vibration magnitude on the individual and median backrest transmissibilities at different measurement locations is shown in Figure 4.7 to Figure 4.9. With the car seat, the transmissibilities at each measurement location from 2 Hz to 10 Hz (at 1/3-octave frequencies) showed significant changes with vibration magnitude ( $p<0.05$ ; Friedman), except at location 5 (at 2 Hz), at locations 3 to 5 (at 3.15 Hz), at locations 1 to 3 (at 4 Hz) and at locations 1, 3 and 4 (at 10 Hz). Significant differences were also found at each measurement location with the foam backrest ( $p<0.05$ ), except at location 1 (at 2 Hz and 2.5 Hz), at locations 1 to 3 (at 3.15 Hz and 4 Hz) and at locations 1 to 2 (at 10 Hz).

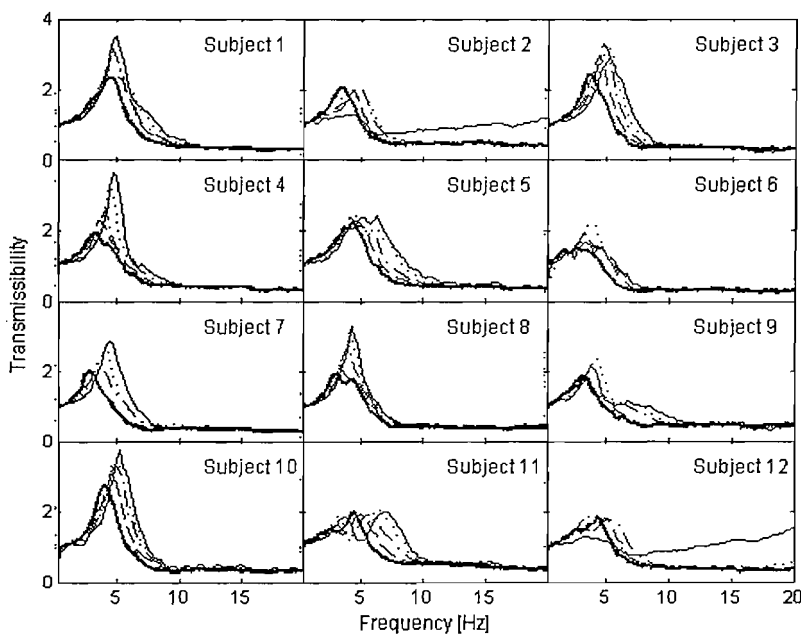


**Figure 4.7:** Fore-and-aft backrest transmissibility for twelve subjects with the car seat at location 3 at  $0.1 \text{ ms}^{-2}$  r.m.s. (—),  $0.2 \text{ ms}^{-2}$  r.m.s. (---),  $0.4 \text{ ms}^{-2}$  r.m.s. (-·-·-),  $0.8 \text{ ms}^{-2}$  r.m.s. (.....) and  $1.6 \text{ ms}^{-2}$  r.m.s. (—).

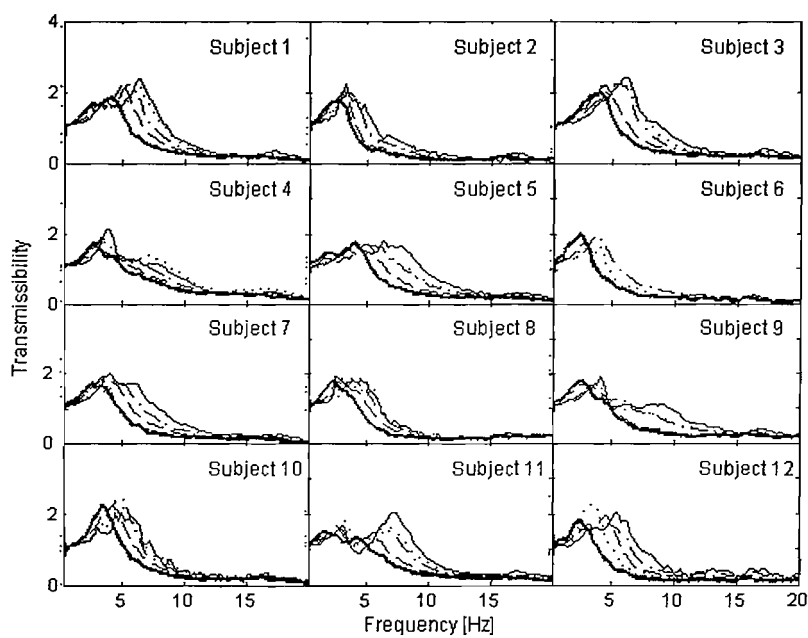


**Figure 4.8:** Fore-and-aft backrest transmissibility for twelve subjects with the foam backrest at location 3 at 0.1 ms<sup>-2</sup> r.m.s. (—), 0.2 ms<sup>-2</sup> r.m.s. (---), 0.4 ms<sup>-2</sup> r.m.s. (-·-·-), 0.8 ms<sup>-2</sup> r.m.s. (.....) and 1.6 ms<sup>-2</sup> r.m.s. (—).

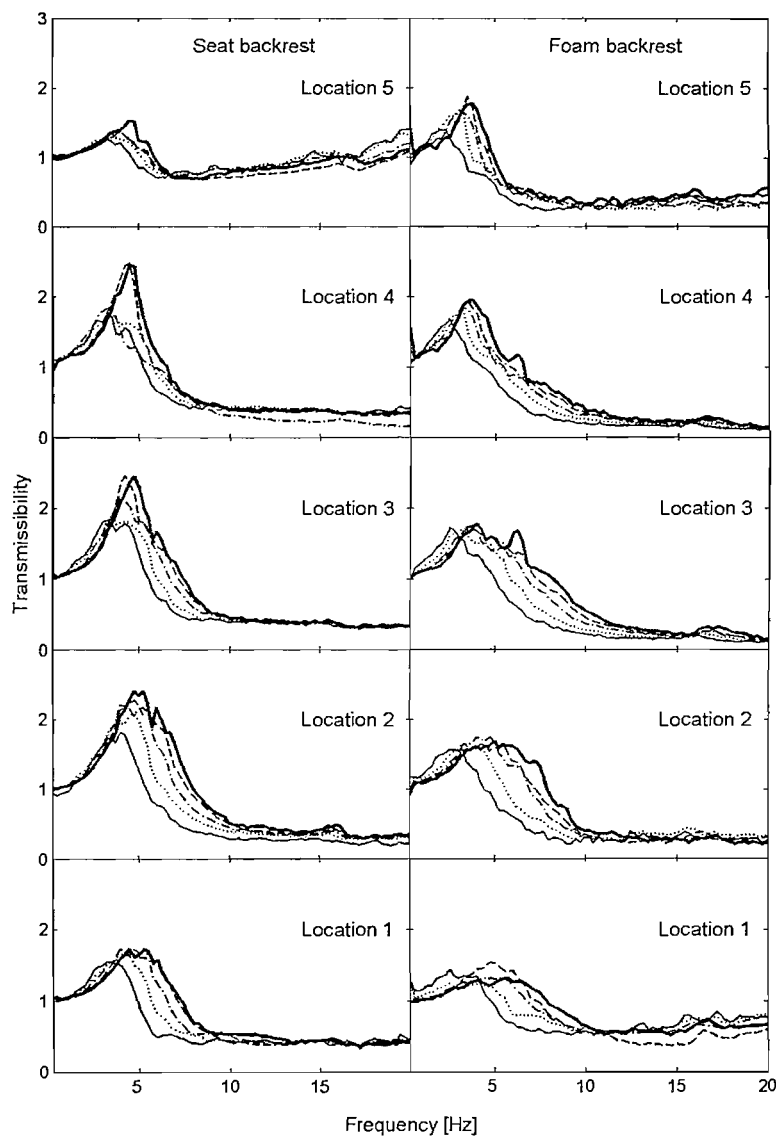


**Figure 4.9:** Median fore-and-aft backrest transmissibilities with twelve subjects for both the car seat and the foam backrests at each of five locations at  $0.1 \text{ ms}^{-2}$  r.m.s. (—),  $0.2 \text{ ms}^{-2}$  r.m.s. (---),  $0.4 \text{ ms}^{-2}$  r.m.s. (-·-·-),  $0.8 \text{ ms}^{-2}$  r.m.s. (·····) and  $1.6 \text{ ms}^{-2}$  r.m.s. (—).

## 4.5 Discussion

Prior to commencing the study, the performance of the 'mini SIT-pad' was compared with a 'SIT-pad' conforming to ISO 10326-1 (1992) with a built-in Entran EGCS-DO-10/V05/L5M accelerometer. The 'mini SIT-pad' was designed to be broadly similar to the mount described in ISO 10326-1 (1992), but sufficiently small to allow several 'mini SIT-pads' to be placed at different locations on the backrest and measure transmissibilities to different locations at the same time (Figure 4.10). The comparison involved measuring the fore-and-aft transmissibility of a foam block used as a backrest (similar to that in this experiment) at the same location in separate measurements. The location of both accelerometer mounts was the same. One subject was used and exposed to two vibration magnitudes (0.2 and 0.8  $\text{ms}^{-2}$  r.m.s.). The results showed minimal differences in the backrest transmissibility measured using the two mounts (Figure 4.11). Both the resonance frequency and the transmissibility at resonance were similar. The relative percentage difference between the measurements was less than 8% over the frequency range 0.25 to 20 Hz. It was concluded that the transmissibilities measured using the 'mini SIT-pads' as in this experiment were similar to those that would have been measured using a full-sized 'SIT-pad' according to ISO 10326-1 (1992).

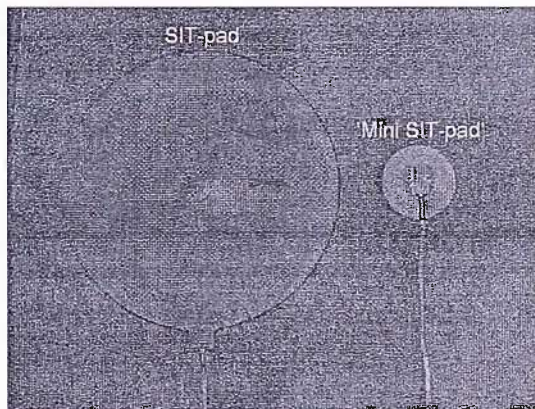
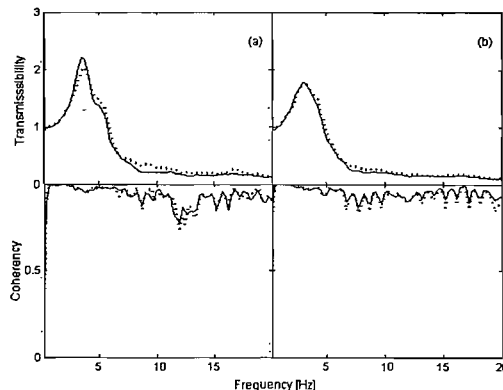


Figure 4.10: Comparison of the size of the 'mini SIT-pad' with the 'SIT-pad', according to ISO 10326-1 (1992).



**Figure 4.11:** Comparison of foam backrest transmissibility measured with the ‘mini SIT-pad’ used in this study (see Figure 4.10) (.....) and a ‘SIT-pad’, according to ISO 10326-1 (1992) (—). Key: (a) at  $0.2 \text{ ms}^{-2}$  r.m.s.; (b) at  $0.8 \text{ ms}^{-2}$  r.m.s.

In a car, the origin of the fore-and-aft vibration on the backrest may be complex: fore-and-aft, pitch and vertical vibration on the floor can all contribute to backrest vibration (Qiu and Griffin, 2003 and 2004). In the present laboratory study, the input vibration at the base of the seat was constrained to the fore-and-aft direction, even though this is often not the case in vehicles. If vertical and pitch vibration of a vehicle floor cause fore-and-aft vibration of a backrest, the variation in vibration with measurement position on the backrest may differ from that found here.

The median resonance frequencies of the backrest transmissibilities of the car seat found in this study (4 to 5 Hz) are similar with the results reported by Qiu and Griffin (2003) who investigated the fore-and-aft transmissibility of the backrest of a car seat with both field and laboratory measurements. They found that the principal resonance frequency of the fore-and-aft backrest transmissibility was in the frequency range 4 to 5 Hz.

The foam backrest showed slightly broader resonances in the frequency range 3 to 6 Hz. The difference is unlikely to be entirely due to different seat adjustment. The seat-pan and foam backrest were horizontal and vertical respectively, compared with a  $10^\circ$  inclination of the seat-pan and a  $17^\circ$  inclination of the backrest angle of the car seat. Other factors, such as a difference in the dynamic stiffness of the car backrest and the foam backrest (see Chapter 8, Section 8.3) would have affected the transmissibilities and resonance frequencies.

For a simple single degree-of-freedom vibrating system, the resonance frequency is proportional to the square root of the stiffness. It is anticipated that the foam backrest had a greater dynamic stiffness than the car seat, based on the higher resonance frequencies in

the individual results. Relating the dynamic stiffnesses of the two backrests to the measured transmissibilities merits further investigation.

The individual results showed that some subjects (four subjects with the car seat and eight subjects with the foam backrest) exhibited one principal resonance. However, other subjects (eight subjects with the car seat and four subjects with the foam backrest) showed a second resonance. The resonances can be associated with modes of the body during fore-and-aft excitation. Kitazaki and Griffin (1997) found that when seated persons were exposed to vertical vibration, the resonance frequency at 4.9 Hz consisted of an entire body mode, including a bending of the upper thoracic spine and the cervical spine. They also observed modes at 5.6 Hz and 8.1 Hz, consisting of bending and pitching modes. Matsumoto and Griffin (1998) found that the pitch transmissibilities of the first thoracic vertebra (T1) and the head had clear peaks between 5 and 7 Hz when subjects were exposed to vertical excitation. It seems possible that the resonances found in this study are related to the modes found by Kitazaki and Griffin (1997) and Matsumoto and Griffin (1998). Measurement of the apparent mass of the back at various vertical positions are required to further understand the responses of the back in the fore-and-aft direction.

The unity transmissibility at location 1 for six subjects with the foam backrest is thought to have arisen because in these subjects at this location there was little or no contact between the back and the backrest. All six subjects had a stature greater than 1.73 m, which may have influenced their sitting posture so that the lower back made less contact with the flat surface of the foam block at this location. However, there were some subjects with a stature greater than 1.73 m who showed good results and clear resonances (Figure 4.6; subjects 3 and 4). For a relatively short subject, the transmissibility at location 1 also showed a clear resonance (Figure 4.6; subject 10). The statistical analysis showed no correlation between the resonance frequency and the stature of the subjects. The unity transmissibility at location 1 in this study may therefore be attributed to some unknown individual response. The unity transmissibility was not observed with the car backrest with the same six subjects. The lumbar support in the car seat encouraged greater contact between the lower back and the backrest than occurred with the flat foam block.

Models for predicting the vertical transmissibility of a seat have assumed one connecting-point representing the interface between the seat cushion and the seated human body (e.g. Fairley and Griffin, 1986 and Wei and Griffin, 1998c). It may be reasonable to make this assumption when predicting vertical seat transmissibility because the principal load-bearing interface between the buttocks and a seat cushion is usually concentrated around the ischial tuberosities. The results of this study suggest that a backrest-back model may require more than one connecting point between the back and the backrest. The points might represent interfaces at the lower part of the backrest (e.g. location 1), the middle

part of the backrest (locations 2 to 4) and the upper part of the backrest (e.g. location 5). The development of a model for predicting the transmissibility of a backrest may require information on both the seat dynamic stiffness and the body impedance at each of these locations, or over an area encompassing these locations (see Chapter 8, Section 8.3).<sup>1</sup>

A non-linearity in fore-and-aft backrest transmissibility has been observed previously. When twelve subjects exposed to three vibration magnitudes in a car seat, the resonance frequency and transmissibility at resonance decreased with increasing vibration magnitude (Qiu and Griffin, 2003). In the present study, a similar 'softening' effect was found to apply at each height and with both types of backrest.

The non-linearity might be due a non-linear response of the body or a non-linear response of the seat, or both. It has been reported that all twelve subjects exposed to fore-and-aft whole-body vibration at four vibration magnitudes (0.125, 0.25, 0.625 and 1.25 ms<sup>-2</sup> r.m.s) showed non-linear changes in the force measured on a flat surface contacting the entire back, and the resonance frequency in the force measured at the back decreased with increasing vibration magnitude (Nawayseh and Griffin, 2005a). A further understanding of the variation in apparent mass of the back with measurement location, body posture and vibration magnitude will be required to develop dynamic models of the body for predicting seat backrest transmissibility during fore-and-aft excitation. To optimise the dynamic responses of backrests, an understanding of the importance of variations in dynamic stiffnesses of backrests with location and vibration magnitude is also required.

## 4.6 Conclusions

Laboratory measurements of the fore-and-aft transmissibilities of a car seat backrest and a foam backrest showed median resonance frequencies in the range 4 to 5 Hz, and 3 to 6 Hz, respectively.

There were large variations in the transmissibilities of both backrests at different vertical positions, although the resonance frequencies showed only small changes with position. With both seats, the median backrest transmissibilities at resonance were greater at the middle than at the top or bottom of the backrest. The transmissibility was least at the top of the car backrest but least at the bottom of the foam backrest.

The backrest transmissibilities were non-linear at all measurement locations: the resonance frequencies and transmissibilities at resonance decreased with increasing vibration magnitude.

# Chapter 5

## Factors affecting transmissibility of backrests

### 5.1 Introduction

In Chapter 4, the fore-and-aft backrest transmissibility was found to be non-linear with vibration magnitude – the resonance frequency tended to decrease with increasing vibration magnitude. The transmission of vibration through the backrest was also shown to vary significantly with vertical height from the seat surface. It is anticipated that there are many factors that can affect the fore-and-aft transmissibility of backrests during fore-and-aft vibration. This chapter describes studies conducted so as to observe the effect of: i) foam thickness, ii) vibration magnitude, iii) backrest inclination, iv) seat-pan inclination, v) push force at feet and vi) horizontal footrest position on the fore-and-aft backrest transmissibility. In all studies, the vibration to the backrest was confined to fore-and-aft excitation.

### 5.2 Effect of foam thickness and vibration magnitude

#### 5.2.1 Introduction

Vertical transmissibility of seats has been extensively studied and the transmissibility of seats showed the principal resonance frequency around 4 Hz. (e.g. Whitham and Griffin, 1977; Fairley and Griffin, 1986; Corbridge *et al.*, 1989 and Wei and Griffin, 1998c). These studies have been conducted in both laboratory and field studies.

Previous researchers have investigated some factors that can affect vertical transmissibility of seats, such as the effects of the foam thickness, subject weight, seat cushion inclination, backrest inclination and posture on the vertical transmissibility of seats.

A thin and soft cushion was found to slightly reduce the vertical transmissibility of seats used in aircraft, whereas a thick and stiffer cushion increased the transmissibility (Payne, 1969). The author concluded that thin cushion could reduce the potential spinal injury during a sudden seat ejection (which the subject was subjected to high magnitude of vibration) compared to the thick foam. Later studies found that the vertical transmissibility of polyurethane foams with twelve subjects was higher with thicker foams than thinner foams at frequencies less than 4 Hz (Ebe, 1997; Ebe and Griffin, 2000). However, at frequencies greater than 4 Hz, thinner foams showed higher transmissibility. The authors also found that thicker foams had lower resonance frequency, but higher transmissibility at resonance compared to thinner foams.

Wei and Griffin (1998a) concluded that as seat cushion inclination increased, seat transmissibility decreased at frequencies below 6 Hz but increased at frequencies above 6 Hz. In a different study, the same authors found that heavier subjects exhibited lower resonance frequency of vertical transmissibility of seats compared to less heavy subjects (Wei and Griffin, 2000). Corbridge *et al.* (1989) reported that when the backrest inclination was increased from 95° to 110° (measured from horizontal), the resonance frequency remains the same but showed slight increased in the transmissibility at resonance.

The vertical transmissibility of seats was also found to be non-linear with vibration magnitude (e.g. Fairley, 1983; Corbridge, 1987, Towards, 2001 and Houghton, 2003). The resonance frequency and transmissibility at resonance of the transmissibility decreased with increasing vibration magnitude. This is due, at least in part, to the non-linearity of body during vertical vibration (e.g. Fairley and Griffin, 1989; Corbridge *et al.*, 1989; Matsumoto and Griffin, 2000; Mansfield and Griffin, 2000 and Nawayseh and Griffin, 2003 and 2004).

Equivalent studies of seat transmissibility in the fore-and-aft direction have rarely been conducted. A study of seat transmissibility in the fore-and-aft direction in a car found several resonances, including a first resonance in the range of 4 to 5 Hz (Qiu and Griffin, 2003). In that study, the fore-and-aft transmissibility of backrest was non-linear with vibration magnitude: the resonance frequency decreased with increasing vibration magnitude. In previous chapter, it was found that the fore-and-aft transmissibility of car seat and foam backrest with twelve subjects during fore-and-aft vibration showed

resonances in the range 4 to 5 Hz, and 3 to 6 Hz, respectively. The transmissibilities of both backrests were also found to be non-linear with vibration magnitude.

In this study, it was hypothesised that the fore-and-aft transmissibility of a foam backrest would be non-linear with vibration magnitude, partly due to non-linearity of the body during fore-and-aft vibration. It was also hypothesised that with increasing foam thickness, the effective stiffness of the foam backrest would reduce – the foam may become ‘softer’, and therefore, it is expected that the resonance frequency would be reduced.

### 5.2.2 Method

#### 5.2.2.1 *Subjects*

Twelve male subjects, with mean age, weight and stature of 26 years, 69.2 kg and 1.75 m participated in the study. The experiment was approved by the Human Experimentation, Safety and Ethics Committee of the Institute of Sound and Vibration Research (ISVR), University of Southampton. Each subject was asked to complete health questionnaire and exposure consent from prior to vibration exposure.

#### 5.2.2.2 *Vibration generation*

The experiment was conducted using a 1-metre electro-hydraulic horizontal vibrator, designed to reproduce motions suitable and safe for the study of human responses to vibration (see Figure 3.1, Section 3.2.1.1). The input motion of the vibrator platform was measured and monitored using Entran EGCS-Y 24-10-D.

#### 5.2.2.3 *Seating and transducers*

A rigid seat with a rigid backrest was securely mounted on the moving platform. The flat seat surface had a 3 mm layer of a high stiffness and a high friction rubber in order to reduce any relative movements between the subjects and the seat due to sliding. Four blocks of polyurethane foam (540 by 355 mm) with thickness of either 25, 50, 100, or 200 mm were placed between the subjects and the backrest.

Two accelerometers were used to measure vibration: an Entran EGCS-Y 24-10-D and an SAE-pad conforming to ISO 10326-1 (see Figure 3.6, Chapter 3). The SAE-pad contained an Entran EGCS-Y-240D\*-10. The Entran accelerometer was mounted at the backrest at a height of 370 mm above the seat surface, while the SAE-pad was attached to the foam surface at the same level as the backrest accelerometer.

The arrangement of the experimental equipment is shown Figure 5.1.

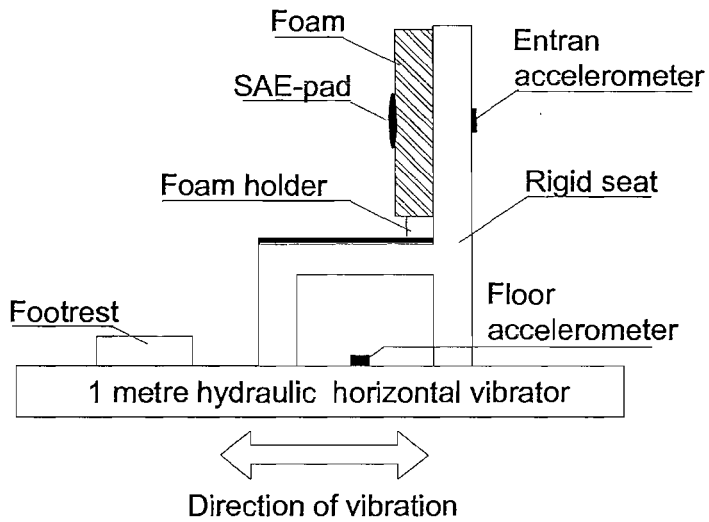


Figure 5.1: Experimental set-up.

#### 5.2.2.4 Subject posture

All subjects were asked to wear a safety belt and adopt an upright posture, making full contact of the upper body with the foam. Their hands rested on their laps and held an emergency stop button. Their upper and lower legs were approximately horizontal and vertical, respectively.

#### 5.2.2.5 Signal generation

All subjects were exposed to five vibration magnitudes (0.1, 0.2, 0.4, 0.8, 1.6  $\text{ms}^{-2}$  r.m.s.) of Gaussian random horizontal vibration with an approximately flat constant bandwidth acceleration power spectrum over the frequency range of 0.25 to 20 Hz. The vibration stimuli were generated using a *HVLab* Data Acquisition and Analysis system (version 3.81). The duration of each vibration exposure was 60 seconds. The acceleration signals were conditioned and acquired directly into an *HVLab* Data Acquisition system at 512 samples per second via 170 Hz anti-aliasing filters.

### 5.2.3 Analysis

All acceleration data were normalised by the *HVLab* Data Acquisition system and used to calculate the modulus, phase and coherency of the backrest transmissibility in each condition. Transfer functions between the backrest of the rigid seat and the SAE-pad were calculated using the ‘cross-spectral density function method’. The transfer function,  $H(f)$ , was determined as the ratio of the cross-spectral density of input and output acceleration,  $G_{io}(f)$ , to the power spectral density of the input acceleration,  $G_{ii}(f)$ :

$$H(f) = \frac{G_{io}(f)}{G_{ii}(f)} \quad (5.1)$$

The coherency between the backrest of the rigid seat and the SAE-pad were calculated to provide an indication of the acceleration at the output that was linearly correlated with the input acceleration:

$$\text{Coherency, } \gamma^2_{io}(f) = \frac{|G_{io}(f)|^2}{G_{ii}(f)G_{oo}(f)} \quad (5.2)$$

where  $G_{oo}(f)$  is the power spectral density of the output acceleration. A resolution of 0.25 Hz was used for the calculation, which gave 60 degrees-of-freedom.

### 5.2.4 Results

#### 5.2.4.1 *Inter-subject variability*

An example of the foam backrest transmissibility with twelve subjects when exposed to  $0.4 \text{ ms}^{-2}$  vibration with all foam thicknesses are shown in Figure 5.2. There is inter-subject variability but the principal resonance is in the range 1.5 to 3.0 Hz for all subjects, with the transmissibility at resonance in the range 1.3 to 2.5. Differences in posture between subjects, as well as variations in body dynamic response may have contributed to the variations in backrest transmissibility. The coherencies of the transmissibility with all foam thicknesses for all subjects and vibration magnitudes were high (more than 0.9)

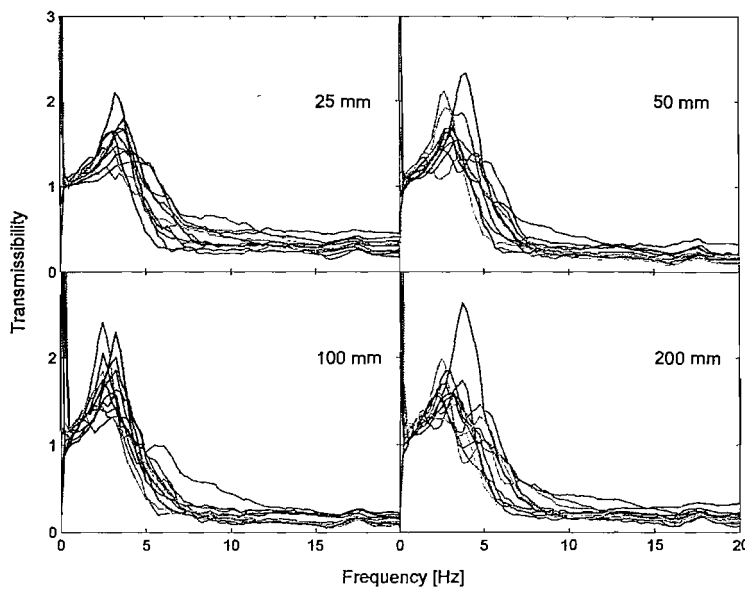


**Figure 5.2:** An example of inter-subject variability in the fore-and-aft transmissibility of foam backrest with 12 subjects at a vibration magnitude of  $0.4 \text{ ms}^{-2}$  r.m.s. The figure shows transmissibility at four different thicknesses of foams.

#### 5.2.4.2 *Effect of foam thickness*

Individual results showed evidence of reduction in the resonance frequency of the fore-and-aft transmissibility of the backrests with increasing foam thicknesses (see Appendix B). As the foam thickness was increased from 100 mm to 200 mm, the change in the resonance frequency at different vibration magnitude was not systematic

Figure 5.3 shows the median fore-and-aft transmissibility of each of the four thicknesses of the backrests at each vibration magnitude. The median principal resonance frequency of the fore-and-aft transmissibility of backrest decreased with increasing foam thickness. With twelve subjects, the resonance frequency decreased significantly as the foam thickness increased at all vibration magnitudes ( $p<0.05$ , Friedman).

With increasing foam thickness of the backrests from 25 to 100 mm, there was an increase in the transmissibility at resonance. However, with a 200 mm of foam thickness, the median transmissibility at resonance was less than the other foam thicknesses, except at  $1.6 \text{ ms}^{-2}$  r.m.s. There was a significant change in the transmissibility at resonance with twelve subjects with increasing foam thicknesses ( $p<0.05$ , Friedman).

The fore-and-aft transmissibility of backrests differed significantly over four thicknesses of foam at the centre frequency of each preferred 1/3-octave from 2 Hz to 10 Hz at all vibration magnitudes ( $p<0.05$ ; Friedman), except at 2.5 Hz (200 mm) and 10 Hz (25 mm).

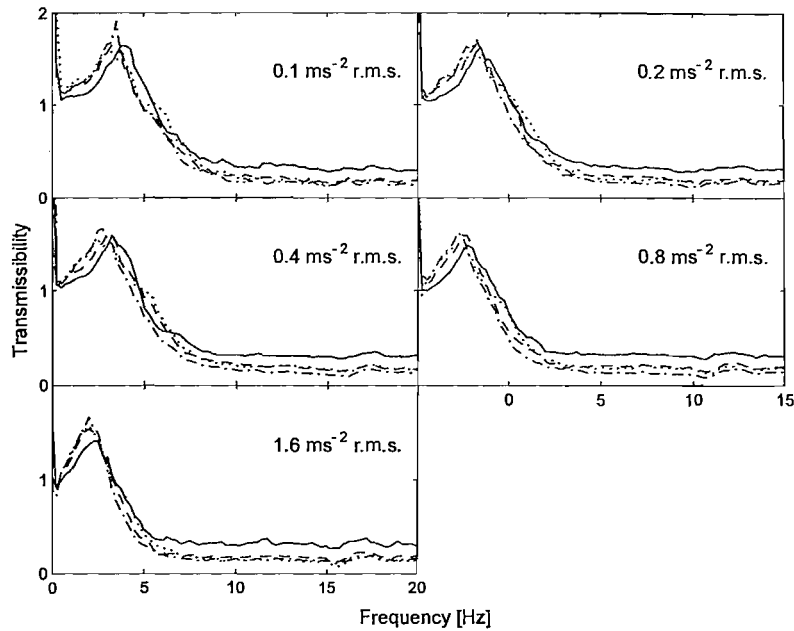


**Figure 5.3:** Median fore-and-aft backrest transmissibility for twelve subjects with foam thickness of 25 mm (—), 50 mm (---), 100 mm (- - -) and 200 mm (.....).

#### 5.2.4.3 Effect of vibration magnitude

With each foam thickness, the transmissibility of the foam backrest was non-linear with vibration magnitude on both the individual and median backrest transmissibility (Figure 5.4). The median principal resonance frequency reduced from 4 to 2 Hz when the vibration magnitude increased from 0.1 to 1.6  $\text{ms}^{-2}$  r.m.s. With twelve subjects, the resonance frequency reduced significantly with increasing vibration magnitude for all foam thicknesses ( $p<0.05$ , Friedman). There was a significant change in the resonance frequency between magnitudes with each foam thickness ( $p<0.05$ , Wilcoxon), except between 0.1 and 0.2  $\text{ms}^{-2}$  r.m.s. (all foams); 0.1 and 0.4  $\text{ms}^{-2}$  r.m.s. (50 mm foam); 0.2 and 0.4  $\text{ms}^{-2}$  r.m.s. (25 and 50 mm foams); 0.4 and 0.8  $\text{ms}^{-2}$  r.m.s. and 0.8 and 1.6  $\text{ms}^{-2}$  r.m.s. (200 mm foam).

The median transmissibility at resonance decreased from approximately 1.9 to 1.4 with increasing vibration magnitude. With twelve subjects, the transmissibility at resonance

decreased significantly with increasing vibration magnitude for all foams ( $p<0.05$ , Friedman). There was significant change in the transmissibility at resonance between paired vibration magnitude with each foam ( $p<0.05$ , Wilcoxon), except between 0.1 and 0.2  $\text{ms}^{-2}$  r.m.s. (25 and 50 mm foams); 0.2 and 0.4  $\text{ms}^{-2}$  r.m.s. (all foams); 0.4 and 1.6  $\text{ms}^{-2}$  r.m.s. (50, 100 and 200 mm foams); 0.8 and 1.6  $\text{ms}^{-2}$  r.m.s. (50, 100 and 200 mm foams); 0.2 and 0.8  $\text{ms}^{-2}$  r.m.s., 0.2 and 1.6  $\text{ms}^{-2}$  r.m.s., 0.4 and 0.8  $\text{ms}^{-2}$  r.m.s. (50 and 200 mm foams)

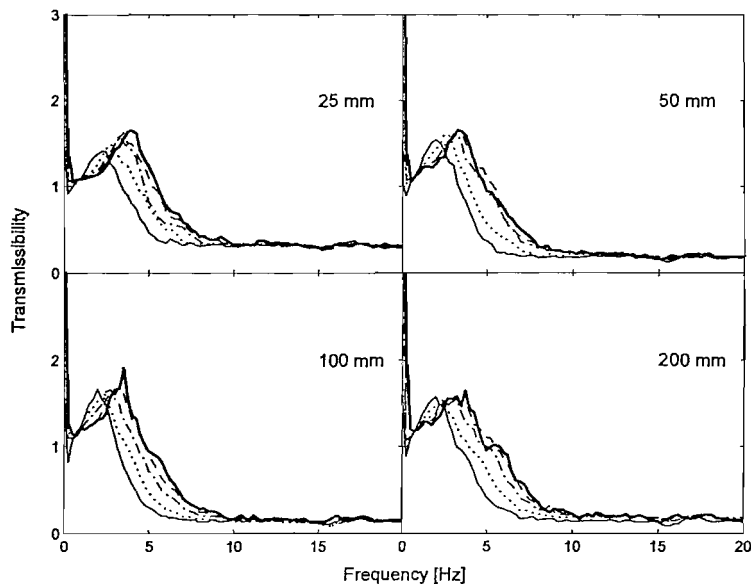


Figure 5.4: Median fore-and-aft backrest transmissibility for twelve subjects with all foam thicknesses at 0.1  $\text{ms}^{-2}$  r.m.s. (thick line), 0.2  $\text{ms}^{-2}$  r.m.s. (---), 0.4  $\text{ms}^{-2}$  r.m.s. (- - -), 0.8  $\text{ms}^{-2}$  r.m.s. (.....) and 1.6  $\text{ms}^{-2}$  r.m.s. (—).

### 5.2.5 Discussion

Although there was appreciable inter-subject variability in the foam transmissibility, the general trend for each subject was similar. The extent to which the variability is due to body characteristics or body posture requires more systematic study of the apparent mass of the back during fore-aft excitation.

Changing the foam thickness affected the fore-and-aft transmissibility of the foam backrests. Both the resonance frequency and transmissibility at resonance were significantly affected. The current study showed that thicker foam had higher

transmissibility at resonance, and higher transmissibility at frequencies less than the resonance frequency. In contrast, at frequencies higher than the resonance frequency, the thinner foam had higher transmissibility than thicker foam at frequencies up to 20 Hz.

With increasing foam thickness, the resonance frequency tended to decrease, except for 200 mm thickness. A similar finding of reducing in resonance frequency with increasing foam thickness was also found by Ebe and Griffin (2000) – a polyurethane foam with a thickness of 50 mm had resonance around 4 Hz and the frequency was lower for a 120 mm foam. When four foams with the same composition but with different thicknesses were compressed to a compression load at a speed of 100 mm/minute, the thicker foams had larger deflection and less gradient on the load-deflection curve compared to the thinner foams (Ebe, 1997). The author concluded that the thicker foam behaved as if it was softer than thinner foam. The findings of Ebe (1997) and Griffin (2000), together with the current study, suggest that that an increase in the foam thickness would reduce the foam stiffness and so reducing the resonance frequency.

As the foam thickness increased from 25 to 100 mm, there was also a significant increase in the transmissibility at resonance, except for the 200 mm foam. In theory, lower transmissibility at resonance corresponds to a high damping. The damping characteristic of foam can be represented by the hysteresis loss in a static load-deflection curve. With increasing foam thicknesses, there was a reduction in the percentage of the hysteresis loss (Ebe, 1997). The author suggested that thin foams had greater damping than thick foams. It is possible that in current study, the 25 mm foam thickness would have greater damping than the 100 mm thickness.

In the previous chapter, it was found that the fore-and-aft transmissibility of backrests varied significantly with vertical height above from the seat surface - the transmissibility around the middle part of the backrest was the greatest. The current study suggests that by increasing the thickness of the backrests cushion, the transmissibility of the foam backrest was reduced at frequencies higher than the resonance frequency. This means that changing the foam thickness can be a useful and a practical method of changing the dynamic properties of the backrests when designing a seat. However, from this study, it was only useful over the foam thickness range from 25 to 100 mm.

With vertical vibration, the effect of vibration magnitude has been linked to a 'softening' of the seat-person system with increased vibration magnitude that lowers the resonance frequency. In the previous chapter, the fore-and-aft transmissibility of a car seat and foam backrests was non-linear with vibration magnitude. It was suggested that the non-linearity might be due a non-linear response of the body or a non-linear response of the seat, or both. A similar finding was apparent in the current study: as the vibration magnitude

increased, the principal resonance frequency and the transmissibility at resonance decreased. The non-linearity in the seat-person system can be influenced by either the non-linearity of the body in response to vibration, or the non-linearity of the properties of the foam. This can be further investigated by measuring the dynamic stiffness of the foams independently of the human body dynamic response.

### 5.2.6 Conclusions

With increasing foam thicknesses of the foam backrest, there was a tendency of the resonance frequency to decrease, although the transmissibility at resonance increased with increasing foam thickness.

The transmissibility of foam backrests with different thicknesses during fore-and-aft vibration has been found to exhibit a non-linearity with vibration magnitude: the principal resonance frequency and transmissibility at resonance decreased with increasing vibration magnitude.

It is concluded that the vibration transmitted through the backrest can be reduced at frequencies greater than the resonance frequency (around 4 Hz) with an increase in foam thickness, and it is a practical and useful way for designing backrests cushion.

## 5.3 Effect of backrest inclination and seat-pan inclination

### 5.3.1 Introduction

Exposures to whole-body vibration in a car involve a variety of sitting postures that partly depend on the seat design. Car seats have inclined seat-pans and inclined backrests. For example, in a study of the transmission of vibration to the backrest of a small car by Qiu and Griffin (2003) the backrest was reclined at 15° to the vertical and the seat-pan was inclined at 12° to the horizontal, as measured with an SAE-manikin (ISO 5353, 1978). The seat-pan and backrest inclinations vary between cars and can often be adjusted by the driver.

Laboratory studies of the vertical transmissibilities of seats have used both car seats (e.g. Mansfield and Griffin, 1996) and rigid seats supporting foam cushions (e.g. Wei and

Griffin, 1998c). In some studies, the angle between the seat and the backrest has been 90°, giving an upright posture. Rakheja *et al.* (2002) suggested that the sitting postures adopted in automotive seats differed considerably from those used in laboratory studies. Both an inclined cushion and an inclined backrest were thought to contribute to the differences in the dynamic responses of subjects compared to a 90° seat-backrest angle. The authors reported that the apparent masses of subjects sitting in an automotive sitting posture showed higher fundamental resonance frequencies (i.e. 6.5 to 8.6 Hz) than those previously reported for subjects with either an upright sitting posture without a backrest or sitting on a seat with a 90° seat-backrest angle (i.e. 4.5 to 5 Hz).

Backrest inclination has been reported to have little effect on the vertical transmissibility of a seat (Corbridge *et al.*, 1989). In that study, with one subject, when the backrest was inclined from 90° to 115°, there was minimal change in the resonance frequency, but the transmissibility at resonance decreased when the backrest was inclined. Toward (2001) also noticed a decrease in the vertical transmissibility at resonance of a seat when the backrest inclination increased from 90° to 110°. Houghton (2003) found that the vertical transmissibility at resonance increased as the backrest inclination increased from 90° to 120°. In that study, subjects were exposed to vertical vibration and the transmissibilities of the seat and the backrest were measured in both the vertical and the fore-and-aft directions. The 'cross-axis' fore-and-aft backrest transmissibility (i.e. the fore-and-aft vibration of the backrest caused by the vertical excitation) showed a resonance around 4 Hz with the frequency increasing with increasing backrest inclination.

When subjects in a rigid seat with a foam cushion were exposed to random vertical vibration, there was a tendency towards increased vertical seat transmissibility at frequencies below the resonance frequency when seat-pan inclination increased from 0° to 20° (Wei and Griffin, 1998a). However, the authors found that seat-pan inclination had little effect on the resonance frequency of vertical seat transmissibility and that the vertical transmissibility at resonance decreased with increasing seat-pan inclination.

In Chapter 4, the fore-and-aft vibration transmitted from the floor to a backrest varied with height above the seat surface. In that study, twelve subjects were exposed to fore-and-aft vibration in both a car seat and a rigid seat with a foam backrest: the fore-and-aft transmissibilities of the backrest measured at five locations showed median resonance frequencies around 4 to 5 Hz for the car seat and in the range of 3 to 6 Hz for the foam backrest. Although the transmissibilities varied with height on both backrests, the resonance frequencies showed minimal changes with height for both backrests.

There is little knowledge of factors that influence the fore-and-aft transmissibilities of seat backrests. Recent studies have found that backrest transmissibility is non-linear with

vibration magnitude (e.g. Qiu and Griffin, 2003). The transmissibility of a foam backrest is affected by foam thickness - there was a tendency of the resonance frequency to decrease with increasing foam thicknesses (see section 5.1). There is no known study of the effect of the backrest inclination or seat-pan inclination on backrest transmissibility in the fore-and-aft direction.

Variations in the inclination of either the seat-pan or the backrest will change the lumbar curve, partly by rotation of the pelvis (Andersson *et al.*, 1979). Rotation of the pelvis will alter sitting posture and the biodynamic responses of the body. If the variations in inclination result in large changes in the fore-and-aft impedance of the back, the transmissibility of the backrest is likely to change, since the backrest transmissibility is determined by the dynamic interaction between the back and the backrest.

The objective of this study was to investigate the effects of backrest inclination and seat-pan inclination on the fore-and-aft transmissibility of the backrest of a car seat and of a backrest consisting of a rectangular block of solid foam supported on a rigid flat vertical plate. It was hypothesized that changing the backrest inclination and changing the seat-pan inclination would change backrest transmissibility.

### 5.3.2 Method

#### 5.3.2.1 Subjects

Twelve male subjects, with ages, weights, statures and seat-to-shoulder heights as shown in Table 5.1, participated in the study. The experiment was approved by the Human Experimentation, Safety and Ethics Committee of the Institute of Sound and Vibration Research (ISVR), University of Southampton. Prior to vibration exposure, each subject completed a health questionnaire and an exposure consent form.

Table 5.1 Subject age, stature, weight and seat-to-shoulder height.

	Age (yrs)	Stature (m)	Weight (kg)	Seat-to-shoulder height (m)
Minimum	20	1.64	50	0.58
Maximum	29	1.78	85	0.64
Median	23.8	1.72	67.7	0.62

### 5.3.2.2 *Vibration generation*

The experiment was performed in the Human Factors Research Unit at ISVR, University of Southampton, using an electro-hydraulic vibrator capable of producing a 1-metre peak-to-peak horizontal displacements (see Figure 3.1, Section 3.2.1.1). The motion of the vibrator was measured using an Entran EGCSY-240D\*-10 accelerometer mounted on the moving platform.

### 5.3.2.3 *Seating and transducers*

Most of the apparatus (seat, accelerometers, etc.) used in this experiment was the same as that used in Chapter 4. The two seats were: (i) a car seat (from a popular current family car) and (ii) a rigid wooden seat with flat surfaces and adjustable backrest and seat-pan inclinations, with the backrest supporting of a block of polyurethane foam (540 mm by 355 mm by 100 mm).

The car seat had contoured surfaces on the cushion and backrest and weighed 19.3 kg. The inclination of the backrest could be changed through a built-in mechanism controlled by a rotating knob, located at the left side of the seat. The seat cushion inclination could be adjusted through a built-in gear mechanism via a rotating lever located beneath the seat pan.

A magnetic protractor, capable of measuring angle to the vertical and horizontal, was used to measure the backrest and seat-pan angles. The protractor was attached at the left side of the backrest using double-sided adhesive tape when measuring the backrest inclination. For measuring the seat-pan inclination, the protractor was placed on the uncompressed surface of the seat cushion. For measurements with the block of foam, the angles of the wooden backrest and seat-pan were adjusted and then secured using bolts and clamps.

The fore-and-aft acceleration at the back-backrest interface was measured using six Entran EGA-125F\*-10-D accelerometers attached to circular wooden plates (50 mm in diameter), similar to that employed in Chapter 4. The total weight of each accelerometer with the wooden block was approximately 5 grams, and is referred to as a 'mini SIT-pad'. The flat surface of the plate faced the backrest with the accelerometer on the side adjacent to the body.

The 'mini SIT-pads' were positioned at six locations on the backrest, corresponding to the locations of specific vertebrae for a 50<sup>th</sup> percentile male (Singley and Haley, 1978). Table 5.2 lists the locations of the 'mini SIT-pads', measured vertically from the seat surface, and

the corresponding vertebrae. The 'mini SIT-pads' were always normal to the surface of the backrest, and so the orientation of the accelerometer varied with backrest inclination.

The experimental set-up is shown in Figure 5.5.

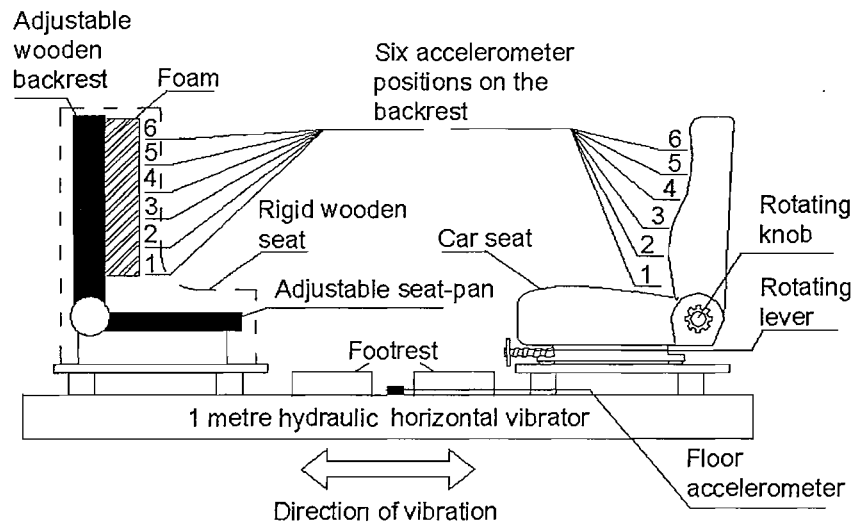


Figure 5.5: Experimental set-up.

Table 5.2 Height of the 'mini SIT-pads' on the backrests and their approximate locations relative to spinal vertebrae (from Singley and Haley, 1978).

Location	Vertical distance, measured to the centre of the mini SIT-pad from the seat surface (mm)	Corresponding spinal position or vertebrae
1	200	Pelvis
2	300	Lumbar 1
3	350	Thoracic 12
4	400	Thoracic 11
5	450	Thoracic 9
6	500	Thoracic 7

#### 5.3.2.4 Subject posture and experimental conditions

Subjects adopted a 'normal' upright posture throughout the experiment. The posture was defined as: '*upper body leaning on the backrest with hands placed on the lap and feet resting*

on the wooden footrest'. The upper and lower legs of subjects were perpendicular to each other throughout the experiment.

Two conditions were studied: the first investigating the effect of backrest inclination and the second investigating the effect of seat-pan inclination (Table 5.3). In both conditions, the backrest transmissibilities were measured in an independent random order of backrest and seat-pan inclination.

**Table 5.3** Experimental conditions.

	Car seat	Foam backrest
Condition (i): effect of backrest inclination.	90°, 95°, 100° and 105° with 10° of seat-pan inclination	90°, 95°, 100° and 105° with 0° of seat-pan inclination
Condition (ii): effect of seat-pan inclination.	10° and 15° with 95° of backrest inclination	0°, 5°, 10° and 15° with 90° of backrest inclination

The footrest height was adjusted at each seat inclination to maintain the same leg posture: upper and lower legs perpendicular to each other at all seat-pan inclinations.

#### 5.3.2.5 Signal generation

All twelve subjects were exposed to  $0.4 \text{ ms}^{-2}$  r.m.s. of Gaussian random vibration having a duration of 60 s with a nominally flat constant bandwidth acceleration spectrum over the frequency range 0.25 to 20 Hz. The vibration stimuli were generated using a *HVLab* Data Acquisition and Analysis system (version 3.81). All acceleration signals were conditioned and acquired directly into the *HVLab* Data Acquisition system at 512 samples per second via 170 Hz anti-aliasing filters.

#### 5.3.3 Analysis

The transfer functions between the floor and the backrest surface at each backrest angle and each seat angle were calculated using the 'cross-spectral density function method' using equation 5.1 (see Section 5.2.3). The coherencies of the transfer functions were calculated using equation 5.2 (see Section 5.2.3). A resolution of 0.25 Hz was used for the calculation, which gave 60 degrees-of-freedom (i.e. the number of independent variables in an estimate).

### 5.3.4 Results

#### 5.3.4.1 Effect of backrest inclination

Individual results suggested that the resonance frequencies of the fore-and-aft transmissibility of the car seat backrest at all locations tended to increase with increasing backrest inclination from 90° to 105° (Figure 5.6). There was also an increase in the transmissibilities at frequencies between 4 and 8 Hz with increasing backrest inclination, so the transmissibilities at resonance also increased with increasing backrest inclination.

With the foam backrest, the results from all twelve subjects showed minimal changes in the resonance frequencies of the fore-and-aft transmissibility of the backrest when the backrest inclination increased from 90° to 105° (Figure 5.7). There was also little change in the transmissibilities at resonance as the backrest inclination varied.

Figure 5.8 shows the median fore-and-aft backrest transmissibilities over the twelve subjects with both the car seat and the foam backrest at all six locations with varying backrest inclination. There was a resonance around 4 Hz for both backrests at all six locations. The median resonance frequencies increased as the backrest inclination increased from 90° to 105° with the car seat, more obviously at the bottom of the backrest (location 1) than at the top of the backrest (location 5). The increase in the resonance frequency of the car seat with increasing backrest inclination was statistically significant at locations 1 to 2 ( $p<0.05$ , Friedman). However, varying the inclination of the foam backrest had no significant effect on the median resonance frequency at any measurement location (Table 5.4,  $p>0.05$ ).

**Table 5.4** Effect of backrest inclination on the median resonance frequencies of the fore-and-aft transmissibilities at all six locations for both the car seat and the foam backrest (median data).

Location	Resonance frequency (Hz)								
	Car seat				Foam backrest				
	90°	95°	100°	105°	90°	95°	100°	105°	
1	3.75	4.5	4.75	4.75	3.75	4	4.25	4	
2	4.25	4.25	4.5	4.5	3.75	3.75	4	4	
3	4	4.25	4.5	4.5	3.75	3.5	4	3.5	
4	4	4	4	4.5	3.75	3.5	4	3.75	
5	4	3.75	4	4.5	3.75	3.5	3.5	3.25	
6	4	3.75	4	4.5	3.75	3.5	3.25	3.25	

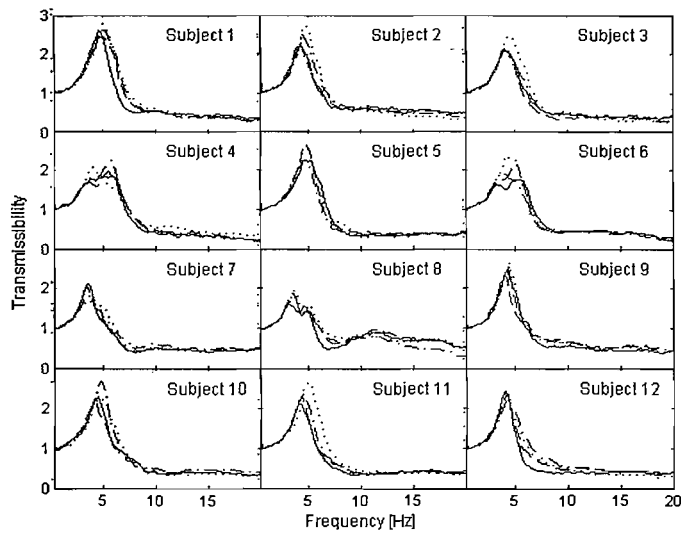


**Figure 5.6:** Fore-and-aft backrest transmissibility for twelve subjects with the car seat measured at location 3 at backrest inclinations of  $90^\circ$  (—),  $95^\circ$  (---),  $100^\circ$  (—·—) and  $105^\circ$  (·····).

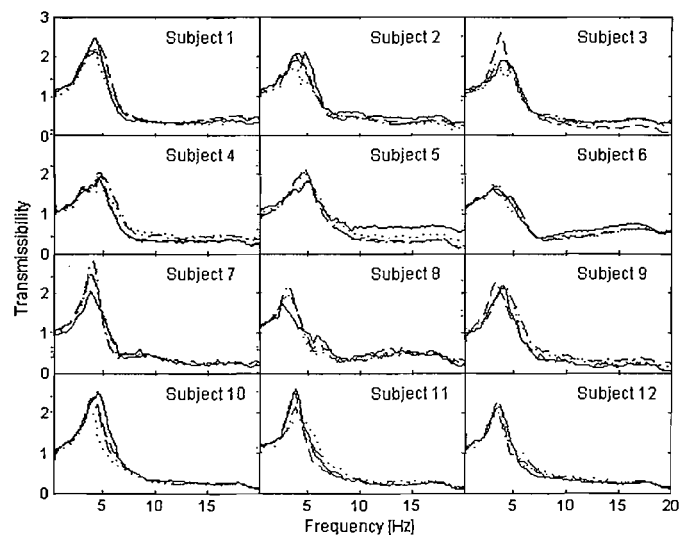


**Figure 5.7:** Fore-and-aft backrest transmissibility for twelve subjects with the foam backrest at location 3 at backrest inclinations of  $90^\circ$  (—),  $95^\circ$  (---),  $100^\circ$  (—·—) and  $105^\circ$  (·····).

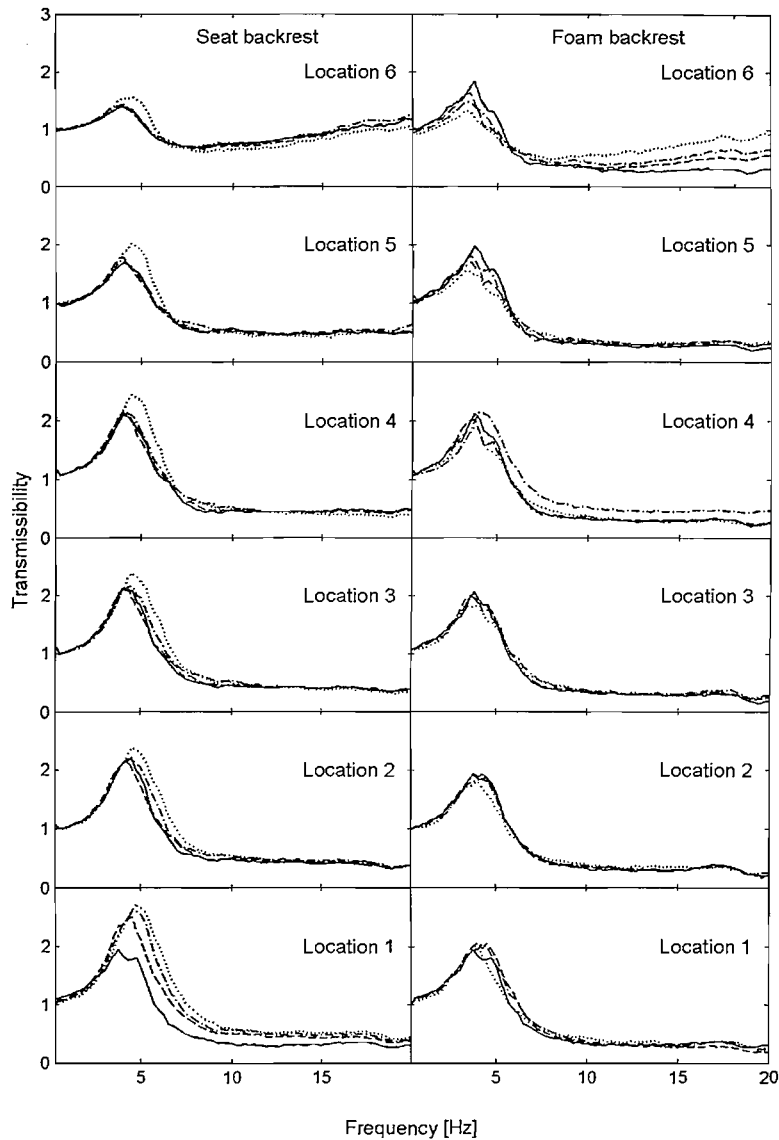


Figure 5.8: Median fore-and-aft backrest transmissibilities with twelve subjects for both the car seat backrest and the foam backrest at each of six locations at backrest inclinations of 90° (—), 95° (---), 100° (-·-·-) and 105° (····).

For the car seat backrest, the median transmissibilities at resonance increased with increasing backrest inclination from 90° to 105°, with the influence most obvious at location 1 (Table 5.5). Statistical analysis with the data from the car seat showed significant increases in the transmissibility at resonance at all locations ( $p<0.05$ , Friedman), except at location 6 ( $p>0.05$ ). With the foam backrest, increasing the backrest inclination resulted in a significant reduction in the transmissibility at resonance at the top of the backrest (i.e. locations 5 and 6,  $p<0.05$ ), but no significant change at other locations on the backrest ( $p>0.05$ ).

**Table 5.5** Effect of backrest inclination on the median transmissibilities at resonance for the fore-and-aft transmissibilities at all six locations for both the car seat and the foam backrest (medians of 12 subjects).

Location	Transmissibility at resonance							
	Car seat				Foam backrest			
	90°	95°	100°	105°	90°	95°	100°	105°
1	1.9	2.48	2.59	2.68	1.91	2.05	2.02	1.97
2	2.19	2.15	2.21	2.36	1.96	1.88	1.88	1.79
3	2.11	2.16	2.17	2.37	2.04	1.98	1.67	1.81
4	2.07	2.10	2.15	2.44	2.11	2.02	2.14	1.85
5	1.67	1.79	1.71	2.01	1.94	1.79	1.68	1.55
6	1.37	1.42	1.41	1.54	1.83	1.63	1.48	1.33

#### 5.3.4.2 Effect of seat-pan inclination

Individual results suggest that increasing the inclination of the seat-pan from 10° to 15° in the car seat and from 0° to 15° in the foam seat tended to decrease the resonance frequency in the fore-and-aft transmissibility of both backrests (Figures 5.9 to 5.10). The transmissibility at resonance increased with increasing seat inclination from 10° to 15° in the car seat but there were only small changes with the foam backrest when the seat inclination increased from 0° to 15°.

The median results appear to show a consistent trend with increasing seat-pan inclination: the resonance frequency tended to decrease with a more inclined seat-pan with both backrests (Figure 5.11 and Table 5.6). However, the influence of the seat-pan inclination on the fore-and-aft transmissibility was not statistically significant with either backrest ( $p>0.05$ , Friedman). With increases in seat-pan inclination from 10° to 15°, the median fore-and-aft transmissibilities of the car seat backrest tended to increase at frequencies

close to, and below, the resonance frequency, but decrease at frequencies greater than the resonance frequency. With variations in seat-pan inclination between  $0^\circ$  and  $15^\circ$ , the median transmissibilities of the foam backrest showed little change at any frequency between 0.25 Hz and 20 Hz.

**Table 5.6** Effect of seat-pan inclination on the median resonance frequencies of the backrest fore-and-aft transmissibilities at all six locations for both the car seat and the foam backrest (medians of 12 subjects).

Location	Resonance frequency (Hz)					
	Car seat		Foam backrest			
	$10^\circ$	$15^\circ$	$0^\circ$	$5^\circ$	$10^\circ$	$15^\circ$
1	4.75	4.25	4.25	4	4	4.25
2	4.5	4.25	3.75	3.75	3.75	3.75
3	4.5	4.5	3.75	3.5	3.5	3.5
4	4	4.25	3.5	3.5	3.5	3.25
5	4	4	3.5	3.5	3.5	3.25
6	4	4	3.5	3.3	3.5	3.25

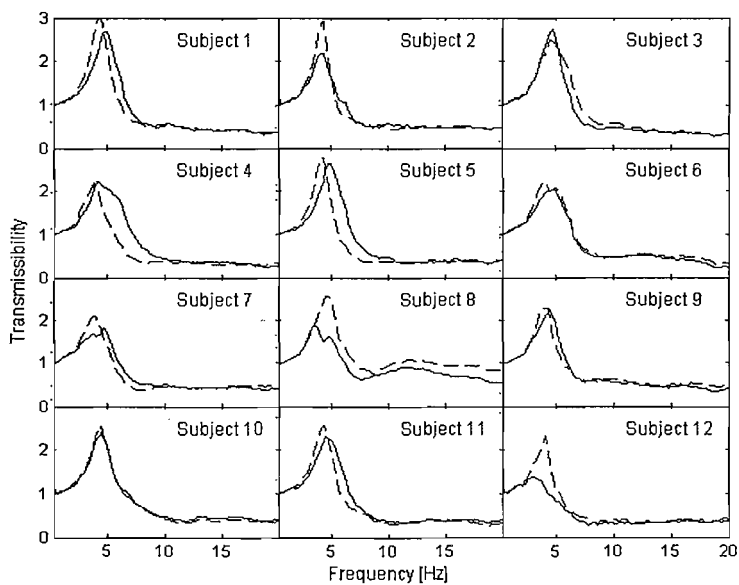


**Figure 5.9:** Fore-and-aft backrest transmissibilities for twelve subjects with the car seat backrest at location 3 at seat-pan inclinations of  $10^\circ$  (—) and  $15^\circ$  (---).

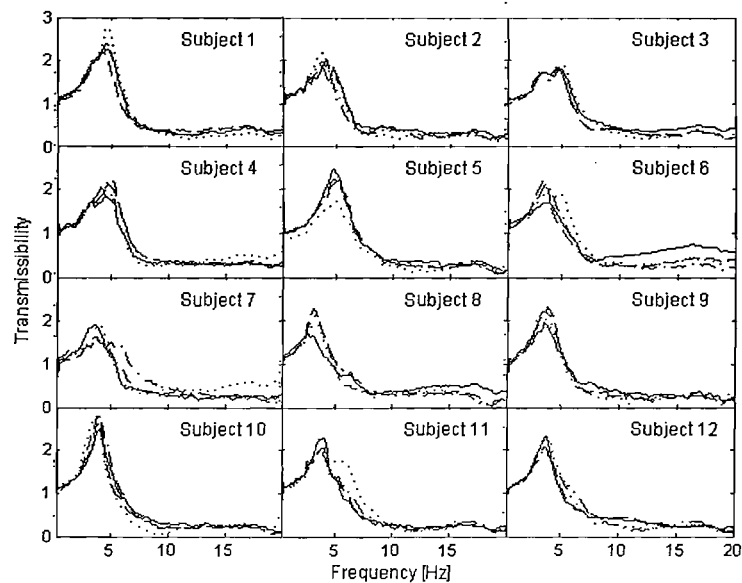
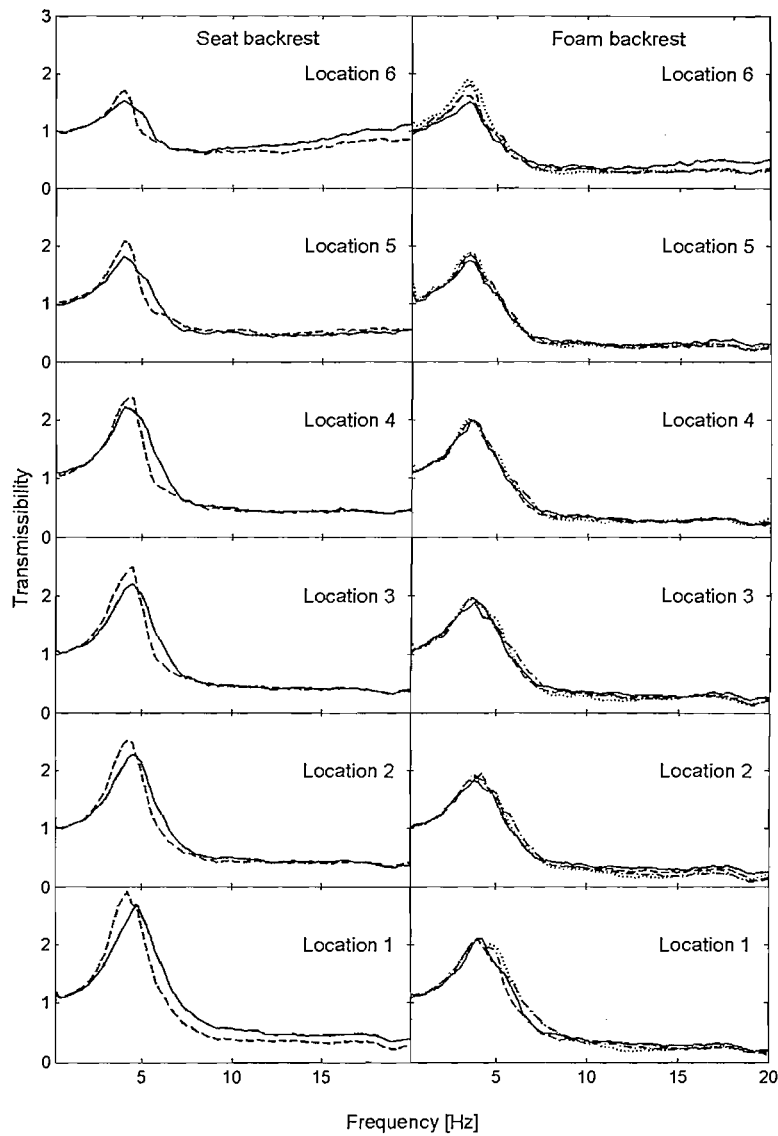


Figure 5.10: Fore-and-aft backrest transmissibilities for twelve subjects with the foam backrest at location 3 at seat-pan inclination of  $0^\circ$  (—),  $5^\circ$  (---),  $10^\circ$  (- · - · -) and  $15^\circ$  (·····).



**Figure 5.11:** Median fore-and-aft backrest transmissibilities with twelve subjects at each of six locations for the car seat backrest and the foam backrest at different seat-pan inclinations. Car seat-pan inclinations:  $10^\circ$  (—),  $15^\circ$  (---),  $0^\circ$  (—),  $95^\circ$  (---),  $100^\circ$  (----) and  $105^\circ$  (.....).

At all measurement locations, there was a significant increase in the median transmissibility at resonance when the inclination of the seat-pan of the car seat increased from 10° to 15° ( $p<0.05$ , Wilcoxon; Table 5.7). However, increasing the seat-pan inclination from 0° to 15° had no significant influence on the median transmissibilities at resonance of the foam backrest at any location ( $p>0.05$ , Friedman), except at location 6 ( $p<0.05$ ; Table 5.7).

**Table 5.7** Effect of seat-pan inclination on the median transmissibilities at resonance for the fore-and-aft backrest transmissibilities at all six locations for both the car seat and the foam backrest (medians of 12 subjects).

Location	Transmissibility at resonance					
	Car seat		Foam backrest			
	10°	15°	0°	5°	10°	15°
1	2.68	2.88	2.12	2.11	2.11	2.07
2	2.27	2.51	1.82	1.95	1.94	1.84
3	2.18	2.47	1.88	1.95	1.96	1.93
4	2.22	2.38	1.97	2.00	2.02	1.97
5	1.82	2.08	1.74	1.83	1.88	1.85
6	1.50	1.67	1.48	1.60	1.78	1.88

### 5.3.5 Discussion

In this experimental study, consideration has been restricted to fore-and-aft excitation of the seats and the fore-and-aft vibration in the seats (i.e. at the back-backrest interface). In vehicles, the vibration entering the seat and the vibration in the seat is more complex. In a car, the fore-and-aft vibration on the backrest can arise from fore-and-aft, pitch and vertical vibration on the floor (Qiu and Griffin, 2003 and 2004). The effects of these vibration inputs on backrest vibration may differ from the effects of pure fore-and-aft excitation found in this study.

#### 5.3.5.1 Effect of backrest inclination

The resonance frequencies and transmissibilities at resonance of the car seat increased with increasing backrest inclination. This is consistent with the results of Houghton (2003) who exposed subjects to vertical vibration and measured vertical backrest transmissibility and 'cross-axis' fore-and-aft backrest transmissibility with various backrest angles using a similar car seat. The seat was exposed to vertical vibration and the 'cross-axis' fore-and-aft

backrest transmissibility was calculated by computing the transfer function between the vertical acceleration at the vibrator platform and the fore-and-aft acceleration measured on the backrest. The 'cross-axis' fore-and-aft transmissibility of the backrest showed a resonance frequency at 4 to 5 Hz, and a transmissibility at resonance that increased with increasing backrest angle.

For both backrests and every backrest inclination in this study, there was little variation in the resonance frequencies with vertical position above the seat surface. This is consistent with the findings in previous chapter (Chapter 4), in which twelve subjects were exposed to five magnitudes of random fore-and-aft vibration and the transmissibilities were measured at five locations above the seat surface with both a car seat and a foam backrest (the same as used in the present experiment). In that study, the resonance frequencies of the fore-and-aft backrest transmissibilities varied only slightly, but the backrest transmissibilities showed significant changes with vertical position above the seat surface.

The vibration measured on the backrest in this study was always normal (i.e. perpendicular) to the backrest and therefore not always horizontal. This is the method employed when measuring vibration at this location in vehicles according to current standards. With more inclined backrests, the 'fore-and-aft' (i.e.  $x$ -axis) component normal to the seat surface will tend to be reduced in proportion to the cosine of the angle between the backrest and the vertical. However, the 'vertical' (i.e.  $z$ -axis) component parallel to the seat surface will tend to increase in proportion to the sine of the angle between the backrest and the vertical. The  $z$ -axis vibration will tend to become increasingly important as the backrest inclination increases since the sine of the angle increases rapidly with increasing angle.

The vibration measured at backrests could be resolved into horizontal and vertical components. Both fore-and-aft seat transmissibilities and human responses to the seat vibration could be calculated from the resolved horizontal components. However, because the reduction in the  $x$ -axis vibration is not great with small deviations from 90°, there would have been only a small effect on the 'fore-and-aft' backrest transmissibility measured in this experiment with backrest inclinations up to 105°. It is anticipated that other effects (e.g., a change in the impedance of the body, a change in pressure on the backrest, and a non-linear coupling between 'vertical' and 'fore-and-aft' vibration of the body) will have had a greater effect on the fore-and-aft transmissibility.

An increase in the dynamic stiffness of the backrest cushion might partly explain the observed increase in the resonance frequency with increased inclination of the car seat backrest. Previous studies have found that the dynamic stiffnesses of foam blocks and seat cushions increase with increasing pre-load force (Wei and Griffin, 1998). There may have

been a change in the dynamic stiffness of the car seat backrest due the increased load supported by the backrest with the more reclined postures. However, the foam backrest showed no significant change in resonance frequency with variations in inclination from 90° to 105°, suggesting little change in foam dynamic stiffness associated with the difference in load at these inclinations.

With the car seat backrest, the changes in the resonance frequencies with variation in backrest inclination were more obvious at the bottom of the backrest (i.e. locations 1 to 2) than at other locations. As the backrest inclination increased from 90° to 105°, the load around this location may have increased and, as a consequence, the variation in dynamic stiffness of the backrest in this area may have been greater than at other locations.

When exposed to a single axis of vibration, the upper body moves in two axes and so there are forces at the back in both the fore-and-aft and the vertical directions (Nawayseh and Griffin, 2004 and 2005a). Some of the forces on the backrest cushion in the present experiment will have arisen from cross-axis movements of the upper body: fore-and-aft excitation producing 'cross-axis' vertical movement. With variations in backrest inclination, these cross-axis motions will have had a varying influence on the vibration measured normal to the backrest surface.

The increase in the resonance frequencies and the increase in the transmissibilities at the resonance of the fore-and-aft backrest transmissibilities with increasing backrest inclination for both backrests may be attributed to a combination of several factors: a change in the biodynamic response of the body with changing posture, a change in the mechanical properties of the backrest cushion due increased dynamic stiffness of the backrests when supporting more weight of the body, and components of acceleration in the 'fore-and-aft' direction due to the inclined orientation of the accelerometers on the backrest.

Even if the vibration at the back-backrest interface were unchanged with variations in backrest inclination it would not imply that human response to the vibration was unaffected by backrest inclination. Studies are required to determine whether the evaluation method in current standards is appropriate with inclined seats: possibly the frequency weighting should be adjusted to allow for variations in sensitivity as the measured 'fore-aft vibration' becomes more vertical in an inclined seat.

### 5.3.5.2 *Effect of seat-pan inclination*

In comparison with the increases in the resonance frequency and transmissibility at resonance with increasing backrest inclination, the effects of seat-pan inclination on the fore-and-aft transmissibility of the car seat backrest were less substantial. There was no

statistically significant influence of seat-pan angle on the resonance frequencies of the car seat backrest and only a small increase in the median transmissibilities at resonance as the seat-pan inclination increased. With the foam backrest, the seat-pan inclination also showed little influence on the resonance frequency and transmissibility at resonance.

The results suggest that there were only small changes in the dynamic stiffnesses of the backrests with increased seat-pan inclination and only small change in the mechanical impedance of the back. However, investigation of vertical and fore-and-aft forces at the backs of seated subjects exposed to whole-body fore-and-aft vibration with varying seat-pan inclination may show changes, especially with greater inclinations than investigated here.

### 5.3.6 Conclusions

Increasing the backrest inclination of a car seat from 90° to 105° increased both the fore-and-aft backrest resonance frequency and the backrest transmissibility at resonance. There was little influence of such changes on the resonance frequency of a foam backrest, but the transmissibility at resonance increased with the more inclined backrest.

Inclination of the seat-pan had little effect on the resonance frequencies in the fore-and-aft backrest transmissibility with either backrest. There was a significant increase in the backrest transmissibility at resonance with the car seat with a more inclined seat-pan angle, but the foam backrest showed little change.

It is concluded that common variations in backrest inclination are likely to have a greater effect on the fore-and-aft transmissibility of backrests than common changes in seat-pan inclination.

## 5.4 Effect of the push force at the feet and the horizontal position of the footrest

### 5.4.1 Introduction

In one study, Radke (1956) investigated the effect of driver's arm and leg effort on the seat transmissibility on conventional and suspension seats with backrests when subjects were exposed to vertical vibration. For both seats, the author found that the transmissibility at

resonance decreased when the subject pushed against the footrest and the steering wheel. However, the resonance frequency showed no change for conventional seat but increased for suspension seat when subjects pushed against the footrest and the steering wheel.

In a different study, variation in the horizontal footrest position had little influence on the vertical seat transmissibility (Corbridge *et al.*, 1989). In that study, thirty subjects (15 males and 15 females) were exposed to vertical excitation while the feet were supported on three footrest positions. The footrest positions were: i) feet flat on the floor in line with the front of the seat cushion, ii) feet flat on the floor 200 mm from the front of the seat and iii) feet resting on heels, legs fully extended. The authors found that when the feet were moved forward from position i) to position ii), there was only little change in the transmissibility. Likewise, when the legs were further extended from position ii) to position iii), the transmissibility of the seat only increased slightly over the frequency range 1 Hz to 4 Hz, and there was only slight decrease in the transmissibility at frequencies greater than 4 Hz and up to 25 Hz.

This study was aimed to further explore the factors that can influence the fore-and-aft backrest transmissibility. The effect of push force at the feet and the horizontal position of the footrest on the fore-and-aft backrest transmissibility were investigated in laboratory measurements. It was hypothesized that the resonance frequency of the fore-and-aft backrest transmissibility would increase with increasing push force at the feet while the hands rested on the laps. This, in part, is due to the effect of stiffening of the back-backrest system, such that the resonance frequency of the backrest transmissibility would increase with increasing stiffness of the back-backrest system. It is also hypothesized that variations in the footrest position would partly change the lower legs posture, and results in changes in the fore-and-aft impedance of the body and therefore it could affect the fore-and-aft transmissibility of the backrest.

#### 5.4.2 Method

The apparatus (seat, accelerometers, etc.) used in this study was the same as that used previously (see Section 5.3). The experiment was conducted using a car seat (Ford Focus, Zetec), which had contoured surfaces on the cushion and backrest and weighed 19.3 kg. The inclination of the backrest and seat cushion could be changed through a built-in mechanism controlled by a rotating knob, located at the left side of the seat, and through a built-in gear mechanism via a rotating lever located beneath the seat pan, respectively.

Six Entran EGA-125F\*-10-D accelerometers were used to measure the fore-and-aft acceleration at the back-backrest interface. Each accelerometer was attached to a circular

wooden plate (50 mm in diameter), similar to that employed in a previous study (Section 5.3) and weighed 5 grams (i.e. the combined weight of the accelerometer and the wooden plate), and is referred to as a 'mini SIT-pad'. The flat surface of the plate faced the backrest with the accelerometer on the side adjacent to the body. The 'mini SIT-pads' were positioned at six locations on the backrest, corresponding to the locations of specific vertebrae for a 50<sup>th</sup> percentile male (Singley and Haley, 1978). Table 5.8 lists the locations of the 'mini SIT-pads', measured vertically from the seat surface, and the corresponding vertebrae. The 'mini SIT-pads' were always normal to the surface of the backrest.

An Entran EGCS-Y 24-10-D accelerometer was attached to the floor beneath the seat using double-sided adhesive tape so as to monitor the input acceleration.

**Table 5.8** Height of the 'mini SIT-pads' on the backrests and their approximate locations relative to spinal vertebrae (from Singley and Haley, 1978).

Location	Vertical distance, measured to the centre of the mini SIT-pad from the seat surface (mm)	Corresponding spinal position or vertebrae
1	200	Pelvis
2	300	Lumbar 1
3	350	Thoracic 12
4	400	Thoracic 11
5	450	Thoracic 9
6	500	Thoracic 7

One 26-year old subject with a 1.76 m stature and weighing 78 kg participated in the study. The subject was exposed to 0.4 ms<sup>-2</sup> r.m.s. of Gaussian random vibration with a nominally flat constant bandwidth acceleration spectrum over the frequency range 0.25 to 20 Hz. The stimulus lasted for 60 seconds in each condition. The vibration stimuli were generated using a *HVLab* Data Acquisition and Analysis system (version 3.81). All acceleration signals were conditioned and acquired directly into the *HVLab* Data Acquisition system at 512 samples per second via 170 Hz anti-aliasing filters.

The subject was asked to adopt a sitting posture with the '*upper body leaning on the backrest with hands placed on the lap and feet resting on the wooden footrest*'. The surface of the wooden footrest was inclined at 5° from the horizontal. Two factors were investigated: effect of push force at the feet (Condition 1) and the effect of horizontal position of the feet (Condition 2).

For Condition 1, the subject was asked initially to 'only rest the feet on the footrest' - this was regarded as 'no force'. The backrest transmissibility was measured. Subsequently, the subject was asked to increase the push force at the feet to either 50 N, or 100 N or 150 N. The push force applied by the feet on the footrest was measured using electronic scales placed on the surface of the footrest (Adam Equipment; model: CPW-150; max. load = 150 kg; SN = AE 16000592). The subject was also asked to maintain the force applied within  $\pm 10\%$  of the required push force by monitoring the panel on the electronic scales.

For Condition 2, the initial position of the footrest was obtained when the lower legs were perpendicular to the upper legs - this position was regarded as '0 mm'. Subsequently, the horizontal footrest position was positioned at 50 mm, 100 mm and 150 mm forward the '0 mm' position.

The experimental set-up and experimental conditions are shown in Figure 5.12.

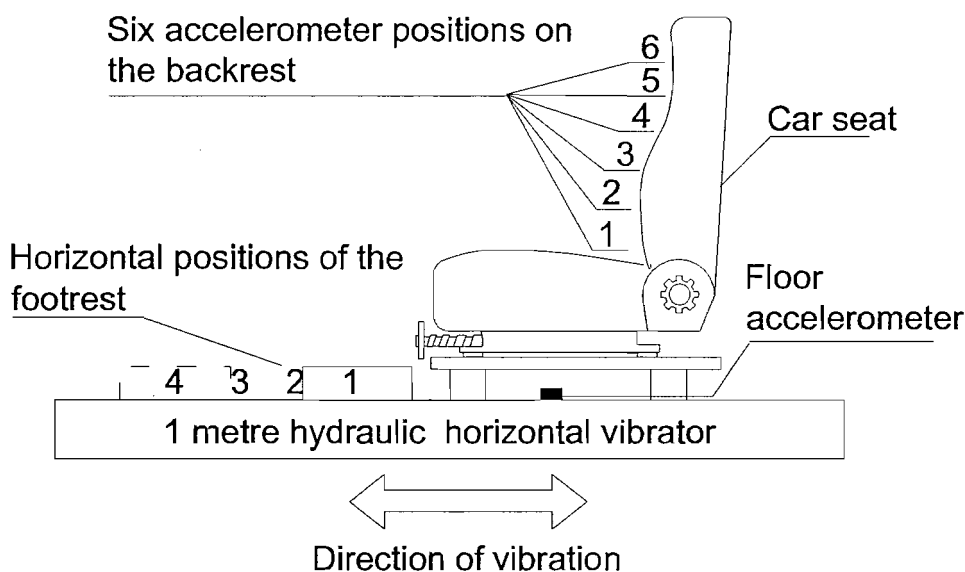


Figure 5.12: Experimental set-up.

### 5.4.3 Analysis

The acquired signals were normalised to remove any d.c. offset from the time histories using the *HVLab* data acquisition system before the transmissibility and the coherency were calculated. The transmissibilities and coherencies of the backrest at each condition

were calculated using equation 5.1 and equation 5.2 respectively (see Section 5.2.3). A resolution of 0.25 Hz was used for the calculation, which gave 60 degrees-of-freedom. The coherency in each condition was more than 0.9.

#### 5.4.4 Results

##### 5.4.4.1 *Effect of the fore-and-aft push force at the feet*

The transmissibility of the car seat backrest was greater with the 'no force' condition at the resonance frequency and at frequencies below the resonance frequency than when additional forces were applied by the feet (Figure 5.13). At frequencies greater than the resonance frequency, the backrest transmissibility increased with increasing push force at the feet. A high coherency (more than 0.95) was found in each condition.

The transmissibility of the backrest with 'no force' showed a principal resonance frequency around 4.2 Hz, and increased with increasing push force at the feet. This trend was apparent at all six measurement locations on the backrest (Table 5.9). The transmissibility at resonance, however, tended to decrease with increasing push force at all locations. The results showed that the transmissibility at resonance reduced from the bottom to the top of the backrest.

**Table 5.9** Resonance frequency and transmissibility at resonance of the fore-and-aft transmissibility of the backrest with increasing push force at the feet.

Location	Resonance frequency (Hz)			Transmissibility at resonance		
	'no force'	50 N	150 N	'no force'	50 N	150 N
1	4.5	5.2	5.2	3.2	2.8	2.9
2	4.5	5.0	5.2	2.6	2.4	2.5
3	4.5	4.7	5.2	2.6	2.3	2.4
4	4.2	4.5	5	2.8	2.5	2.5
5	4.2	4.5	4.7	2.4	2.3	2.2
6	4.2	4.5	4.5	1.8	1.7	1.8

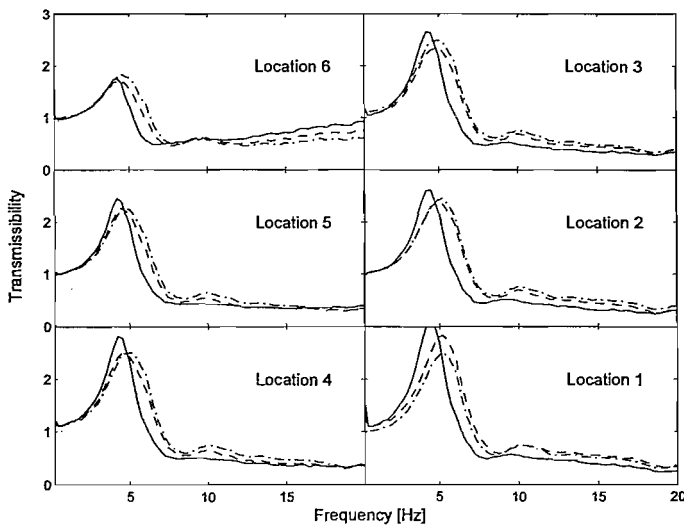


**Figure 5.13:** Fore-and-aft backrest transmissibility for one subject with car seat backrest with '0 N' (—), 50 N (---) and 150 N (·---·) of push force at the feet.

#### 5.4.4.2 *Effect of the horizontal position of the footrest*

There was little influence of the horizontal footrest position on the fore-and-aft transmissibility of the car seat backrest at frequencies less than the principal resonance frequency (around 4.7 Hz) with the '0 mm' footrest position (Figure 5.14). This trend was evident at all six measurement locations. Variations in the horizontal position of the footrest had little effect on the principal resonance frequency of the backrest transmissibility. However, when the footrest was at 150 mm forward the '0 mm' position, the principal resonance frequency reduced to 4.5 Hz at locations 2 to 6.

At frequencies greater than the principal resonance frequency and up to 10 Hz, the transmissibility of the backrest tended to decrease with increasing horizontal distance of the footrest. The transmissibility of the backrest, however, tended to increase at frequencies greater than 10 Hz with increasing horizontal distance of the footrest, except at location 1.

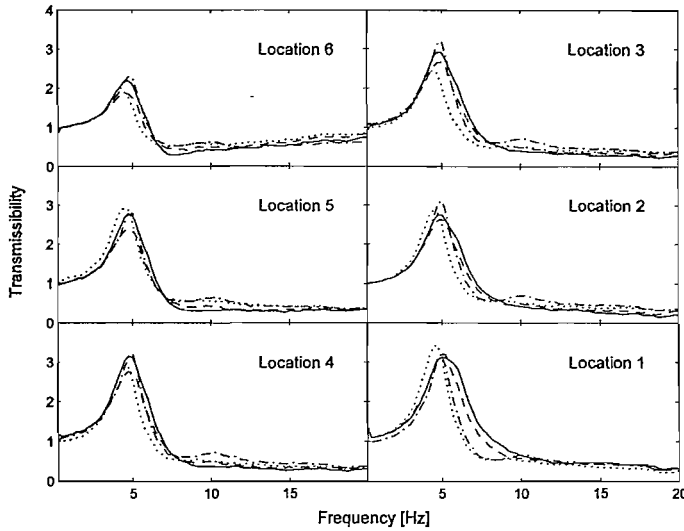


**Figure 5.14:** Fore-and-aft backrest transmissibility for one subject with the car seat at '0 mm' (—), 50 mm (---), 100 mm (-----) and 150 mm (.....) of horizontal footrest positions.

### 5.4.5 Discussion

#### 5.4.5.1 Effect of the fore-and-aft push force at the feet

The results with one subject suggest that the stiffness of the back-backrest system may increase with increasing push force at the feet, and so increase the resonance frequency – also known as the '*stiffening*' effect. Previous studies have found that the dynamic stiffness of a foam cushion increased with increasing pre-load on the foam (Wei and Griffin, 1998c). An increased resonance frequency in a backrest transmissibility with increased force at the feet, as found in this study, may be partly due to increased dynamic stiffness of the backrest cushion as a result of the increased force on the backrest cushion. A study of the effect of push force at the feet on the apparent mass of the back during fore-and-aft excitation merits further investigation.

The results of the current study showed that the transmissibility at resonance decreased with increasing push force, although the resonance frequency increased with increasing push force against the footrest. This is similar to the results found by Radke (1956), whose exposed subject seated on a suspension seat to vertical excitation and measured the

vertical transmissibility while subject was asked to apply push force at the feet against the footrest and push against the steering wheel using their hands. In that study, the resonance frequency of the vertical transmissibility of the suspension seat increased from 2.1 Hz to 2.8 Hz, and the transmissibility at resonance decreased when subject pushed against the steering-wheel and applied push force at the feet. The results of this study, together with the results of Radke (1956), suggest that the resonance frequency in the transmissibility of seats would increase when subjects apply additional push force at either the feet, or against the steering-wheel, as the results of increasing stiffness in the seat-seated person system.

#### 5.4.5.2 *Effect of the horizontal position of the footrest*

Corbridge *et al.* (1989) reported that by moving the feet forward 200 mm from a position in line with the front of a seat cushion, and subsequently further forward to a position where the subjects could just rest their feet on their heels, had little influence on the transmissibility of seat in the vertical direction. In the current study, the effect of footrest position on the fore-and-aft backrest transmissibility was small. The resonance frequency in the transmissibility of the backrest showed only small changes, suggesting little change in either the stiffness of the body or backrest. A study investigating the apparent mass of the back with variations in the leg postures (i.e. variations in the horizontal footrest position) merits further investigation.

#### 5.4.6 Conclusion

Results of one study showed that with increasing push force at the feet, the resonance frequency of the backrest transmissibility increased, although the transmissibility at resonance reduced. Varying the horizontal footrest position had little influence on the fore-and-aft backrest transmissibility.

The results of this study suggest that during fore-and-aft vibration, the application of the force at the feet has greater effect on the backrest transmissibility than a change in the fore-and-aft position of the footrest.

# Chapter 6

## Fore-and-aft apparent mass of the back

### 6.1 Introduction

When seated persons are exposed to whole-body vibration, dynamic forces are applied to the body by the supporting seat surface and a backrest. The forces can be measured and used to calculate the mechanical impedance, or apparent mass, of the body at the seat and the backrest.

The apparent mass provides information on the dynamic responses of the human body that can assist the development of biodynamic models and advance understanding of the coupling between the body and compliant seating. There have been extensive studies of the apparent mass of seated persons in the vertical direction (Fairley and Griffin, 1989; Mansfield and Griffin, 2002; Matsumoto and Griffin, 2002; Nawayseh and Griffin, 2003 and 2004). With vertical excitation, the human body shows a clear resonance at 4 to 5 Hz (e.g., Fairley and Griffin, 1989) that has been associated with a mode of the entire body (Kitazaki and Griffin, 1997; Matsumoto and Griffin, 2001), although variations in body posture or muscle tension can alter this resonance frequency (Mansfield and Griffin, 2002; Matsumoto and Griffin, 2002).

Some studies have investigated the apparent mass of the seated body in horizontal directions; i.e. with fore-and-aft or lateral excitation (e.g., Fairley and Griffin, 1990; Holmlund and Lundström, 1998 and Mansfield and Lundström, 1999a). Most measurements of the apparent mass of the body have been obtained with subjects seated on rigid seats without a backrest

With both vertical and horizontal excitation, a backrest will contribute to the dynamic forces applied to a seated person. With vertical vibration, a backrest may produce a shear force on the back, stiffening the upper body and increasing the resonance frequency (Mansfield and Griffin, 2002 and Nawayseh and Griffin, 2004). With fore-and-aft vibration, a backrest may also restrict body movements: without a backrest, the fore-and-aft apparent masses of seated persons have been found to have resonances at 0.7 Hz and 2.5 Hz, but with a backrest only one resonance was evident, around 3.5 Hz (Fairley and Griffin, 1990). The authors of that study suggested that the increase in the resonance frequency with the backrest was due to stiffening of the upper body.

With seated subjects exposed to whole-body fore-and-aft vibration in a rigid seat, three resonances in apparent masses have been found from the forces and accelerations at a flat backrest: less than 2 Hz, 3 to 5 Hz and 4 to 7 Hz (Nawayseh and Griffin, 2005a). The first and third resonances were clearer at low vibration magnitudes than at high magnitudes. In another study, a first resonance around 3 Hz was evident in the 'cross-axis' fore-and-aft apparent mass of the back when subjects were exposed to vertical vibration ('cross-axis' apparent mass is calculated from the force in a direction other than the direction of excitation and the acceleration in the direction of excitation; Nawayseh and Griffin, 2004). In the same study, all subjects showed a 'cross-axis' fore-and-aft resonance of the back between 5 and 10 Hz, with two peaks evident in this frequency range.

Without a backrest the apparent mass of the seated human body in the fore-and-aft direction is non-linear with vibration magnitude: the resonance frequency of the second peak (i.e. around 2.5 Hz) decreasing with increasing vibration magnitude – but the vibration magnitude appears to have no effect on the first peak around 0.7 Hz (Fairley and Griffin, 1990). A similar non-linearity: i.e. a reduction in the frequency of the principal resonance frequency around 3 to 5 Hz with increasing vibration magnitude has been reported by Holmlund and Lundström (1998). Nawayseh and Griffin (2005b) found that the fore-and-aft apparent mass of the back during fore-and-aft excitation of seated subjects was similarly non-linear with vibration magnitude.

The study of the fore-and-aft transmissibility of backrests, as described in Chapter 4, showed that the transmission of vibration through backrests varied significantly across the vertical height of the backrest from the seat surface. This might partly be caused by the variations in the dynamic stiffness of the backrest and partly by differences in the apparent mass of the back at different locations on the back with other points unsupported. The present study was designed to investigate the forces at different locations on the back when subjects were exposed to whole-body fore-and-aft excitation. It was hypothesised that the apparent mass of the back would vary with the location on the back. The fore-and-aft backrest transmissibility was also found to be non-linear with vibration magnitude: the

resonance frequency decreased with increasing vibration magnitude. The non-linearity of the backrest transmissibility in the fore-and-aft direction was probably due to the non-linearity of the impedance of the human body with vibration magnitude. Hence, it was also expected that with increasing level of the magnitude of the vibration, the apparent mass of the back will respond non-linearly, such that the resonance frequency will decrease with increasing vibration magnitude.

## 6.2 Method

### 6.2.1 Subjects

Twelve male subjects, with ages, weights, statures and seat-to-shoulder heights as shown in Table 6.1, participated in the study. The experiment was approved by the Human Experimentation, Safety and Ethics Committee of the Institute of Sound and Vibration Research (ISVR), University of Southampton. Prior to vibration exposure, each subject completed a health questionnaire and an exposure consent form.

Table 6.1 Subject age, stature, weight and seat-to-shoulder height.

	Age (yrs)	Stature (m)	Weight (kg)	Seat-to-shoulder height (m)
Minimum	20	1.64	50	0.58
Maximum	29	1.78	85	0.64
Median	23.8	1.72	67.7	0.62

### 6.2.2 Apparatus

#### 6.2.2.1 Vibration generation

The experiment was performed using an electro-hydraulic vibrator in the Human Factors Research Unit at ISVR, University of Southampton, capable of producing a 1-metre peak-to-peak horizontal displacement. The motion of the vibrator was measured using an Entran EGCSY-240D\*-10 accelerometer mounted on the moving platform.

### 6.2.2.2 Seating and transducers

A rigid seat with a horizontal flat rigid seat-pan and a vertical flat rigid backrest was securely mounted on the vibrator platform. A force platform (Kistler 9421A) capable of measuring forces normal to the backrest surface was secured on the rigid flat vertical backrest of the seat. The force plate (600 mm by 400 mm) consisted of four quartz force transducers. The signals from each of the force transducers were summed and conditioned using a Kistler 5007 charge amplifier. The acceleration of the backrest was measured using an Entran EGCSY-240D\*-10 accelerometer positioned 350 mm above the horizontal seat surface.

A wooden block (600 mm by 120 mm by 50 mm) was placed between the force platform and the back at one of five different heights so as to measure the fore-and-aft force at the back at different heights above the seat surface. The block was securely attached to the surface of the force platform using clamps. The five areas were obtained by dividing the height of the force platform into five equal bands, with each band 120 mm in height. Table 6.2 lists the vertical distance of each location, measured from the horizontal seat surface to the centre of the block at each location.

**Table 6.2** Location of the wooden block on the force plate with the corresponding height, measured from the seat surface to the centre of the block at each location.

Location	Vertical distance, measured from the centre of the block at each location to the seat surface (mm)
1	60
2	180
3	300
4	420
5	600

The arrangement of the experimental equipment is shown in Figure 6.1.

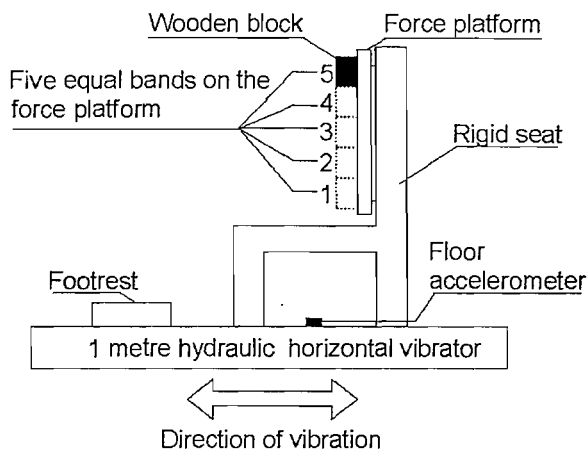


Figure 6.1: Experimental set-up.

#### 6.2.2.3 Subject posture

A loose safety belt was fastened around the subjects for safety but did not impinge on their movements. Subjects were asked to sit so as to make contact between their backs and the wooden block and maintain the same posture throughout the experiment. For measurements with the entire back in contact with the backrest, the wooden block was removed. Subjects were instructed to adopt upright posture with the back leaning against the backrest.

With the wooden block at locations 1 and 2, there was a gap between the middle and upper back and the force plate of only 50 mm (i.e. the thickness of the wooden block). In a preliminary study, when a subject was exposed to fore-and-aft vibration, the middle and upper back were observed to 'accidentally' touch the force plate when the wooden block was positioned at either location 1 or location 2. To prevent any effect on the force measurements at these locations, subjects were instructed to maintain the sitting posture and avoid the back touching the force plate directly.

The legs of subjects' rested on a horizontal footrest with the height of the footrest adjusted for each subject so as to make the upper and lower legs horizontal and vertical, respectively. The hands of subjects rested on their laps and held an emergency stop button.

### 6.2.2.4 Signal generation

A Gaussian random signal with a duration of 60 s and a nominally flat constant bandwidth acceleration spectrum over the frequency range of 0.25 to 10 Hz was generated by using a *HVLab* version 3.81 Data Acquisition and Analysis system. Each subject was exposed to five vibration magnitudes (0.1, 0.2, 0.4, 0.8, 1.6 ms<sup>-2</sup> r.m.s.). All acceleration signals were conditioned and acquired directly into the *HVLab* Data Acquisition system at 512 samples per second via 170 Hz anti-aliasing filters.

### 6.2.3 Analysis

All acquired signals were normalised to remove any d.c. offset from the time histories using the *HVLab* data acquisition system before they were used to calculate the apparent mass at the back.

The apparent masses of the back at five locations were calculated using the cross-spectral density method (CSD):

$$M_B(\omega) = \frac{F(\omega)}{a(\omega)} \quad (6.1)$$

where  $M_B(\omega)$ , is the apparent mass of the back,  $F(\omega)$ , is the cross-spectral density of the force and acceleration, and  $a(\omega)$ , is the power spectral density of the input acceleration. The results are a complex function that is capable of giving modulus and phase. A resolution of 0.25 Hz was used, which gave 60 degrees-of-freedom.

#### 6.2.3.1 Mass cancellation

The measured fore-and-aft forces at the back were influenced by the apparent mass of the subject, the mass of the force plate supported on the force transducer, the mass of the wooden block and also the masses of the clamps. Hence, a method of mass cancellation (i.e. the force acting on the plate of the force platform is subtracted from the total measured force acting with the subject and the plate) by using equation 3.9 (see Section 3.4.2.1) was applied to subtract the masses 'above' the force plate (28.8 kg for the plate, 1.2 kg for the wooden block, 0.8 kg for the clamps) from the measured fore-and-aft apparent mass of the back at each location.

## 6.3 Results

### 6.3.1 Apparent mass of the back at five locations above the seat surface

Inter-subject variability was observed in the apparent masses of the backs of the twelve subjects at all five locations. There was a tendency towards less variability at greater vibration magnitudes at all locations, and less variability at locations 4 and 5 at frequencies greater than 6 Hz at all vibration magnitudes (Figure 6.2).

There was a first peak in the apparent mass around 2 Hz in most individual data and at all locations – although most visible at the middle and the lower back (locations 1 to 3). A second, clearer, peak was present around 4 to 5 Hz at the upper back (locations 4 to 5), and at a higher frequency at the middle and the lower back (locations 1 to 3) – between 5 and 8 Hz. A third peak, around 7 Hz, appeared in the responses of a few subjects – clearer at locations 3 and 4 at 0.2, 0.4 and 0.8  $\text{ms}^{-2}$  r.m.s.

The coherencies were generally high (more than 0.85) at all locations, except at frequencies less than 5 Hz at 0.1  $\text{ms}^{-2}$  r.m.s. and greater than 5 Hz at 1.6  $\text{ms}^{-2}$  r.m.s. at all locations (where coherencies were less than 0.85). This might have arisen from noise in the system at the lowest vibration magnitude and a tendency of the back to lose contact with the wooden block at the highest magnitude.

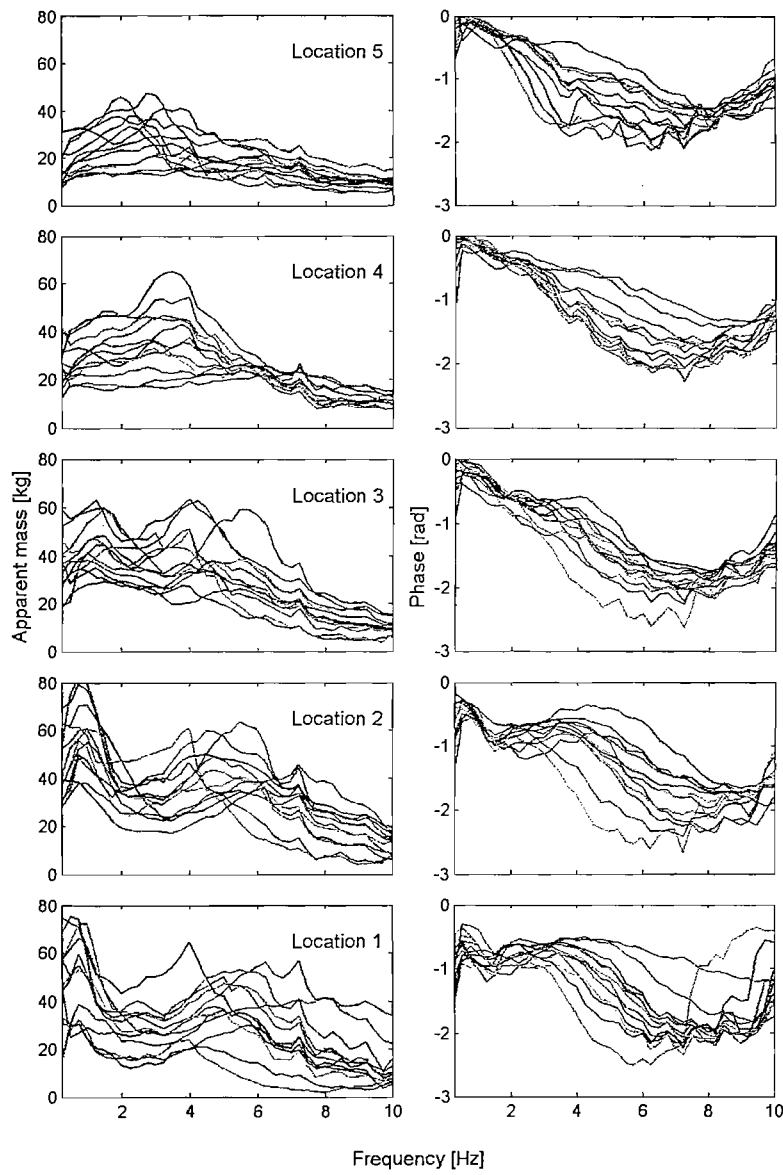


**Figure 6.2:** Inter-subject variability in the apparent masses and phases of the backs of twelve subjects at five locations above the seat surface at a vibration magnitude of  $0.8 \text{ ms}^{-2}$  r.m.s.

An example of typical moduli and phases of the apparent mass at all locations for one subject are shown in Figure 6.3. At 0.5 Hz, there were high forces at the lower back, with decreasing forces with increasing height above the seat surface. A first peak around 1 to 2 Hz is visible at all locations – more pronounced at the middle and the lower back (i.e. locations 1 to 3) with a frequency around 1 Hz and with a greater apparent mass at resonance than at the upper back (i.e. locations 4 to 5). A second peak is evident between 5 and 8 Hz – clearer at the middle and the lower back, but not very clear at the upper back at lower frequencies (between 4 and 5 Hz).

A trough in the apparent mass was observed between 2 and 4 Hz at the middle and the lower back. However, high forces were observed at the upper back at these frequencies, with a tendency to become a peak. Generally, forces at the lower back were greatest at frequencies less than 1.5 Hz and at frequencies greater than 5 Hz, whereas between 1.5 and 5 Hz the middle back produced greatest forces.

Clear differences with location above the seat surface can be seen in the individual apparent masses of the backs of the 12 subjects (Figures 6.4 to 6.5). At low frequency (0.5 Hz), there was a significant difference in apparent mass at the different locations ( $p<0.05$ , Friedman). The moduli of the apparent masses at the lower back (locations 1 to 2) were greater than at the middle and the upper back (locations 3 to 5). There was also a significant difference in apparent mass over the five measurement locations at all vibration magnitudes and at each preferred 1/3-octave centre frequency from 1 to 10 Hz ( $p<0.05$ , Friedman), except at 6.3 Hz (at 0.1  $\text{ms}^{-2}$  r.m.s.) and at 10 Hz (at 0.4 and 0.8  $\text{ms}^{-2}$  r.m.s.).

At 0.5 Hz, there was an increasing phase shift, by up to approximately  $28^\circ$  (0.5 radians), from the upper to the lower back at all vibration magnitudes (see Figures 6.2-6.3, 6.5). The phase shift was observed in the results of all subjects, although the extent of the phase shift varied between subjects and vibration magnitudes.

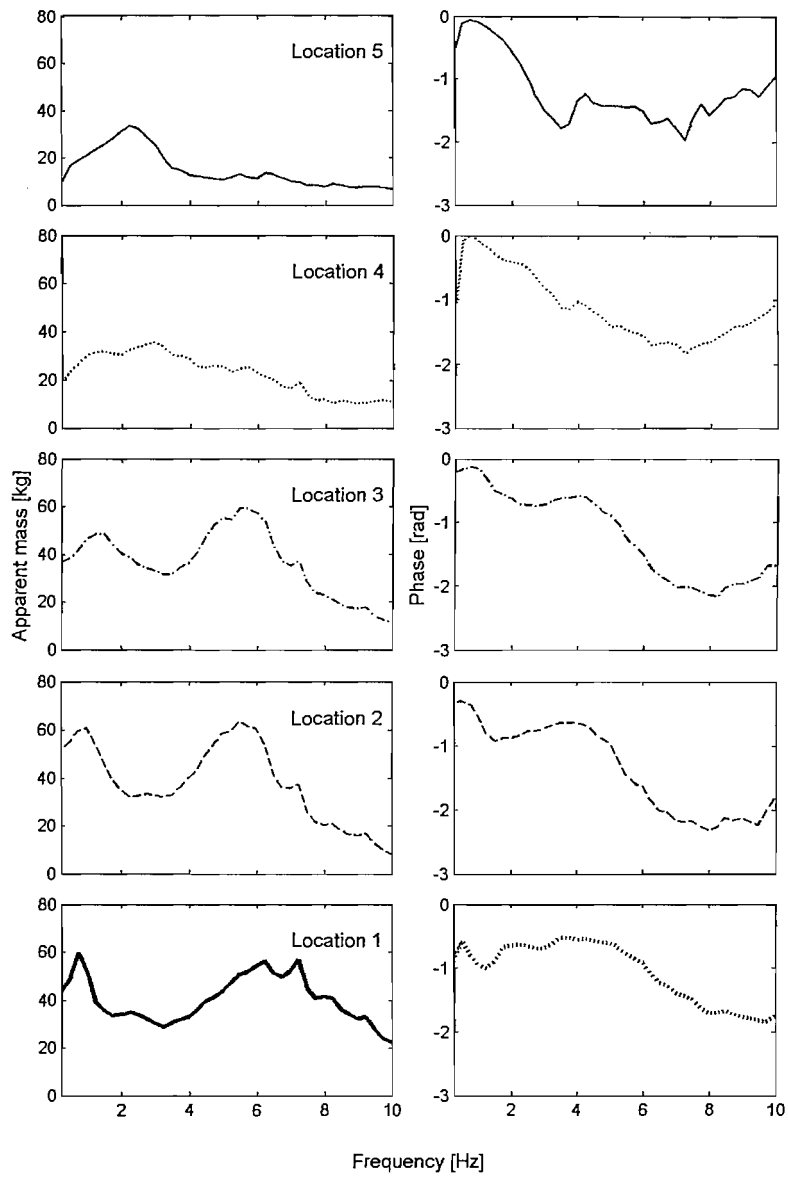
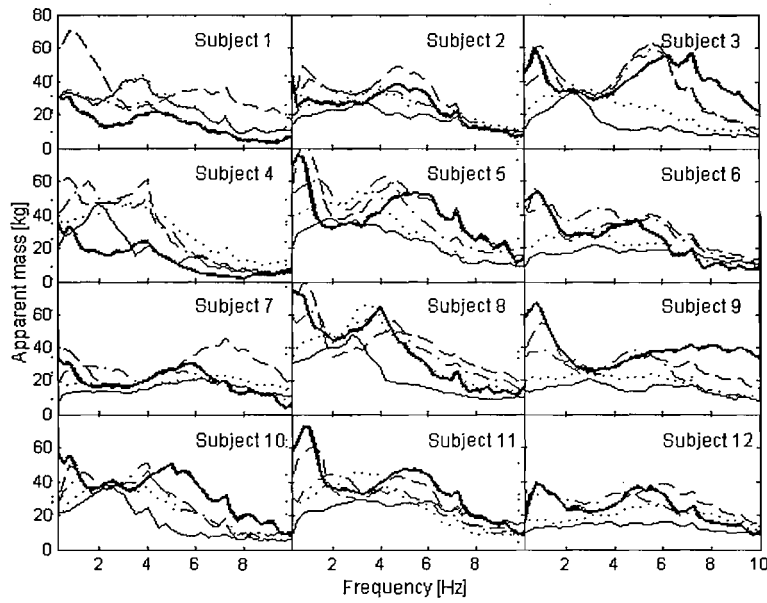
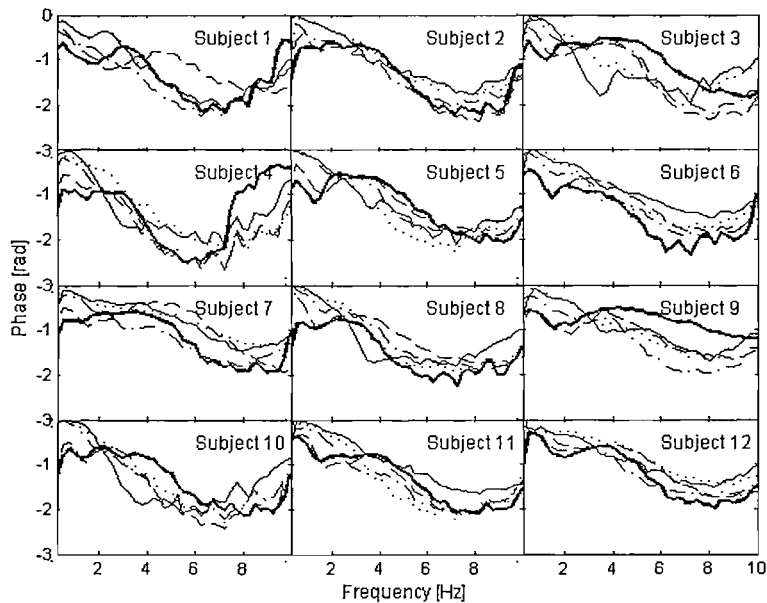


Figure 6.3: Example of a typical apparent mass moduli and phases measured at of the back of one subject at  $0.8 \text{ ms}^{-2}$  r.m.s.



**Figure 6.4:** The effect of measurement location on the moduli of the apparent masses measured at the backs of twelve subjects at a vibration magnitude of  $0.8 \text{ ms}^{-2}$  r.m.s.: location 1 (thick line), location 2 (---), location 3 (- - -), location 4 (.....), and location 5 (—).



**Figure 6.5:** The effect of measurement location on the phases of the apparent masses measured at the backs of twelve subjects at a vibration magnitude of  $0.8 \text{ ms}^{-2}$  r.m.s.: location 1 (thick line), location 2 (---), location 3 (- - -), location 4 (.....), and location 5 (—).

### 6.3.1.1 Effect of vibration magnitude

The apparent masses at the back varied non-linearly with vibration magnitude at all five locations (Figures 6.6 to 6.7). The resonance frequencies and the apparent masses at resonance tended to decrease with increasing vibration magnitude at all locations. At each location and at each preferred 1/3-octave centre frequency, from 1 Hz to 10 Hz, the statistical significance of the variations in the modulus of the apparent masses were investigated. The apparent mass at the lower and upper back (locations 1 and 5) varied non-linearly with vibration magnitude at frequencies greater than 5 Hz and 1.25 Hz, respectively ( $p<0.05$ , Friedman). The apparent mass around the middle back (locations 2 to 4) varied non-linearly at frequencies greater than 2.5 Hz ( $p<0.05$ ).

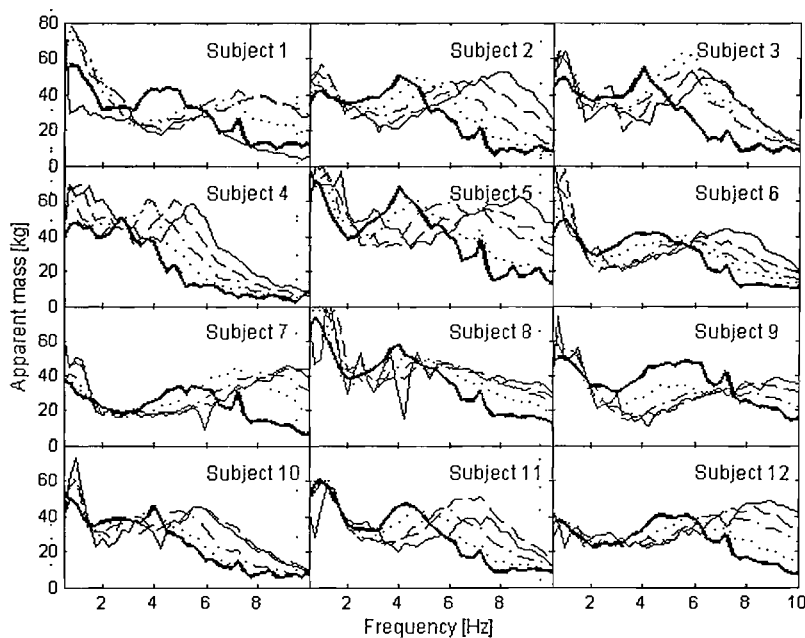


**Figure 6.6:** Effect of vibration magnitude on the fore-and-aft apparent masses measured at the backs of twelve subjects at location 3:  $0.1 \text{ ms}^{-2}$  r.m.s. (—),  $0.2 \text{ ms}^{-2}$  r.m.s. (---),  $0.4 \text{ ms}^{-2}$  r.m.s. (-·-·-),  $0.8 \text{ ms}^{-2}$  r.m.s. (·····) and  $1.6 \text{ ms}^{-2}$  r.m.s. (thick line).

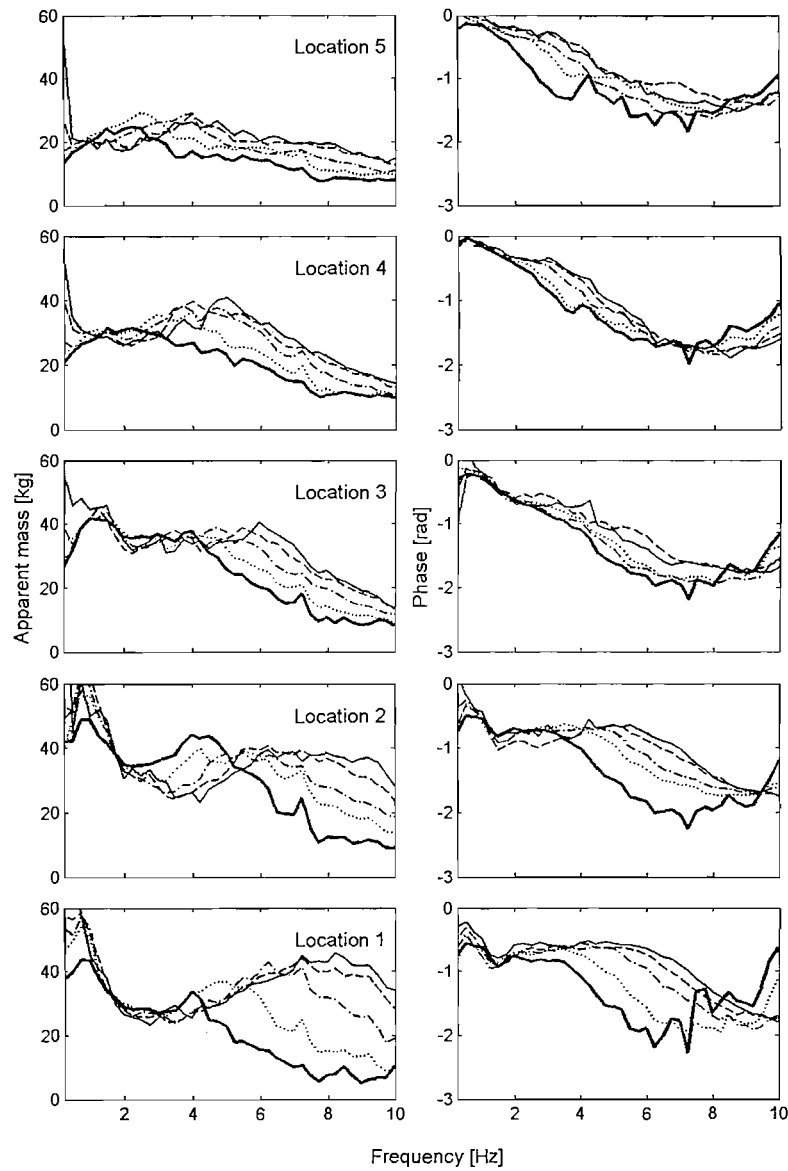


**Figure 6.7:** Effect of vibration magnitude on the median moduli and phases of the fore-and-aft apparent masses of the back at each of five locations:  $0.1 \text{ ms}^{-2}$  r.m.s. (—),  $0.2 \text{ ms}^{-2}$  r.m.s. (---),  $0.4 \text{ ms}^{-2}$  r.m.s. (-·-·-),  $0.8 \text{ ms}^{-2}$  r.m.s. (····), and  $1.6 \text{ ms}^{-2}$  r.m.s. (thick line).

### 6.3.2 Apparent mass of the entire back

The large subject variability in the fore-and-aft apparent masses of the back at the five locations was also present in the fore-and-aft apparent masses of the entire backs of ten subjects (Figure 6.8). (Note: the results of subjects 1 and 2 were excluded due to an experimental problem).

A first peak in the apparent mass around 2 Hz was observed in most of the ten subjects. A second, more pronounced peak was observed between 4 and 6 Hz. A third, less profound peak, was noticed in some of the individual responses between 7 and 8 Hz.

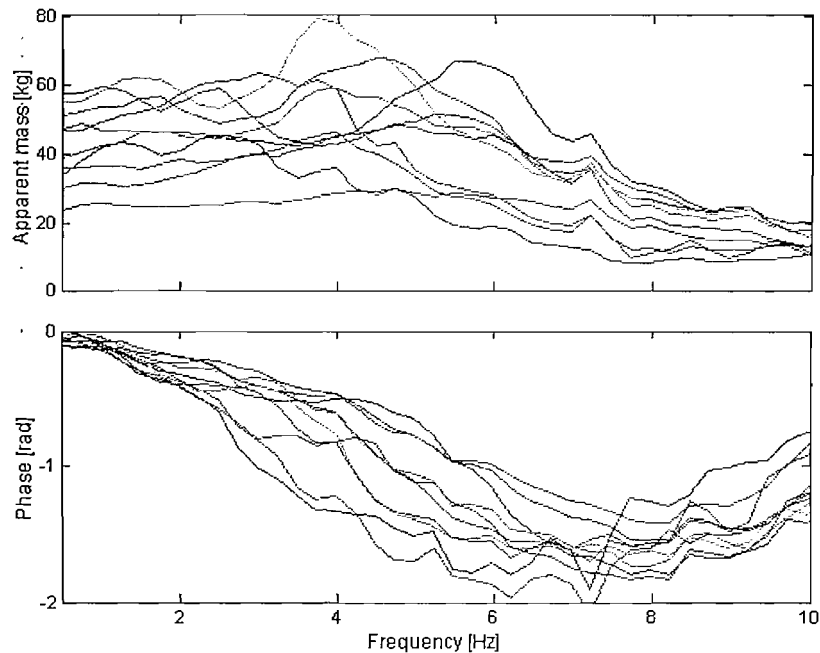


**Figure 6.8:** Inter-subject variability in the moduli and phases of the apparent mass of the entire back of ten subjects at  $0.8 \text{ ms}^{-2}$  r.m.s.

There were positive correlations between total body mass and the modulus of the apparent mass of the entire back at low frequency (0.5 Hz) ( $p<0.05$ , Spearman). However, body stature and the seat-to-shoulder height were not significantly correlated with the apparent mass of the entire back at 0.5 Hz ( $p>0.05$ ). The frequency of the first peak of the apparent mass of the entire back (around 2 Hz) was positively correlated with total body mass at all vibration magnitudes ( $p<0.05$ ), except at  $1.6 \text{ ms}^{-2}$  r.m.s., but there were no significant correlations between the second and third peak and total body mass ( $p>0.05$ ). The

statures and seat-to-shoulder heights of the subjects were also uncorrelated with the apparent mass of the second and third peaks ( $p>0.05$ ).

### 6.3.2.1 Effect of vibration magnitude

With an increase in vibration magnitude, there were reductions in the modulus of the apparent mass and increases in the phase lag measured with the entire back. The changes were statistically significant at frequencies greater than 5 Hz ( $p<0.05$ , Friedman; Figure 6.9).

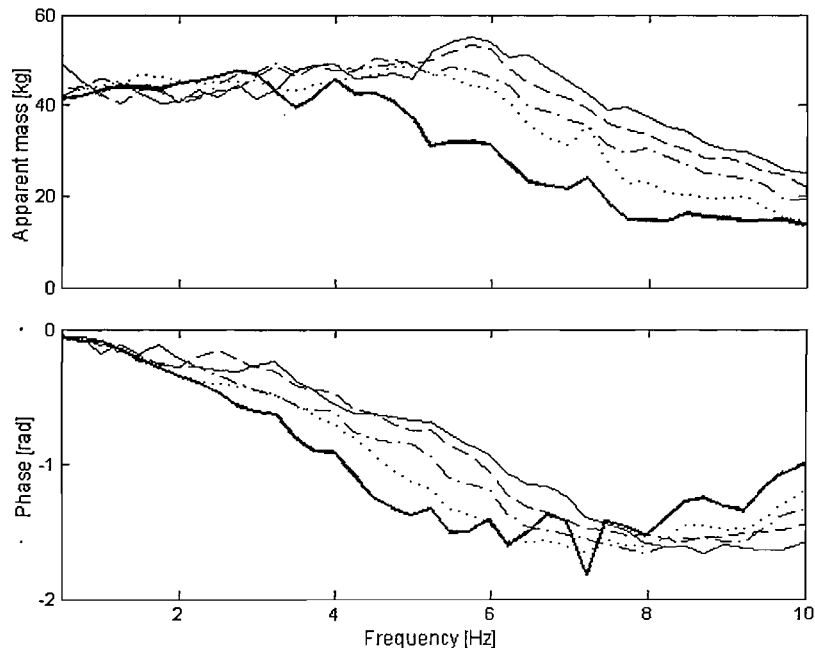


**Figure 6.9:** Effect of vibration magnitude on the median moduli and phases of the fore-and-aft apparent mass of the entire back with ten subjects.  $0.1 \text{ ms}^{-2}$  r.m.s. (—),  $0.2 \text{ ms}^{-2}$  r.m.s. (---),  $0.4 \text{ ms}^{-2}$  r.m.s. (-·-·-),  $0.8 \text{ ms}^{-2}$  r.m.s. (·····) and  $1.6 \text{ ms}^{-2}$  r.m.s. (thick line).

### 6.3.3 Comparison of the apparent mass of the back measured at five locations and with the entire back

The median apparent mass of the back at each location for ten subjects was compared with the median apparent mass of the entire back for the same ten subjects (Figure 6.10). At frequencies less than 2 Hz, the forces of the entire back were 30% greater than those of the upper back and 10% greater than those of the middle back. The forces of the back near the shoulder area (location 5) were about half those of the entire back. The forces at the lower back were 40% greater than those of the entire back. At frequencies greater than 2 Hz, the forces of the entire back were greater than at any of the five locations on the back. The forces at the back near the shoulder area were the least – 50% less than the entire back. Generally, at frequencies below 7 Hz, the forces of the entire back showed similar trends to those of the middle back, but the former produced greatest force. At frequencies greater than 7 Hz, the response of the entire back was closest to the response at location 2 (the lower back).

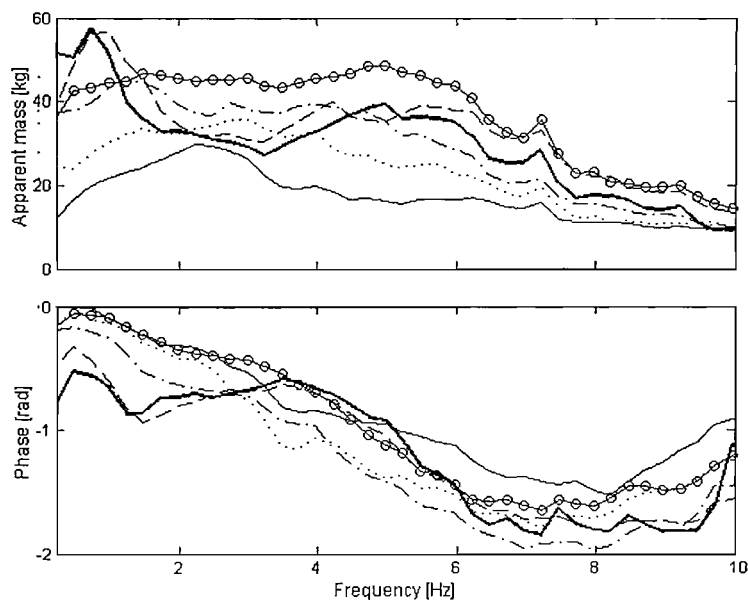


**Figure 6.10:** Comparison of median moduli and phases of the apparent masses of the back at five locations with the median apparent mass of the entire back at a vibration magnitude of  $0.8 \text{ ms}^{-2}$  r.m.s. Key: Location 1 (—); Location 2 (---); Location 3 (-·-·-); Location 4 (····); Location 5 (—); Entire back (-o-o-o-o-). (Median of 10 subjects).

## 6.4 Discussion

In previous studies, sitting posture has been found to affect the apparent mass of the body measured on the seat in the vertical excitation, with increasing apparent mass on the seat between 4 and 8 Hz and increasing resonance frequency of the apparent mass when the posture changed from 'slouched' to 'very erect' – consistent with a 'stiffening' of the body (e.g. Fairley ad Griffin, 1989). There is no known study of the effects of such variations in sitting posture on the apparent mass at a backrest during fore-and-aft excitation. With a rigid vertical backrest, a change in posture (e.g. 'relaxed' to 'erect') will change the curvature of the spine, may alter the location of the interface between the back and the backrest and the location of the vibration input to the back. A 'relaxed' posture will tend to result in less upper-back contact with a backrest but more contact around the middle back, whereas an 'erect' posture will tend to have more contact with a backrest in the lower and the upper back. The five locations studied here may resemble the various interface points between the back and a rigid flat backrest with different sitting postures. A cushioned backrest will tend to follow the contours of the back and so some contact over the entire back may occur irrespective of variations in the curvature of the spine in different postures.

### 6.4.1 Modes of vibration of the body

The three peaks in the apparent masses of the back observed in this study are consistent with the peaks found by Nawayseh and Griffin (2005a), who exposed twelve subjects to four magnitudes of fore-and-aft vibration and measured the apparent mass of the entire back in the fore-and-aft direction and the 'cross-axis' apparent mass in the vertical and lateral directions. They found a first peak in the fore-and-aft apparent mass of the entire back at a frequency less than 2 Hz, with a second peak between 3 and 5 Hz, and a third peak in the frequency range 4 to 7 Hz. A previous study by the same authors found that in subjects exposed to vertical vibration the 'cross-axis' fore-and-aft apparent mass at the back had a principal resonance between 5 to 10 Hz, with evidence of a first resonance in the range 2 to 3 Hz for some subjects (Nawayseh and Griffin, 2004).

During vertical excitation, a bending deformation of the spine between 2 and 3 Hz results in two body modes associated with fore-and aft motion of the head and the pelvis in opposite phase and in phase, respectively (Kitazaki and Griffin, 1997), and a pitching mode in the pelvis (Matsumoto and Griffin, 2001). If the body has a pitching mode during vertical excitation at 2 to 3 Hz, the same mode may be expected to occur during fore-and-

aft excitation. Nawayseh and Griffin (2005a) reported a first peak of the apparent mass of the entire back at a similar frequency (1 to 2 Hz), when they exposed seated subjects to whole-body fore-and-aft excitation. They suggested that the first mode at the back might be associated with a pitching mode of the body. In this study, the first peak at the back was observed at 2 Hz, with the peak clearer at the middle and lower back. This, together with the findings of previous studies, suggests that the first peak in the apparent mass of the back in the fore-and-aft direction may be associated with a pitching mode of the pelvis.

In this study, the upper back showed a second resonance around 4 to 5 Hz, while the middle and lower back showed second peaks at higher frequencies (around 5 and 8 Hz). When using a backrest, there is a pronounced peak in the transmission of fore-and-aft seat vibration to the head around 6 Hz (Paddan and Griffin, 1988b). A pitching mode of the head and a bending mode of the entire spine around 5 Hz have been extracted from a modal analysis of the human body in the vertical direction using a finite element model of the human body (Kitazaki and Griffin, 1997). It seems possible that the second resonance of the apparent mass of upper back may be associated with combined pitching of the head and bending of the entire spine and the upper body.

A bending mode of the lumbar and the lower thoracic spine of the body during vertical vibration has been reported at 5.6 Hz, which may arise from pitching motion of the upper body (Kitazaki and Griffin, 1998). The authors also found pitching in the pelvis around 8 Hz. Possibly, the second peak in apparent mass at the middle and lower back are associated with a mode of the entire body involving combined bending in the lower thoracic spine and pitching of the pelvis and the upper body.

A third peak was found around 7 Hz, and was clearest at the middle back. Nawayseh and Griffin (2005) reported a third broad peak in the frequency range of 4 to 7 Hz in the fore-and-aft apparent mass of the entire back, but they did not suggest any associated mode. A resonance at approximately 6 Hz has been reported in the transmission of vertical seat vibration to fore-and-aft vibration at the abdomen (Mansfield and Griffin, 2000). Fore-and-aft transmissibilities to the tenth thoracic spine (T10) also showed a resonance around 6 Hz (Matsumoto and Griffin, 2001). Although it is not clear which body mode was associated with the third resonance of the apparent mass of the back found here, it may have been influenced by the same mechanisms producing peaks in the fore-and-aft transmissibility to the abdomen and the lower spine during vertical excitation.

#### 6.4.2 Biodynamic responses at low frequency (i.e. near 0 Hz)

During vertical excitation at very low frequencies (near to 0 Hz), the human body is rigid: the vertical apparent mass of a seated body is approximately equal to its static sitting mass and the force and acceleration are in phase. In the fore-and-aft direction, the interaction between the back and backrest are more complex. The results of this study suggest that at low frequencies (i.e. near to static conditions), the fore-and-aft forces at the back vary with the location of measurement: forces at the lower back were greater than at the middle and upper back and not solely determined by the acceleration and the mass in contact with the backrest.

If the back was only coupled to the backrest, it would be reasonable to expect the mass of the back to equal the apparent mass at low frequencies (similar to the static mass of the body equalling the low frequency vertical apparent mass of a person sitting without support from a backrest or footrest). With the subjects supported in the current experiment on a surface that oscillated them backwards and forwards with the same vibration as appeared at the back, the situation is more complex, and the measured apparent mass different from that which would have been measured without this movement at the supporting seat. Other studies have found that during fore-and-aft excitation without a backrest but with feet supported and exposed to the vibration, the apparent mass of the body measured on a seat at low frequencies was about 80% of the subject static mass (Nawayseh and Griffin, 2005b), but this reduced to about 35% of the static mass when a vertical backrest was present (Nawayseh and Griffin, 2005a). The apparent mass of the back measured in this study indicates the forces present at the back when the seat and back move together. During low frequency fore-and-aft oscillation, the sum of the forces at back, the seat and the feet would be expected to equal the product of the acceleration and the subject static mass.

The positive correlation between subject mass and the apparent mass of the entire back at low frequencies (e.g. 0.5 Hz) in the current study means that heavier subjects produced a greater apparent mass of the back than lighter subjects at low frequencies. Fore-and-aft excitation was applied by a vertical surface normal to the surface of the backs of subjects, similarly to vertical vibration being applied normal to the horizontal surface that supports a seated person. A large part of the variability in the apparent masses of subjects measured at surfaces supporting seated persons during vertical excitation is due to differences in subject weights on the seat (Fairley and Griffin, 1989). It seems possible that some of the variability in fore-and-aft apparent mass at the back in the current study was also due to differences in subject mass.

At low frequencies there were increasing phase shifts between the force and the acceleration as the measurement location moved down from the upper back to the lower back (Figures 6.2 to 6.3). In addition to the influence of vibration on the supporting seat surface, the phase shifts may have arisen from reduced coherency at low frequencies as a result of measurement noise (e.g. due to, the body losing contact with the back – as may be expected at greater vibration magnitudes). Alternatively, the phase shift may have arisen from some muscle activity attempting to stabilise the body and maintain an upright posture during low frequency oscillation. Matsumoto and Griffin (2002) found a phase shift in the apparent mass of the body when subjects were exposed to sinusoidal vertical vibration. The authors suggested that the phase shift could have been caused by the variation in the vibration magnitude or it could be related to change in the back muscle activity. Previous study by Robertson and Griffin (1989) found gradual increased in the amplitude of the EMG (electromyographic) activity from the erector spinae muscle over the first cycle of the sinusoidal oscillation around 2 Hz and 4 Hz. Based on the studies of Matsumoto and Griffin (2002) and Robertson and Griffin (1989), may suggest that the phase shift observed at low frequencies is likely to arise from some muscle activity.

#### 6.4.3 Variation in apparent mass of the back

When subjects with foot height adjusted to produce ‘average thigh contact’ on a seat were exposed to vertical vibration, the ‘cross-axis’ fore-and-aft apparent mass at the back was greater than when there was ‘maximum thigh contact’ or their feet were hanging, but the ‘cross-axis’ fore-and-aft apparent mass was greatest when there was ‘minimum thigh contact’ (Nawayseh and Griffin, 2004). The authors suggested that when the feet were raised (i.e. minimum thigh contact), a greater contact force between the back and the backrest might have arisen from push forces applied by the feet reacting to the pitch motion of the body, and this may have also increased the fore-and-aft dynamic force on the backrest during vertical excitation. During fore-and-aft vibration, a backrest may provide postural stability and reduce some effects of vibration, in particular at frequencies less than 4 Hz (Nawayseh and Griffin, 2005a). However, the fore-and-aft vibration at the backrest may increase the vibration at frequencies greater than 4 Hz and may also cause the body to pitch, and result in a reaction force from the feet to control the pitching motion (Nawayseh and Griffin, 2005a). The variation of the force at the back during fore-and-aft excitation as found in the current study may arise from the variations in push force at the feet reacting with pitch movements of the upper body during fore-and-aft excitation.

At frequencies less than 2 Hz, the apparent mass of the back at locations 1 and 2 were greater than the apparent mass of the entire back. Possibly, this may have arisen from some push force at the feet to react with the pitching motion of the body as the rest of the

upper back were not in contact with the force platform. Although at low frequencies, the backrest may provide postural stability and reduce some effects of vibration, prior to the experiment, the preliminary run showed that there was a tendency of the subject to 'accidentally' touch the force platform at these locations and some 'active control of the muscle within the body' is required to maintain the upright posture due to the upper part of the back being unsupported and can freely sway forward and backward in response to vibration.

Alternatively, the increase of the apparent mass of the back at these two locations compared to the entire back may have arisen from the effect of the vibration on the seat surface. At these location, the forces may come from the shear force between the thigh and the seat surface, although these forces (between the thigh and the seat surface) were not measured in the current study.

#### 6.4.4 Non-linearity of the body with vibration magnitude

Previous studies have found that the response of the body is non-linear with vibration magnitude during vertical excitation – the resonance frequency of the body decreases with increasing vibration magnitude (e.g. Sandover, 1978; Fairley and Griffin, 1989; Mansfield and Griffin, 2000; Mansfield and Griffin, 2002; Matsumoto and Griffin, 2002 and Nawayseh and Griffin, 2003 and 2004). The causes of the non-linearity are not understood but may include muscle activity and non-linear mechanical properties of the soft tissues (Huang, 2004). It has been suggested that the non-linearity seen in biodynamic responses during vertical excitation is associated with involuntary changes in muscle tension within the body (e.g. Fairley and Griffin, 1989). With increases in vibration magnitude, Matsumoto and Griffin (2002) found that the resonance frequency of the body decreased when both the buttock and abdomen muscles were tensed and they suggested the non-linearity may be partly caused by involuntary changes in muscle tension. A few studies have monitored the activity of muscles using electromyography (EMG) and observed phasic contractions of erector spinae muscles in subjects exposed to whole-body vertical or lateral vibration at low frequencies (e.g. Seidel *et al.*, 1986 and Robertson and Griffin, 1989). There is a variation in muscle activity with vibration magnitude (Robertson and Griffin, 1989) that may cause, or contribute to, the non-linearity.

A few studies have investigated the non-linearity of the body during fore-and-aft excitation, mainly measuring the response at a seat surface supporting subjects without backrest (e.g. Fairey and Griffin, 1990; Mansfield and Lundström, 1999, Holmlund and Lundström, 1998; Nawayseh and Griffin, 2005b). When seated with a backrest, Nawayseh

and Griffin (2005a), found that the apparent mass of the back varied non-linearly with vibration magnitude, similarly to the present study.

#### 6.4.5 Biodynamic model

Biodynamic models of seated persons in the vertical direction generally have one connecting point at the interface between the seat and the body, assumed to be at the principal load-bearing area around the ischial tuberosities (e.g. Fairley and Griffin, 1986; Wei and Griffin, 1998c and Nawayseh, 2002). The principal area bearing the static load between the back and a backrest may either be the lower back (around the lumbar area), or the middle back, or the whole back (Andreoni *et al.*, 2002). The present study has shown that the fore-and-aft dynamic response of the back is highly dependent on the location on excitation of the back. This suggests that a dynamic model of the back of a seated person should be represented by at least two points representing two different responses of the back, the middle and lower back, and the upper back. A biodynamic model of the fore-and-aft response of a combined backrest and body may need to represent the impedance of the back at these locations, as well as the fore-and-aft impedance of the body at the interface between the buttocks and the seat surface. Such a model of the back might be combined with a backrest cushion model so as to predict, and optimise, backrest transmissibility.

### 6.5 Conclusions

Three resonances were evident in forces measured at the back-backrest interfaces of seated subjects exposed to fore-and-aft vibration. A first resonance around 2 Hz was visible at all five measurement locations on the back. There was a clearer, second, resonance between 4 and 5 Hz at the upper back (and with the entire back), and between 5 and 8 Hz at the middle and lower back. A third resonance was observed around 7 Hz at all locations, although only for some subjects.

The forces at the back varied greatly with location on the back. The lower back showed greatest force and the upper back showed the least force. The forces measured with the entire back differed from those measured at all five locations, but showed some similarity with forces at the middle back.

The apparent mass of the back measured at all locations, and with the entire back, was significantly non-linear: the principal resonance frequency and the apparent mass at resonance tended to decrease with increasing vibration magnitude.

The results suggest that biodynamic models of the seated human body used to predict fore-and-aft vibration at the back, including the transmission of fore-and-aft vibration through backrests, should recognize the variation in forces with both measurement location and vibration magnitude.

# **Chapter 7**

## **Factors affecting apparent mass of the back**

### **7.1 Introduction**

In Chapter 6, the apparent mass of back showed a principal resonance frequency around 5 Hz during fore-and-aft excitation. It also vary non-linearly with vibration magnitude: the principal resonance frequency of the apparent mass of the back tended to decrease with increasing vibration magnitude. It is anticipate that there are many factors that can affect the apparent mass of the back during fore-and-aft vibration. This chapter describes studies conducted to explore the factors that could affect the apparent mass of the back during exposure to whole-body fore-and-aft vibration. The effect of backrest inclination, seat-pan inclination, push force at the feet and horizontal footrest position on the apparent mass of the back were investigated.

### **7.2 Effect of backrest inclination and seat-pan inclination**

#### **7.2.1 Introduction**

Exposure to whole-body vibration in one direction can cause the body to respond in a direction other than the direction of excitation – a ‘cross-axis’ response. Matsumoto and Griffin (2002) found that during vertical excitation, the ‘cross-axis’ fore-and-aft forces at the seat varied up to 40% of the static weight of subjects. With vertical excitation,

Nawayseh and Griffin (2003 and 2004) measured the forces in the vertical, fore-and-aft and lateral directions on a seat without backrest (Nawayseh and Griffin, 2003) and on both a seat and backrest (Nawayseh and Griffin, 2004). On a seat without backrest they found high vertical forces and appreciable 'cross-axis' fore-and-aft forces, with low 'cross-axis' lateral forces (Nawayseh and Griffin, 2003). On a seat with a rigid vertical backrest, the vertical forces on the seat were increased at frequencies greater than 5 Hz, but the vertical forces on the backrest were low (Nawayseh and Griffin, 2004). The backrest modified the 'cross-axis' fore-and-aft forces on the seat and there were considerable fore-and-aft forces at the backrest, whereas the 'cross-axis' lateral forces on the seat and the backrest were relatively low. Nawayseh and Griffin performed similar studies with fore-and-aft excitation, both without a backrest (Nawayseh and Griffin, 2005b) and with a rigid vertical backrest (Nawayseh and Griffin, 2005a). Without a backrest they found high fore-and-aft forces on the seat and considerable 'cross-axis' vertical forces on the seat, but 'cross-axis' lateral forces were relatively small (Nawayseh and Griffin, 2005b). With a backrest, there were high fore-and-aft forces at the backrest and the fore-and-aft forces on the seat depended on support for the feet (whether supported or not). The 'cross-axis' vertical forces were high on the seat but not on the backrest, while the forces in the lateral direction were low on both the seat and the backrest (Nawayseh and Griffin, 2005a). The findings of Matsumoto and Griffin (2002) and Nawayseh and Griffin (2003, 2004, 2005a and 2005b), confirm that the body produces high forces on a seat and a backrest in the direction of excitation, and also show that there are appreciable 'cross-axis' forces on a seat and a backrest when the body is exposed to vertical or fore-and-aft excitation.

During vertical excitation, the biodynamic responses of a seated person can be affected by many factors, including sitting posture (e.g. 'erect (stiff)' or 'slouched (relaxed)') or seating conditions (e.g. with or without a backrest, or inclined seat-pan, or inclined backrest). It has been suggested that when subjects adopt an erect sitting posture the body stiffness increases and the resonance frequency of the apparent mass of the body also increases (Fairley and Griffin, 1989 and Kitazaki and Griffin, 1998). A relaxed sitting posture (i.e. 'slouched') may reduce tension in the body and reduce the resonance frequency (Fairley and Griffin, 1989).

Sitting postures are influenced by the seat. A vertical backrest affects the apparent mass of the body during vertical vibration (Fairley and Griffin, 1989 and Wang *et al.*, 2004). With vertical excitation, Rakheja *et al.* (2002) measured the vertical apparent mass on a seat while subjects adopted an automotive sitting postures (i.e. inclined seat-pan and inclined backrest); the apparent mass of subjects had higher principal resonance frequencies (i.e. 6.5 to 8.6 Hz) than previously reported with either an upright sitting posture without a backrest or sitting on a seat with a vertical backrest and horizontal seat-pan (i.e. 4.5 to 5

Hz; Fairley and Griffin, 1989; Mansfield and Lundström, 2002 and Nawayseh and Griffin, 2004).

With fore-and-aft excitation, Nawayseh and Griffin found three peaks in the fore-and-aft apparent mass measured on the seat with no backrest (at about 1 Hz, between 1 and 3 Hz and between 3 and 5 Hz; Nawayseh and Griffin, 2005b). When a vertical backrest was used, they found only one resonance (between 2 and 6 Hz) on the seat, with an additional resonance between 1 and 2 Hz in a 'feet hanging' posture (Nawayseh and Griffin, 2005a).

Although a rigid vertical backrest modifies the responses of the body on the seat during fore-and-aft excitation, there is little knowledge of factors that influence the fore-and-aft forces and 'cross-axis' vertical forces at the backrest during fore-and-aft excitation. In Chapter 6, the fore-and-aft apparent mass of the back is non-linear with vibration magnitude. Nawayseh and Griffin (2005a) reported that both the fore-and-aft and 'cross-axis' vertical response at the backrest were non-linear with vibration magnitude when subjects were exposed to fore-and-aft excitation.

The present study investigated the effect of backrest inclination and seat-pan inclination on the fore-and-aft apparent mass of the back and the 'cross-axis' vertical apparent mass of the back during fore-and-aft whole-body excitation. It was expected that considerable force would be found at the backrest in the vertical direction. It was hypothesised that changing the backrest inclination and the seat-pan inclination would change the sitting posture, thus altering the apparent mass of the back in the fore-and-aft and 'cross-axis' vertical directions.

## 7.2.2 Method

### 7.2.2.1 Subjects

The experiment was conducted with twelve male subjects with the median and ranges of the age, weight, stature and seat-to-shoulder height as listed in Table 7.1. The experiment was approved by the Human Experimentation, Safety and Ethics Committee of the Institute of Sound and Vibration Research (ISVR), University of Southampton. Prior to vibration exposure, each subject completed a health questionnaire and an exposure consent form.

**Table 7.1** Subject age, stature, weight and seat-to-shoulder height.

	Age (yrs)	Stature (m)	Weight (kg)	Seat-to-shoulder height (m)
Minimum	20	1.64	50	0.58
Maximum	29	1.78	85	0.64
Median	23.8	1.72	67.7	0.62

#### 7.2.2.2 *Vibration generation*

Fore-and-aft vibration was produced by using a 1-metre peak-to-peak horizontal displacement electro-hydraulic vibrator, available in the Human Factors Research Unit at the ISVR, University of Southampton (see Figure 3.1, Chapter 3). The fore-and-aft motion of the vibrator platform was measured using an Entran EGCSY-240D\*-10 accelerometer (see Figure 3.3a, Chapter 3) mounted on the moving platform.

#### 7.2.2.3 *Seating and transducers*

A wooden rigid seat, with an adjustable seat-pan and backrest was securely mounted on the vibrator platform. Both the seat-pan and the backrest had flat surfaces. A tri-axial force platform (Kistler 9821B; see Figure 3.9a, Chapter 3) capable of measuring forces in three directions simultaneously (i.e.  $x$ ,  $y$  and  $z$ ) was secured to the flat backrest of the wooden seat so as to measure the forces at the back of seated person with varying backrest inclinations. The force plate (600 mm by 400 mm by 20 mm) consisted of four quartz piezoelectric force transducers. The force signal from each of the force transducers in both directions were summed and conditioned using Kistler 5007 charge amplifiers.

Figure 7.1 shows the experimental set-up.

#### 7.2.2.4 *Subject posture and experimental conditions*

Two conditions were studied: the first investigated the effect of backrest inclination and the second investigated the effect of seat pan inclination (Table 7.2). In both conditions, the forces on the backrest were measured in the 'fore-and-aft' direction (normal to the force platform) and in the 'cross-axis vertical' direction (parallel to the force platform). The conditions were presented in an independent random order of backrest, or seat-pan inclinations.

When varying the backrest and seat-pan inclination, the vertical height of the footrest on the vibrator platform was adjusted for each subject so as to make the upper and lower legs perpendicular to each other. In every condition, subjects were asked to '*maintain full contact of the upper body against the backrest with upper and lower legs always perpendicular to each other*'.

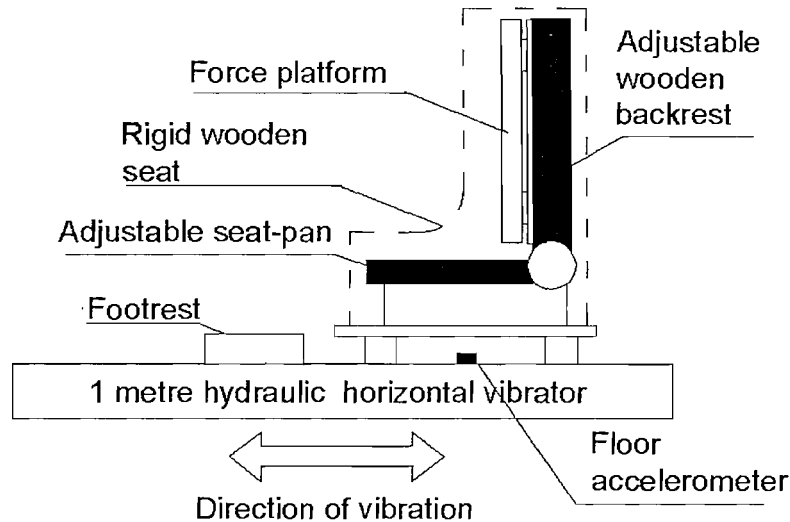


Figure 7.1: Experimental set-up.

Table 7.2 Experimental conditions (Note: All inclinations were measured from the horizontal).

	Parameters tested
Condition (i): effect of backrest inclination.	90°, 95°, 100° and 105° with 0° of seat-pan inclination
Condition (ii): effect of seat-pan inclination.	0°, 5°, 10° and 15° with 95 ° of backrest inclination

#### 7.2.2.5 Signal generation

All subjects were exposed to  $0.4 \text{ ms}^{-2}$  r.m.s. of a Gaussian random vibration having a duration of 60 s with a nominally flat constant bandwidth spectrum over the frequency range of 0.25 to 10 Hz. The vibration stimuli were generated using *HVLab* Data

Acquisition and Analysis system (version 3.81). All acceleration and forces signals were conditioned and acquired directly to the *HVLab* Data Acquisition system at 512 samples per second via 170 Hz anti-aliasing filters.

### 7.2.3 Analysis

Components of acceleration normal and parallel to the backrest (i.e. the force platform) could be related to the forces measured normal and parallel to the backrest so as to calculate the fore-and-aft apparent mass and the 'cross-axis' vertical apparent mass of the back. However, with constant fore-and-aft acceleration but increasing backrest inclination, the magnitudes of the accelerations in these directions changed during the experiment. As a consequence, the calculated 'fore-and-aft' and 'cross-axis vertical' apparent mass of the back at different backrest inclinations will have varied due to the combined effects of changing backrest angle and the non-linearity of the body.

Alternatively, the fore-and-aft apparent mass of the back and 'cross-axis' vertical apparent mass of the back could be calculated from the force measured normal to the backrest surface,  $F_F$ , and the force measured parallel to the backrest,  $F_V$ , resolved into fore-and-aft components ( $F_{Ff}$  and  $F_{Vf}$ ; Figure 7.2) and vertical components ( $F_{Fv}$  and  $F_{Vv}$ ; Figure 7.2). The 'true' fore-and-aft apparent mass of the back and the 'true' 'cross-axis vertical' apparent mass of the back could then be calculated from the applied fore-and-aft acceleration,  $a_f$ , and the resultant forces in the fore-and-aft and vertical directions. However, since previous studies have shown that the response of the body is non-linear in both directions, this simple resolving and adding of force components may not be suitable.

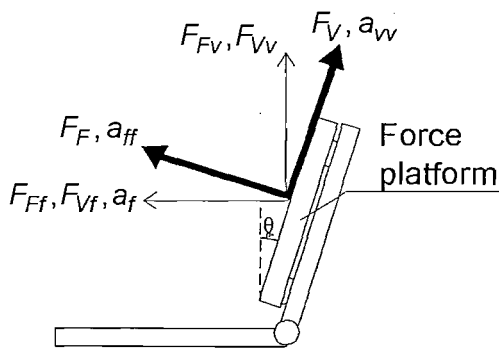


Figure 7.2: Forces and acceleration vectors diagram at the backrest.

In this study, at each backrest inclination, the measured forces on the backrest (i.e. the force normal to the backrest surface,  $F_F$ , and the forces parallel to the backrest surface,  $F_V$ , were compared directly with the applied fore-and-aft acceleration,  $a_f$ , to give what is called here the 'fore-and-aft' apparent mass of the back and the 'cross-axis vertical' apparent mass of the back (see Figure 7.2). Both frequency response functions were calculated using the cross-spectral density method:

$$M_{BF}(\omega) = \frac{F_F(\omega)}{a_f(\omega)} \quad (7.1)$$

or

$$M_{BV}(\omega) = \frac{F_V(\omega)}{a_f(\omega)} \quad (7.2)$$

where  $M_{BF}(\omega)$ , is the 'fore-and-aft' apparent mass of the back (or the 'cross-axis vertical' apparent mass of the back,  $M_{BV}(\omega)$ ),  $F_F(\omega)$ , is the cross-spectral density of the normal force and acceleration (or the cross-spectral density of the parallel force and acceleration,  $F_V(\omega)$ ) and  $a_f(\omega)$ , is the power spectral density of the input acceleration. The results are complex functions capable of giving modulus and phase.

#### 7.2.3.1 Mass cancellation

The measured 'fore-and-aft' and 'cross-axis vertical' forces at the back were influenced by the apparent mass of the subject and the mass of the force plate supported on the force transducer. Hence, mass cancellation was applied in the time domain so as to remove the effect of the mass of the aluminium plate of the force platform (15 kg) mounted 'above' the force cells at each backrest inclination. The force produced by the aluminium plate of the force platform in the 'fore-and-aft' direction (i.e. normal to the backrest) was 15 kg x acceleration x cosine  $\theta$  (assuming 90° for an upright backrest and  $\theta$  is small angle from the upright backrest) and was subtracted from the measured 'fore-and-aft' force,  $F_F$ . Likewise, the force produced by the aluminium plate of the force platform in the 'cross-axis vertical' direction (i.e. parallel to the backrest) was 15 kg x acceleration x sine  $\theta$  (assuming 90° for an upright backrest and  $\theta$  is small angle from the upright backrest) and was also subtracted from the measured 'cross-axis vertical' force,  $F_V$ . The 'corrected' 'fore-and-aft' and 'cross-axis vertical' forces at the backrest at each backrest inclination were used to calculate the 'fore-and-aft' and 'cross-axis vertical' apparent masses of the back.

## 7.2.4 Results

### 7.2.4.1 *Effect of backrest inclination*

#### 7.2.4.1.1 ‘Fore-and-aft’ apparent mass

The ‘fore-and-aft’ apparent masses of the backs of all twelve subjects with varying backrest inclinations are shown in Figure 7.3. The ‘fore-and-aft’ apparent mass of the back tended to decrease with increasing backrest inclination at frequencies less than 7 Hz - more obvious between 4 Hz and 7 Hz. At frequencies greater than 7 Hz, the apparent mass increased with increasing backrest inclination. A clear resonance around 5 Hz is apparent in some of the individual results (e.g. subjects 1,2 and 12) with the frequency decreasing with increasing backrest inclination. The apparent mass at resonance also tended to decrease with increasing backrest inclination.

There was a little ‘unusual’ trend of the apparent mass of the back in the results of subject 7 at frequencies less than 4 Hz for all conditions. However, since the coherency between 0.25 to 10 Hz was high for that subject, it was decided to include the results in the median calculation.

The median ‘fore-and-aft’ apparent mass of the backs of the twelve subjects showed similar trends to the individual results: with increasing backrest inclination, the apparent mass of the back tended to decrease at frequencies less than 7 Hz but increase at frequencies greater than 7 Hz (Figure 7.4). The median results suggest a principal resonance around 5 Hz with an upright backrest (i.e. 90°), with the frequency decreasing with increasing backrest inclination. When the backrest inclination was varied from 90° to 110°, there was a significant difference in the apparent mass at each of the preferred 1/3-octave centre frequencies, from 0.25 Hz to 10 Hz ( $p<0.05$ , Friedman), except at 0.25 Hz, 3.15Hz and 4 Hz ( $p>0.05$ ).

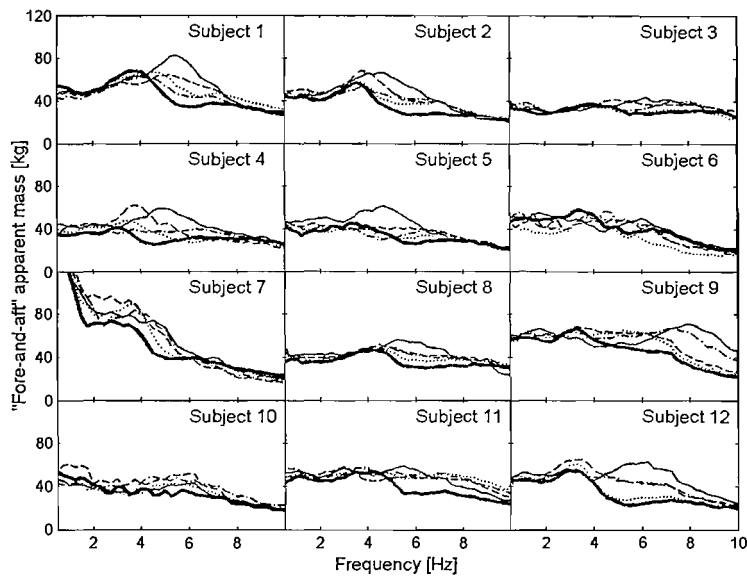


**Figure 7.3:** 'Fore-and-aft' apparent mass of the back for twelve subjects at backrest inclination of  $90^\circ$  (—),  $95^\circ$  (---),  $100^\circ$  (-·-·-),  $105^\circ$  (.....) and  $115^\circ$  (thick line).

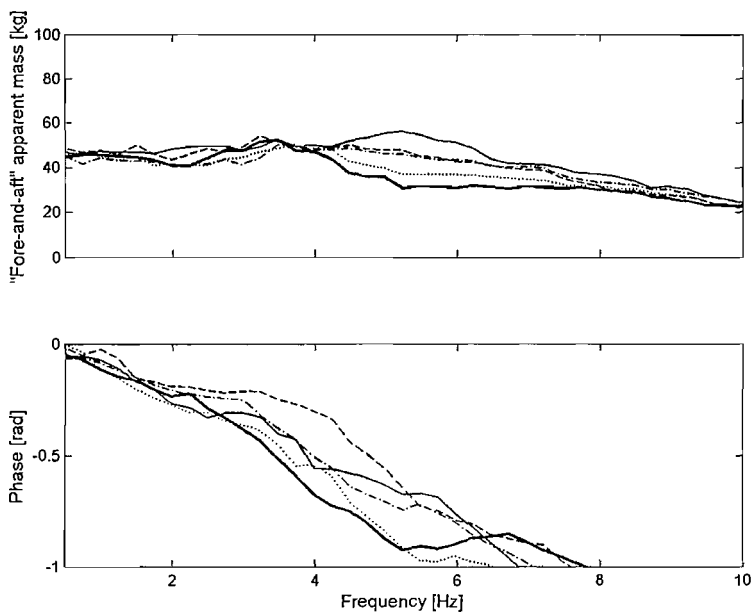


**Figure 7.4:** Median moduli and phases of the 'fore-and-aft' apparent mass of the back with twelve subjects at backrest inclination of  $90^\circ$  (—),  $95^\circ$  (---),  $100^\circ$  (-·-·-),  $105^\circ$  (.....) and  $115^\circ$  (thick line).

#### 7.2.4.1.2 'Cross-axis vertical' apparent mass

The twelve subjects showed a consistent trend: the 'cross-axis vertical' apparent mass of the back increased with a more inclined backrest (Figure 7.5). There was a clear resonance frequency around 5 Hz with upright backrest, with the resonance frequency decreasing with increasing backrest inclination. The apparent mass at resonance increased with increasing inclination of the backrest.

The median 'cross-axis vertical' apparent masses of the twelve subjects increased with increasing backrest inclination. At each preferred 1/3-octave centre frequency, from 0.25 Hz to 10 Hz, the 'cross-axis vertical' apparent mass of the back increased significantly with increasing backrest inclination (Figure 7.6;  $p<0.05$ , Friedman).

The median resonance frequency of the 'cross-axis vertical' apparent mass of the back decreased significantly when the backrest inclination was increased from 90° to 110° ( $p<0.05$ ). The median apparent mass at resonance increased significantly when the backrest inclination increased from 90° to 110° ( $p<0.05$ ).

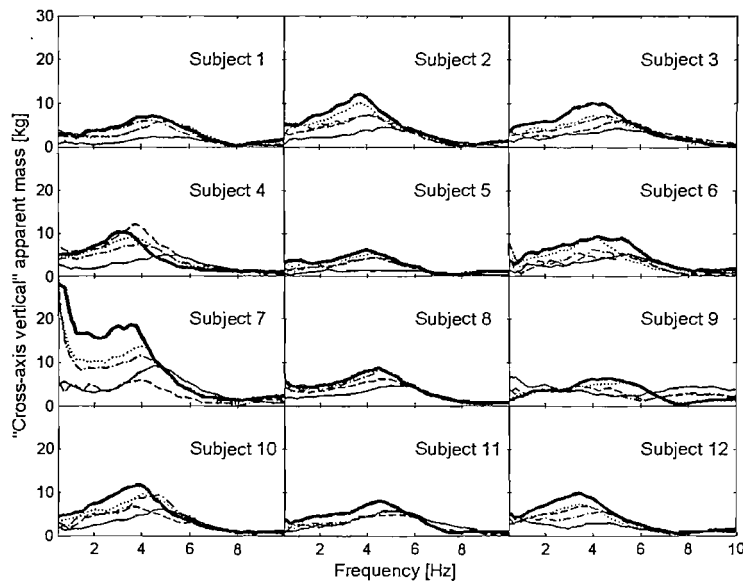
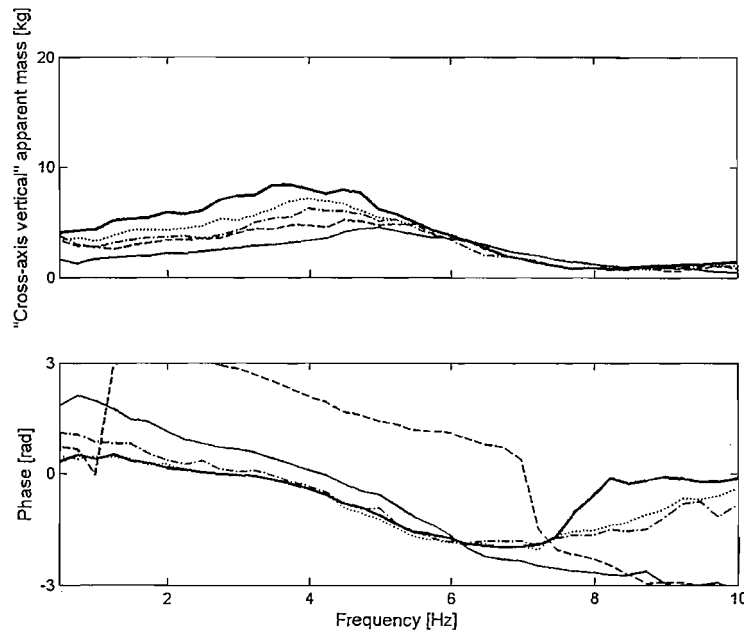


Figure 7.5: 'Cross-axis vertical' apparent mass of the back for twelve subjects at backrest inclination of 90° (—), 95° (---), 100° (-----), 105° (.....) and 115 ° (thick line).



**Figure 7.6:** Median moduli and phases of the 'cross-axis vertical' apparent mass of the back with twelve subjects at backrest inclination of 90° (—), 95° (---), 100° (-----), 105° (.....) and 115° (thick line).

#### 7.2.4.2 *Effect of seat pan inclination*

##### 7.2.4.2.1 'Fore-and-aft' apparent mass

As the seat-pan inclination increased from 0° to 15°, there was little change in the 'fore-and-aft' apparent mass of the back at lower frequencies (i.e. less than 4 Hz), but tendency for the apparent mass to increase at frequencies greater than 4 Hz (Figure 7.7). The seat-pan inclination had no obvious systematic influence on the resonance frequency of the 'fore-and-aft' apparent mass of the backs of the twelve subjects.

The median 'fore-and-aft' apparent mass of the backs of the twelve subjects is shown in Figure 7.8. At frequencies less than 4 Hz, there was no statistically significant in the 'fore-and-aft' apparent mass of the back at preferred 1/3-octave centre frequencies, from 0.25 Hz to 4 Hz ( $p>0.05$ , Friedman). However, at each preferred 1/3-octave centre frequency, from 5 to 10 Hz, the 'fore-and-aft' apparent mass of the back increased significantly with increasing seat-pan inclination from 0° to 15° ( $p<0.05$ ).

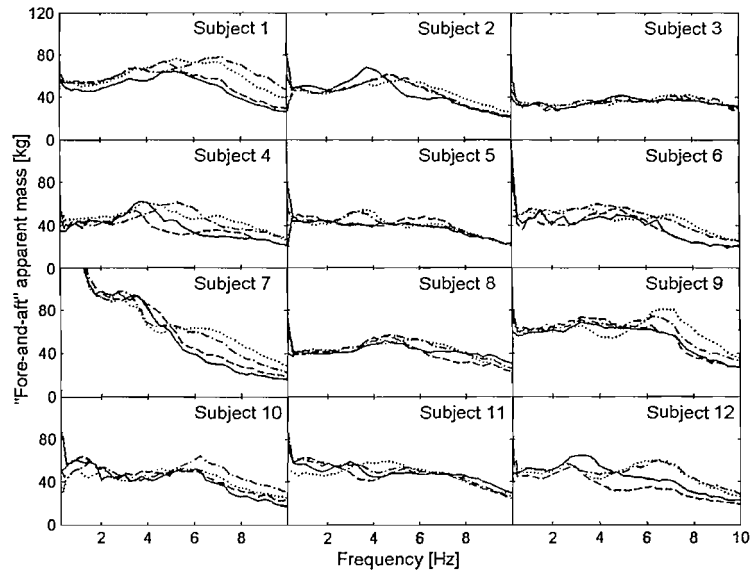


Figure 7.7: 'Fore-and-aft' apparent mass of the back for twelve subjects at seat-pan inclination of  $0^\circ$  (—),  $5^\circ$  (---),  $10^\circ$  (-·-·-) and  $15^\circ$  (····).

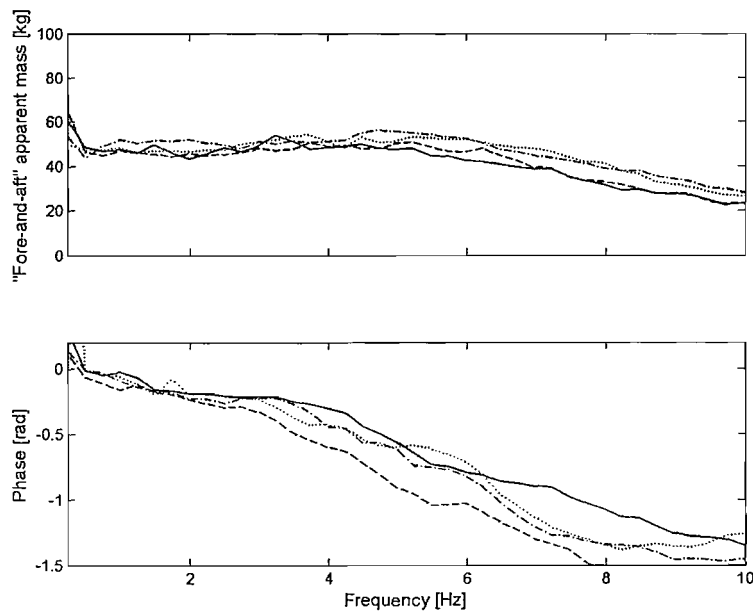


Figure 7.8: Median moduli and phases of the 'fore-and-aft' apparent mass of the back with twelve subjects at seat-pan inclination of  $0^\circ$  (—),  $5^\circ$  (---),  $10^\circ$  (-·-·-) and  $15^\circ$  (····).

#### 7.2.4.2.2 'Cross-axis vertical' apparent mass

Increasing seat-pan inclination had little influence on the 'cross-axis vertical' apparent mass of the back of twelve subjects (Figure 7.9). There was a resonance around 4 Hz but the resonance frequency was not systematically affected by the seat-pan inclination. Varying the seat-pan inclination also had little influence on the apparent mass at resonance.

Figure 7.10 shows the median 'cross-axis' vertical apparent mass of the backs of the twelve subjects at the four seat-pan inclinations. There was no significant change in the 'cross-axis vertical' apparent mass of the back due to seat-pan inclination at preferred 1/3-octave centre frequencies, from 0.25 Hz to 10 Hz ( $p>0.05$ , Friedman), except at 5 Hz and 6.3 Hz ( $p<0.05$ ). With varying seat-pan inclination, there was also no significant change in the principal resonance frequency or apparent mass at resonance of the 'cross-axis vertical' apparent mass of the back among the twelve subjects ( $p>0.05$ ).

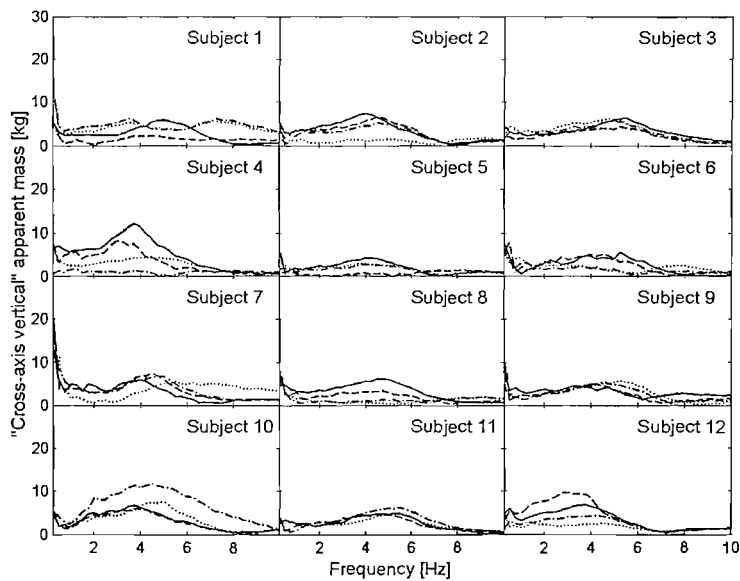
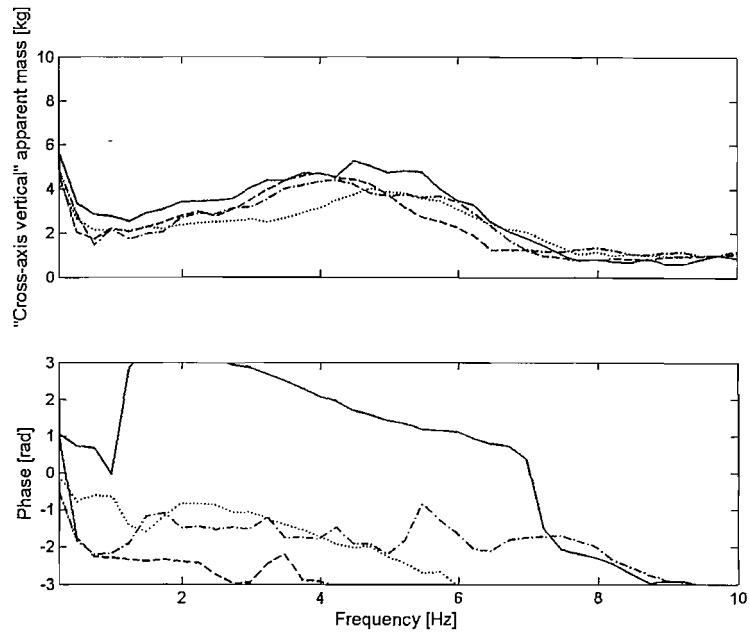


Figure 7.9: 'Cross-axis vertical' apparent mass of the back for twelve subjects at seat-pan inclination of 0° (—), 5° (---), 10° (-·-·-) and 15° (.....).



**Figure 7.10:** Median moduli and phases of the ‘cross-axis vertical’ apparent mass of the back with twelve subjects at seat-pan inclination of  $0^\circ$  (—),  $5^\circ$  (---),  $10^\circ$  (-·-·-) and  $15^\circ$  (····).

### 7.2.5 Discussion

#### 7.2.5.1 Effect of analysis method

The ‘fore-and-aft’ and ‘cross-axis vertical’ apparent masses of the back were calculated such that the measured ‘fore-and-aft’ force at the backrest (i.e. the force normal to the backrest),  $F_F$ , and the ‘cross-axis vertical’ force at the backrest (i.e. the force parallel to the backrest) were compared with the true fore-and-aft acceleration,  $a_f$  (Method A). The ‘fore-and-aft’ apparent mass of the back could have been calculated by comparing the normal forces at the backrest to the resolved fore-and-aft acceleration component,  $a_{ff}$  (i.e. ‘fore-and-aft’ acceleration normal to the backrest; see Figure 7.2). Likewise, the parallel forces to the backrest could have been compared with the resolved ‘vertical’ acceleration,  $a_{vv}$  (i.e. parallel to the backrest) so as to obtain the ‘cross-axis vertical’ apparent mass of the back at each backrest inclination (Method B). The acceleration normal to the backrest will reduce with increasing backrest inclination, proportion to the cosine of the angle between the backrest and the vertical. The acceleration parallel to the backrest will increase with increasing backrest inclination, proportion to the sine of the angle between the backrest and the vertical. Example results are shown in Figures 7.11 to 7.12.

Differences between the 'fore-and-aft' apparent mass of the back calculated using Method A (as presented in this chapter) and Method B are small. This is due to the small reduction in the 'fore-and-aft' acceleration with small deviations from the vertical. However, there were large differences in the 'cross-axis vertical' apparent mass between the two analysis methods. This is due to the great increase of the 'cross-axis vertical' acceleration, which is proportional to the sine of the angle of the backrest inclination. The 'cross-axis vertical' apparent mass calculated using Method B therefore showed different trends in the response from those given by Method A.

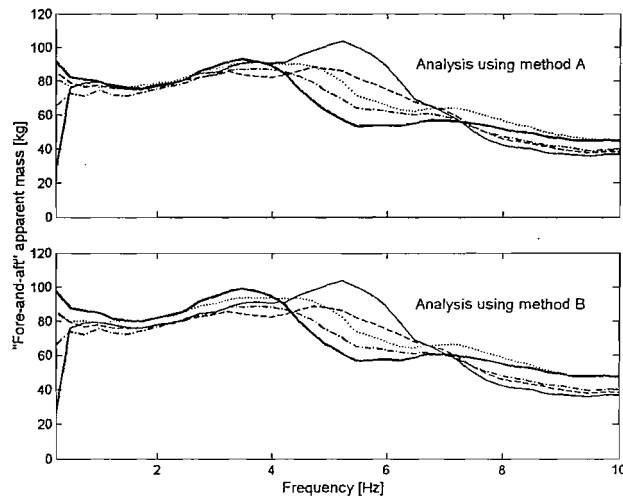


**Figure 7.11:** Comparison of the apparent masses of the back at five backrest inclinations of one subject using analysis method A (calculated from the forces measured normal to the backrest and the applied fore-and-aft acceleration; top graph) and method B (calculated from the forces measured normal to the backrest and the resolved 'fore-and-aft' acceleration at the backrest, i.e. normal to the backrest; bottom graph). Key: 90° (—), 95° (---), 100° (-----), 105° (.....) and 115° (—).

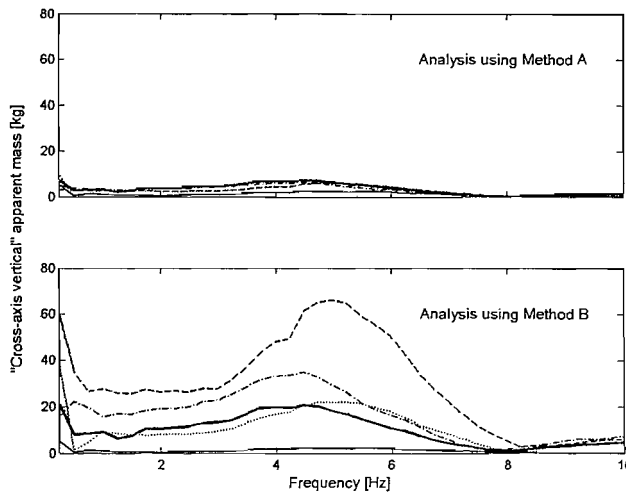


**Figure 7.12:** Comparison of the 'cross-axis' vertical apparent masses of the back at five backrest inclinations of one subject using analysis method A (calculated from the forces measured parallel to the backrest and the applied fore-and-aft acceleration; top graph) and method B (calculated from the forces measured parallel to the backrest and the resolved 'vertical' acceleration at the backrest, i.e. parallel to the backrest; bottom graph). Key: 90° (—), 95° (---), 100° (----), 105° (.....) and 115° (—).

### 7.2.5.2 Effect of backrest inclination

#### 7.2.5.2.1 'Fore-and-aft' apparent mass

The 'fore-and-aft' apparent mass of the back showed a resonance around 5 Hz with a vertical backrest (i.e. 90°), but the frequency decreased with increasing backrest inclination. Demic *et al.* (2002) found that the resonance frequency in fore-and-aft seat-to-head transmissibility during fore-and-aft excitation decreased when the backrest inclination was increased from an upright backrest (i.e. 90°) to 104° with subjects adopting a driving position (i.e. hands on the steering wheel). A change in body posture when sitting with a more inclined backrest might change the body responses – in this study it might be inferred that the body stiffness reduced.

Alternatively, the percentage of the body mass supported on the seat and the inclined backrest differ from that when seated with a vertical backrest. Anderson *et al.* (1979) reported decreased myoelectric activity (reflecting decreased muscle activity) in the lumbar area with a more inclined backrest, and inferred that the decrease was associated with a reduction in the disc pressure, possibly due to a transfer of body weight to the backrest.

When subjects adopted an automotive sitting posture (i.e. with inclined seat-pan and inclined backrest), the percentage of the body mass supported on the seat was 70%, while around 30% was supported on the inclined backrest (Rakheja *et al.*, 2002). With vertical excitation, Wang *et al.* (2004) found a resonance frequency in the whole-body apparent mass around 5 Hz with an upright backrest, with the resonance frequency increasing when the backrest was inclined up to 12° from the vertical. A decrease in the proportion of the body mass supported on the seat with the inclined backrest may, in part, cause the resonance frequency of the whole-body apparent mass to increase. By analogy with the findings with vertical vibration (Rakheja *et al.*, 2002 and Wang *et al.*, 2004), a decrease in the resonance frequency of the 'fore-and-aft' apparent mass of the back may be partially due to an increased proportion of the mass of the body being supported on the backrest.

The reduced resonance frequency in the 'fore-and-aft' apparent mass of the back with increased backrest inclination may be attributed to a combination of changes in the biodynamic responses of the body with changing posture and an increased proportion of the body mass supported on the backrest with a more inclined backrest.

If the backrest were inclined further than the vertical, the backrest would receive additional loading in the 'fore-and-aft' direction (i.e. normal to the backrest) - the apparent mass of the back in the 'fore-and-aft' direction will change. Although more mass is supported on the backrest with greater inclined backrest, it could be expected that the 'fore-and-aft' apparent mass of the back and the resonance frequency would reduce. This is due to the reduction in the 'fore-and-aft' vibration at the backrest (i.e. normal to the backrest), which is proportion with the cosine of the angle between the backrest and the vertical (i.e. 90°). Therefore, the influence of the additional load would affect the resonance frequency of the 'fore-and-aft' apparent mass of the back.

In Chapter 5, it was found that the resonance frequency of the 'fore-and-aft' transmissibility (i.e. the transmissibility in a direction normal to the backrest surface) increased with increasing backrest inclination. The current results suggest that an increase in the resonance frequency of the 'fore-and-aft' backrest transmissibility may be partly due to an increase in the dynamics stiffness of the backrest cushion with a more inclined backrest, which can be associated with an increase body mass supported on the backrest cushion.

During vertical vibration and at low frequencies, i.e. near 0 Hz, the apparent mass of the body at this frequency is approximately equal to the subject static weight supported by the seat, which is approximately 75% of subject's weight (Griffin, 1990; Wei and Griffin, 1998c and Nawayseh and Griffin, 2004). It may be expected that at the same frequencies, the apparent mass of the back during fore-and-aft excitation equals to the mass of the back

supported on the backrest. In Chapter 6, the apparent mass of the back at low frequency was found to be approximately 45% of the subjects' weight. However, during static condition, the forces measured at vertical backrest were approximately 10% of the subject's weight (Nawayseh and Griffin, 2005a). An increase in the forces of the back at the backrest during fore-and-aft excitation compared to the forces at the backrest in static condition suggests that the forces at the backrest do not directly indicate the total mass of the back supported on the backrest. This is because they indicate forces at the back when the seat and the backrest move together. The increase in the forces at the back at low frequencies during fore-and-aft excitation may be the results of the involuntary push force at the feet which pushes the body to lean to the backrest in reacting with the pitching motion of the upper body.

The 'fore-and-aft' forces at the back with a vertical backrest (i.e. 90°) were greatest at frequencies between 4 and 8 Hz. In Chapter 6, the body exhibited a mode around 5 Hz, and it is suggested that this mode was associated with the entire body bending in the lower thoracic spine and pitching in the pelvis and the upper body. The high 'fore-and-aft' forces against the vertical backrest at frequencies between 4 and 8 Hz may arise from push forces at the feet reacting with pitching movements of the body and pushing the back against the backrest. This would increase the static and dynamic 'fore-and-aft' forces at the backrest. With a more inclined backrest, the upper body 'rests' against the backrest, and possibly the centre of gravity (COG) of the body moves forward. Therefore, the forces required to stabilise the body are no longer needed since the body does not pitch forward beyond the COG.

#### 7.2.5.2.2 'Cross-axis vertical' apparent mass

Nawayseh and Griffin (2005a) found 'cross-axis vertical' forces at the back when sitting against an upright backrest during fore-and-aft excitation. In a single subject study, they found that the resonance frequency of the 'cross-axis vertical' apparent mass of the back varied between 5 Hz and 7 Hz during fore-and-aft vibration, depending on the vibration magnitude. The current study also shows the 'cross-axis vertical' apparent mass of the back with a resonance around 5 Hz when sitting against an upright backrest, but the frequency decreased with increasing backrest inclination. The reduction in the resonance frequency with increasing inclination may partly be attributed to increased mass supported on the backrest in the 'cross-axis vertical' direction (i.e. parallel to the seat back).

A previous study found low 'cross-axis vertical' forces at an upright backrest for one subject during fore-and-aft excitation (Nawayseh and Griffin, 2005a) and it was suggested that '*the low vertical forces at the back were the results of some vertical motion of the spine*

accompanying the pitching mode of the pelvis, spine and upper body'. In the current study, the 'cross-axis vertical' apparent mass of the back with an upright backrest were very low for all subjects in the frequency range 0.25 to 10 Hz. However, with increasing backrest inclination, the 'cross-axis vertical' forces increases. As the backrest inclination increased, it is suggested that COG of the body moves forward and resulting in the body 'resting' against the backrest (since the body does not pitch forward beyond the COG). At this condition, the 'cross-axis vertical' acceleration (i.e. parallel to the backrest) increases proportional to the sine angle of the backrest from vertical. An increase in the vibration at the backrest may increase 'vertical' motion of the body (i.e. parallel to the backrest) and therefore increases the 'cross-axis vertical' forces at the back

#### 7.2.5.3 *Effect of seat-pan inclination*

##### 7.2.5.3.1 'Fore-and-aft' apparent mass

Changing the seat-pan inclination could change the sitting posture of a subject, and thereby the biodynamic responses. However, in the present study, the backrest inclination and the leg postures remained the same with all four seat-pan inclinations. Any differences in the responses between the four seat-pan inclinations are therefore assumed to be due to the changes in the sitting posture (e.g. due to pelvis rotation).

Increasing the seat-pan inclination had little influence on the 'fore-and-aft' apparent mass of the back at frequencies less than 4 Hz, above which the 'fore-and-aft' forces at the backrest tended to increase with increasing seat pan inclination. With a horizontal seat pan (i.e. 0° inclination), the 'fore-and-aft' forces on the seat (i.e. parallel to the seat-pan) could influence the 'fore-and-aft' forces at the backrest. With increasing seat-pan inclination, the 'fore-and-aft' acceleration on the seat decreased in proportion to the cosine of the angle between the seat-pan and the horizontal. Possibly, the 'reduced' forces on the seat may be partially transferred to the backrest, as there was a tendency for increased 'fore-and-aft' forces with increased seat-pan inclination at frequencies greater than 4 Hz.

##### 7.2.5.3.2 'Cross-axis vertical' apparent mass

The resonance frequency of the 'cross-axis vertical' apparent mass of the back was not affected by the seat-pan inclination. Although changing the seat-pan inclination may change sitting posture, there was not much of increase in the shear forces between the back and the backrest with increased seat-pan inclination because the backrest inclination was the same for all conditions. A reduction in the 'cross-axis vertical' forces at the backrest with increasing seat-pan inclination may be caused by the 'cross-axis vertical' vibration on

the seat (i.e. normal to the seat surface), which increases in proportion to the sine of the angle between the seat-pan and the horizontal, although the forces on the seat were not measured here.

### 7.2.6 Conclusion

Varying the backrest inclination (from 90° to 110°) had more influence on the 'fore-and-aft' apparent mass (calculated from the forces measured normal to the backrest and the applied fore-and-aft acceleration) and the 'cross-axis vertical' apparent mass of the back (calculated from the forces measured parallel to the backrest and the applied fore-and-aft acceleration) than varying the seat-pan inclination (from 0° to 15°).

With increased backrest inclination, there was a reduction in the resonance frequency of both the 'fore-and-aft' and the 'cross-axis vertical' apparent masses of the back. The forces at the backrest in both the 'fore-and-aft' and the 'cross-axis vertical' directions were significantly affected when the backrest inclination was increased from 90° to 110°. However, with four seat-pan inclinations (0°, 5°, 10° and 15°), the resonance frequencies of both the 'fore-and-aft' and the 'cross-axis vertical' apparent masses of the back were unaffected. Furthermore, increasing the seat-pan inclination had no significant effect on the forces at the backrest in either the 'fore-and-aft' or 'cross-axis vertical' directions.

## 7.3 Effect of the push force at the feet and the horizontal position of the footrest

### 7.3.1 Introduction

The apparent mass of the back of a seated person exposed to whole-body fore-and-aft vibration shows a principal resonance around 5 Hz (Nawayseh and Griffin, 2005a). Some of the factors that can affect the apparent mass of the back during fore-and-aft vibration have been explored. Raising the height of a moving footrest (so that subjects adopted different leg postures and had different thigh contact with the seat surface) had little influence on the apparent mass of the back during fore-and-aft excitation (Nawayseh and Griffin, 2005a). In the same study, the authors found that the body produces vertical oscillatory forces at the backrest – also known as a 'cross-axis' response when exposed to fore-and-aft vibration. Increasing the height of a footrest had little influence on the 'cross-axis' vertical apparent mass of the back.

This study was designed to explore further the factors that can affect the apparent mass of the back during fore-and-aft excitation. The effect of push force at the feet and the horizontal position of a footrest on the apparent mass of the back were investigated. It was hypothesised that, due to a stiffening of the back, the resonance frequency of the fore-and-aft apparent mass of the back would increase with increases in the force applied by the feet against the footrest. It was hypothesised that changing the footrest position would change the posture of the lower legs and thereby affecting the apparent mass of the back in both the 'fore-and-aft' and 'cross-axis vertical' directions.

### 7.3.2 Method

A wooden rigid seat, with an adjustable seat-pan and backrest was securely mounted on the vibrator platform. Both the seat-pan and the backrest had flat surfaces. A tri-axial force platform (Kistler 9821B) capable of measuring forces in three directions was secured to the flat backrest of the wooden seat so as to measure the forces normal and parallel to the backrest surface. The forces at the backrest are referred to as 'fore-and-aft' and 'cross-axis vertical' forces in this section, although when the seat was inclined they were not truly fore-and-aft and vertical. The force plate (600 mm by 400 mm by 20 mm) consisted of four quartz piezoelectric force transducers. The force signals from each of the force transducers were summed and conditioned using a Kistler 5007 charge amplifier.

An Entran EGCS-Y 24-10-D accelerometer was attached to the floor beneath the seat using double-sided adhesive tape so as to monitor the input acceleration.

One 26-year old subject with a 1.76 m stature and weighing 78 kg participated in the study. The subject was exposed to  $0.4 \text{ ms}^2$  r.m.s. of Gaussian random vibration with a nominally flat constant bandwidth acceleration spectrum over the frequency range 0.25 to 10 Hz. The stimulus lasted for 60 seconds in each condition. The vibration stimuli were generated using a *HVLab* Data Acquisition and Analysis system (version 3.81). All acceleration signals were conditioned and acquired directly into the *HVLab* Data Acquisition system at 512 samples per second via 170 Hz anti-aliasing filters.

The subject was asked to adopt a sitting posture with the '*upper body leaning on the backrest with hands placed on the lap and feet resting on the wooden footrest*'. The surface of the wooden footrest was inclined at  $5^\circ$  from the horizontal. Two factors were investigated: effect of push force at the feet (Condition 1) and the effect of horizontal position of the feet (Condition 2).

For Condition 1, the subject was asked initially to 'only rest the feet on the footrest' - this was regarded as 'no force'. The apparent mass of the back were measured. Subsequently,

the subject was asked to increase the push force at the feet to either 50 N, or 100 N or 150 N. The push force applied by the feet on the footrest was measured using electronic scales placed on the surface of the footrest (Adam Equipment; model: CPW-150; max. load = 150 kg; SN = AE 16000592). The subject was also asked to maintain the force applied within  $\pm 10\%$  of the required push force by monitoring the panel on the electronic scales.

For Condition 2, the initial position of the footrest was obtained when the lower legs were perpendicular to the upper legs – this position was regarded as ‘0 mm’. Subsequently, the horizontal footrest position was positioned at 50 mm, 100 mm and 150 mm forward the ‘0 mm’ position. The experimental arrangement is shown in Figures 7.13.

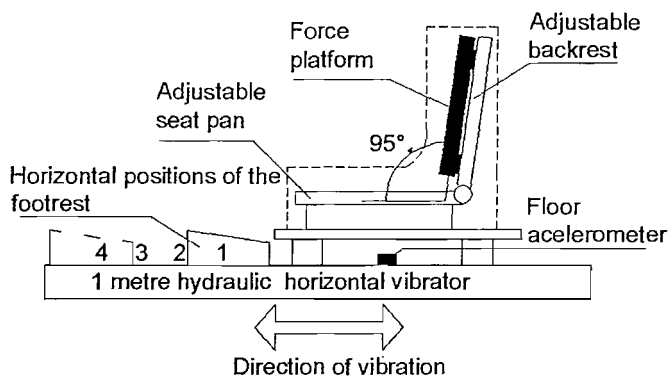


Figure 7.13: Experimental set-up.

### 7.3.3 Analysis

All acquired signals were normalised to remove any d.c. offset from the time histories using the *HVLab* data acquisition system before they were used to calculate the apparent mass at the back. A resolution of 0.25 Hz was used, giving 60 degrees-of-freedom.

The ‘fore-and-aft’ and ‘cross-axis vertical’ apparent masses of the back in each condition were also calculated using the CSD method using equations 7.1 and 7.2 respectively (see Section 7.2.3).

### 7.3.3.1 Mass cancellation

The measured 'fore-and-aft' and 'cross-axis vertical' forces at the back were influenced by the apparent mass of the subject and the mass of the force plate supported on the force transducers. Hence, mass cancellation was applied in the time domain so as to remove the effect of the mass of the aluminium plate of the force platform (15 kg) mounted 'above' the force cells. The force produced by the aluminium plate of the force platform in the 'fore-and-aft' direction (i.e. normal to the backrest) was  $15 \text{ kg} \times \text{acceleration} \times \cosine \theta$  (assuming  $90^\circ$  for an upright backrest and  $\theta$  is small angle from the upright backrest) and was subtracted from the measured 'fore-and-aft' force. Likewise, the force produced by the aluminium plate of the force platform in the 'cross-axis vertical' direction (i.e. parallel to the backrest) -  $15 \text{ kg} \times \text{acceleration} \times \sin \theta$  (assuming  $90^\circ$  for an upright backrest and  $\theta$  is small angle from the upright backrest) was subtracted from the measured 'cross-axis vertical' forces at the backrest. The 'corrected' 'fore-and-aft' and 'cross-axis vertical' forces at the backrest were used to calculate the 'fore-and-aft' and 'cross-axis vertical' apparent masses of the back

## 7.3.4 Results

### 7.3.4.1 Effect of the push force at the feet

There were high 'fore-and-aft' forces at the backrest and appreciable forces in the 'cross-axis vertical' direction (Figure 7.14). While the 'fore-and-aft' forces at the backrest tended to increase with increasing push force at the feet, the forces at the backrest in the 'cross-axis vertical' direction tended to reduce with increased push force. The increase in the 'fore-and-aft' forces at the backrest with increasing push force is more obvious at frequencies greater than the principal resonance frequency (i.e. greater than 4.7 Hz). Conversely, there is a reduction in the 'cross-axis vertical' forces at the backrest with increased push force at frequencies less than the resonance frequency around 4.5 Hz.

With increasing push force at the feet, the principal resonance frequency of both the 'fore-and-aft' and 'cross-axis vertical' apparent masses of the back increased from 4.7 to 5.5 Hz and from 4.5 to 5.2 Hz, respectively. There is evidence of a second resonance frequency in the 'fore-and-aft' apparent mass of the back around 7 Hz ('no force'), that shows a slight increase to 7.1 Hz when the subject exerted a 150 N push force at the feet.

The apparent mass at resonance in the 'fore-and-aft' direction with 'no force' was around 73 kg, and increased to around 75 kg with both 50 N and 100 N push force, after which the

apparent mass further increased to 90 kg with 150 N push force. However, with greater push force at the feet, the 'cross-axis vertical' apparent mass of the back at resonance reduced from 3.7 to 2 kg with a push force of 50 N, after which there was little change in the apparent mass at resonance when the push force was increased from 50 N to 150 N.

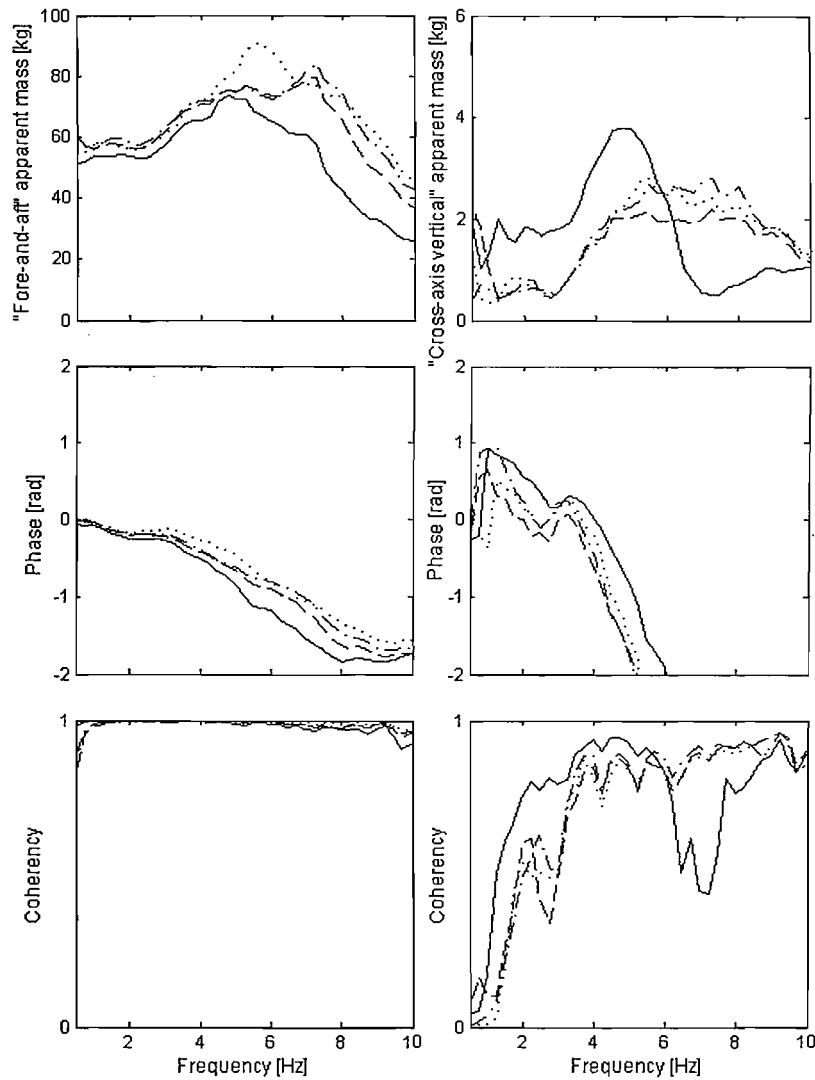


Figure 7.14: Moduli and phases of the 'fore-and-aft' and 'cross-axis vertical' apparent masses of the back for one subject with 'no force' (—), 50 N (---), 100 N (- · - · -) and 150 N (.....) of push force at the feet.

#### 7.3.4.2 *Effect of horizontal footrest position*

The 'fore-and-aft' apparent mass of the back tended to increase at frequencies below the resonance frequency (around 5 Hz with '0 mm' footrest position), after which the forces in the 'fore-and-aft' direction tended to decrease at frequencies greater than the resonance frequency (Figure 7.15). The 'fore-and-aft' forces were least over the frequency range (0.25 to 10 Hz) when the footrest was positioned furthest from the front edge of the seat cushion. However, at this footrest position (i.e. when the footrest was furthest away from the seat cushion), the 'cross-axis vertical' forces at the backrest were greatest from 0.25 Hz up to 7 Hz.

Varying the horizontal position of the footrest had little influence on the principal resonance frequency of the 'fore-and-aft' apparent mass of the back around 4.7 Hz. Similarly, there is a peak around 4.7 Hz in the 'cross-axis vertical' apparent mass of the back that was not affected by the horizontal position of the footrest. Between the '0 mm' and '100 mm' footrest position, there was little change in the moduli of the apparent mass at resonance in either the 'fore-and-aft' or the 'cross-axis vertical' directions. However, with the footrest at 150 mm, the 'fore-and-aft' apparent mass at resonance was lowest while the 'cross-axis vertical' apparent mass at resonance was highest.

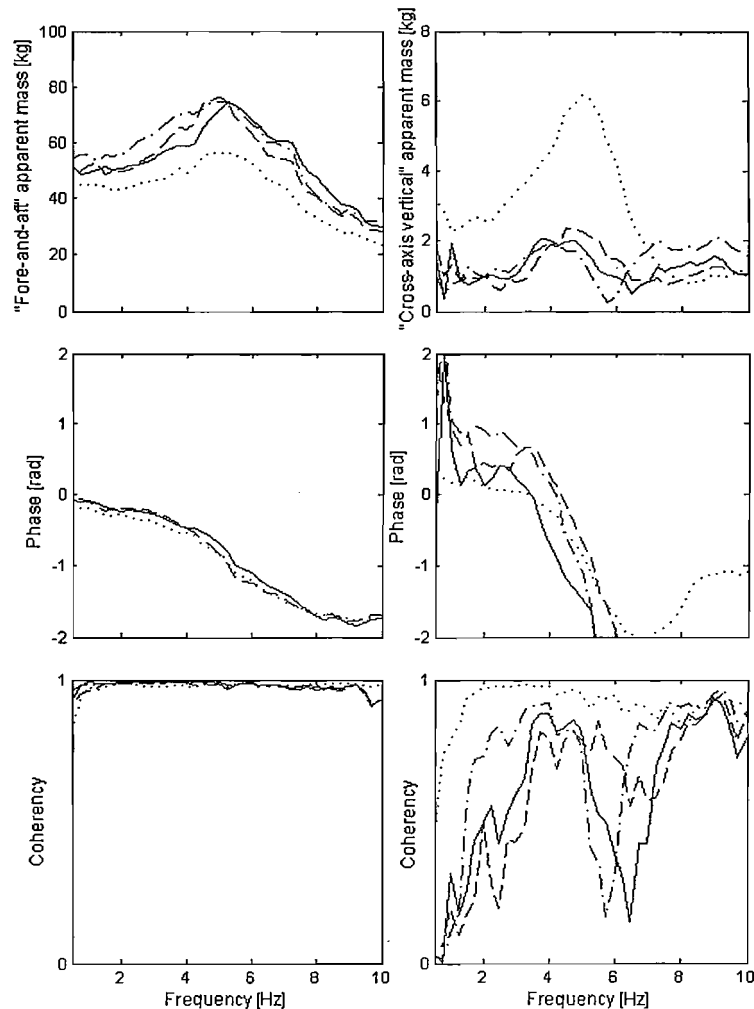


Figure 7.15: 'Fore-and-aft' and 'cross-axis vertical' apparent masses and phases of the back for one subject at horizontal footrest's position of '0 mm' (—), 50 mm (---), 100 mm (- · - · -) and 150 mm (·····).

### 7.3.5 Discussion

#### 7.3.5.1 *Effect of the fore-and-aft push force at the feet*

The results of only one subject in the current study suggest that force applied by muscles (such as increasing the push force at the feet on a footrest) can increase the stiffness of the body. An increase in the resonance frequency of both the 'fore-and-aft' and 'cross-axis vertical' apparent masses of the back may be the result of an increase in the body stiffness. Similarly, the results of previous studies show that when subjects adopt an 'erect' sitting posture, the resonance frequency of the apparent mass is greater than when sitting in a relaxed posture during vertical excitation, consistent with a stiffening effect of the body (e.g. Fairley and Griffin, 1989 and Kitazaki and Griffin, 1997).

When subjects changed sitting posture from 'slouched' to 'erect', there was a significant increase in the resonance frequency of the apparent mass and the apparent mass of the body between 4 Hz and 10 Hz (Fairley and Griffin, 1989). However, when subjects further tensed their body postures from 'erect' to 'very erect', the resonance frequency peak became broader and there was only a small increase in the apparent mass of the body between 4 Hz and 10 Hz. Likewise, in the present study, when the subject increased the push force at the feet from 'no force' to 50 N, there was a clear increase in the fore-and-aft apparent mass of the back between 5 Hz and 10 Hz. However, when the push force at the feet was further increased from 50 N to 150 N, although the fore-and-aft forces at the backrest were increased the change was not as clear as that when the force increased from 'no force' to 50 N. This, together with the results of Fairley and Griffin (1989), may suggest that the biodynamic responses change significantly if the body stiffness changes from 'normal' to 'stiff', but when the stiffness of the body is further tensed, the difference between the 'stiff' and the 'stiffest' condition is small.

With increased push force at the feet, it was anticipated that the body would become stiffer as the body was pushed against the backrest. The 'cross-axis' vertical movement of the upper body may have become restricted when the body was pushed against the backrest. As suggested by Nawayseh and Griffin (2005a), the vertical forces at the backrest when the body is exposed to fore-and-aft excitation could be the results of some vertical motion of the spine accompanying the pitching mode of the pelvis, spine and upper body. However, in their study, subjects did not impose any additional push force at the feet, hence allowing the body to respond in a 'natural' movement. Notwithstanding the 'cross-axis' vertical movement of the spine during fore-and-aft excitation, it can be anticipated that by restricting the body response in the direction of the excitation (i.e. by exerting a

push force at the feet so as to push the upper body against the backrest), the accompanying vertical movement of the spine with the fore-and-aft and pitching motions of the upper body may also be restricted. This may partially explain why the 'cross-axis vertical' forces at the backrest reduced with increasing push force at the feet.

The apparent mass of the back during fore-and-aft excitation has been found to vary non-linearly with vibration magnitude – the resonance frequency of the fore-and-aft apparent mass of the back tended to decrease with increasing vibration magnitude (Nawayseh and Griffin, 2005a). It is anticipated that the forces at the feet will be proportional the fore-and-aft acceleration and stabilise the pitching movement of the body while allowing the 'natural' softening response of the body with increasing vibration magnitude. The results of current study suggest that the 'softening' response of the body (i.e. the reduction in the resonance frequency of the apparent mass of the back with increasing vibration magnitude) may be affected if the feet exert additional force at higher vibration magnitudes. With greater push force at the feet, the forces at the backrest will tend to increase and so increase the resonance frequency of both the apparent mass of the back and the backrest transmissibility.

Previous studies have found that the dynamic stiffness of a foam cushion increased with increasing pre-load on the foam (Wei and Griffin, 1998c). An increased resonance frequency in a backrest transmissibility with increased force at the feet as found in the Chapter 5 (Section 5.4), may be partly due to increased dynamic stiffness of the backrest cushion as a result of the increased force on the backrest cushion.

#### 7.3.5.2 *Effect of the horizontal position of the footrest*

When subjects sat with their feet 75 mm forward of the 'normal' position (i.e. a comfortable stable posture), the effect of the horizontal foot position on the vertical apparent mass of the body was negligible at frequencies less than 40 Hz (Rakheja *et al.*, 2002). In the current study, the effect of footrest position on the 'fore-and-aft' apparent mass at the back was small. The resonance frequency in the apparent mass at the back showed only small changes, suggesting little change in either the stiffness of the body or backrest.

There were appreciable 'cross-axis vertical' forces at the backrest with all positions of the footrest, although with different footrest positions the 'cross-axis vertical' forces changed little. When the legs were stretched to rest the feet on the footrest (i.e. at 150 mm), the 'cross-axis vertical' forces at the backrest were greatest. In this condition, the body may have been more free to move, as there would be reduced push force at the feet, allowing more pitch motion of the upper body.

### **7.3.6 Conclusion**

Results from one subject show that with increased push force at the feet there was an increase in the resonance frequency of the 'fore-and-aft' and 'cross-axis vertical' apparent mass of the back. Increased 'fore-and-aft' forces at the backrest were measured with increased push forces at the feet. Varying the fore-and-aft position of the footrest had little influence on the apparent mass of the back in either direction (i.e. the 'fore-and-aft' or 'cross-axis vertical' apparent mass). The results of this study suggest that during fore-and-aft excitation the application of force at the feet has a greater effect on the biodynamic responses of the back than a change in the fore-and-aft position of the feet.

# Chapter 8

## Predicting fore-and-aft backrest transmissibility

### 8.1 Introduction

The drivers, occupants, operators, of vehicles are exposed to vibration of body through the seats. Most modern seats are compliant – they modify the vibration by amplifying it at low frequencies and attenuating it at high frequencies. A good seat should be able to provide a good sitting environment for the occupant (e.g. comfortable to sit over long period) and should not prevent any activities the occupant has to perform.

There have been extensive studies of the vibration transmitted through seats during vertical excitation. A few studies have investigated the transmissibility of seats during fore-and-aft excitation. Most of the studies involve the measurement of seat transmissibility with subjects sitting in the seat, with either laboratory measurements, or field measurements. Although such measurements are ‘real’ (as human subjects are involved), the method: i) is time consuming, ii) requires a suitable vibrator (in the case of laboratory measurements) to reproduce the vibration that is suitable and safe for exposure to human subjects, which can be very expensive, and iii) there are *‘inherent risks that exposure to the mechanical vibration or shock which the experiment is intended to reproduce may lead to injury or ill-health, either immediately or at some time in the future’* (British Standard BS 7085, 1989).

Previous studies have shown that it is possible to predict the vibration transmitted through seats in the vertical direction without using human subjects. The alternative methods were: i) the use of anthropodynamic dummies with appropriate mechanical impedance to replace the human subjects (e.g. Suggs *et al.* 1969 and Mansfield and Griffin,

1996), or ii) the use of mathematical models based on separate measurements of the impedance of the body and the impedance of the seat (e.g. Fairley and Griffin, 1986 and Wei and Griffin, 1998c).

There is no known study reporting the prediction of backrest transmissibility during fore-and-aft excitation. The objective of this chapter is to investigate the method of predicting seat transmissibility in the vertical direction as reported by Fairley and Griffin (1986) and Wei and Griffin (1998c) as a method of predicting fore-and-aft backrest transmissibility. This chapter is divided into three main sections: (i) developing a lumped parameter model that can adequately represents the apparent mass of the back, (ii) obtaining the dynamic properties of the backrest cushion (stiffness and damping coefficients) from an indenter test and (iii) using the developed lumped parameter model and measured impedance of the backrest cushion to predict backrest transmissibility.

## 8.2 Modelling apparent mass of the back

### 8.2.1 Introduction

Models representing the impedance of a seated person exposed to vertical excitation have been extensively reported (e.g. Suggs *et al.*, 1969; Fairley and Griffin, 1989; Nawayseh, 2002). The apparent mass of the seated person during vertical vibration, in the simplest way, can be presented by a single degree-of-freedom model (e.g. Wei and Griffin, 1998c). Many models adequately represent the apparent mass of the seated person with no backrest during vertical excitation, although they could not represent the mechanisms involved.

There has been little study of models of the apparent mass of seated person during fore-and-aft excitation. Mansfield and Lundström (1999) showed that a three-degree-of-freedom model (three mass-spring-damper systems arranged in parallel) can adequately represent the apparent mass of the body during fore-and-aft and lateral excitation. Nawayseh (2004) also showed that a three-degree-of-freedom model, with a rotational capability can represent the fore-and-aft apparent mass of the body during fore-and-aft excitation. The latter model was also capable of representing the 'cross-axis' vertical apparent mass of the body during fore-and-aft vibration. However, both models (by Mansfield and Lundström, 1999 and Nawayseh, 2004) only considered the apparent mass of the body when were subjects seated with upright posture and with no backrest. No study has reported a model of the apparent mass of the back during fore-and-aft excitation.

In the next section, a simple two-degree-of-freedom lumped parameter model is developed to predict the apparent mass of the back during fore-and-aft excitation. This model is not a mechanistic model, it does not represent the mechanisms involved during the responses of the body to vibration. The model was developed so that when it is combined with a backrest cushion model, the new seat-person model could be used to predict the backrest transmissibility.

### 8.2.2 Lumped parameter model

A simple two degrees-of-freedom model was developed in an attempt to predict the fore-and-aft apparent mass of the back (Figure 8.1). The model consisted of two mass-spring-damper systems, arranged in parallel.

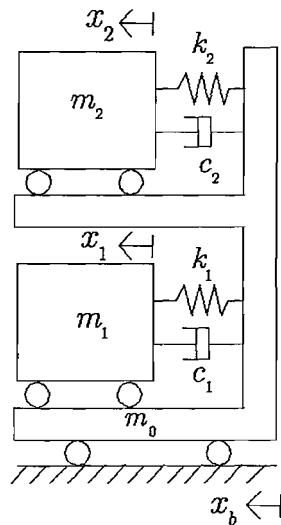


Figure 8.1: Two degree-of-freedom lumped parameter model.

From the diagram:

$m_0$ ,  $m_1$  and  $m_2$ : Masses of mass 0, mass 1 and mass 2. Mass 0 can be regarded as the support frame of the model.

$k_1$  and  $k_2$ : Stiffness coefficient of the springs of sub-systems containing mass 1 and mass 2, respectively.

$c_1$  and  $c_2$ : Damping coefficient of sub-system containing mass 1 and mass 2, respectively.

The equations of motion of the model can be described as:

$$m_1 \ddot{x}_1 + c_1 (\dot{x}_1 - \dot{x}_b) + k_1 (x_1 - x_b) = 0 \quad (8.1)$$

$$m_2 \ddot{x}_2 + c_2 (\dot{x}_2 - \dot{x}_b) + k_2 (x_2 - x_b) = 0 \quad (8.2)$$

By using the *Laplace Transform* on the assumption that  $x(0) = 0$ ,  $\dot{x}(0) = 0$ ,  $x_b(0) = 0$  and  $\dot{x}_b(0) = 0$ , and by some mathematical manipulation, the equations of motion can be written as:

$$(m_1 s^2 + c_1 s + k_1) X_1(s) = (c_1 s + k_1) X_b(s) \quad (8.3)$$

$$(m_2 s^2 + c_2 s + k_2) X_2(s) = (c_2 s + k_2) X_b(s) \quad (8.4)$$

By Newton's second law of motion:

$$F(t) = m_0 \ddot{x}_b + m_1 \ddot{x}_1 + m_2 \ddot{x}_2 \quad (8.5)$$

$$F(s) = m_0 s^2 X_b(s) + m_1 s^2 X_1(s) + m_2 s^2 X_2(s) \quad (8.6)$$

where  $F(t)$  is the total force acting on the model. The apparent mass of the model can be computed by dividing both sides with  $s^2 X_b(s)$ , such that:

$$M(s) = m_0 + m_1 \frac{B}{A} + m_2 \frac{D}{C} \quad (8.7)$$

where

$$\begin{aligned} A &= m_1 s^2 + c_1 s + k_1 \\ B &= c_1 s + k_1 \\ C &= m_2 s^2 + c_2 s + k_2 \\ D &= c_2 s + k_2 \end{aligned} \quad (8.8)$$

By replacing the *Laplace Transform* variable,  $s$ , with the angular frequency,  $\omega$ , based on the relation  $s = i\omega$ , the modulus,  $|M|$ , and phase,  $\arctan^{-1}(M)$  of the apparent mass of the model can be calculated.

### 8.2.3 Fitting with experimental data

The parameters of Model 1 were optimised by comparing the response of the model with the measured apparent mass of the back (whole-back in contact with the backrest) with a vibration magnitude of  $0.4 \text{ ms}^{-2}$  r.m.s., as reported in Chapter 6 (see Section 6.3.2). The apparent masses of 10 subjects were measured in the frequency range of 0.25 to 10 Hz. The median results, as well as the individual responses, were used in optimising the parameters of the model.

A curve fitting method was used to obtain the model parameters  $m_n$ ,  $k_n$  and  $c_n$  ( $n = 0, 1, 2$ ) from the magnitude and phase of apparent mass,  $M$ . The least-square-error method with an optimisation algorithm was utilized (i.e. the constrained non-linear multivariable function in Matlab - *fmincon*). The parameters in the equation of each model were refined to minimize the error function over the whole frequency range, such that:

$$\text{error} = \sum_{i=1}^N (M_P(i) - M_T(i))^2 + F * \sum_{i=1}^N (P_P(i) - P_T(i))^2 \quad (8.9)$$

where:

$M_P(i)$  and  $P_P(i)$  are the corresponding apparent mass and phase from the curve fit at the  $i$ th frequency,

$M_T(i)$  and  $P_T(i)$  are the measured apparent mass and phase data, respectively.

$F$  is arbitrary constant.

From a preliminary run, Model 1, generally, showed a good fit only with the modulus of the apparent mass data, but not with the phase data. The fitting with the phase was improved when the error function of the phase was weighted by a scalar factor,  $F$ . It should be mentioned that  $F$  is an arbitrary value used to improve the fitting of both the apparent mass and phase.

Figures 8.2 to 8.4 show the curve fitting obtained from Model 1 with the median and individual apparent masses of the back with 10 subjects at  $0.4 \text{ ms}^{-2}$  r.m.s. For the optimisation process, all parameters were constrained such that the value of any parameter would be either zero, or a positive value – this is to give a physical meaning to the model, or, to make it possible to construct the model. An exception was the mass  $m$  (i.e. support frame) such that the minimum value was fixed to 1 kg – this is to avoid a massless frame

(which would be difficult if the model is to be constructed). The optimised parameters are listed in Table 8.1 (median) and Table 8.2 (individual).

**Table 8.1** Optimised parameter of Model 1 from the median apparent mass of the back with 10 subjects.

Model	$m$ (kg)	$m_1$ (kg)	$m_2$ (kg)	$k_1$ (N/m)	$k_2$ (N/m)	$c_1$ (Ns/m)	$c_2$ (Ns/m)
1	1	21.5	19	24753	2775.6	486	379

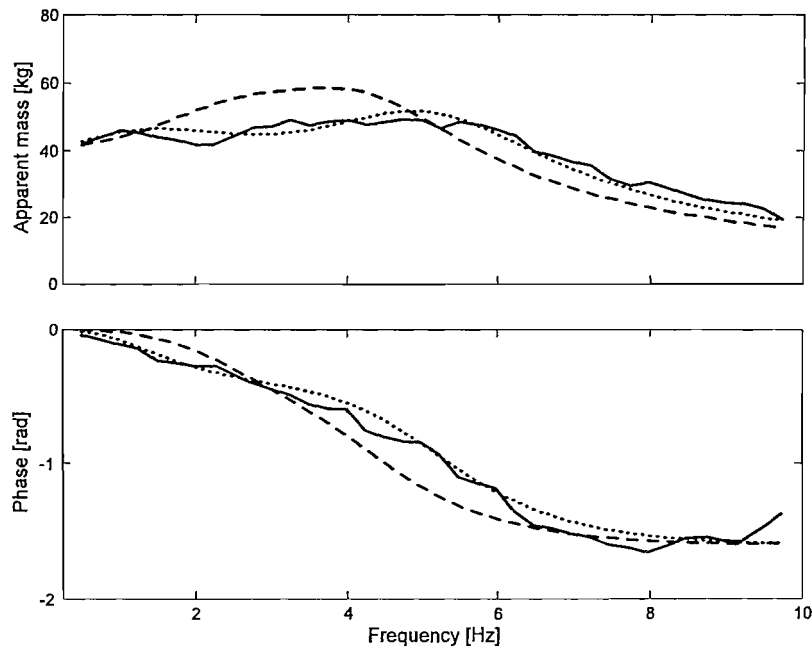


**Figure 8.2:** Median apparent mass and phase (with full back) with 10 subjects at  $0.4 \text{ ms}^{-2}$  r.m.s. with optimised response of the Model 1. Experiment (—); optimised response with the median data (····); approximated apparent mass using the median parameter of mass, spring and damping of individual fitted response – see Table 8.2 (---).

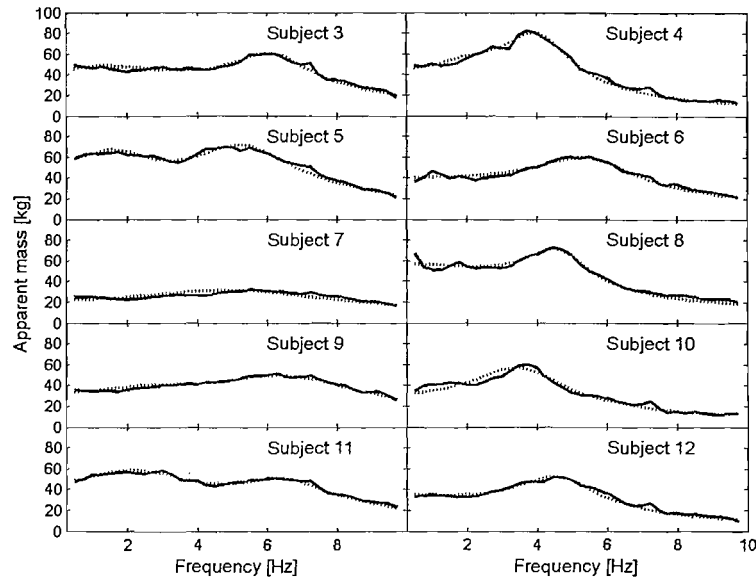


**Figure 8.3:** Individual apparent masses of the back 10 subjects (with full back) at  $0.4 \text{ ms}^{-2}$  r.m.s. with optimised response of Model 1. Experiment (—); model (.....).

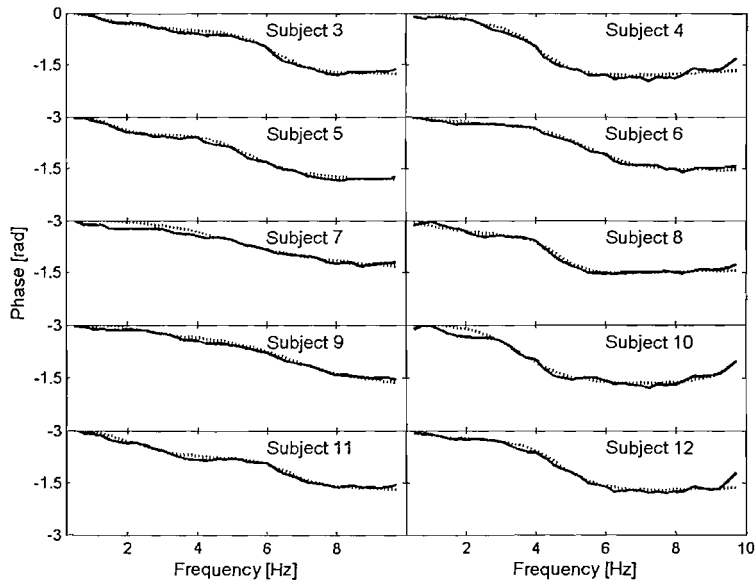


**Figure 8.4:** Individual phases of the apparent mass of the back of 10 subjects (with full back) at  $0.4 \text{ ms}^{-2}$  r.m.s. with optimised response of Model 1. Experiment (—); model (.....).

**Table 8.2** Optimised parameter of Model 1 from the individual responses of the apparent masses of the back with 10 subjects.

Subject	$m$ (kg)	$m_1$ (kg)	$m_2$ (kg)	$k_1$ (N/m)	$k_2$ (N/m)	$c_1$ (Ns/m)	$c_2$ (Ns/m)
3	1	26.8	16	4055.6	25159.5	632	250.7
4	1	40.1	0.4	25227	1716.8	586.9	0.2
5	1	28.2	27.1	34205.9	4413.9	542.4	387.7
6	1	21.7	18	28191.4	0	434.4	617.7
7	1	16.9	9.4	26084	0	589.5	130.3
8	1.2	38.4	17.2	130.1	15273.8	900	208.9
9	1	21.6	11	40646.1	5163.1	580.5	257.6
10	4.1	26.6	6.4	16129	678.6	398.8	42.3
11	1	35	11.7	10140.8	20405.6	761.1	206.2
12	1.9	19	14.8	17251.7	0	283.5	250.5
<b>Median</b>	<b>1</b>	<b>27</b>	<b>13</b>	<b>21239</b>	<b>4297</b>	<b>584</b>	<b>229</b>

Model 1 showed a good fit with the median apparent mass and phase and was able to depict both resonance frequencies of the apparent mass of the back around 1 Hz and 4 Hz. It also showed a good fit with the individual responses, with both the moduli of the apparent mass and the phase response.

In Figure 8.2, the dashed-line showed the approximated apparent mass of the back using the median of the individual mass (M), spring (K) and damping (C) values. In comparison with the optimised curve from the median apparent mass data (i.e. dotted-line), the approximated curve using the median of the individual MKC showed clear difference.

#### 8.2.3.1 Discussion and concluding remarks

The logical reason of using the median data (see Figure 8.2; solid line) to develop the human body model is such that the data have an appropriate overall shape showing roughly the same number of resonances with the same relationships between resonances as most individual responses (see Figure 8.3; solid line). From Figure 8.2, the median data showed roughly two resonances around 1 Hz and a major resonance around 5 Hz. The optimised curve of Model 1 using the median data (dotted line in Figure 8.2) also showed two resonances; around 1 Hz and 5 Hz, similar to the median data. In the individual responses (see Figure 8.3), subjects 5 and 11 roughly having the same shape and

resonances with the median data. Other subjects, such as subjects 3, 6, 9 and 12 showed major resonance between 5 and 6 Hz, which is similar to the major resonance of the median data, although the first resonance around 1 Hz was not clearly visible. In contrast, the apparent mass curve based on the median of the individual fitted MKC values (dashed line in Figure 8.2) showed only one major resonance around 4 Hz. Only subjects 4 and 10 showed roughly the similar shape as the approximated apparent mass curve using the median of the individual MKC values. Based on this simple analysis, the median data is preferred in developing the human body model. Although it may not be able to approximate the apparent mass of the back of every individuals but it might be able to approximate the apparent mass of the back of most people.

### 8.2.4 Sensitivity analysis

A parameter sensitivity test was carried out to determine which one of the mass-spring-damping systems is responsible for producing the resonance frequency of the apparent mass of the back (Figure 8.5). The test was performed on Model 1 and the parameters were based on the fit with the median results. All the parameters were varied  $\pm 50\%$  of the optimised parameters.

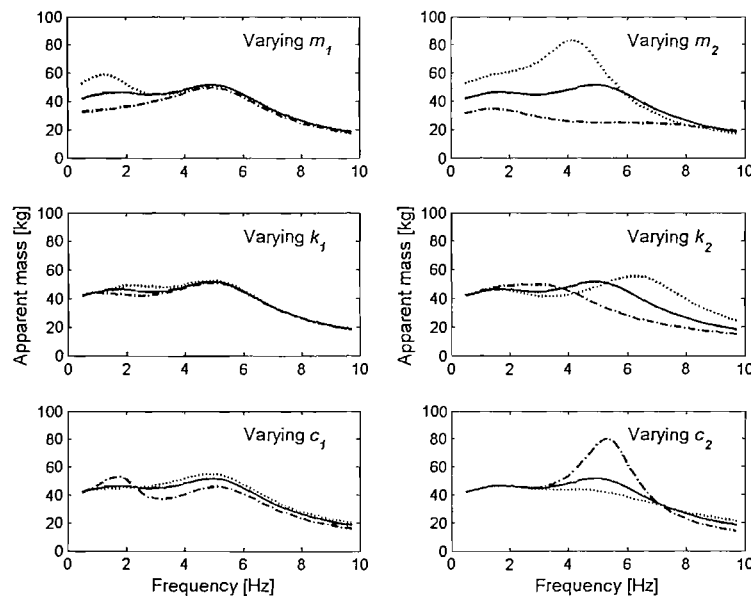


**Figure 8.5:** Sensitivity of the apparent mass prediction to  $\pm 50\%$  changes in the optimised parameters of the Model 1. Response of the optimised parameter (—);  $+50\%$  of the optimised parameter (·····) and  $-50\%$  of the optimised parameter (—·—·—).

From the sensitivity test, the apparent mass of the back at low frequencies was affected by varying  $m_1$  - the apparent mass increases with increasing  $m_1$ , while lowering it reduces the modulus. Increasing the mass of  $m_2$  had a greater effect on the apparent mass of the back than increasing the mass of  $m_1$ . The apparent mass of the back increased from up to 6 Hz with an increased in the mass of  $m_2$ . The spring and damper of the sub-system containing mass  $m_2$  were controlling the principal resonance of the apparent mass of the back, which is around 5 Hz. Varying these coefficients showed a greater effect on the apparent mass of the back than varying the spring and damper of the sub-system containing mass  $m_1$ . The sub-system of  $m_1$  is responsible of controlling the resonance around 2 Hz.

## 8.3 Measurement of seat mechanical impedance with an indenter

### 8.3.1 Introduction

Fairley and Griffin (1986) showed that it is possible to predict the vertical transmissibility of seats based on separate measurements of the impedance of seat and the impedance of human body. In that study, the dynamic properties of the seat cushion (stiffness and damping coefficients) were obtained from an indenter test, in which a seat cushion was loaded with a rigid indenter; the indenter shape was similar to a SIT-BAR (Whitham and Griffin, 1977). The force on the seat cushion (measured by a force transducer on the indenter) and the acceleration on the vibrating plate (which hold the seat cushion) were obtained and, therefore, the dynamic stiffness of the seat cushion was calculated (i.e. the ratio of the force and the displacement of the seat cushion; the displacement was obtained by integrating the acceleration twice).

Wei and Griffin (1998c) further explored the indenter test method to obtain the impedance of seat cushions. The authors found that the dynamic stiffness and damping of the seat cushions changed with variations in the pre-load such that the stiffness and damping increased with increasing pre-load in the seat cushions. Different vibration magnitudes and inclination angles of the seat had little effect on the measured dynamic stiffness of the seat cushions, although the effect of contact area was complex (Wei, 2000).

In this section, the indenter test method was used to measure the dynamic properties of both a car seat backrest and a 100 mm foam block. The effect of different pre-loads on the backrest cushion was investigated - this may correspond to different loads applied by the

back to the backrest cushion with different subjects. Based on the results of Wei and Griffin (1998c), it was expected that the dynamic stiffness and damping of both the seat backrest and the foam block would increase with increasing pre-load.

### 8.3.2 Method and analysis

The measurements were conducted separately with the backrest cushion of the car seat and with a 100 mm foam block (Figure 8.6). For the backrest cushion, the backrest was dismantled from the seat pan, and only the backrest was used in the test (Figure 8.6 (b)). The backrest cushion had a contoured surface and weighted 19 kg.

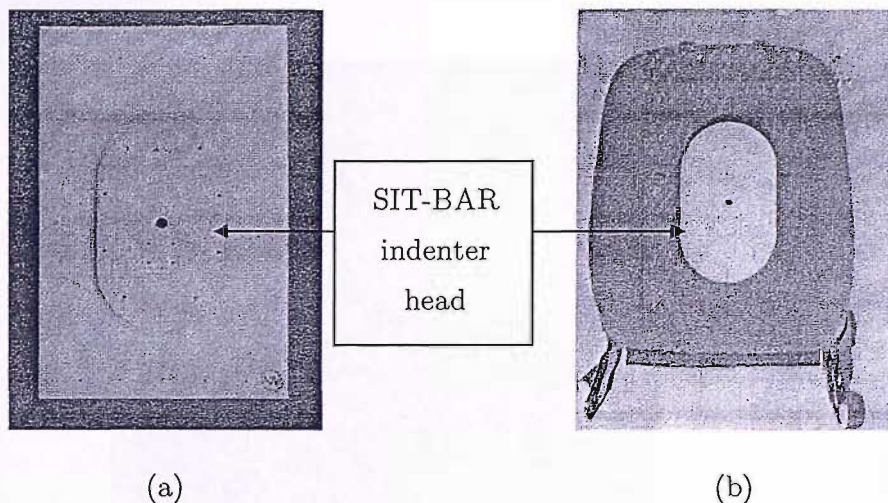


Figure 8.6: Orientation of the SIT-BAR indenter head on: (a) the foam block and (b) the backrest cushion.

An indenter rig capable of conducting vertical, lateral, cross-axis and arbitrary angle quasi-static and dynamic indenter testing of seats and seat components was used in the experiment (Figure 8.7).

The backrest cushion or the foam backrest was supported on the flat vibrator platform. In the case of the car seat, the contoured surface faced upward, toward the indenter. For the foam block, either the flat surface on either side can face the upward.

The indenter, having the shape of a SIT-BAR (Whitham and Griffin, 1977), was used to compress the backrest cushion and the foam backrest. The SIT-BAR was attached to a moving shaft, which was moved by a motor controlled via a control box. The SIT-BAR was placed at the middle of both backrests and was oriented as in Figure 8.6.

An Entran EGCSY-240\*-10 accelerometer was securely attached beneath the vibrator platform. The force on the backrest cushion was measured using a Kistler tri-axial force transducer (which was calibrated to the indenter head to give the correct reading), and was conditioned using a Kistler 5007 charge amplifier.

A Gaussian random signal with a duration of 100 s and a nominally flat constant bandwidth acceleration spectrum over the frequency range of 0.25 to 20 Hz at a vibration magnitude of at  $0.4 \text{ ms}^{-2}$  r.m.s. was generated by using a *HVLab* version 3.81 Data Acquisition and Analysis system. The vibration was produced by an electrodynamic vibrator (VP85 6LA).

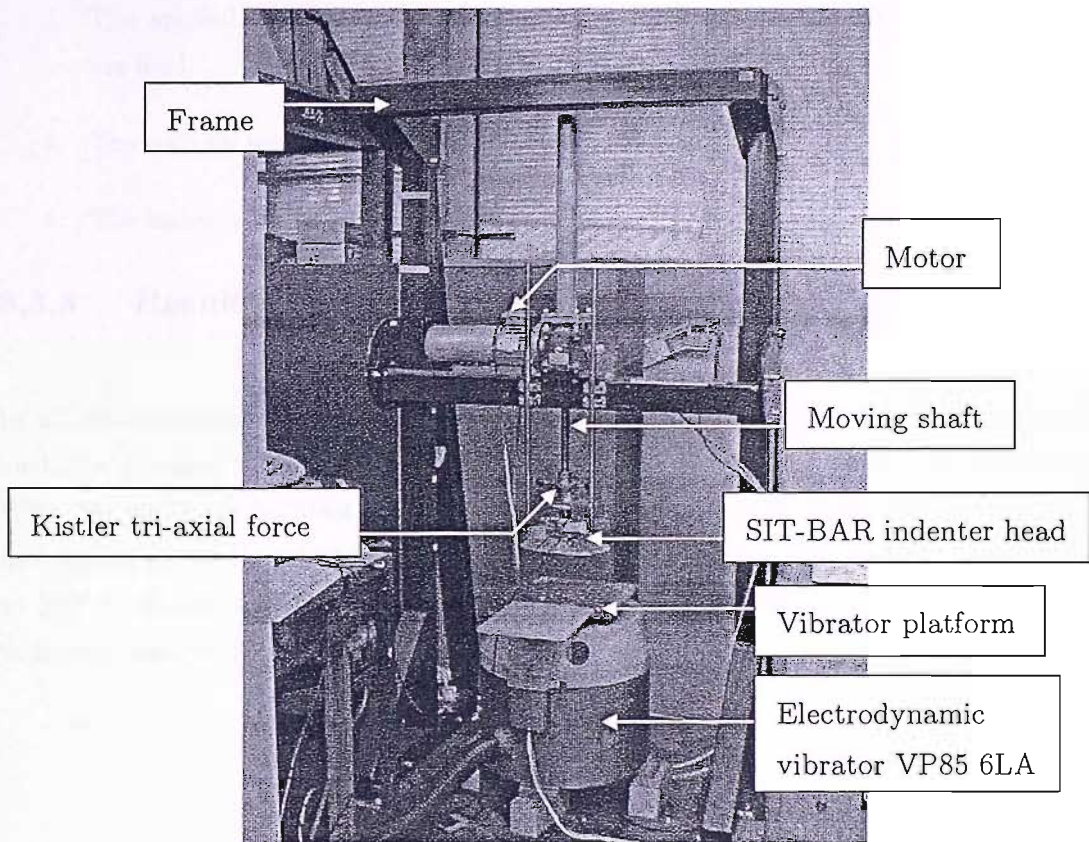


Figure 8.7: Indenter rig.

Four loads (50N, 100N, 150N and 200N) were used as the pre-load, which was applied to both the car seat backrest and the foam block before the measurements of force and acceleration were taken.

All acceleration and force signals were conditioned and acquired directly into the *HVLab* Data Acquisition system at 256 samples per second via 85 Hz anti-aliasing filters.

The procedures of acquiring the measurements were:

1. The cushion was compressed at 25% greater than the desired pre-load (50N or 100N or 150N or 200 N).
2. The cushion was allowed to settle for approximately 5 minutes.
3. The applied pre-load was checked so that the load was within 5% of the desired pre-load.
4. The cushion was allowed to settle for another 1 minute.
5. The measurements of the force and acceleration were acquired.

### 8.3.3 Results and Discussion

In all measurement, the coherency was high (i.e. greater than 0.9). With increasing pre-load, the dynamic stiffness and damping for the car seat backrest increased (Figure 8.8). With 100 mm foam backrest, the dynamic stiffness showed a small change as the pre-load increased from 50 N to 150 N, but was greatly increased when the pre-load was increased to 200 N (Figure 8.9). This may be due to a 'bottoming' effect (where the foam was 'squashed' near to the vibrator plate)

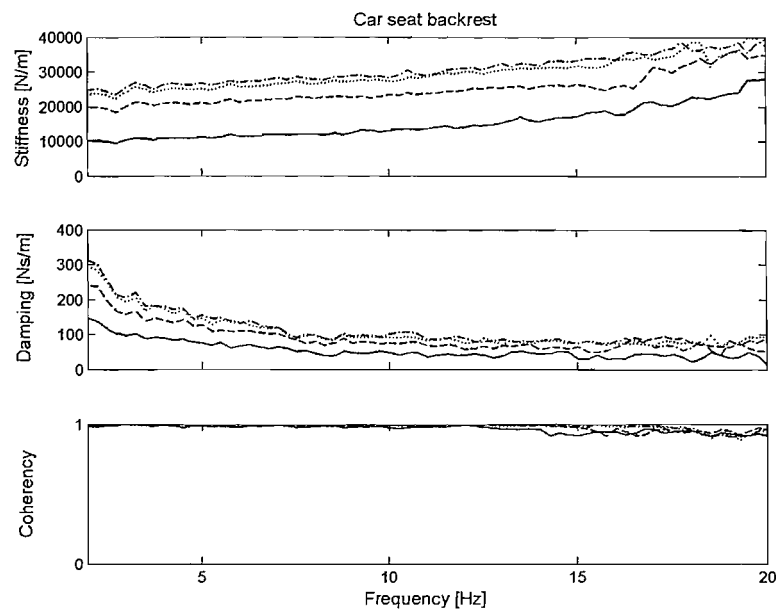


**Figure 8.8:** The measured dynamic stiffness and damping of car seat backrest at 50N (—); 100N (---), 150N (-----) and 200 N (.....) of pre-load.

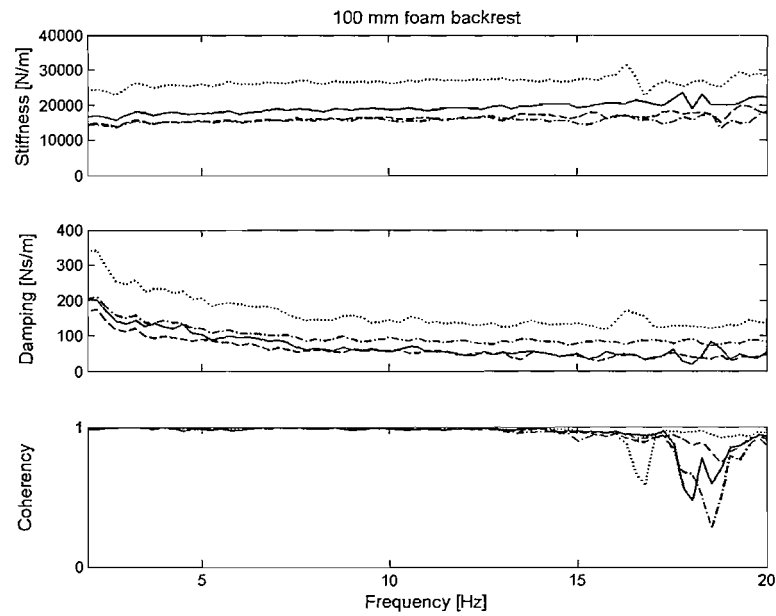


**Figure 8.9:** The measured dynamic stiffness and damping of 100 mm foam backrest at 50N (—); 100N (---), 150N (-----) and 200 N (.....) of pre-load.

### 8.3.4 Backrest cushion model

It is desirable to have a single value of the stiffness,  $K$ , and damping,  $C$ , coefficients of the backrest cushion, which later can be used with the optimised parameters of Model 1 (representing the apparent mass of the back) to predict the backrest transmissibility. This can be achieved by fitting the measured data with a simple model of the backrest cushion, which consist of spring and damper, arranged in parallel (Figure 8.10).

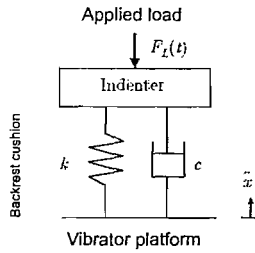


**Figure 8.10:** Schematic diagram of the backrest cushion and the indenter to obtain the dynamic properties of the backrest cushion.

The frequency response of the backrest cushion or foam block when a load was applied can be written as:

$$F(t) = Kx + C\dot{x} \quad (8.10)$$

where  $F(t)$  is the equivalent force from the platform with the applied load on the backrest/foam,  $K$  is the stiffness (i.e. a spring stiffness) and  $C$  is the damping of the backrest/foam (i.e. a viscous damping). The displacement,  $x$ , and the velocity,  $\dot{x}$ , can be obtained by double and single integration of the measured the acceleration,  $\ddot{x}$ , respectively. Using *Laplace Transform* on the assumption that  $x(0) = 0$  and  $\dot{x}(0) = 0$  and replacing the *Laplace Transform* variable  $s$  with the angular frequency  $\omega$  based on the relation of  $s = i\omega$ , the equation 8.10 can be written as:

$$F_L(\omega) = (K + Cs)X(s) \quad (8.11)$$

The dynamic stiffness of the backrest cushion/foam is:

$$\frac{F_L(\omega)}{X(\omega)} = S(\omega) = K + C\omega i \quad (8.12)$$

From equation 8.12, the stiffness,  $K$  and damping,  $C$ , of the backrests are the real and imaginary of the dynamic stiffness of the backrest/foam,  $S(\omega)$ , respectively.

A curve fitting method was used to obtain the parameters of the backrest cushion model from the real and imaginary components of dynamic stiffness,  $S(\omega i)$ . This method was used by Wei and Griffin (1998c) to obtain the stiffness and damping of the seat cushion model for predicting vertical seat transmissibility from the measured apparent mass of the body and the measured impedance of the backrest cushion. The least square error method with an optimisation algorithm was utilized (i.e. constrained non-linear multivariable function in Matlab - *fmincon*). The parameters in the equation of the dynamic stiffness were refined to minimize the error function over the whole frequency range, such that:

$$\text{error} = \sum_{i=1}^N (S_P(i) - S_T(i))^2 \quad (8.13)$$

where:

$S_P(i)$  is the corresponding modulus of the dynamic stiffness from the curve fit at the  $i$ th frequency,

$S_T(i)$  is the measured modulus dynamic stiffness.

With values of parameters chosen at random as starting values, the parameters were varied systematically by using the optimisation algorithm. The measured and calculated values of the modulus of the dynamic stiffness, ( $|S| = \sqrt{K^2 + (C\omega)^2}$ ) of the seat backrest and the foam block are shown in Figures 8.11 to 8.12. The calculated values of the stiffness and damping are listed in Table 8.3.

**Table 8.3** Optimised parameter of  $K$  and  $C$  from the measured modulus dynamic stiffness of both the car seat backrest and foam block at four pre-loads.

Pre-load (N)	Stiffness (N/m)		Damping (Ns/m)	
	Car seat	Foam backrest	Car seat	Foam backrest
50	11324	17053	142	126
100	21176	14496	187	109
150	27242	14844	201	103
200	25595	24505	208	193

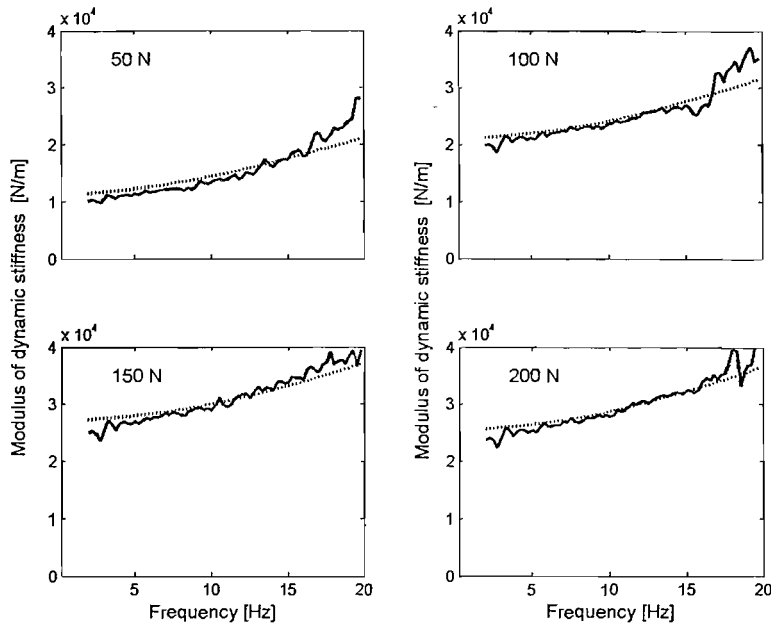


Figure 8.11: Modulus of dynamic stiffness of the car seat backrest and fitted model for four pre-loads. Measured values (—); fitted values (·····).

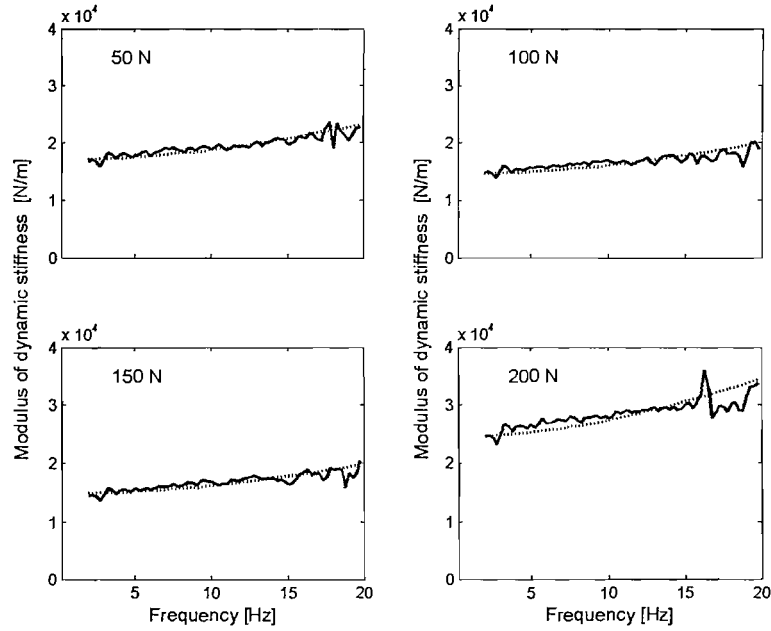


Figure 8.12: Modulus of dynamic stiffness of the 100 mm foam backrest and fitted model for four pre-loads. Measured values (—); fitted values (·····).

The optimised parameters of both seat backrest and foam block showed that the seat backrest was more than 50% stiffer than the foam block with 100 N and 150 N pre-loads, but not at 50 N and 200 N of pre-loads. With the highest pre-load, the stiffness of both backrests was similar. The car seat had 200% higher damping than the foam block at 100 N and 150 N pre-loads, while at 50 N and 200 N of pre-loads showed similar damping for both backrests.

### 8.3.5 Conclusions

It was possible to measure the dynamic properties of the seat backrest and the foam block from the indenter test method. The dynamic stiffness and damping of both backrests generally tended to increase with increasing pre-load. When fitting the measured data with a simple backrest cushion model (spring and damper arranged in parallel), it is possible to obtain a single value for both the stiffness and the damping coefficient.

## 8.4 Predicting backrest transmissibility

In this section, the transmissibilities of both the seat backrest and the foam block were predicted from the apparent mass model of the back developed earlier (Model 1) and from the dynamic properties of the backrest cushion obtained from the indenter test. The transmissibility model (Model 1a) corresponding to Model 1 is shown in Figure 8.13. The backrest cushion is represented by  $K$  and  $C$ .

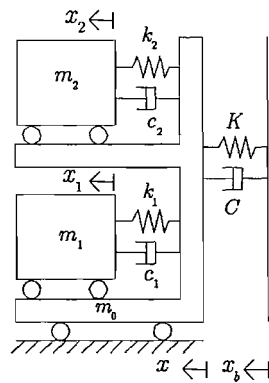


Figure 8.13: Model 1a: transmissibility of backrest cushion based on Model 1 and  $K$  and  $C$  (in parallel, representing the backrest cushion).

### 8.4.1 Mathematical equation of the transmissibility model

The equations of motion of Model 1a can be written as:

$$\begin{aligned} m_0 \ddot{x} + C(\dot{x} - \dot{x}_b) + c_1(\dot{x} - \dot{x}_1) + c_2(\dot{x} - \dot{x}_2) + \dots \\ K(x - x_b) + k_1(x - x_1) + k_2(x - x_2) = 0 \end{aligned} \quad (8.14)$$

$$m_1 \ddot{x}_1 + c_1(\dot{x}_1 - \dot{x}) + k_1(x_1 - x) = 0 \quad (8.15)$$

$$m_2 \ddot{x}_2 + c_2(\dot{x}_2 - \dot{x}) + k_2(x_2 - x) = 0 \quad (8.16)$$

The transmissibility of the backrest (through  $K$  and  $C$ ) can be written as:

$$H(\omega) = \frac{\ddot{x}(\omega)}{\ddot{x}_b(\omega)} \quad (8.17)$$

By using the *Laplace Transform* on the assumption that  $x(0) = 0$ ,  $\dot{x}(0) = 0$ ,  $x_b(0) = 0$  and  $\dot{x}_b(0) = 0$ , and by some mathematical manipulation, the transmissibility of Model 1a can be written as:

$$H(s) = \frac{X(s)}{X_b(s)} = \frac{D}{AA} \quad (8.18)$$

where

$$\begin{aligned} AA &= A - \frac{B^2}{E} - \frac{C^2}{F} \\ A &= ms^2 + Cs + c_1s + c_2s + K + k_1 + k_2 \\ B &= c_1s + k_1 \\ C &= c_2s + k_2 \\ D &= Cs + K \\ E &= m_1s^2 + c_1s + k_1 \\ F &= m_2s^2 + c_2s + k_2 \end{aligned} \quad (8.19)$$

By substituting the parameters describing the apparent mass of the back (Table 8.1) and stiffness and damping coefficient of the backrest cushion (Table 8.3), the transmissibility of both the seat backrest and the 100 mm foam backrest can be predicted.

### 8.4.2 Results and discussion

The predicted transmissibility of both the car seat backrest and the 100 mm foam backrest were compared with the median transmissibilities of both backrests with twelve subjects, measured at the middle location with a vibration magnitude of  $0.4 \text{ m}^{-2}$  r.m.s. (Figures 8.14 to 8.15). The results showed that the predicted transmissibility of both backrests did not agree with the measured data at any pre-load, although the human body model (i.e. Model 1) adequately predicted the apparent mass of the back at the same location and vibration magnitude.

The results suggested that the backrests were stiffer than the measured data. Possibly because the dynamic stiffnesses were measured over a small area (i.e. area of the SIT-BAR) whereas the area of the interface between the back and the backrest are larger than the size of the SIT-BAR. In contrast, the results in Chapter 6 showed that the area of the back does not affect the apparent mass of the back. The apparent mass of the middle back (measured over a small area of a wooden block) was similar to the apparent mass of the back when measured with the entire back in contact with the backrest.

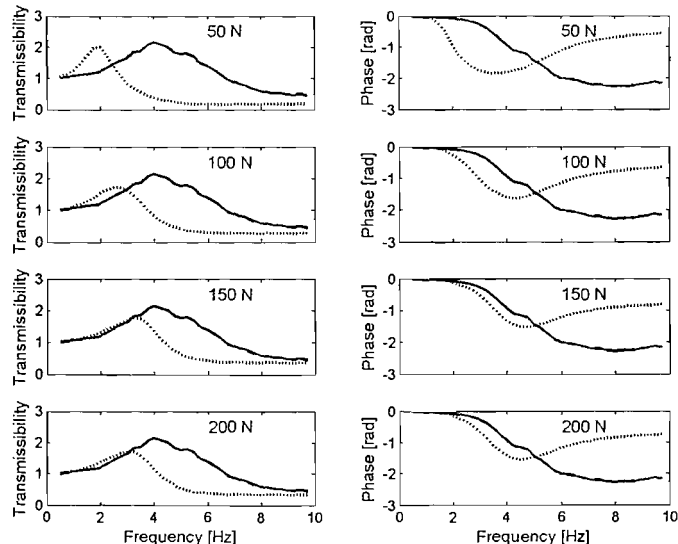


**Figure 8.14:** Comparison of median car seat backrest transmissibility and phase with twelve subjects and predicted backrest transmissibility and phase when using Model 1a. Measured transmissibility and phase (—); predicted transmissibility and phase (.....).

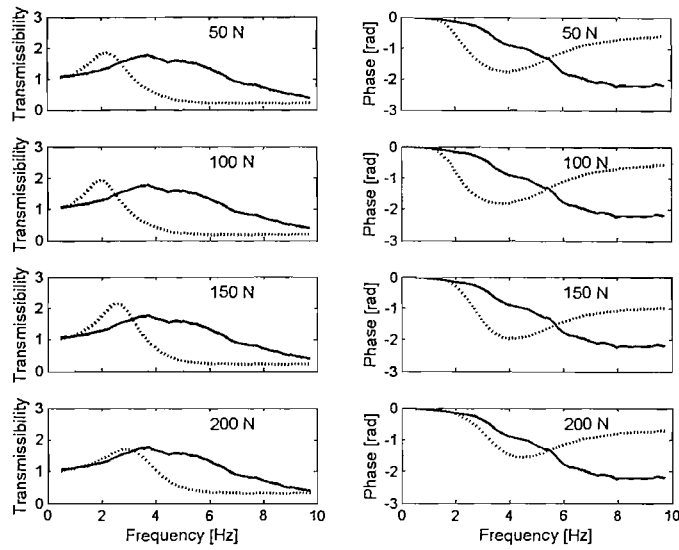


**Figure 8.15:** Comparison of median 100mm foam backrest transmissibility and phase with twelve subjects and predicted backrest transmissibility and phase when using Model 1a. Measured transmissibility and phase (—); predicted transmissibility and phase (·····).

## 8.5 Alternative models for predicting backrest transmissibility

The results in the previous section showed that, although Model 1 was capable of predicting the apparent mass of the back during fore-and-aft excitation at a vibration magnitude of  $0.4 \text{ ms}^{-2}$  r.m.s, combining the model with a backrest cushion model (i.e. spring and damping in parallel) did not show a good prediction of the transmissibilities of either the car seat or the foam backrests. There are two possibilities: either i) the model of the body is ‘wrong’ or ii) the dynamic stiffness of the backrest cushion is ‘wrong’. In the following section, both possibilities were investigated so as to improve the predictions of backrest transmissibility.

### 8.5.1 Alternative models of the apparent mass of the back

In this section, three alternative models of the human body are developed. These models were fitted with median apparent mass of the back at  $0.4 \text{ ms}^{-2}$  r.m.s., after which the models were used to predict both the backrest transmissibility of the car seat and the foam backrest.

The three models representing the apparent mass of the back are shown in Figure 8.16.

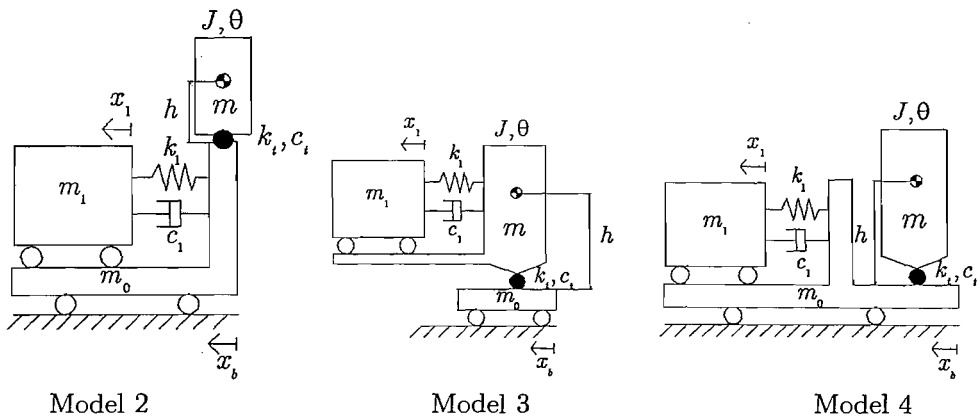


Figure 8.16: Three alternative models representing the apparent mass of the back.

Descriptions of each model are as follows:

**Model 2:** Model 2 consists of sub-system containing  $m_1$ ,  $k_1$  and  $c_1$  connected to a support frame,  $m_0$ . A mass  $m$ , which can rotate is connected to  $m_0$ . The COG of  $m$  is in line with the pivot.

**Model 3:** Model 3 consists of a sub-system containing mass  $m_1$ ,  $k_1$  and  $c_1$ , which is connected to mass,  $m$ . Mass  $m$  is connected to  $m_0$  and can rotate about the pivot.  $h$  is the height of the COG and is in line with the pivot.

**Model 4:** The sub-system containing  $m_1$  is connected to the base mass and only move translational. Mass  $m$  moves together with  $m_0$ , which can also rotate about the pivot. The COG of  $m$  is in line with the pivot.

For each model, the equations of motion were derived using *Lagrange's* equation (example of derivation of the equations of motion of Model 2 is shown in Appendix D). All the model parameters were optimised using a similar optimisation method as described in Section 8.2.3. The parameters in the equation of each model were refined to minimize the error function over the whole frequency range using equation 8.9.

All parameters were constrained such that the value of any parameter would be either zero, or a positive value. However, in each model, the support mass,  $m_0$ , was set to the minimum value of 1 kg (this is to avoid a massless frame) and the height of the COG of the mass  $m$  to the pivot was constrained in the range 0.1 m (minimum value) to 0.5 m

(maximum value). This was to give a reasonably logical  $h$  value, which may correspond to the COG of the upper body such as reported in the literature (e.g. Nawayseh, 2002).

### 8.5.1.1 Fitting with experimental data

All three alternative models showed a visually good fitting with the moduli and phase of the measured apparent mass of the back at  $0.4 \text{ ms}^{-2}$  r.m.s. (Figure 8.17). Table 8.4 lists the optimised parameters obtained from the models. For all models, the optimised moment of inertia showed a low value, although the corresponding mass was high.

**Table 8.4** Optimised parameters of Models 2, 3 and 4 from the median apparent mass of the back with 10 subjects.

Model	$m_0$ (kg)	$m$ (kg)	$m_1$ (kg)	$k_1$ (N/m)	$k_t$ (N/m)	$c_1$ (Ns/m)	$c_t$ (Ns/m)	$h$ (m)	$J$ (kgm <sup>2</sup> )
2	1	18	22	4531	8096	339	130	0.5	1
3	1	24.2	18.9	1	13812	446	174	0.5	1
4	1	24.2	15.9	3021	8759	310	160	0.5	1

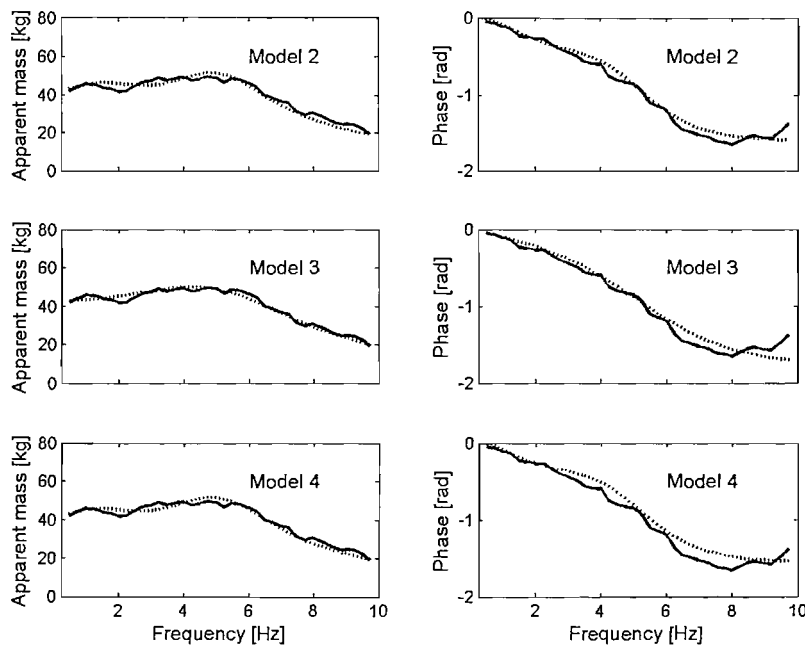


**Figure 8.17:** Median apparent mass and phase (with full back) with 10 subjects at  $0.4 \text{ ms}^{-2}$  r.m.s. with optimised response of the Models 2,3 and 4. Experiment (—); model (·····).

Models 2, 3 and 4 were also optimised with the individual apparent masses of the backs of ten subjects, as shown in Figures 8.18 to 8.23. Generally, all models showed a visually good fit with the individual apparent masses of the backs of the ten subjects. The optimised parameters of each model for each subject are listed in Tables 8.5 to 8.7.

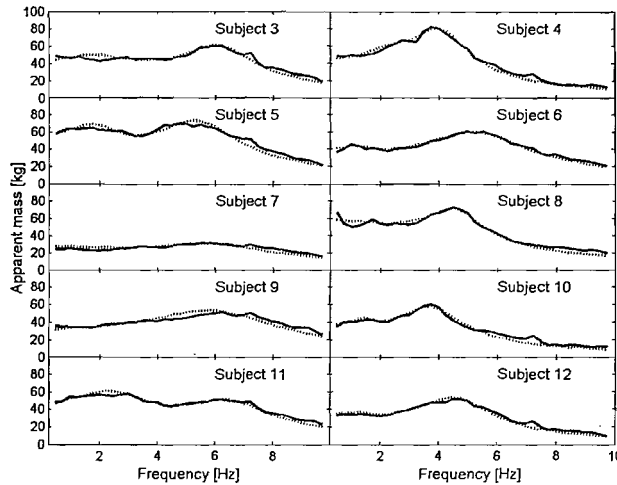


**Figure 8.18:** Individual apparent masses of the back 10 subjects (with full back) at  $0.4 \text{ ms}^{-2}$  r.m.s. with optimised response of Model 2. Experiment (—); model (·····).

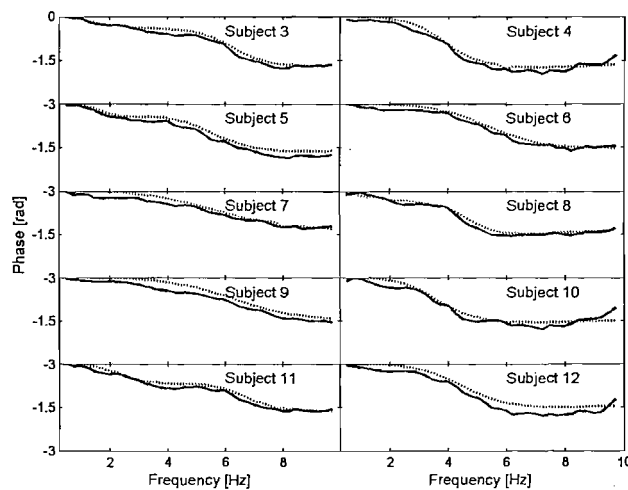


**Figure 8.19:** Individual phases of the apparent mass of the back 10 subjects (with full back) at  $0.4 \text{ ms}^{-2}$  r.m.s. with optimised response of Model 2. Experiment (—); model (·····).

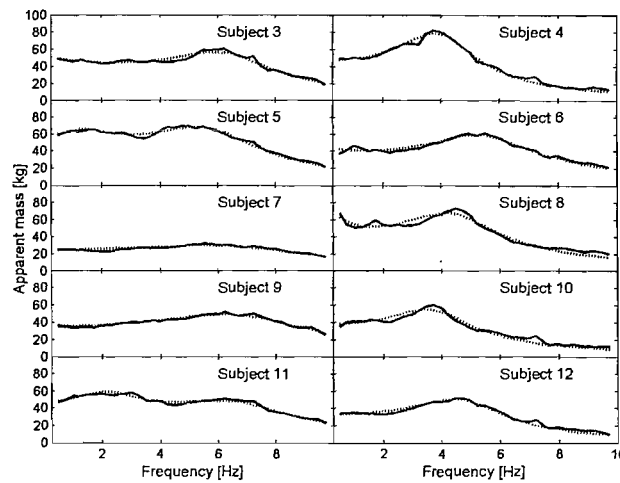


**Figure 8.20:** Individual apparent masses of the back of 10 subjects (with full back) at  $0.4 \text{ ms}^{-2}$  r.m.s. with optimised response of Model 3. Experiment (—); model (.....).

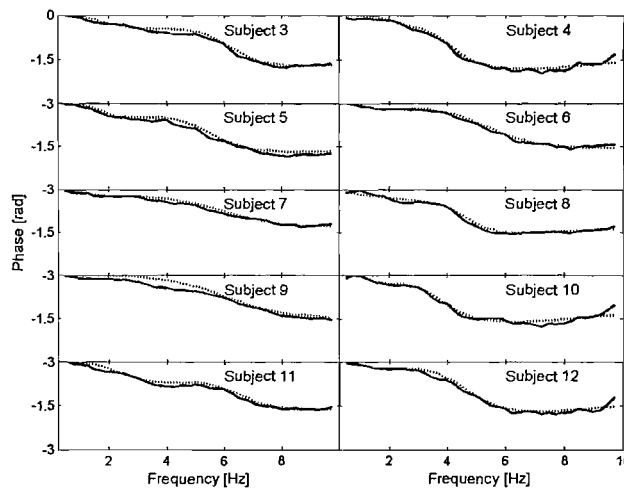


**Figure 8.21:** Individual phases of the apparent mass of the back of 10 subjects (with full back) at  $0.4 \text{ ms}^{-2}$  r.m.s. with optimised response of Model 3. Experiment (—); model (.....).

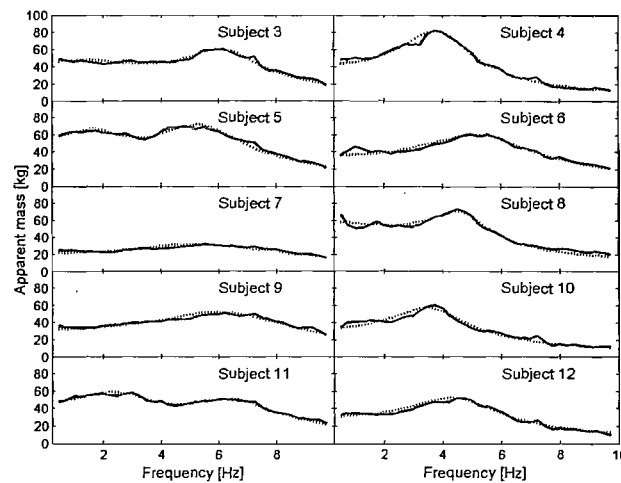


**Figure 8.22:** Individual apparent masses of the back of 10 subjects (with full back) at  $0.4 \text{ ms}^{-2}$  r.m.s. with optimised response of Model 4. Experiment (—); model (.....).

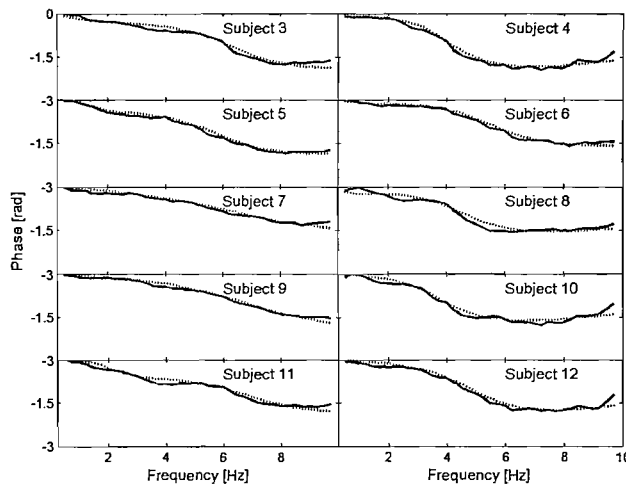


**Figure 8.23:** Individual phases of the apparent mass of the back of 10 subjects (with full back) at  $0.4 \text{ ms}^{-2}$  r.m.s. with optimised response of Model 4. Experiment (—); model (.....).

**Table 8.5** Optimised parameter of Model 2 from the individual responses of the apparent masses of the back with 10 subjects.

Subject	$m_0$ (kg)	$m$ (kg)	$m_1$ (kg)	$k_1$ (N/m)	$k_t$ (N/m)	$c_1$ (Ns/m)	$c_t$ (Ns/m)	$h$ (m)	$J$ (kgm <sup>2</sup> )
3	1	20.4	21.7	4436	9673	433	96	0.5	1
4	1	34.7	9.2	2447	6706	102	125	0.5	1
5	1	30.8	24.8	4420	10831	329	158	0.5	1
6	1	32.4	6.9	583	11564	58	208	0.5	1
7	1	16.5	10.6	0	8213	172	144	0.5	1
8	1	23	34.5	0	6061	658	90	0.5	1
9	1	31	0	3001	14355	454	250	0.5	1
10	1	29.7	6.5	701	5166	43	124	0.5	1
11	1	16	30.6	9613	8748	582	87	0.5	1
12	1	24.5	8.2	610	6499	87	107	0.5	1
<b>Median</b>	1	10.4	23.8	1567	8477	190	124	0.5	1

**Table 8.6** Optimised parameter of Model 3 from the individual responses of the apparent masses of the back with 10 subjects.

Subject	$m_0$ (kg)	$m$ (kg)	$m_1$ (kg)	$k_1$ (N/m)	$k_t$ (N/m)	$c_1$ (Ns/m)	$c_t$ (Ns/m)	$h$ (m)	$J$ (kgm <sup>2</sup> )
3	1	28.3	20.2	19	13501	242	129	0.5	1.1
4	1	40.8	5	14610	0	41	196	0.48	1
5	1	36.7	19.8	2095	13805	283	181	0.5	1
6	1	33.2	8.5	0	12673	65	213	0.5	1
7	1	18.9	5	310	10375	79	169	0.5	1
8	1	40.6	19.7	161	10728	111	223	0.5	1.7
9	1	29	5	1534	15080	89	211	0.5	1
10	1	31	5	403	5366	41	130	0.5	1
11	1	28.2	17.07	4171	13244	297	164	0.5	1
12	1	26	5	318	7208	63	117	0.5	1
<b>Median</b>	1	30	6.8	360	11700	84	175	0.5	0.1

**Table 8.7** Optimised parameter of Model 4 from the individual responses of the apparent masses of the back with 10 subjects.

Subject	$m_0$ (kg)	$m$ (kg)	$m_1$ (kg)	$k_l$ (N/m)	$k_t$ (N/m)	$c_l$ (Ns/m)	$c_t$ (Ns/m)	$h$ (m)	$J$ (kgm <sup>2</sup> )
3	1	21.8	21	2936	10344	419	111	0.5	1
4	1	39	10	63	7215	80	151	0.5	1
5	1	31.8	23.7	3979	11333	335	180	0.5	1
6	1	31.8	2.3	29093	11845	564	203	0.5	1
7	1	19.6	1	28852	9394	1000	176	0.5	1
8	1	37.8	4.7	28722	8838	671	201	0.5	1
9	1	23.9	8.4	4877	13775	177	174	0.5	1
10	1	30.3	1	29302	5413	4617	131	0.5	1
11	1	26.2	17	6045	12243	199	186	0.5	1
12	1	27.2	1	24915	7217	2252	131	0.5	1
Median	1	28.7	6.6	15480	9869	492	175	0.5	1

### 8.5.1.2 Sensitivity analysis

Sensitivity analyses were performed on all three alternative models. The analyses were performed on the median optimised parameters.

Generally, the tests showed that the principal resonance of the apparent mass of the back and the apparent mass at resonance were most affected when the values of mass  $m$ ,  $k$  and  $c_t$  were changed. A variation in  $c_t$  greatly affected the apparent mass at the principal resonance. It can also be seen that varying the COG of mass  $m$  in all models significantly affected the general response of the apparent mass of the back.

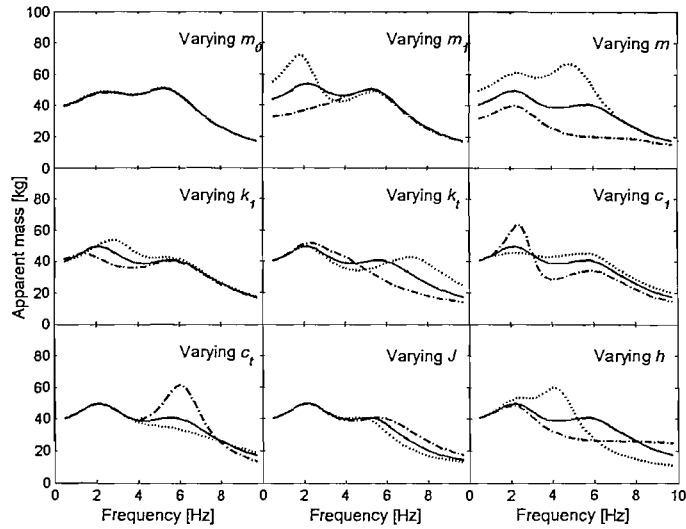


**Figure 8.24:** Sensitivity of the apparent mass prediction to  $\pm 50\%$  changes in the optimised parameters of the Model 2. Response of the optimised parameter (—);  $+50\%$  of the optimised parameter (.....) and  $-50\%$  of the optimised parameter (----).

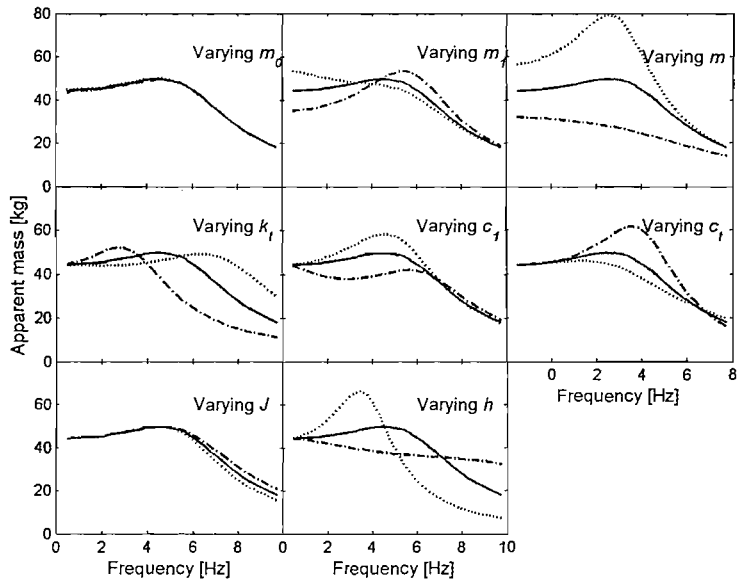


**Figure 8.25:** Sensitivity of the apparent mass prediction to  $\pm 50\%$  changes in the optimised parameters of the Model 3. Response of the optimised parameter (—);  $+50\%$  of the optimised parameter (.....) and  $-50\%$  of the optimised parameter (----).

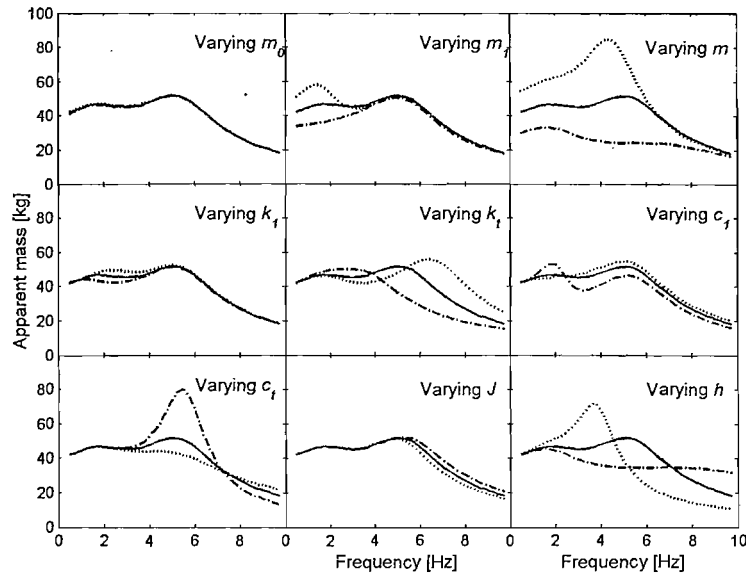


**Figure 8.26:** Sensitivity of the apparent mass prediction to  $\pm 50\%$  changes in the optimised parameters of the Model 4. Response of the optimised parameter (—);  $+50\%$  of the optimised parameter (·····) and  $-50\%$  of the optimised parameter (—·—·—).

#### 8.5.1.3 Predicting backrest transmissibility

Each of the alternative models (Model 2, Model 3 and Model 4) was combined with the backrest cushion model ( $K$  and  $C$ , arranged in parallel) to predict the transmissibility of the car seat and the foam backrests. These models are shown in Figure 8.27.

All the equations of motion for each model were derived using *Lagrange's* equation. By substituting the parameters describing the apparent mass of the back (Tables 8.4) and stiffness and damping coefficients of the backrest cushion (Table 8.3), the transmissibility of both the seat backrest and the 100 mm foam block can be predicted.

The predicted transmissibility of both the car seat backrest and the 100 mm foam backrest were compared with the median transmissibilities of both backrests with twelve subjects, measured at the middle location at a vibration magnitude of  $0.4 \text{ m}^{-2}$  r.m.s. (Figures 8.28 to 8.29).

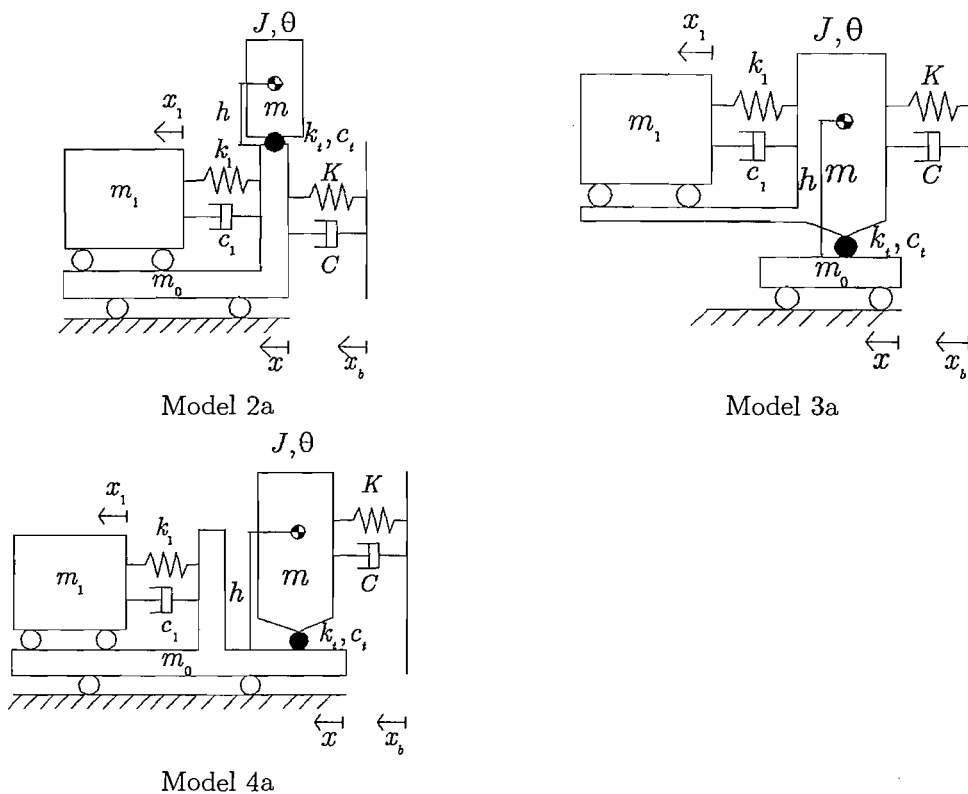


**Figure 8.27:** All three transmissibility models obtained from combination of all three alternative models (see Figure 8.16) with a backrest cushion model (comprises of  $K$  and  $C$  arranged in parallel).

It can be seen that Model 2a did not predict well the transmissibility of either backrest, even with different values of  $K$  and  $C$  corresponding to different pre-loads.

Model 3a showed encouraging predictions of the transmissibility of the seat backrest, compared with the median data, except with the  $K$  and  $C$  values corresponding to the 50 N pre-load. However, the prediction of foam transmissibility with the same model was over-estimated.

Model 4a also showed promising prediction of the transmissibility of the seat backrest. The prediction of transmissibility of the foam backrest using this model is better than Model 3a, although a good fitting was only obtained with a 200 N pre-load. With the 50 N pre-load, the model did not yield a good prediction for either backrest.

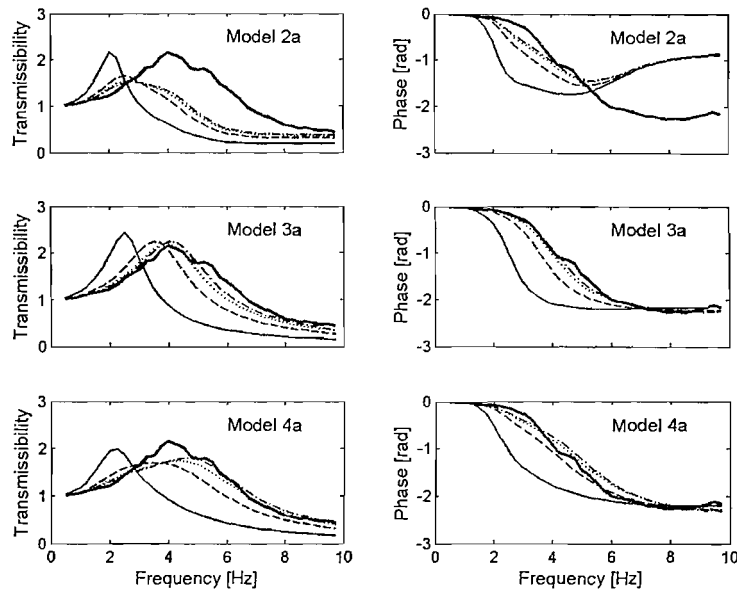


**Figure 8.28:** Fore-and-aft backrest transmissibility of car seat cushion. Experiment (—); predicted transmissibility with per-load of: 50 N (—); 100 N (---); 150 N (—·—) and 200 N (····).

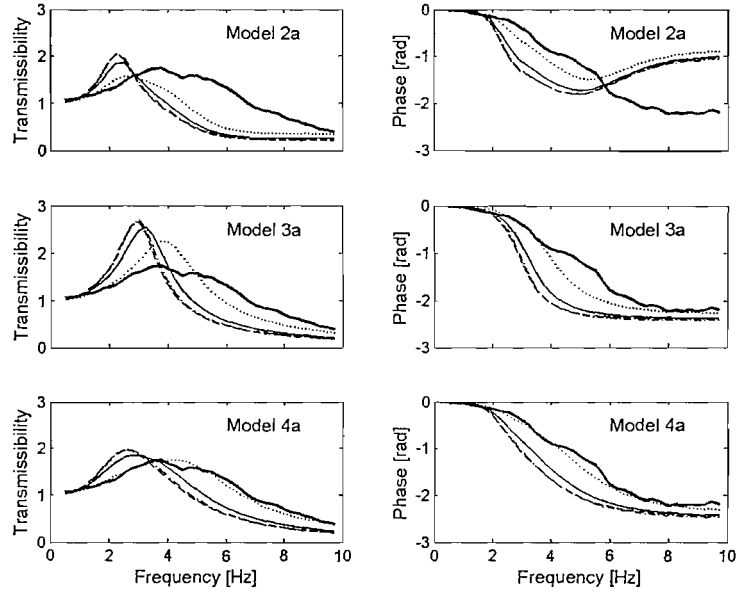


**Figure 8.29:** Fore-and-aft backrest transmissibility of 100 mm foam backrest. Experiment (—); predicted transmissibility with per-load of: 50 N (—); 100 N (---); 150 N (—·—) and 200 N (····).

#### 8.5.1.4 Discussion and concluding remarks

The prediction of backrest transmissibilities with Model 3a and Model 4a showed encouraging results compared to Model 2a and Model 1a. The principal difference between Models 3a and 4a, and Models 2a and 1a is that the force was applied to a mass that can rotate in the former models while in the latter models, the force was applied to the mass that can only translate.

Although none of the models is a mechanistic model, it is tempting to suggest that the rotating mass  $m$  about the pivot in Models 3a represents the pitching motion of the body about the pelvis. The sub-system containing  $m_1$ ,  $k_1$  and  $c_1$ , may represent the movement of the viscera.

In conclusion, the prediction of backrest transmissibility showed encouraging results when the backrest cushion was attached with the mass of the seated-person in a model that can rotate. However, the modelling merits further development.

#### 8.5.2 Alternative dynamic impedance of the backrest

In this section, the dynamic stiffness and damping of the seat backrest and the foam backrest were approximated to represent a larger area of contact between the back and the backrest than the area of contact between the SIT-BAR and the backrest as used in the indenter test.

For simplicity, it was assumed that the orientation of the SIT-BAR would have small effect on the measured dynamic stiffness of both backrests. Figure 3.30 shows the arrangement of the SIT-BAR to approximate the contact area between the back and the backrest.

Based on the simple model of the backrest cushion consisting of a spring and a damper arranged in parallel (see Section 8.3.4), the 'new' dynamic stiffness and damping for both backrests are now represented with two springs and two dampers arranged in parallel to estimate the whole area (i.e. the area underneath the two SIT-BARs and the backrest cushion as shown in Figure 3.30). Table 8.8 lists the 'new' dynamic stiffness and damping of both backrests with different pre-loads (the 'new' dynamic stiffness and damping is twice the measured value, assuming that both springs (or dampers) are identical to each other; see Table 8.3). It should be noted that the pre-loads corresponding to the 'new' dynamic stiffness and damping were also increased.

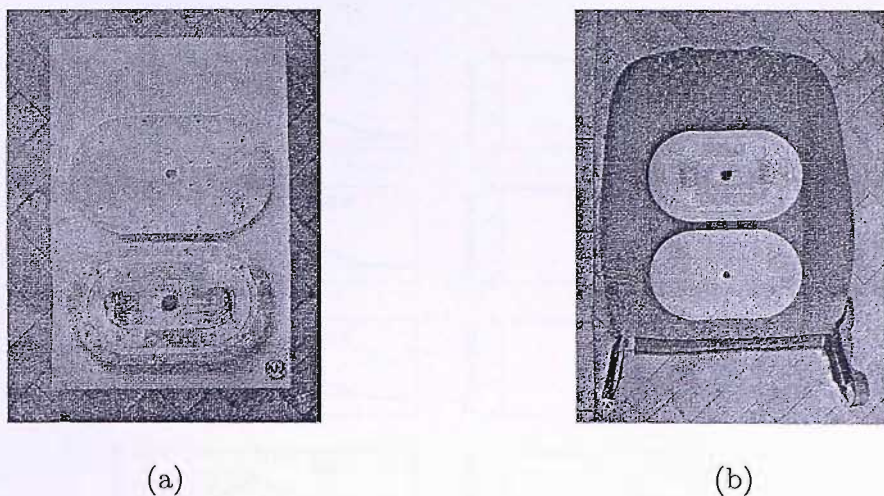


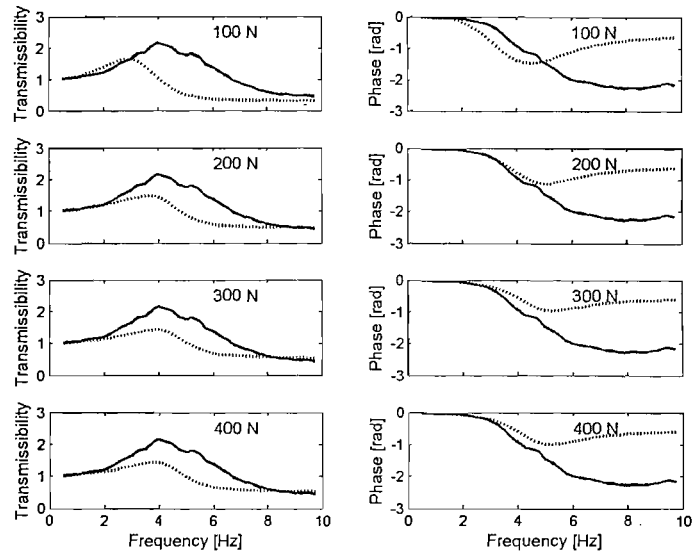
Figure 8.30: The arrangements of the SIT-BAR for approximating the stiffness of the backrest cushions. (a) On the foam block; (b) on the backrest cushion.

Table 8.8 The 'new' dynamic stiffness and damping for the seat backrest and the foam backrest.

Pre-load		Stiffness (N/m)				Damping (Ns/m)			
		Car seat		Foam backrest		Car seat		Foam backrest	
'old'	'new'	'old'	'new'	'old'	'new'	'old'	'new'	'old'	'new'
50	100	11324	22648	17053	34106	142	284	126	252
100	200	21176	42352	14496	28992	187	374	109	218
150	300	27242	54484	14844	29688	201	402	103	206
200	400	25595	51190	24505	49010	208	416	193	386

### 8.5.2.1 Predicting backrest transmissibility

Using the 'new' values of the dynamic properties of the backrests, the transmissibilities of both backrests were predicted using all models (Models 1a to 4a) and are shown in Figure 8.31 to Figure 8.34.



**Figure 8.31:** Comparison of median car seat backrest transmissibility and phase with twelve subjects and predicted backrest transmissibility and phase when using Model 1a with the ‘new’ stiffness and damping of the backrest cushion. Measured transmissibility and phase (—); predicted transmissibility and phase (·····).

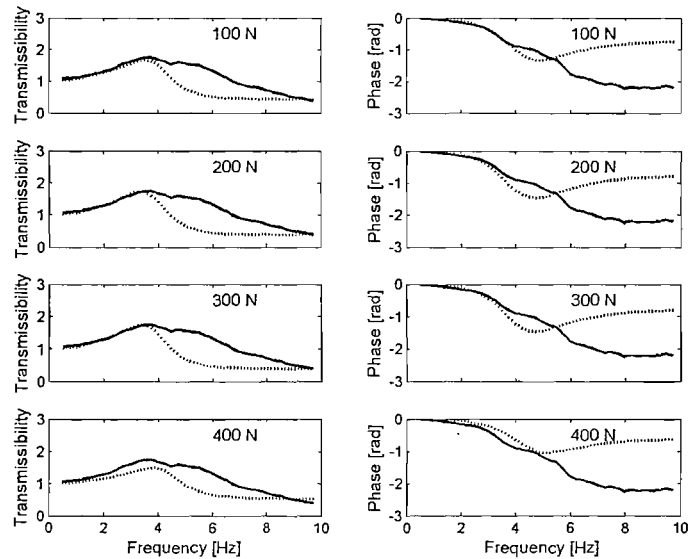


**Figure 8.32:** Comparison of median 100mm foam backrest transmissibility and phase with twelve subjects and predicted backrest transmissibility and phase when using Model 1a with the ‘new’ stiffness and damping of the backrest cushion. Measured transmissibility and phase (—); predicted transmissibility and phase (·····).

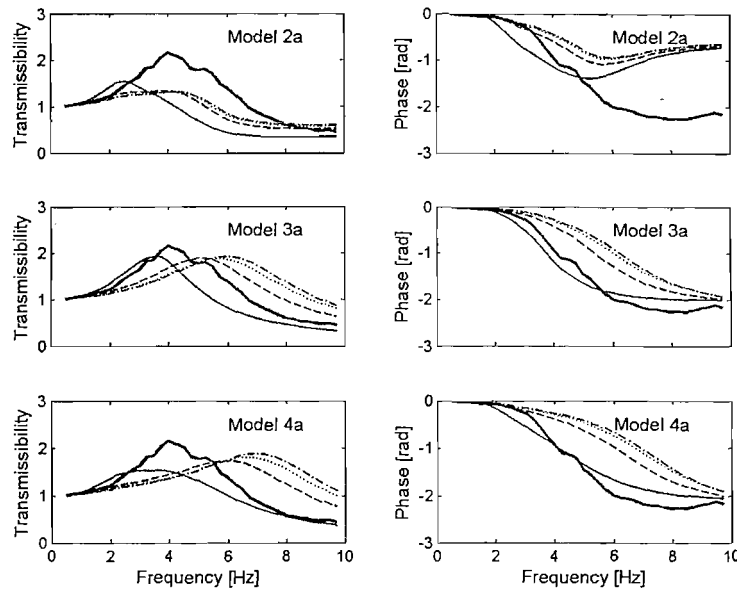


**Figure 8.33:** Fore-and-aft backrest transmissibility of car seat cushion. Experiment (—); predicted transmissibility with the ‘new’ dynamic stiffness and damping at pre-load of: 100 N (—); 200 N (---), 300 N (—·—) and 400 N (····).

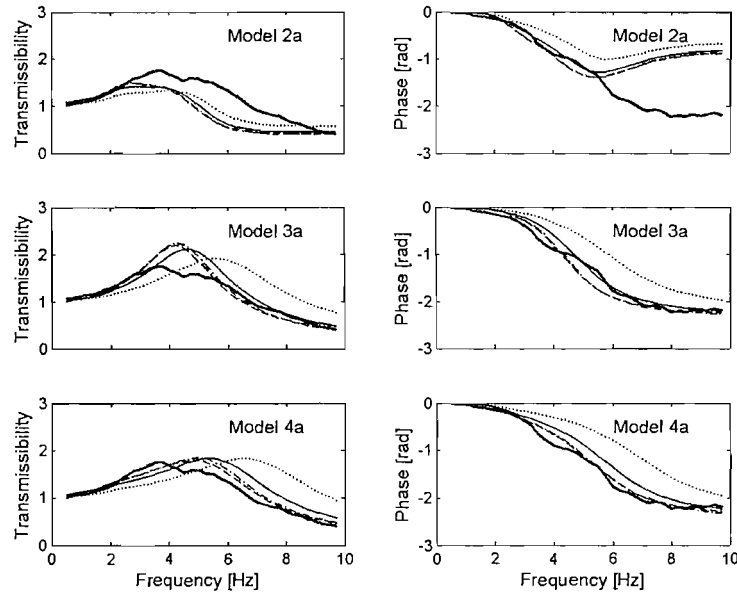


**Figure 8.34:** Fore-and-aft backrest transmissibility of 100 mm foam backrest. Experiment (—); predicted transmissibility with the ‘new’ dynamic stiffness and damping at pre-load of: 100 N (—); 200 N (---), 300 N (—·—) and 400 N (····).

Using Model 1a and with the 'new' dynamic stiffness values, the predictions of both backrests were improved compared to when using the measured dynamic stiffness. With the 'new' dynamic stiffness, Model 1a was able to predict the resonance frequency of the transmissibility of both backrests, although the predictions of the transmissibilities were underestimated compared to the measured data.

It can be seen that Model 2a did not predict well the transmissibility of either backrest, even with the 'new' dynamic stiffness of the backrests.

The predictions of the transmissibility of the seat backrests using Model 3a showed visually good agreement with the measured data only with the 'new' dynamic stiffness corresponding to a pre-load of 100 N. With other pre-loads, the predictions seem to overestimate the measured transmissibility. However, predictions for the foam backrest with the same model showed good agreement with the measured data when using the 'new' dynamic stiffness corresponding to 100 N, 200 N and 300 N pre-loads.

The predictions of the transmissibility of the seat backrests using Model 4a did not show good agreement with measured values when using any 'new' dynamic stiffness. However, the model showed promising predictions of the transmissibility of the foam backrest when using the 'new' dynamics stiffness corresponding to 100 N, 200 N and 300 N pre-loads.

#### 8.5.2.2 *Discussion and concluding remarks*

Despite some of the predictions of the transmissibility of both backrests with Model 3a and 4a showing visually good agreement with the measured data, the corresponding pre-loads were too high to correspond to the loads of the back to the backrest cushion with seated persons.

In conclusion, it is possible to improve the prediction of the transmissibility of backrests when using the approximate values of the dynamic stiffness of the backrest cushions to correspond to a larger area than the area of the indenter head, but the method merits further investigation.

## 8.6 Discussion

The transmissibility models were developed from the seated-person models based on measurements of the apparent mass of the back only. Recent studies have shown that the effect of vibration on the seat can affect responses at the backrest during fore-and-aft excitation (Nawayseh and Griffin, 2005a). It is anticipated that the inclusion of the effect of vibration on the seat may improve the prediction of backrest transmissibility.

The SIT-BAR was designed such that: i) the upper surface of the mount must be hard and flat to provide firm contact with the ischial tuberosities, and ii) the lower surface should be of a similar shape and size to that portion of the human buttocks normally in contact with a seat (Whitham and Griffin, 1977). Using the SIT-BAR as the indenter head showed good results when measuring the seat cushion dynamic properties and showed encouraging prediction for vertical seat transmissibility when combined with the seated-person model (Wei and Griffin, 1998c). However, the interaction at the back-backrest, and the load bearing at the backrest may be more complex than on the seat cushion. A reasonable shape that can possibly represent the interaction at the back-backrest interface, possibly like the part that represent the torso of the SAE-mannequin in the International Standard ISO 5353, (1978) merits further development.

The prediction of the transmissibility of backrests may be improved if the 'correct' dynamic properties of the backrest cushions are used. For example, the prediction of Model 3a showed encouraging results with higher pre-loads (100N to 200 N). However, a higher pre-load did not correspond to the 'correct' pre-load on the backrest with subjects. A recent study by Nawayseh and Griffin (2004) reported that the static forces at the backrest were 52.5 N with an 'average thigh contact' posture (i.e. upper legs parallel with the seat surface) for subjects weighting around 73 kg. Based on this study, less than 10% of the body weight is supported on the backrest, compared to around 75% of the body weight supported on the seat cushion (e.g. Wei and Griffin, 1998c).

The indenter test assumes that the backrest cushion is made of a simple spring and damper arranged in parallel. However, the backrest cushion is more complex than a spring-damper arranged in parallel. Possibly, the indenter test to measure the dynamic properties of backrest cushion should consider the construction of the backrest cushion.

The prediction assumed that the fore-and-aft vibration at the backrest was always translational. Qiu and Griffin (2005) found that the pitch and roll vibration of a car, together with the translational vibration at the seat base, made significant contributions to the seat backrest vibration. With the seat backrest attached to the seat cushion via a pivot (see Figure 4.1), there is a possibility that the fore-and-aft vibration at the backrest may also include the pitching of the backrest. However, this was not quantified in the measurements. Possibly, the prediction of fore-and-aft backrest transmissibility should take into account the pitch vibration of the backrest.

## 8.7 Conclusions

A simple linear two-degree-of-freedom lumped parameter model (Model 1) showed good prediction of the apparent mass of the back. However, when combined with a backrest cushion model (spring and damper arranged in parallel), the prediction of the transmissibility of the car seat backrest and the foam backrest did not show good agreement with the measured data.

Three alternatives models (Models 2, 3 and 4), representing the human-body were developed and showed good prediction of the apparent mass of the back. However, only Model 3 and Model 4 showed encouraging predictions of the backrest transmissibility when combined with the backrest cushion model. For these models, the backrest cushion was attached to a mass which can rotate.

The dynamic stiffness and damping of the seat backrest and the foam backrest were estimated to correspond to a larger area of contact between the back and the backrest than the size of SIT-BAR. Using the 'new' dynamic stiffness, the predictions of the transmissibility of both backrests using Model 1a were improved, although the predicted transmissibilities were under-estimate. When using the 'new' stiffness with the alternative models, only Model 3a showed good agreement with the measured data.

Although promising predictions of the transmissibility of both backrests were obtained with some of the alternative models of the human-body model, or when using an scaled value of the dynamic stiffness of the backrest cushion, further development is needed to improve the predictions of the transmissibility of backrests.

# Chapter 9

## General discussion

### 9.1 Introduction

In each chapter, the equivalent findings have been discussed. This chapter considers the validity of using a linear technique to analyse the responses of the human body to vibration and presents a general discussion of the equivalent results presented in Chapter 4 to Chapter 8 of this thesis.

### 9.2 Validity of using linear method

The biodynamic responses of the body, such as the fore-and-aft apparent mass of the back and the ‘cross-axis’ response during fore-and-aft excitation as reported in Chapter 6 and Chapter 7 have been calculated using the ‘cross-spectral density’ (CSD) method. This CSD method is a linear analysis technique and has been used widely in previous studies to analyse biodynamic responses of the human body to vibration. An advantage of using this method is that it only includes energy at the output that is linearly related to the input, and that linearity can be observed by calculating the coherency of the transfer function (see Section 3.4.1). A high coherency (greater than 0.9) indicates that the output signal is linearly correlated with the input signal. In addition, the CSD transfer function is a complex function: both the modulus and phase of the transfer function can be calculated.

The transfer functions of the biodynamic responses of the body can also be calculated using the ‘power-spectral density’ (PSD) method. Using this method, for example, the apparent mass of the back during fore-and-aft excitation can be calculated as the square root of the ratio of the PSD of the output (i.e. force) and the PSD of the input (i.e. acceleration). Unlike the CSD method, the latter method only produces the modulus of the apparent mass. It also includes both correlated and uncorrelated signals and therefore includes ‘noise’ and does not assume linearity.

Previous studies have shown that the human body responds non-linearly in response to vibration. In Chapter 6, the apparent mass of the back was found to be significantly non-linear with vibration magnitude. However, there was generally high coherency between fore-and-aft acceleration and the fore-and-aft forces (or 'cross-axis vertical' forces) at the back during each measurement, possibly suggesting that the body was behaving approximately linearly during each measurement. Therefore, it is of interest to compare fore-and-aft (and the 'cross-axis' vertical) apparent mass of the back calculated using the CSD method with the PSD method. An example of the results is shown in Figure 9.1.

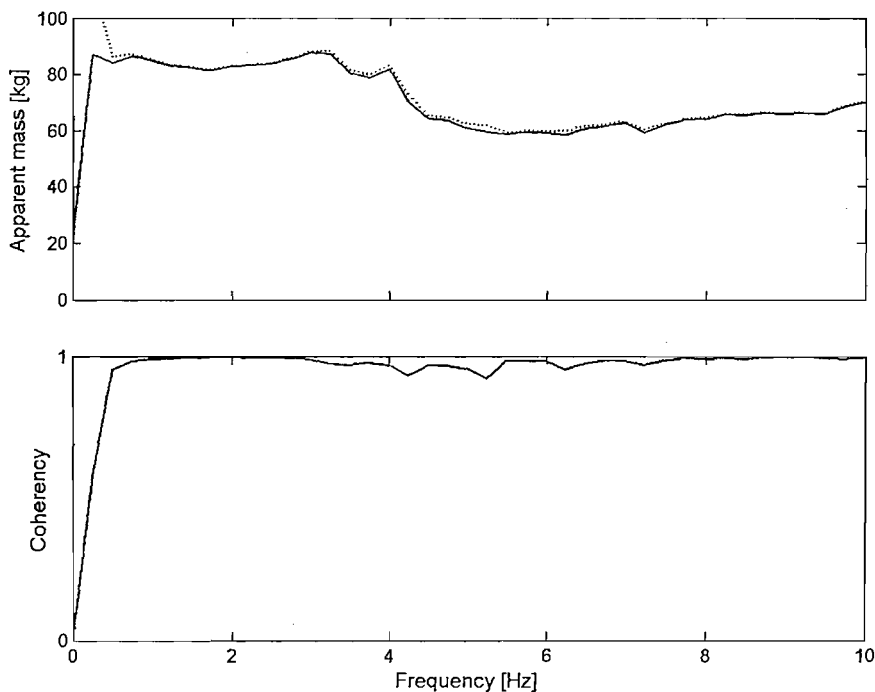


**Figure 9.1:** Comparison of apparent mass of the back at location 3 (middle back) of one subject at  $0.4 \text{ ms}^{-2}$  r.m.s. calculated using CSD method (—) and PSD method (·····).

It may be seen that the CSD and PSD methods gave similar results. This suggests that the CSD method used in Chapter 6 and Chapter 7 give representative values for the fore-and-aft (and 'cross-axis vertical') apparent mass of the back at different condition, and that the use of linear technique (such as in this study) has not produced misleading results.

## 9.3 General discussion

The results shown in Chapter 4 and Chapter 5 were based on the analysis of the transfer function between the vibrator platform (or in some case, between the back of the backrest) and the acceleration at the interface of the back-backrest at any location. Previous studies by Fairley and Griffin (1984) and Qiu and Griffin (2004) showed that the magnitude of the fore-and-aft transmissibility of the seat was near unity, suggesting that the vibration at the seat-person interface is approximately similar to the input vibration (either from the floor or the seat base). Therefore, the results Chapter 4 and Chapter 5 were presented with the assumption that the fore-and-aft vibration between the seat and the thigh had little effect on the vibration at the back-backrest interface.

Likewise, the results presented in Chapter 6 and Chapter 7 also based on the assumption that the vibration on seat had little effect on the vibration at the backrest. Recent study by Nawayseh and Griffin (2004a) showed the apparent mass on the body on the seat during fore-and-aft vibration is affected when a vertical backrest was used, such that backrest reduced the forces on the seat at frequencies less than 4 Hz but increased the forces at frequencies greater than 4 Hz. However, the extent of the effect of vibration on the seat affecting the vibration at the backrest and vice-versa is not fully uncovered and remains unknown. Based on the results of Nawayseh and Griffin (2004a), it can be assumed that the decreased in the apparent mass on the seat at frequencies less than 4 Hz and increased at frequencies greater than 4 Hz with vertical backrest may have arisen from the coupled-effect of the vibration on the seat and the backrest. However, notwithstanding the mechanism involved, the results in Chapter 6 and Chapter 7 were analysed with the assumption that the high apparent mass of the body on the seat, as shown by Nawayseh and Griffin (2004a) would produce high shear forces between the seat surface and the thigh, resulting in only small forward and backward of the body movement in response to fore-and-aft excitation. Based on this analogy, it is assumed that the effect of vibration on the seat may have little effect on the responses at the back-backrest interface.

### 9.3.1 Mode of vibration of the body

The vibration transmitted through backrests depends on the responses of the occupants. In Chapter 4, the principal resonance frequency of the transmissibility of backrests was found around 5 Hz, which coincides with the principal resonance frequency of the apparent mass of the back as reported in Chapter 6. It is possible that the resonance frequency of the backrest transmissibility is related to the mode of vibration of the body during fore-and-aft

excitation. If the body has a rotational mode during vertical excitation, the same mode would be expected during fore-and-aft excitation. Kitazaki and Griffin (1997) showed that there was a mode of the entire body involving combined bending in the lower thoracic spine and pitching of pelvis and the upper body at the principal resonance frequency of the body during vertical excitation. Matsumoto and Griffin (1998) suggested that the motion of the body at the principal resonance of the body involved a combined bending in the lumbar spine, coupled with a rocking motion of the upper thoracic spine about the lower thoracic spine and a pitching motion of the pelvis. Based on the results of Kitazaki and Griffin (1997) and Matsumoto and Griffin (1998), it is suggested that the principal resonance frequency of the apparent mass of the back could be associated with a mode of the vibration of the entire body involving combined bending in the thoracic spine and pitching of the pelvis and the upper body.

### 9.3.2 Variation in the transmissibility of backrests

The median resonance frequencies of the backrest transmissibilities of the car seat found in Chapter 4 (4 to 5 Hz) are similar with the results reported by Qiu and Griffin (2003) who investigated the fore-and-aft transmissibility of the backrest of a car seat (similar to the seat used in this study) with both field and laboratory measurements. The authors found that the principal resonance frequency of the fore-and-aft backrest transmissibility was in the frequency range 4 to 5 Hz. It is anticipated that with different seats, there would be slight difference in the transmissibility of backrests and in the resonance frequency of the backrest transmissibility since the transmissibility of seats does not only depend on the responses of the occupants, but also depends on the mechanical properties of the seats, which may vary between seats.

The results in Chapter 4 showed that the transmissibility of a car seat and a foam backrest was significantly varied across the vertical positions on the backrest from the seat surface, although the resonance frequency showed little change with vertical position. It is anticipated that variation in the apparent mass of the back during fore-and-aft vibration may have contributed to the variation in the transmissibility of the backrest with vertical position.

The variation of the apparent mass of the back with vertical positions on the back was investigated in Chapter 6. In that study, the apparent mass of the back was measured using a rigid block of wood (120 mm in height) placed between the back and the force platform at five locations to the back so as to investigate the variation in the apparent mass of the back with vertical position. Prior to the test, subjects were instructed to adopt an upright posture with the back making contact with the block while maintaining the

posture at all locations. Assuming that subjects adopted a similar posture at all locations, the results obtained from this study may be representative of the variation in the apparent mass of the back as if the whole-back in contact with the backrest (i.e. the wooden block is removed between the back and the force platform). However, for locations at the lower back, it was found 'necessary' for the subjects to make some voluntary muscle control of the posture to avoid the upper back touching the force platform since there was a gap between the upper back and the force platform. This has a potential of altering the body posture as well as the muscle stiffness within the body and could affect the responses. Ideally, five 'mini' force platforms were required to measure the variation in the forces between the back and the backrest with the whole-back in contact with the backrest, but due to the limitations in the equipments, the former method was used. Nevertheless, the results in Chapter 6 showed that the apparent mass of the back varied significantly with vertical location on the back. The apparent mass of the lower and the middle back were greater than at the upper back at frequencies less than 10 Hz.

Upon assuming that the changes in posture with vertical location had little effect on the apparent mass of the back during fore-and-aft excitation, the results of Chapter 6 showed that during fore-and-aft excitation, two resonance frequencies were clearly observed around 2 Hz and 5 Hz, where the resonance at 5 Hz was a major resonance. As suggested earlier, the mode of vibration of the body at the principal resonance frequency could be associated with a mode of vibration of the entire body involving combined bending in the thoracic spine and pitching of the pelvis and the upper body. The resonance frequency of the apparent mass of the upper back around 2 and 3 Hz could be associated with the pitching of the body, similar to the mode of vibration of the body around 2 Hz found by Nawayseh and Griffin (2005a) which they suggested to be associated with pitching mode of the body during fore-and-aft excitation.

The modes of vibration of the body during fore-and-aft excitation could cause relative movement over the spine during the vibration exposure. Matsumoto and Griffin (1998) measured the transmissibility to the first, fifth and tenth thoracic vertebra (T1, T5, and T10), and to the first, third and fifth lumbar vertebra (L1, L3 and L5) and to the pelvis (the posterior-superior iliac spine) from the seat surface at the principal resonance frequency of the body during vertical excitation so as to investigate the movement of the upper-bodies of seated persons. The authors showed that there was a clear relative motion between the locations over the spine at the principal resonance frequency: all measurement points did not move in the same manner. They found bending and rocking motions in the spine appeared to be dominant at frequencies around the principal resonance frequency of the body. The upper thoracic spine, between T1 and T10, tended to rock about a point on the lower thoracic spine in the sagittal plane, with some slight bending. In the lower

thoracic spine and the lumbar spine region, bending motion along the spine was more significant than in the upper thoracic spine. Some pitch motion of the pelvis occurred at this frequency, although the pitch resonance of the pelvis is at a higher frequency. There was also pitch motion of the head at the principal resonance of the body. There was also slight compression and expansion between the measurement points on the spine at the principal resonance frequency. Therefore, the results of Chapter 6, together with the findings of Kitazaki and Griffin (1997), Matsumoto and Griffin (1998) and Nawayseh and Griffin (2005a), suggest that the variation in the transmissibility of the backrest during fore-and-aft vibration could be caused by the relative movement along the spinal column due to different modes of the body, associated with the variation in the apparent mass of the back.

### 9.3.3 Non-linearity

A non-linearity in the fore-and-aft backrest transmissibility with vibration magnitude found in Chapter 4 has also been observed previously (Qiu and Griffin, 2003). The non-linearity in the transmissibility might be due to a non-linear response of the body or a non-linear response of the seat, or both. In Chapter 6, the apparent mass of the back was shown to be significantly non-linear with vibration magnitude. Nawayseh and Griffin (2005a) also found that the fore-and-aft apparent mass of the back during whole-body fore-and-aft vibration was non-linear with vibration magnitude. Wei and Griffin (1997) concluded that the vibration magnitudes did not have an important influence on the stiffness or the damping of a foam block. Therefore, the non-linearity in the body is likely to have a greater influence in the non-linearity of the transmissibility of backrests than the non-linearity in the dynamic properties of the backrests with vibration magnitude.

The causes of the non-linearity of the body with vibration magnitude during exposure to fore-and-aft vibration are not known. Possible causes include changes in muscle activity, change in posture, the geometry of the body and non-linear mechanical properties of the soft tissue.

A possibility causing the non-linearity of the back during exposure to fore-and-aft vibration could be associated with the 'softening' effect of the body with increasing vibration magnitude, combined with involuntary changes in the muscle tension within the body. Matsumoto and Griffin (2002) suggested that the non-linearity of the body during vertical excitation may be partly caused by involuntary changes in the muscle tension. It is suggested that with increasing vibration magnitude, the feet involuntarily applied some push force proportional to the fore-and-aft acceleration so as to stabilise the pitching movement of the body while at the same time allowing the 'natural' softening response of

the body. Nawayseh and Griffin (2005a) found that the apparent mass of the back was significantly non-linear with vibration magnitude and there was an evident of non-linearity in the fore-and-aft apparent mass of the feet with vibration magnitude during exposure to fore-and-aft whole-body vibration (Nawayseh and Griffin, 2005b). Therefore, it is anticipated that the non-linearity in the apparent mass of the back may be associated with the combined effect of the 'softening' effect of the body with the involuntary push force at the feet with increasing vibration magnitude.

The non-linearity of the body with vibration magnitude during fore-and-aft excitation may be partly caused by the shear deformation of the tissue beneath between the thigh and the seat surface. Kitazaki and Griffin (1997) showed that the shear deformation of the buttock tissue can contribute to the decrease in the natural frequency of the entire body mode and the principal resonance frequency of the body during vertical excitation, due to the much lower shear stiffness and axial stiffness of tissue. Nawayseh (2004) suggested that the shear deformation of the tissue beneath the pelvis to have contributed to the non-linearity in the fore-and-aft 'cross-axis apparent mass' of the body during vertical vibration. It is possible that this shear deformation of the tissue beneath the pelvis may have partly contributed to the non-linearity of the body during fore-and-aft excitation.

There also could be an effect of the viscera on the non-linearity of the body during fore-and-aft excitation. Although there is no study reported on the effect of viscera on the non-linearity of the body during fore-and-aft excitation, Mansfield and Griffin (2002) showed that by restricting the visceral movement (by the elasticated belt worn by subjects around the abdomen) the resonance frequencies of the apparent mass of the body was significantly higher compared to when subjects seated an upright posture without wearing the belt. A similar study to investigate the effect of the visceral movement on the non-linearity of the apparent mass of the back merits further study.

### 9.3.4 Factors affecting transmissibility of backrests

The transmissibility of a backrest is largely depended on the apparent mass of the back. Any factors that could affect the apparent mass of the back would have an effect to the transmissibility of backrests.

In Chapter 7 (Section 7.2), the resonance frequency of the apparent mass of the back decreased with increasing backrest inclination and this is probably due to an increase in the percentage of the body mass supported on the inclined backrest. Rakheja *et al.* (2002) found that the resonance frequency of the apparent mass of the body when subjects adopted an automotive sitting posture (i.e. with inclined seat-pan and inclined backrest)

was between 6.5 and 8.6 Hz, which is higher than most previous studies where subjects have sat with a vertical backrest (approximately around 5 Hz; e.g. Fairley and Griffin, 1989; Mansfield and Griffin, 2000 and Nawayseh and Griffin, 2003). In that study, it was found that the percentage of the body mass supported on the seat was 70%, while around 30% was supported on the inclined backrest. Wang *et al.* (2004) also found that the resonance frequency of the apparent mass of the body on the seat showed resonance around 5 Hz with a vertical backrest during vertical excitation, and increased when the back was supported by an inclined backrest (up to 12° from vertical). A reduction in the percentage of body mass supported on the seat with an inclined backrest may, in part, cause an increased in the resonance frequency of the apparent mass of the body during vertical excitation. Consequently, an increase in the percentage of body mass supported on the backrest with increasing backrest inclination may have contributed to an increase in the dynamic stiffness of the backrest. This might partly explain the increase in the resonance frequency of the fore-and-aft backrest transmissibility with increasing backrest inclination, as found in Chapter 5 (Section 5.3).

With increasing push force at the feet, there was an increase in the resonance frequency of the apparent mass of the back (see Chapter 7, Section 7.3). Possibly, this is due to the 'stiffening' effect of the body. With increasing push force at the feet, the apparent mass of the back was increased, suggesting that the loads on the backrest were also increased. This may have contributed to an increase in the dynamic stiffness of the backrest cushion. With increasing push force at the feet, the resonance frequency of the fore-and-aft backrest transmissibility was increased (Chapter 5, Section 5.4). It is reasonable to suggest that an increase in the resonance frequency of the fore-and-aft backrest transmissibility with increasing push force at the feet is most probably due to an increase in the loads on the backrest from the push force at the feet, which may have contributed to an increase in the dynamic stiffnesses of the backrests.

In contrast, varying the seat-pan inclination (see Chapter 7, Section 7.2) and varying the fore-and-aft footrest position (see Chapter 7, Section 7.3) showed little effect on the apparent mass of the back and consequently had little effect on the fore-and-aft transmissibility of backrests (Chapter 5, Sections 5.3 and 5.4).

### **9.3.5 Biodynamic responses at low frequency (i.e. near 0 Hz)**

During vertical excitation and at low frequencies (i.e. near 0 Hz), the apparent mass at this frequency is approximately equal to the subject static weight supported by the seat (Griffin, 1990). Some studies have found that the weight supported on the seat is approximately 75% of the subject's weight (e.g. Wei and Griffin, 1998c and Nawayseh and

Griffin, 2004). In Chapter 6, the apparent mass of the full back at low frequency was approximately 45% of the subjects' weight. However, in static conditions, the forces measured at vertical backrest were approximately 10% of the subject's weight (Nawayseh and Griffin, 2005a). An increase in the apparent mass at low frequency during fore-and-aft excitation compared to the forces at the backrest in static condition suggests that the apparent mass of the back at low frequency: i) did not equate with the static mass of the upper body leaning against the backrest, and ii) it only indicates the dynamic forces between the back and the backrest during fore-and-aft excitation.

### 9.3.6 Conceptual model

Exposure to whole-body vibration causes complex dynamic responses of the body. This may cause unpleasant sensations giving rise to discomfort. As the transmission of vibration to the backrest of a seat can cause the discomfort of drivers and passengers, the ultimate aim of studying the biodynamic responses of the body and the transmissibility of backrest is to change, for example, a seated person from saying, "I am feeling **uncomfortable**" to "I am feeling **comfortable**". However, dealing with this problem needs a systematic study to understand the causes of discomfort, which include the study of the vibration being transmitted to the body through the seat and the biodynamic responses at the seat-person interfaces, such as investigated in this thesis.

British Standard BS 6841 (1987) suggests that during fore-and-aft vibration in a rigid seat, the backrest would primarily cause the discomfort to the occupants at frequencies greater than about 2 Hz if a cushion and backrest have the same level of vibration. In practice, seats are not rigid. The seat and backrest cushions can amplify the vibration through the seat cushion, or the backrest. Furthermore, any fore-and-aft resonance of the backrest and variation in the fore-and-aft vibration at the backrest will increase further the importance of backrest vibration to ride comfort. A recent study by Price *et al.* (2005) showed that during fore-and-aft vibration, the presence of a rigid vertical backrest caused increased sensitivity to vibration between 2 and 6 Hz. In the same study, the authors found that greatest discomfort was experienced in the upper body in the frequency range 0.5 to 16 Hz at all vibration magnitudes tested (0.05, 0.2 and 0.8 ms<sup>2</sup> r.m.s.). The most discomfort in the upper body was experienced at 4 Hz with 0.2 and 0.8 ms<sup>2</sup> r.m.s. vibration magnitude. They suggested that the discomfort experienced in the upper body was due to the backrest transmitting vibration directly to the upper torso. They also found that the vibration frequency had a greater effect on the location on discomfort than the vibration magnitude. The results in Chapter 4 showed that there was a principal resonance of the fore-and-aft backrest transmissibility around 5 Hz and the vibration transmitted to the

back varied significantly across the vertical height from the seat surface between 2 and 10 Hz. The effect of vibration magnitude on the transmissibility of backrests was also apparent. It is reasonable to suggest that the greatest discomfort felt by the seated subjects around 4 Hz in the study of Price *et al.* (2005) may be attributed to the resonance frequency of the backrest transmissibility around the same frequency as found in Chapter 4. In addition, the greatest transmissibility was measured at the middle part of the backrests (see Chapter 4). Furthermore, the results in Chapter 5 showed that the fore-and-aft vibration on the backrest was significantly modified with increasing inclination of the backrest and with increasing push force at the feet (i.e. the back was pushed against the backrest). The results in Chapter 4 and Chapter 5, suggest that the sensitivity of the back may not only depend on the vibration frequency and vibration magnitude, but also may depend on the location at the backrest as well as other factors, such as the backrest inclination and variation in push force at the feet. These factors are important when considering the effect of backrest vibration on ride discomfort.

The human-body lumped parameter models developed in Chapter 8 to predict the apparent mass were based on the measurements of the apparent mass of the back only. Nawayseh and Griffin (2005a and 2005b) showed that the effect of the vibration of the seat can affect the responses at the backrest of the seated person during fore-and-aft excitation. In addition, the apparent mass of the back was influenced by different sitting thigh contact between the seat surface and the backrest from 'maximum thigh contact' to 'minimum thigh contact'. The human-body model merits further development, which could include the measurement of the apparent mass on the seat during fore-and-aft excitation.

The seat-person models were developed in Chapter 8 so as to predict the backrest transmissibility of the backrest during fore-and-aft excitation. The models showed good prediction on the transmissibility of backrest, although further development is required. Having a mathematical seat-person model, such as in Chapter 8 would enable the prediction of fore-and-aft backrest transmissibility, which can be used, for example, by the seat designer to optimise the seat design as well as to improve the comfort. However, the models were developed based on the measurements of the apparent mass of the back (Chapter 6) and the impedance of the backrest cushions (Chapter 8) such that the input vibration at the base of the seat was constrained to the fore-and-aft direction, even though this is often not the case in vehicles. Qiu and Griffin (2003) conducted field and laboratory studies to measure the fore-and-aft transmissibility from the seat base to the seat surface and to the backrest. The authors found that the fore-and-aft transmissibility from the floor to the backrest laboratory test exhibited three resonance frequencies at about 5 Hz, 28 Hz and 48 Hz. Similar resonances of the transmissibility of backrest were also obtained in the car test measurements. However, due to lower coherency and the multi-input vibrations,

the peaks in the field test were less visible compared to the laboratory study. In the field test results, the fore-and-aft transmissibility to the backrest tended to be higher than the fore-and-aft transmissibility to the seat. The authors suggested that this may be due to the effect of pitch and roll motions on the seat pan were not as significant as on the backrest. In addition, they found that the contribution of the vertical input to the seat pan is small compared to the backrest due to smaller inclined angle of the seat pan. While the results from the laboratory tests provided a much better coherency for the transmissibility and the vibration input spectra can be controlled and manipulated, the field test may incorporate the multi-axis vibration input and that the subject may adopt the real sitting posture in vehicles. The authors (Qiu and Griffin, 2004 and 2005) also evaluated the vibration transmitted to the backrest of car seat using single-input and multi-input models to determine the vibration input at the seat base that can induce the fore-and-aft vibration at the backrest. The authors found that the fore-and-aft vibration and the vertical vibration, but not the lateral vibration at the four corners of the seat base, contributed to the fore-and-aft vibration (Qiu and Griffin, 2004). Using the same single-input and multi-input models model, they found that the pitch vibration, together with the translational vibration at the seat base, made significant contributions to the fore-and-aft backrest vibration (Qiu and Griffin, 2005). It seems important to investigate the effect of pitching vibration at the backrest to the biodynamic responses of the body and the transmissibility of backrests as this could advance the development of the seat-person model for predicting backrest transmissibility.

# Chapter 10

## General conclusions and future work

### 10.1 General conclusions

The vibration transmitted through backrests with seated subjects showed a principal resonance frequency of the transmissibility of backrests around 5 Hz (see Chapter 4). This coincides with the principal resonance frequency of the apparent mass of the back (see Chapter 6). It is possible that the resonance frequency of the backrest transmissibility is related to the mode of vibration of the body during fore-and-aft excitation. It is suggested that at the principal resonance frequency, the apparent mass of the back is associated with a mode of vibration of the entire body involving combined bending in the thoracic spine and pitching of the pelvis and the upper body. An additional resonance frequency of the body around 2 Hz might be associated with pitching a mode of the body during fore-and-aft excitation.

The fore-and-aft transmissibility of a seat backrest and a foam backrest varied significantly between 2 Hz and 10 Hz when measured at five vertical locations of the backrest above the seat surface varied significantly between 2 Hz and 10 Hz, although the resonance frequencies showed little changed (see Chapter 4). It is anticipated that the variation in the transmissibility of the backrest during fore-and-aft vibration may be attributed to relative movement along the spinal column caused by the different modes of the body which can be associated with the variation in the apparent mass of the back (see Chapter 6).

There was a systematic decrease in the principal resonance frequency of the apparent mass of the entire back and significant reductions in the apparent mass of the back at frequencies greater than 5 Hz with increasing vibration magnitude (see Chapter 6). The non-linearity of the body is suggested to have greatly influenced the non-linearity in the transmissibility of backrest with vibration magnitude. With increasing vibration magnitude, the fore-and-aft backrest transmissibilities of the car seat and the foam

backrest at five locations showed significant changes at frequencies between 2 Hz and 10 Hz (see Chapter 4). The resonance frequencies and transmissibilities at resonance for both backrests at all locations decreased with increasing vibration magnitude.

An increase in the resonance frequency of the fore-and-aft backrest transmissibility with increasing backrest inclination and with increasing push force at the feet found in Chapter 5 is probably due to an increase in the dynamic stiffness of the backrest cushions which can be associated with an increase in the loads on the backrest cushion from: i) an increased in the percentage of body mass supported on the backrest with increasing backrest inclination (see Section 7.2, Chapter 7) and ii) from the voluntary push force at the feet (see Section 7.3, Chapter 7). Conversely, varying the seat-pan inclination (see Section 7.2, Chapter 7) and varying the fore-and-aft footrest position (see Section 7.3, Chapter 7) had little effect on the apparent mass of the back and consequently had little effect on the fore-and-aft transmissibility of backrests.

At low frequencies (near to 0 Hz), there was a significant difference in the apparent mass of the back with different input locations to the back. The apparent mass of the back at the lower back was greater than at the middle back and the upper back. The results suggest that the interaction between the back and the backrest are complex and the modulus of the apparent mass at low frequencies does not represent the mass of the back supported on the backrest.

When a linear two degree-of-freedom model of the seated-person without a rotational degree-of-freedom was combined with a backrest cushion model (obtained from the indenter test), the predicted transmissibility of the backrests did not show a good fit with the measured data, although the seated-person model can predict the fore-and-aft apparent mass of the back. The prediction of the resonance frequency of the backrest transmissibility was improved when the value of the stiffness and damping of the backrest cushion was approximated to the area of contact between the back and the backrest. With an alternative model of the body with rotational capability, the prediction of the backrest transmissibility showed good agreement with the measured data between 0.5 Hz and 10 Hz. The seat-person model developed in this study is a first step towards developing a standardised method for predicting backrest transmissibility and requires further development.

## 10.2 Future work

This thesis focuses on the biodynamic responses of the body and the transmissibility of the backrests due to fore-and-aft excitation only. As seated persons in the real world are

exposed to multi-axis input excitation, it would be wise to further the studies of the biodynamic responses of the body and the transmissibility of seats to multi-axis vibration. There is an evident that the biodynamic responses of seated persons obtained in vehicle multi-axis measurements indicated a slight different outcome compared to the single-axis measurements, in particular in the  $x$ -direction such that the mechanical impedance of the body measured in multi-axis vibration input were much greater than the impedance of the body measured in a laboratory with a single-axis input vibration between 3 and 20 Hz (Holmlund and Lundström, 2001). This could be further investigated by measuring the apparent mass of the body at the seat and at the backrest in vertical, fore-and-aft and lateral directions simultaneously when the seated persons are exposed to multi-axis input vibration. This could help to extend the knowledge of the responses of the body and help to uncover the underlying mechanisms of the responses of the body to a real vibration input. Furthermore, the measurement of the biodynamic responses of body and transmissibility of seats exposed to multi-axis input vibration would enable researchers to develop mathematical models to predict the transmissibility of seats and backrests simultaneously in vertical, fore-and-aft and lateral directions.

The results in Chapter 5 showed that backrest inclination and push force at the feet have significant influences on the fore-and-aft vibration at the back-backrest interface. This suggests that sensitivity at the back-backrest interface may change with different inclinations of backrest or with different push force at the feet. Further study on the sensitivity of the back (discomfort) with varying backrest inclination and varying push force at the feet during fore-and-aft excitation merits investigation.

In Chapter 6, three body modes were suggested based on the driving point responses, but it was difficult to identify the mechanisms that cause these modes. However, it is possible to identify the mechanisms causing the body modes by measuring the transmissibilities to different locations on body, such as the study of Matsumoto and Griffin (1998). This knowledge will help to improve the modelling of the seated-body, in particular, when developing a mechanistic model.

The seated-person model developed in this study to predict the apparent mass of the back is a linear model. It can only predict the apparent mass of the back at a specific vibration magnitude. The non-linearity of the body response at different vibration magnitudes revealed in Chapter 6 suggests a non-linear body model is needed to represent the non-linear response of the body.

The biodynamic models of a seated person developed in Chapter 8 exclude the effects of vibration on the seat surface. A study by Nawayseh and Griffin (2005a) reported that vibration on the seat surface has a significant influence on the responses at the backrest.

The next logical step is to include the measurements of the apparent mass on the seat and the apparent mass at the backrest for predicting the impedance of the body at both surfaces.

The indenter test method used in Section 8.3 (Chapter 8) provides reasonable dynamic properties for both backrests. However, this method was originally developed to obtain the dynamic stiffness and damping of seat cushions during vertical vibration, and for simplicity, the seat cushion is assumed to be made of simple spring and damping arranged in parallel. In addition, the indenter head used (i.e. SIT-BAR) is a good approximation of the interface between the buttock and the seat surface. A new design for the indenter head that may represent the interaction between the principal load bearing at the back-backrest interface merits further study.

## Appendix A

# Fore-and-aft transmissibility of backrests: individual data

### A.1 Characteristics of subjects

Table A.1 Characteristics of subjects used in the experiment described in Chapter 4.

Subject no.	Age (year)	Stature (m)	Mass (kg)	Seat-to-shoulder (m)
1	25	1.76	78	0.61
2	23	1.76	78	0.59
3	20	1.75	61	0.62
4	28	1.75	72	0.61
5	26	1.74	72	0.62
6	25	1.73	65	0.60
7	22	1.82	70	0.67
8	23	1.70	80	0.63
9	32	1.69	67	0.60
10	22	1.65	58	0.58
11	27	1.86	99	0.69
12	22	1.78	67	0.64

## A.2 Instructions to subjects prior the experiment

### INSTRUCTION TO SUBJECT

You will be participating in a study investigating the variation of the **transmissibility of backrest above the seat surface**.

This experiment will last approximately 60 minutes.

Through the experiment, please try to ensure that you:

1. Adopt an upright posture
2. Maintain full contact of your upper body with the backrest
3. Adopt a leg posture such that the upper and the lower legs always perpendicular
4. Maintain your head position by looking forward
5. Rest your hands on your lap and hold the emergency button

**Important:**

In case of emergency during the test, please do not hesitate to press the STOP button. The vibrator will come to rest.

Thank you for your participation.

### A.3 Individual results

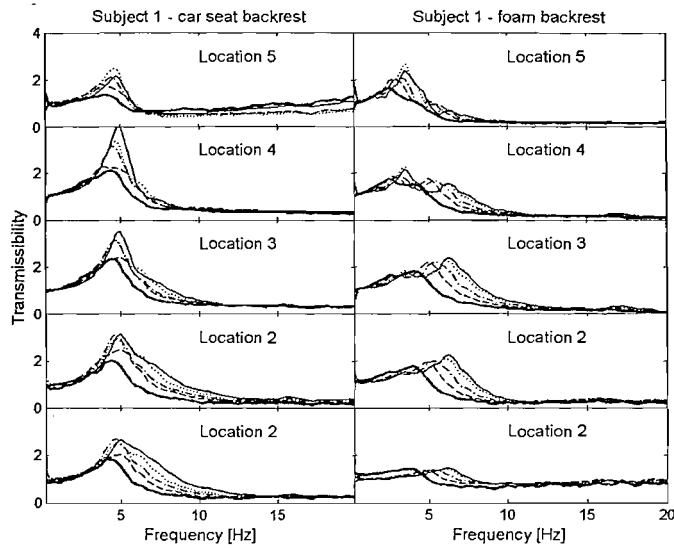


**Figure A.1:** The transmissibilities of a seat backrest and a foam backrest at all locations for subject 1 at all five vibration magnitudes.  $0.1 \text{ ms}^{-2}$  r.m.s. (—),  $0.2 \text{ ms}^{-2}$  r.m.s. (---),  $0.4 \text{ ms}^{-2}$  r.m.s. (-·-·-),  $0.8 \text{ ms}^{-2}$  r.m.s. (····) and  $1.6 \text{ ms}^{-2}$  r.m.s. (—).

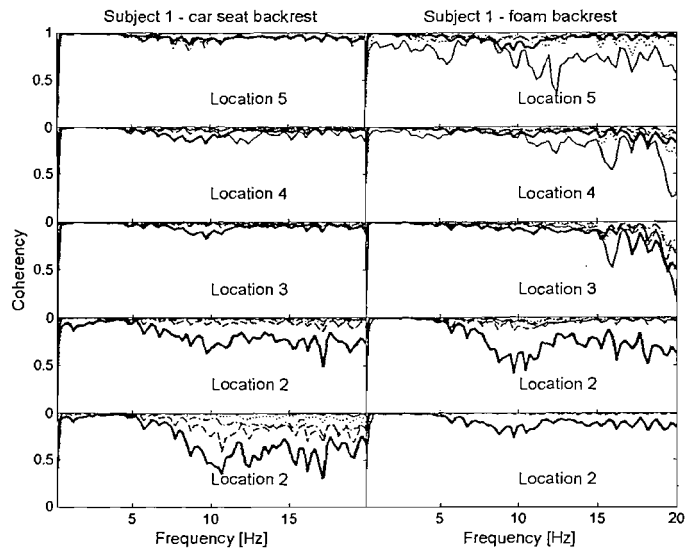


**Figure A.2:** The coherencies of the transmissibility of a seat backrest and a foam backrest at all locations for subject 1 at all five vibration magnitudes.  $0.1 \text{ ms}^{-2}$  r.m.s. (—),  $0.2 \text{ ms}^{-2}$  r.m.s. (---),  $0.4 \text{ ms}^{-2}$  r.m.s. (-·-·-),  $0.8 \text{ ms}^{-2}$  r.m.s. (····) and  $1.6 \text{ ms}^{-2}$  r.m.s. (—).

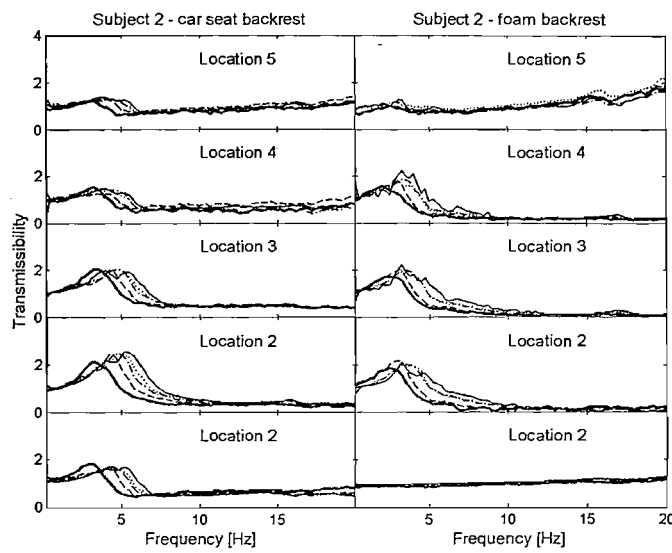


**Figure A.3:** The transmissibilities of a seat backrest and a foam backrest at all locations for subject 2 at all five vibration magnitudes.  $0.1 \text{ ms}^{-2}$  r.m.s. (—),  $0.2 \text{ ms}^{-2}$  r.m.s. (---),  $0.4 \text{ ms}^{-2}$  r.m.s. (-·-·-),  $0.8 \text{ ms}^{-2}$  r.m.s. (.....) and  $1.6 \text{ ms}^{-2}$  r.m.s. (—).

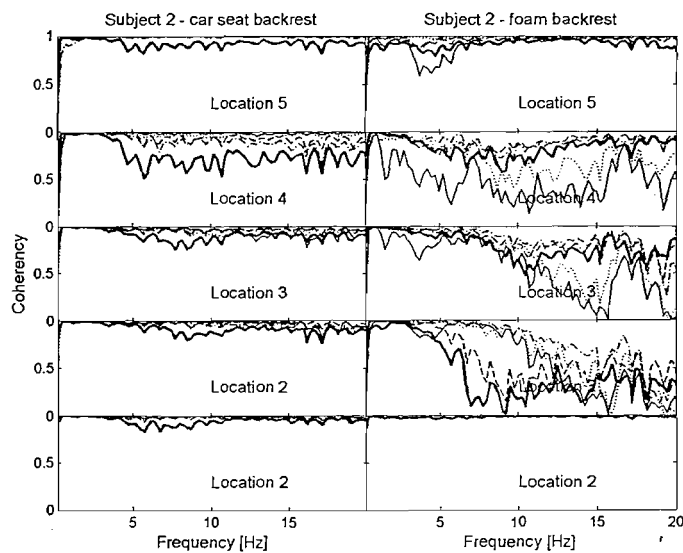


**Figure A.4:** The coherencies of the transmissibility of a seat backrest and a foam backrest at all locations for subject 2 at all five vibration magnitudes.  $0.1 \text{ ms}^{-2}$  r.m.s. (—),  $0.2 \text{ ms}^{-2}$  r.m.s. (---),  $0.4 \text{ ms}^{-2}$  r.m.s. (-·-·-),  $0.8 \text{ ms}^{-2}$  r.m.s. (.....) and  $1.6 \text{ ms}^{-2}$  r.m.s. (—).

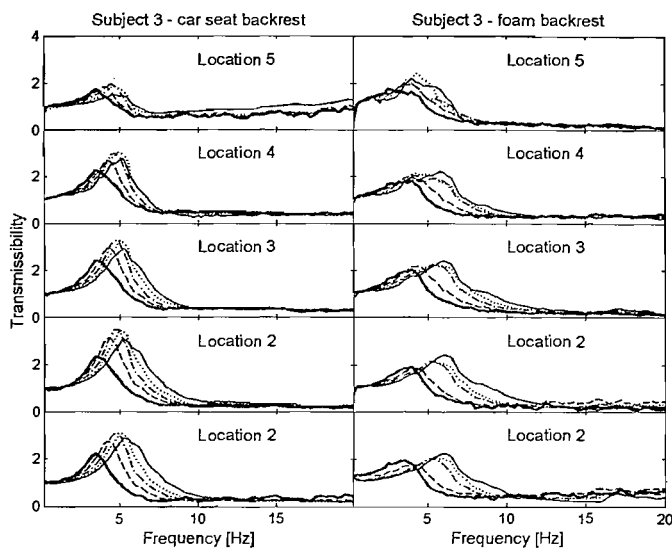


**Figure A.5:** The transmissibilities of a seat backrest and a foam backrest at all locations for subject 3 at all five vibration magnitudes.  $0.1 \text{ ms}^{-2}$  r.m.s. (—),  $0.2 \text{ ms}^{-2}$  r.m.s. (---),  $0.4 \text{ ms}^{-2}$  r.m.s. (—·—),  $0.8 \text{ ms}^{-2}$  r.m.s. (····) and  $1.6 \text{ ms}^{-2}$  r.m.s. (—).

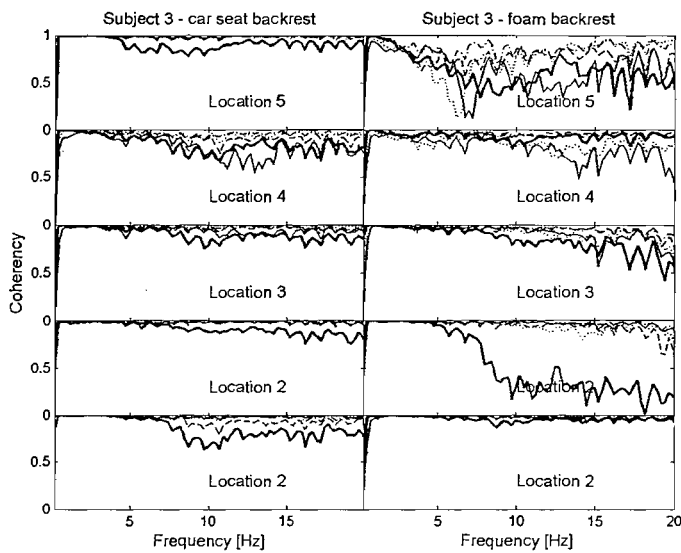


**Figure A.6:** The coherencies of the transmissibility of a seat backrest and a foam backrest at all locations for subject 3 at all five vibration magnitudes.  $0.1 \text{ ms}^{-2}$  r.m.s. (—),  $0.2 \text{ ms}^{-2}$  r.m.s. (---),  $0.4 \text{ ms}^{-2}$  r.m.s. (—·—),  $0.8 \text{ ms}^{-2}$  r.m.s. (····) and  $1.6 \text{ ms}^{-2}$  r.m.s. (—).

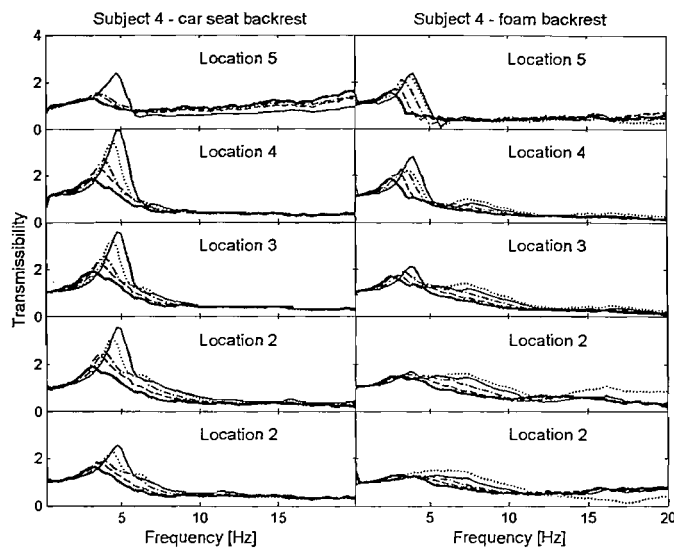


**Figure A.7:** The transmissibilities of a seat backrest and a foam backrest at all locations for subject 4 at all five vibration magnitudes.  $0.1 \text{ ms}^{-2}$  r.m.s. (—),  $0.2 \text{ ms}^{-2}$  r.m.s. (---),  $0.4 \text{ ms}^{-2}$  r.m.s. (-·-·-),  $0.8 \text{ ms}^{-2}$  r.m.s. (·····) and  $1.6 \text{ ms}^{-2}$  r.m.s. (—).

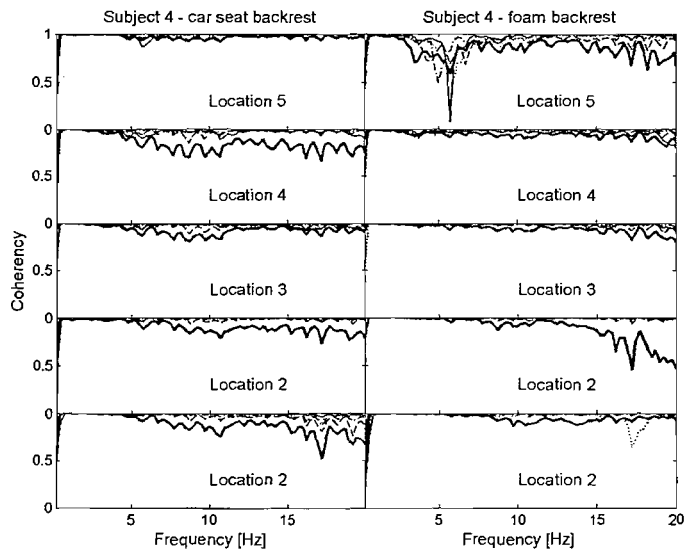


**Figure A.8:** The coherencies of the transmissibility of a seat backrest and a foam backrest at all locations for subject 4 at all five vibration magnitudes.  $0.1 \text{ ms}^{-2}$  r.m.s. (—),  $0.2 \text{ ms}^{-2}$  r.m.s. (---),  $0.4 \text{ ms}^{-2}$  r.m.s. (-·-·-),  $0.8 \text{ ms}^{-2}$  r.m.s. (·····) and  $1.6 \text{ ms}^{-2}$  r.m.s. (—).

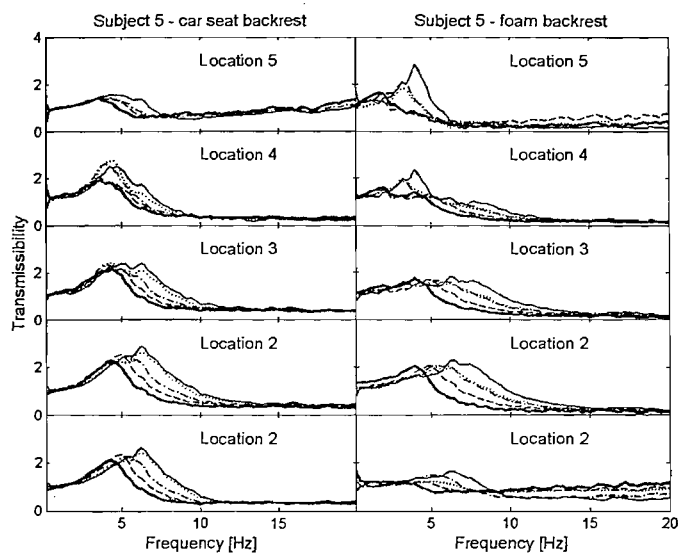


**Figure A.9:** The transmissibilities of a seat backrest and a foam backrest at all locations for subject 5 at all five vibration magnitudes.  $0.1 \text{ ms}^{-2}$  r.m.s. (—),  $0.2 \text{ ms}^{-2}$  r.m.s. (---),  $0.4 \text{ ms}^{-2}$  r.m.s. (—·—·—),  $0.8 \text{ ms}^{-2}$  r.m.s. (·····) and  $1.6 \text{ ms}^{-2}$  r.m.s. (—).

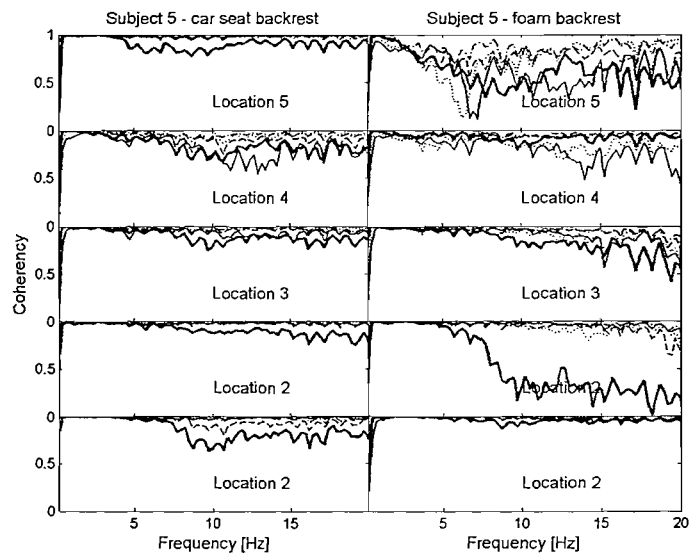


**Figure A.10:** The coherencies of the transmissibility of a seat backrest and a foam backrest at all locations for subject 5 at all five vibration magnitudes.  $0.1 \text{ ms}^{-2}$  r.m.s. (—),  $0.2 \text{ ms}^{-2}$  r.m.s. (---),  $0.4 \text{ ms}^{-2}$  r.m.s. (—·—·—),  $0.8 \text{ ms}^{-2}$  r.m.s. (·····) and  $1.6 \text{ ms}^{-2}$  r.m.s. (—).

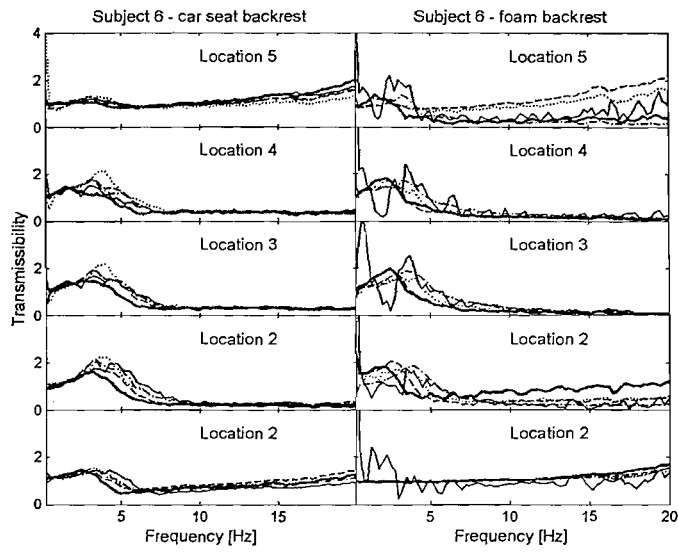


**Figure A.11:** The transmissibilities of a seat backrest and a foam backrest at all locations for subject 6 at all five vibration magnitudes.  $0.1 \text{ ms}^{-2}$  r.m.s. (—),  $0.2 \text{ ms}^{-2}$  r.m.s. (---),  $0.4 \text{ ms}^{-2}$  r.m.s. (-·-·-),  $0.8 \text{ ms}^{-2}$  r.m.s. (····) and  $1.6 \text{ ms}^{-2}$  r.m.s. (—).

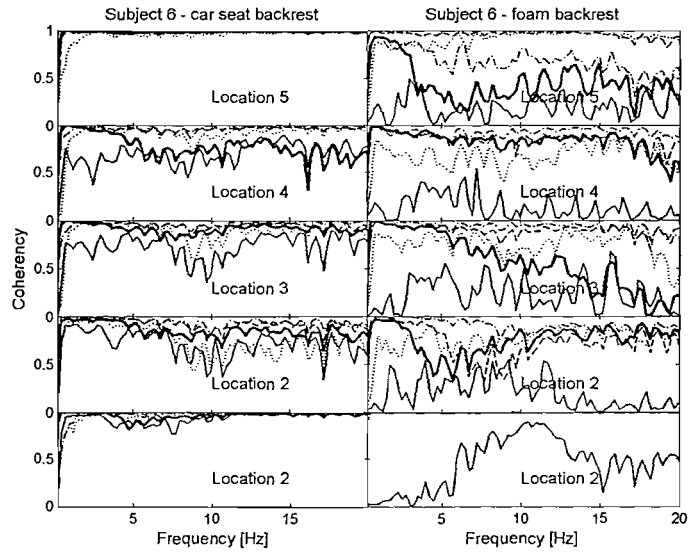


**Figure A.12:** The coherencies of the transmissibility of a seat backrest and a foam backrest at all locations for subject 6 at all five vibration magnitudes.  $0.1 \text{ ms}^{-2}$  r.m.s. (—),  $0.2 \text{ ms}^{-2}$  r.m.s. (---),  $0.4 \text{ ms}^{-2}$  r.m.s. (-·-·-),  $0.8 \text{ ms}^{-2}$  r.m.s. (····) and  $1.6 \text{ ms}^{-2}$  r.m.s. (—).

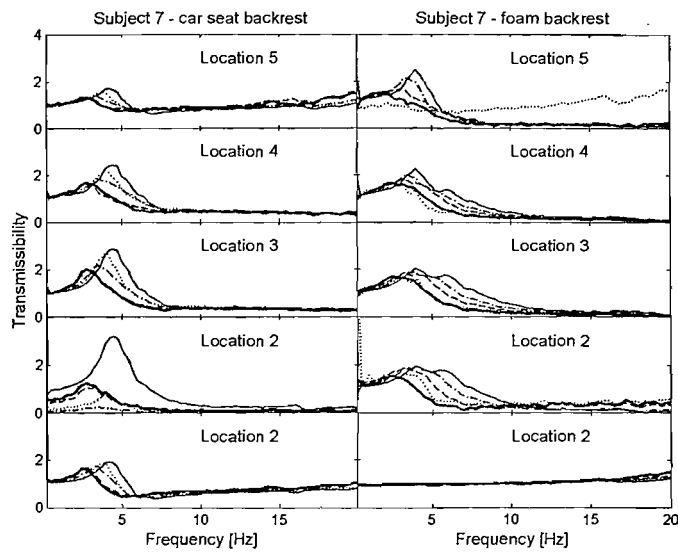


**Figure A.13:** The transmissibilities of a seat backrest and a foam backrest at all locations for subject 7 at all five vibration magnitudes.  $0.1 \text{ ms}^{-2}$  r.m.s. (—),  $0.2 \text{ ms}^{-2}$  r.m.s. (---),  $0.4 \text{ ms}^{-2}$  r.m.s. (-----),  $0.8 \text{ ms}^{-2}$  r.m.s. (.....) and  $1.6 \text{ ms}^{-2}$  r.m.s. (—).

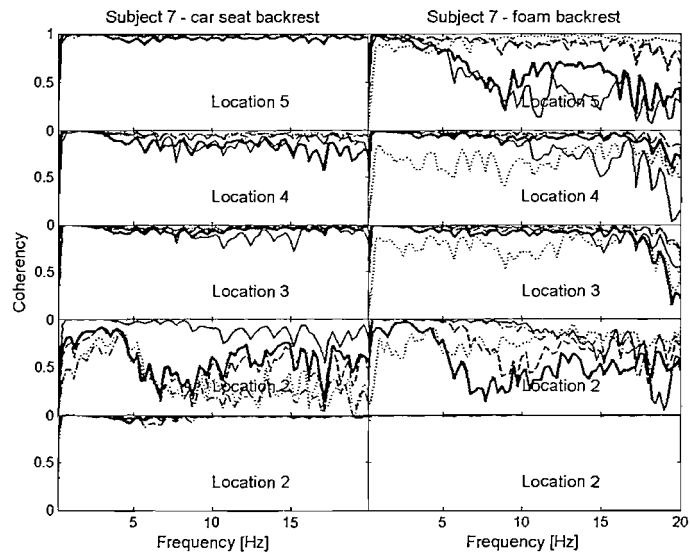


**Figure A.14:** The coherencies of the transmissibility of a seat backrest and a foam backrest at all locations for subject 7 at all five vibration magnitudes.  $0.1 \text{ ms}^{-2}$  r.m.s. (—),  $0.2 \text{ ms}^{-2}$  r.m.s. (---),  $0.4 \text{ ms}^{-2}$  r.m.s. (-----),  $0.8 \text{ ms}^{-2}$  r.m.s. (.....) and  $1.6 \text{ ms}^{-2}$  r.m.s. (—).

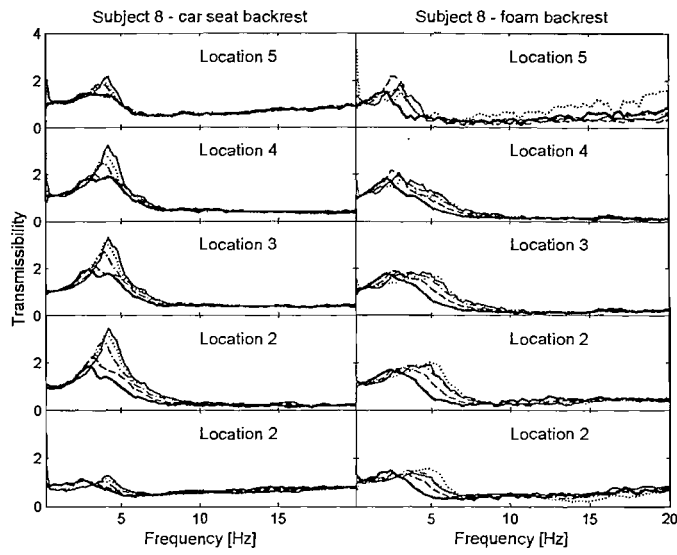


**Figure A.15:** The transmissibilities of a seat backrest and a foam backrest at all locations for subject 8 at all five vibration magnitudes.  $0.1 \text{ ms}^{-2}$  r.m.s. (—),  $0.2 \text{ ms}^{-2}$  r.m.s. (---),  $0.4 \text{ ms}^{-2}$  r.m.s. (—·—),  $0.8 \text{ ms}^{-2}$  r.m.s. (····) and  $1.6 \text{ ms}^{-2}$  r.m.s. (——).

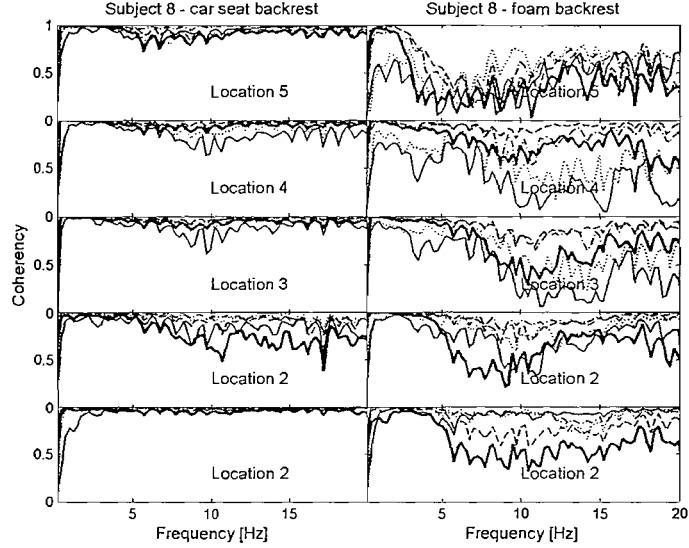


**Figure A.16:** The coherencies of the transmissibility of a seat backrest and a foam backrest at all locations for subject 8 at all five vibration magnitudes.  $0.1 \text{ ms}^{-2}$  r.m.s. (—),  $0.2 \text{ ms}^{-2}$  r.m.s. (---),  $0.4 \text{ ms}^{-2}$  r.m.s. (—·—),  $0.8 \text{ ms}^{-2}$  r.m.s. (····) and  $1.6 \text{ ms}^{-2}$  r.m.s. (——).

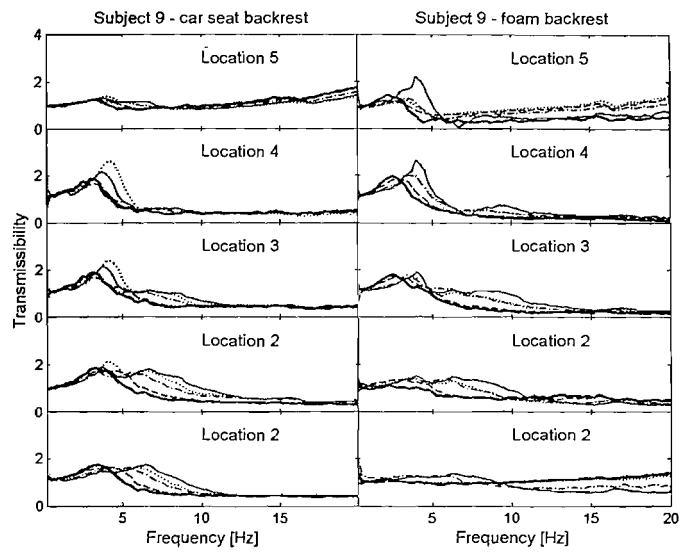


**Figure A.17:** The transmissibilities of a seat backrest and a foam backrest at all locations for subject 9 at all five vibration magnitudes.  $0.1 \text{ ms}^{-2}$  r.m.s. (—),  $0.2 \text{ ms}^{-2}$  r.m.s. (---),  $0.4 \text{ ms}^{-2}$  r.m.s. (-·-·-),  $0.8 \text{ ms}^{-2}$  r.m.s. (····) and  $1.6 \text{ ms}^{-2}$  r.m.s. (—).

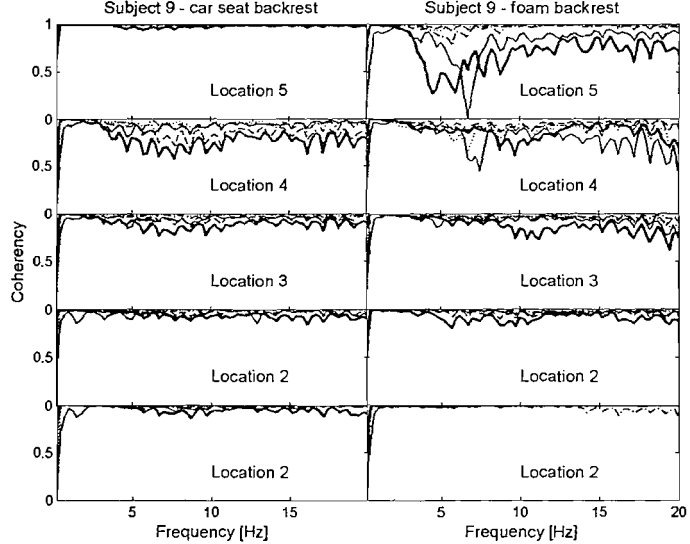


**Figure A.18:** The coherencies of the transmissibility of a seat backrest and a foam backrest at all locations for subject 9 at all five vibration magnitudes.  $0.1 \text{ ms}^{-2}$  r.m.s. (—),  $0.2 \text{ ms}^{-2}$  r.m.s. (---),  $0.4 \text{ ms}^{-2}$  r.m.s. (-·-·-),  $0.8 \text{ ms}^{-2}$  r.m.s. (····) and  $1.6 \text{ ms}^{-2}$  r.m.s. (—).

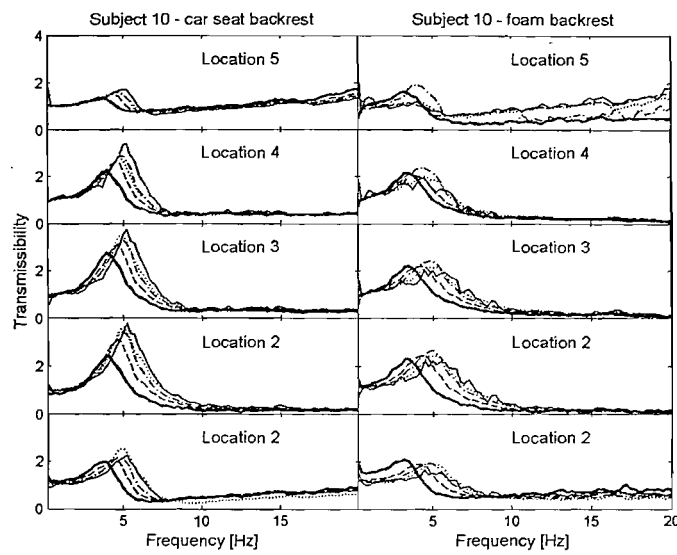


**Figure A.19:** The transmissibilities of a seat backrest and a foam backrest at all locations for subject 10 at all five vibration magnitudes.  $0.1 \text{ ms}^{-2}$  r.m.s. (—),  $0.2 \text{ ms}^{-2}$  r.m.s. (---),  $0.4 \text{ ms}^{-2}$  r.m.s. (—·—),  $0.8 \text{ ms}^{-2}$  r.m.s. (····) and  $1.6 \text{ ms}^{-2}$  r.m.s. (—·—).

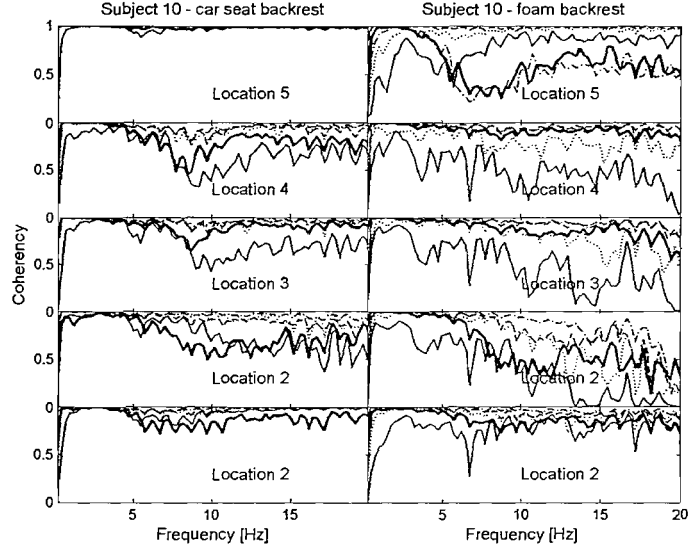


**Figure A.20:** The coherencies of the transmissibility of a seat backrest and a foam backrest at all locations for subject 10 at all five vibration magnitudes.  $0.1 \text{ ms}^{-2}$  r.m.s. (—),  $0.2 \text{ ms}^{-2}$  r.m.s. (---),  $0.4 \text{ ms}^{-2}$  r.m.s. (—·—),  $0.8 \text{ ms}^{-2}$  r.m.s. (····) and  $1.6 \text{ ms}^{-2}$  r.m.s. (—·—).

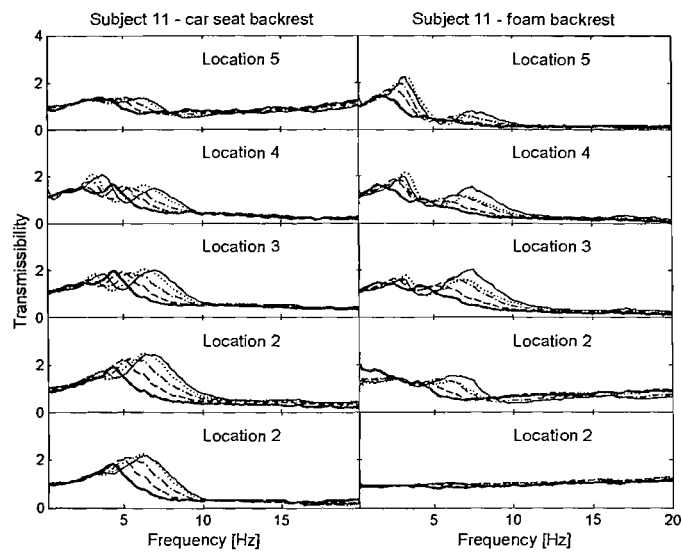


**Figure A.21:** The transmissibilities of a seat backrest and a foam backrest at all locations for subject 11 at all five vibration magnitudes.  $0.1 \text{ ms}^{-2}$  r.m.s. (—),  $0.2 \text{ ms}^{-2}$  r.m.s. (---),  $0.4 \text{ ms}^{-2}$  r.m.s. (—·—·—),  $0.8 \text{ ms}^{-2}$  r.m.s. (·····) and  $1.6 \text{ ms}^{-2}$  r.m.s. (—).

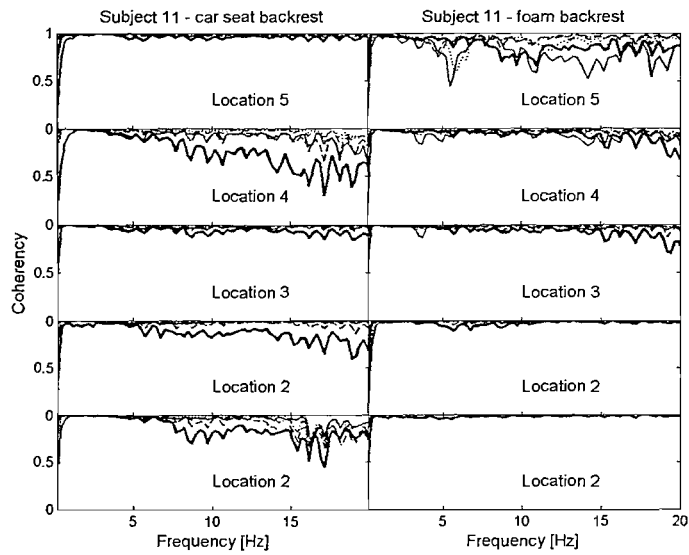


**Figure A.22:** The coherencies of the transmissibility of a seat backrest and a foam backrest at all locations for subject 11 at all five vibration magnitudes.  $0.1 \text{ ms}^{-2}$  r.m.s. (—),  $0.2 \text{ ms}^{-2}$  r.m.s. (---),  $0.4 \text{ ms}^{-2}$  r.m.s. (—·—·—),  $0.8 \text{ ms}^{-2}$  r.m.s. (·····) and  $1.6 \text{ ms}^{-2}$  r.m.s. (—).

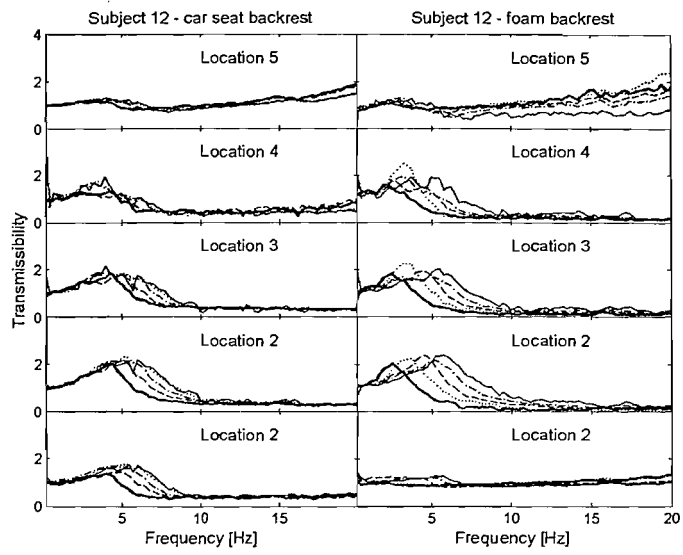


**Figure A.23:** The transmissibilities of a seat backrest and a foam backrest at all locations for subject 12 at all five vibration magnitudes.  $0.1 \text{ ms}^{-2}$  r.m.s. (—),  $0.2 \text{ ms}^{-2}$  r.m.s. (---),  $0.4 \text{ ms}^{-2}$  r.m.s. (-·-·-),  $0.8 \text{ ms}^{-2}$  r.m.s. (····) and  $1.6 \text{ ms}^{-2}$  r.m.s. (—).

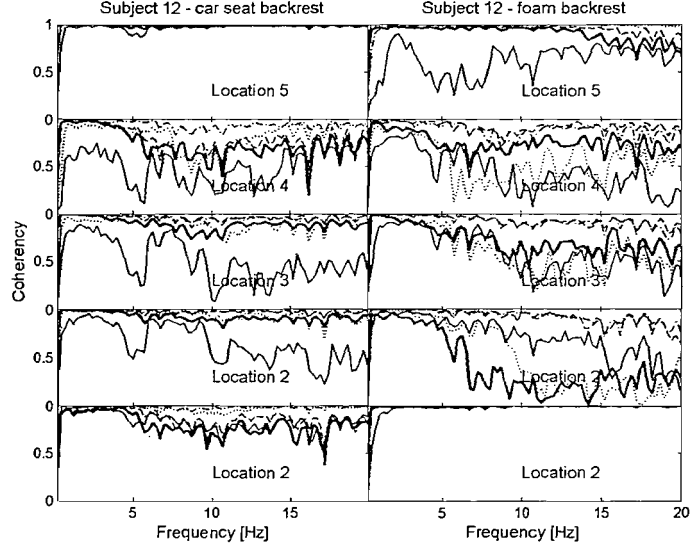


**Figure A.24:** The coherencies of the transmissibility of a seat backrest and a foam backrest at all locations for subject 12 at all five vibration magnitudes.  $0.1 \text{ ms}^{-2}$  r.m.s. (—),  $0.2 \text{ ms}^{-2}$  r.m.s. (---),  $0.4 \text{ ms}^{-2}$  r.m.s. (-·-·-),  $0.8 \text{ ms}^{-2}$  r.m.s. (····) and  $1.6 \text{ ms}^{-2}$  r.m.s. (—).

## Appendix B

# Effect of foam thickness: individual data

### B.1 Characteristics of subjects

Table B.1 Characteristics of subjects used in the experiment described in Chapter 5, Section 5.2.

Subject no.	Age (year)	Stature (m)	Mass (kg)
1	21	1.63	56
2	22	1.70	60
3	32	1.70	67
4	38	1.83	87
5	21	1.84	74
6	26	1.85	93
7	25	1.79	65
8	27	1.70	65
9	26	1.68	75
10	26	1.75	72
11	25	1.75	73
12	24	1.75	73

## B.2 Instructions to subjects prior the experiment

### INSTRUCTION TO SUBJECT

You will be participating in a study investigating the effect of foam thickness on the transmissibility of backrest.

This experiment will last approximately 60 minutes.

Through the experiment, please try to ensure that you:

6. Adopt an upright posture
7. Maintain full contact of your upper body with the backrest
8. Adopt a leg posture such that the upper and the lower legs always perpendicular
9. Maintain your head position by looking forward
10. Rest your hands on your lap and hold the emergency button

#### **Important:**

In case of emergency during the test, please do not hesitate to press the STOP button. The vibrator will come to rest.

Thank you for your participation.

### B.3 Individual results

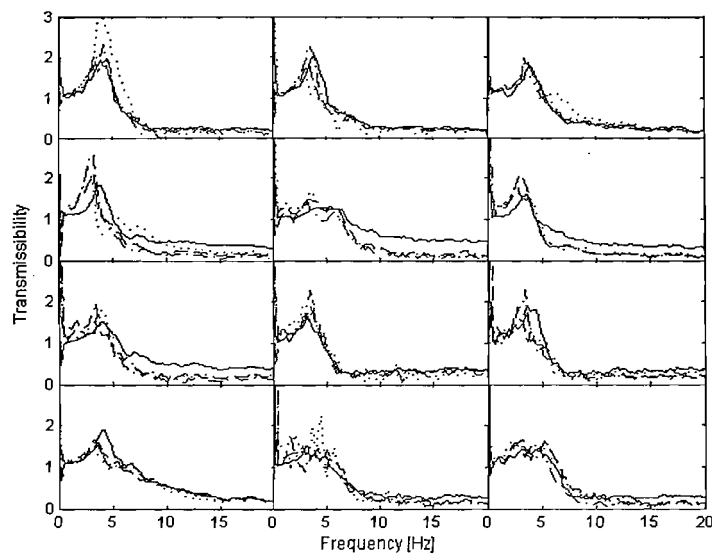


**Figure B.1:** The transmissibilities of foam backrest with twelve subjects at a vibration magnitude of  $0.1 \text{ ms}^{-2}$  r.m.s.: 25 mm (—), 50 mm (---), 100 mm 3 (-·-·-) and 200 mm (····).

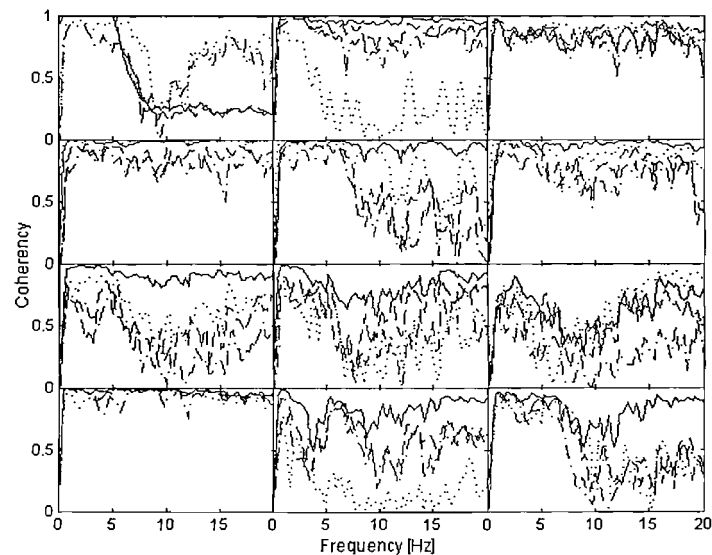


**Figure B.2:** The coherencies of the transmissibility of foam backrest with twelve subjects at a vibration magnitude of  $0.1 \text{ ms}^{-2}$  r.m.s.: 25 mm (—), 50 mm (---), 100 mm 3 (-·-·-) and 200 mm (····).

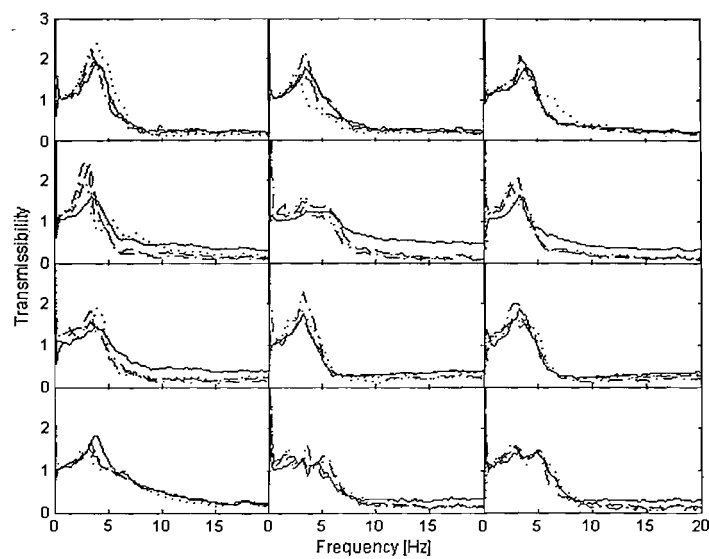


**Figure B.3:** The transmissibilities of foam backrest with twelve subjects at a vibration magnitude of  $0.2 \text{ ms}^{-2}$  r.m.s.: 25 mm (—), 50 mm (---), 100 mm 3 (-·-·-) and 200 mm (····).

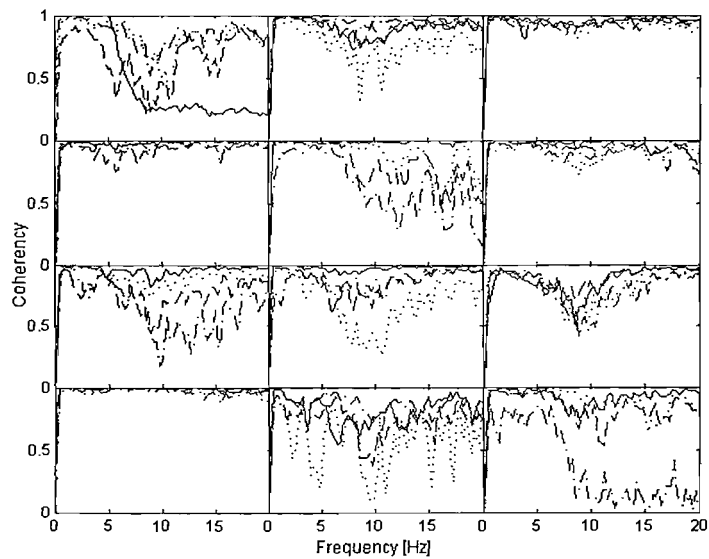


**Figure B.4:** The coherencies of the transmissibility of foam backrest with twelve subjects at a vibration magnitude of  $0.2 \text{ ms}^{-2}$  r.m.s.: 25 mm (—), 50 mm (---), 100 mm 3 (-·-·-) and 200 mm (····).

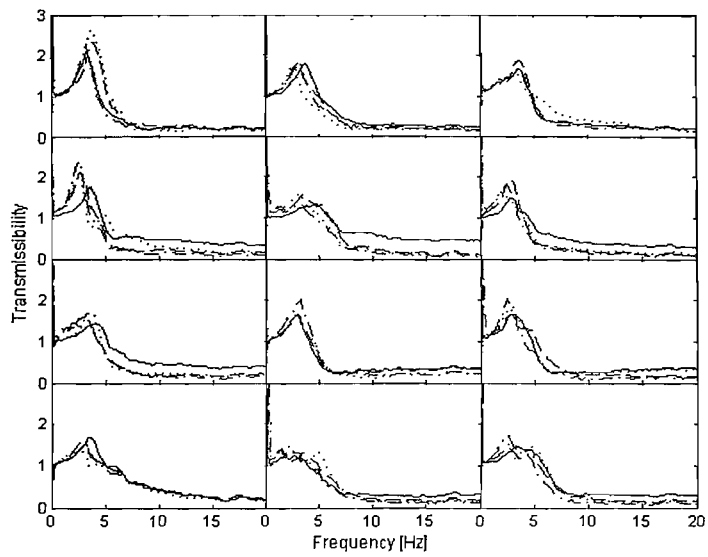


**Figure B.5:** The transmissibilities of foam backrest with twelve subjects at a vibration magnitude of  $0.4 \text{ ms}^{-2}$  r.m.s.: 25 mm (—), 50 mm (---), 100 mm 3 (-·-·-) and 200 mm (····).

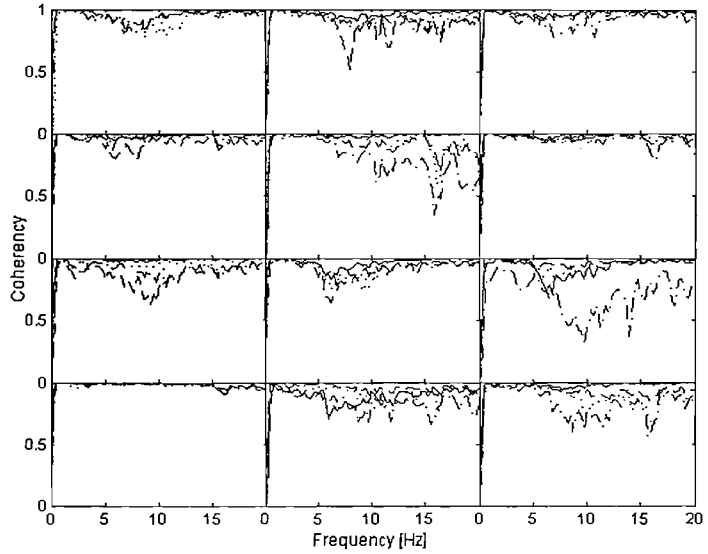


**Figure B.6:** The coherencies of the transmissibility of foam backrest with twelve subjects at a vibration magnitude of  $0.4 \text{ ms}^{-2}$  r.m.s.: 25 mm (—), 50 mm (---), 100 mm 3 (-·-·-) and 200 mm (····).

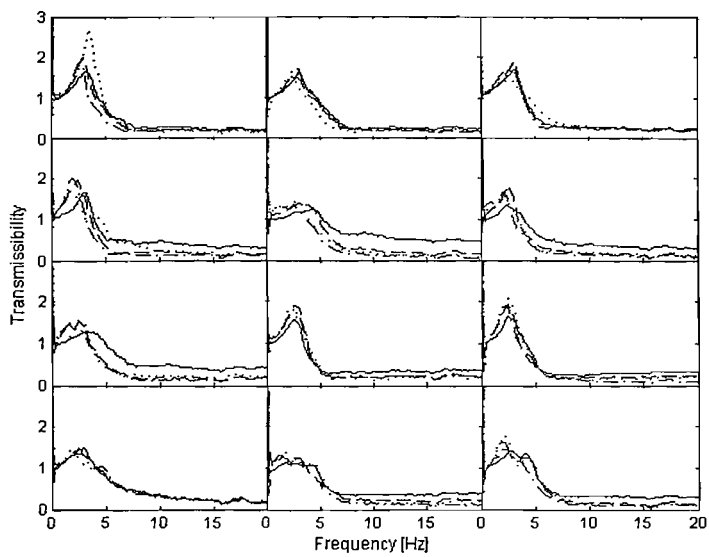


**Figure B.7:** The transmissibilities of foam backrest with twelve subjects at a vibration magnitude of  $0.8 \text{ ms}^{-2}$  r.m.s.: 25 mm (—), 50 mm (---), 100 mm 3 (-·-·-) and 200 mm (····).

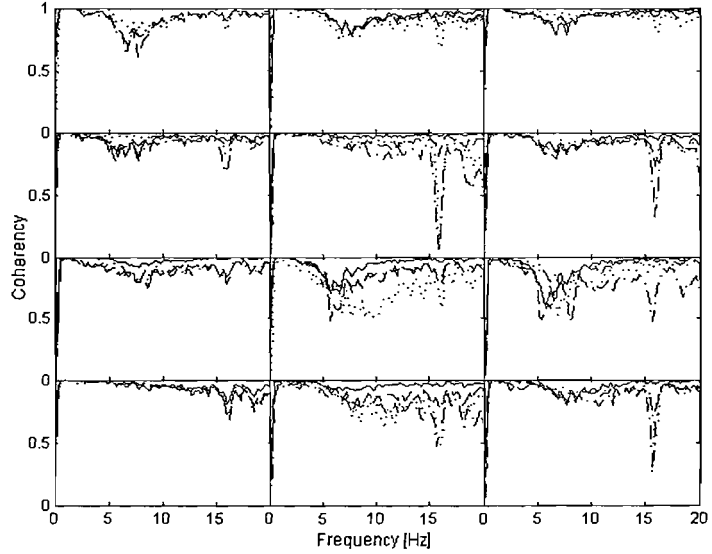


**Figure B.8:** The coherencies of the transmissibility of foam backrest with twelve subjects at a vibration magnitude of  $0.8 \text{ ms}^{-2}$  r.m.s.: 25 mm (—), 50 mm (---), 100 mm 3 (-·-·-) and 200 mm (····).

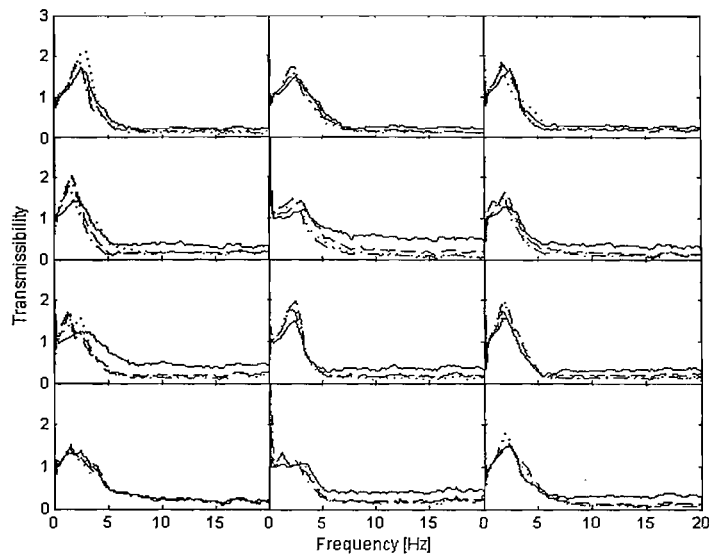


**Figure B.9:** The transmissibilities of foam backrest with twelve subjects at a vibration magnitude of  $1.6 \text{ ms}^{-2}$  r.m.s.: 25 mm (—), 50 mm (---), 100 mm 3 (-·-·-) and 200 mm (····).

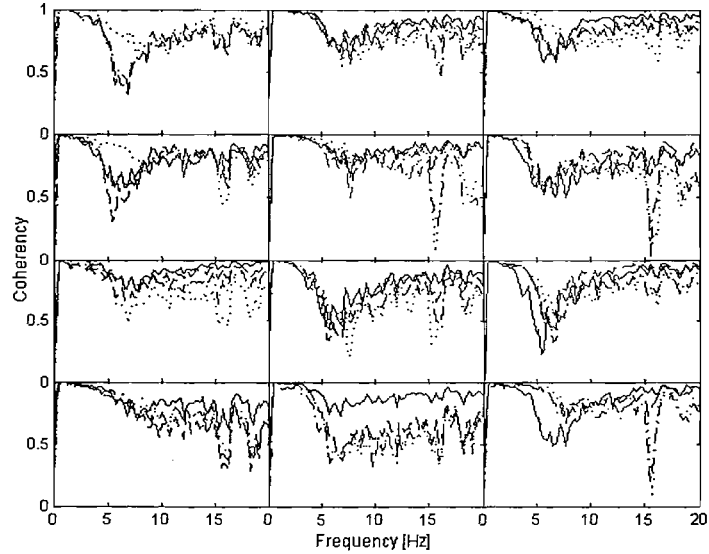


**Figure B.10:** The coherencies of the transmissibility of foam backrest with twelve subjects at a vibration magnitude of  $1.6 \text{ ms}^{-2}$  r.m.s.: 25 mm (—), 50 mm (---), 100 mm 3 (-·-·-) and 200 mm (····).

## Appendix C

# Apparent mass of the back: individual data

### C.1 Characteristics of subjects

Table C.1 Characteristics of subjects used in the experiment described in Chapter 6.

Subject no.	Age (year)	Stature (m)	Mass (kg)	Seat-to-shoulder (m)
1	22	1.78	67	0.64
2	20	1.75	61	0.62
3	23	1.71	64	0.58
4	23	1.70	80	0.63
5	26	1.74	72	0.62
6	21	1.78	63	0.64
7	21	1.64	50	0.59
8	23	1.76	78	0.59
9	28	1.70	55	0.60
10	26	1.73	70	0.63
11	27	1.66	85	0.60
12	22	1.65	67	0.64

## C.2 Instructions to subjects prior the experiment

### INSTRUCTION TO SUBJECT

You will be participating in a study investigating the variation of the apparent mass of the back with different input location to the back.

This experiment will last approximately 60 minutes.

A wooden block will be placed between your back and the force platform. Through the experiment, please try to ensure that you:

11. Adopt an upright posture
12. Maintain contact of your back with the wooden block
13. Adopt a leg posture such that the upper and the lower legs always perpendicular
14. Maintain your head position by looking forward
15. Rest your hands on your lap and hold the emergency button

At the lower locations (i.e. Location 1 and Location 2), please maintain the upright posture and ensure your upper back not touching the force platform. A practice session will be given before the actual vibration exposure. It is important that you DO NOT touch your upper back with the force platform at these two locations.

#### **Important:**

In case of emergency during the test, please do not hesitate to press the STOP button. The vibrator will come to rest.

Thank you for your participation.

### C.3 Individual results

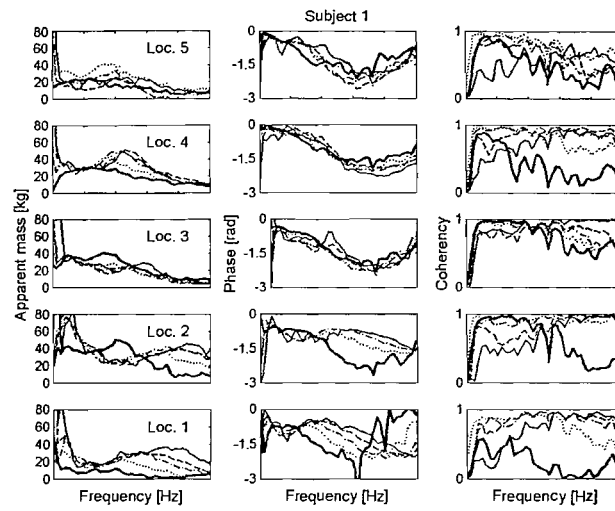


**Figure C.1:** The moduli of the apparent mass of the back and the corresponding phase and coherency at all locations for subject 1 at  $0.1 \text{ ms}^{-2}$  r.m.s. (—),  $0.2 \text{ ms}^{-2}$  r.m.s. (---),  $0.4 \text{ ms}^{-2}$  r.m.s. (—·—·—),  $0.8 \text{ ms}^{-2}$  r.m.s. (····) and  $1.6 \text{ ms}^{-2}$  r.m.s. (—).

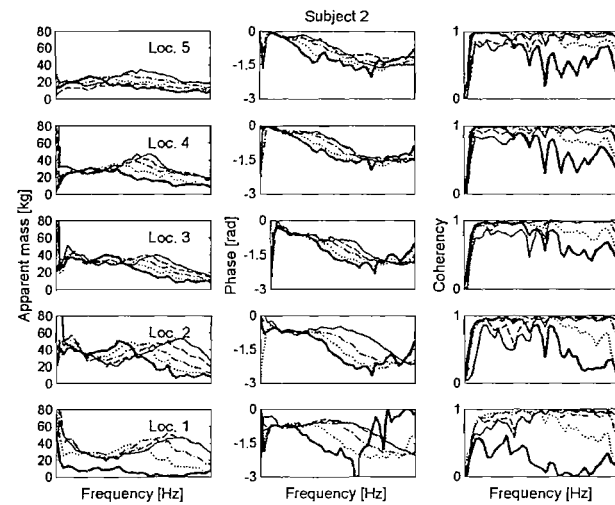


**Figure C.2:** The moduli of the apparent mass of the back and the corresponding phase and coherency at all locations for subject 2 at  $0.1 \text{ ms}^{-2}$  r.m.s. (—),  $0.2 \text{ ms}^{-2}$  r.m.s. (---),  $0.4 \text{ ms}^{-2}$  r.m.s. (—·—·—),  $0.8 \text{ ms}^{-2}$  r.m.s. (····) and  $1.6 \text{ ms}^{-2}$  r.m.s. (—).

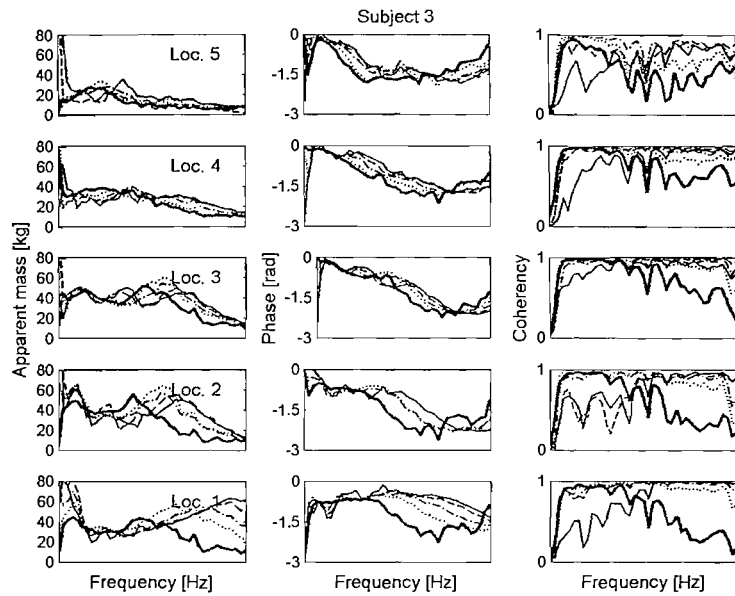


**Figure C.3:** The moduli of the apparent mass of the back and the corresponding phase and coherency at all locations for subject 3 at  $0.1 \text{ ms}^{-2}$  r.m.s. (—),  $0.2 \text{ ms}^{-2}$  r.m.s. (---),  $0.4 \text{ ms}^{-2}$  r.m.s. (—·—),  $0.8 \text{ ms}^{-2}$  r.m.s. (····) and  $1.6 \text{ ms}^{-2}$  r.m.s. (—).

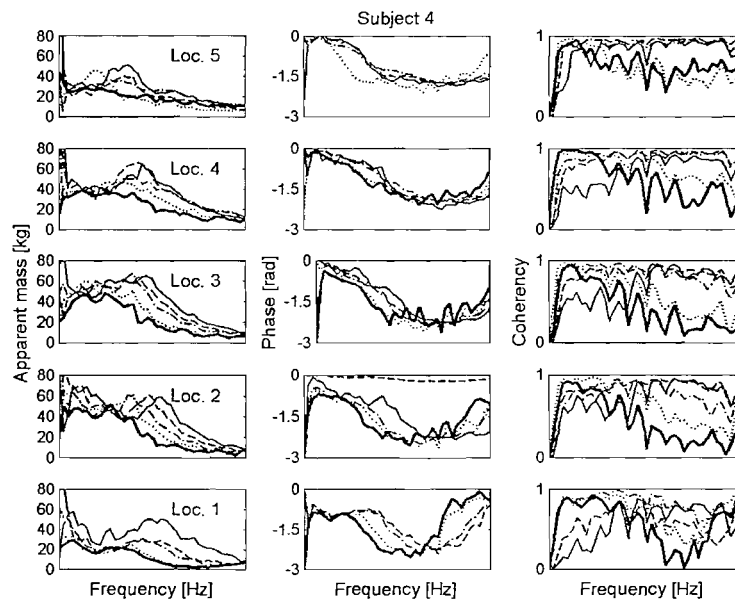


**Figure C.4:** The moduli of the apparent mass of the back and the corresponding phase and coherency at all locations for subject 4 at  $0.1 \text{ ms}^{-2}$  r.m.s. (—),  $0.2 \text{ ms}^{-2}$  r.m.s. (---),  $0.4 \text{ ms}^{-2}$  r.m.s. (—·—),  $0.8 \text{ ms}^{-2}$  r.m.s. (····) and  $1.6 \text{ ms}^{-2}$  r.m.s. (—).

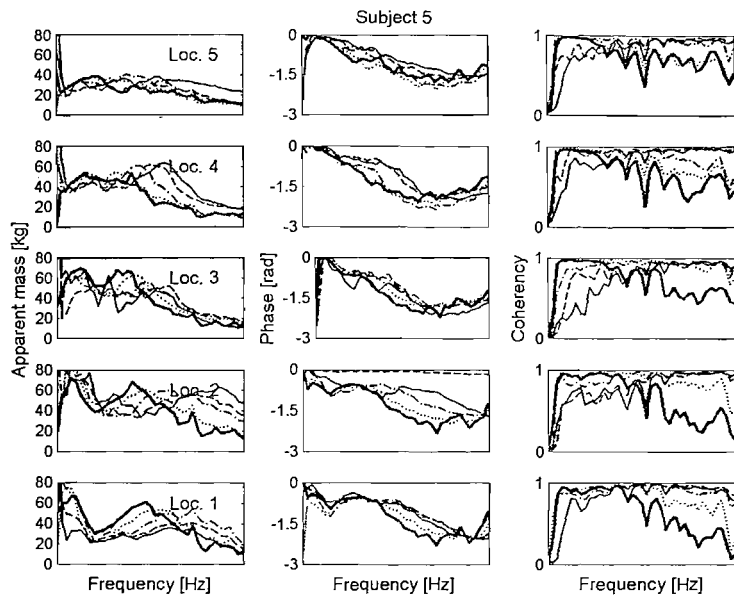


**Figure C.5:** The moduli of the apparent mass of the back and the corresponding phase and coherency at all locations for subject 5 at  $0.1 \text{ ms}^{-2}$  r.m.s. (—),  $0.2 \text{ ms}^{-2}$  r.m.s. (---),  $0.4 \text{ ms}^{-2}$  r.m.s. (—·—),  $0.8 \text{ ms}^{-2}$  r.m.s. (····) and  $1.6 \text{ ms}^{-2}$  r.m.s. (—·—).

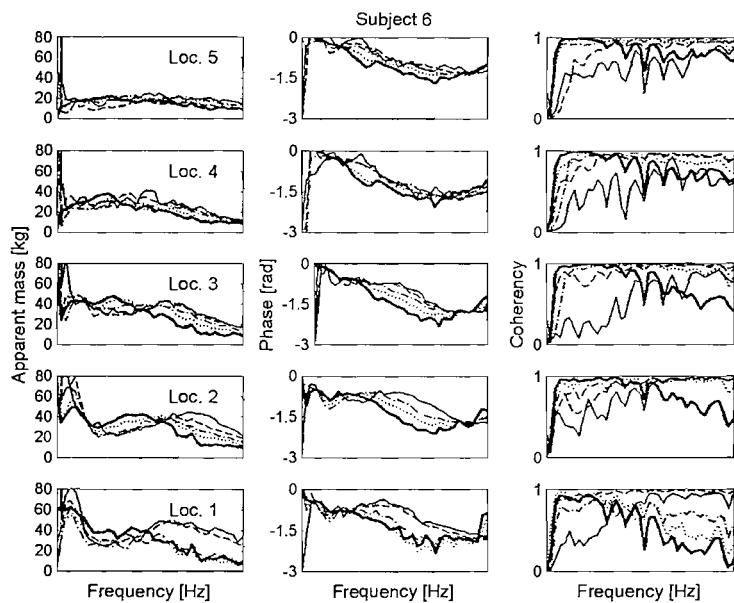


**Figure C.6:** The moduli of the apparent mass of the back and the corresponding phase and coherency at all locations for subject 6 at  $0.1 \text{ ms}^{-2}$  r.m.s. (—),  $0.2 \text{ ms}^{-2}$  r.m.s. (---),  $0.4 \text{ ms}^{-2}$  r.m.s. (—·—),  $0.8 \text{ ms}^{-2}$  r.m.s. (····) and  $1.6 \text{ ms}^{-2}$  r.m.s. (—·—).

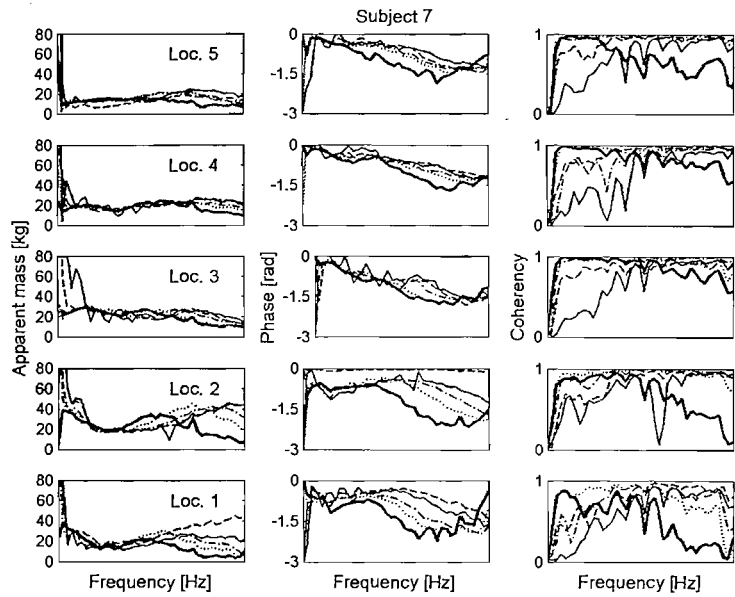


**Figure C.7:** The moduli of the apparent mass of the back and the corresponding phase and coherency at all locations for subject 7 at  $0.1 \text{ ms}^{-2}$  r.m.s. (—),  $0.2 \text{ ms}^{-2}$  r.m.s. (---),  $0.4 \text{ ms}^{-2}$  r.m.s. (—·—·—),  $0.8 \text{ ms}^{-2}$  r.m.s. (······) and  $1.6 \text{ ms}^{-2}$  r.m.s. (—·—).

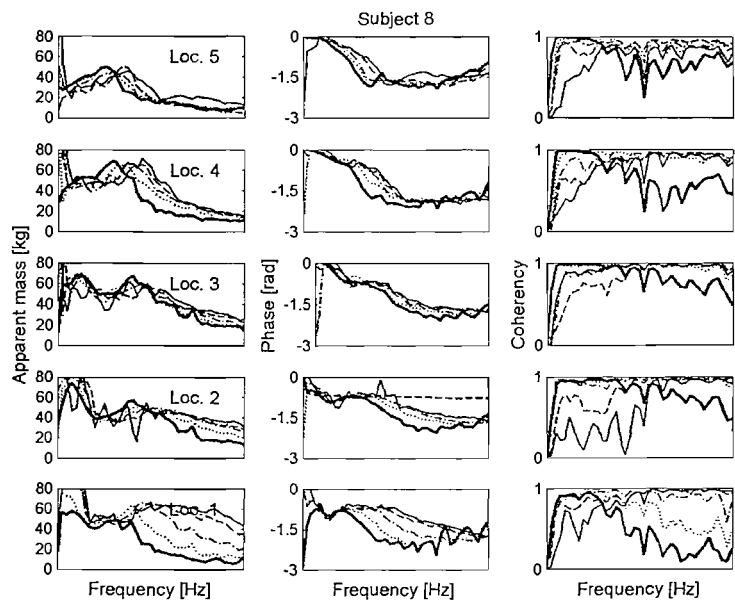


**Figure C.8:** The moduli of the apparent mass of the back and the corresponding phase and coherency at all locations for subject 8 at  $0.1 \text{ ms}^{-2}$  r.m.s. (—),  $0.2 \text{ ms}^{-2}$  r.m.s. (---),  $0.4 \text{ ms}^{-2}$  r.m.s. (—·—·—),  $0.8 \text{ ms}^{-2}$  r.m.s. (······) and  $1.6 \text{ ms}^{-2}$  r.m.s. (—·—).

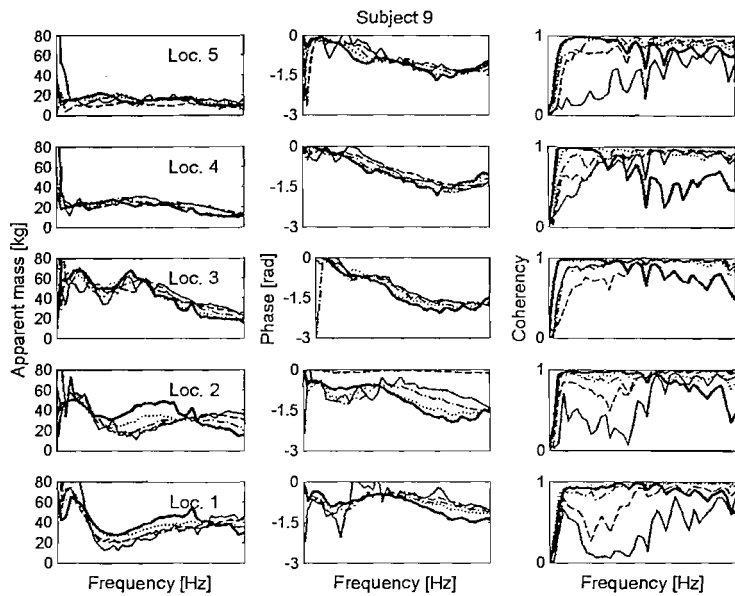


**Figure C.9:** The moduli of the apparent mass of the back and the corresponding phase and coherency at all locations for subject 9 at  $0.1 \text{ ms}^{-2}$  r.m.s. (—),  $0.2 \text{ ms}^{-2}$  r.m.s. (---),  $0.4 \text{ ms}^{-2}$  r.m.s. (-----),  $0.8 \text{ ms}^{-2}$  r.m.s. (.....) and  $1.6 \text{ ms}^{-2}$  r.m.s. (—).

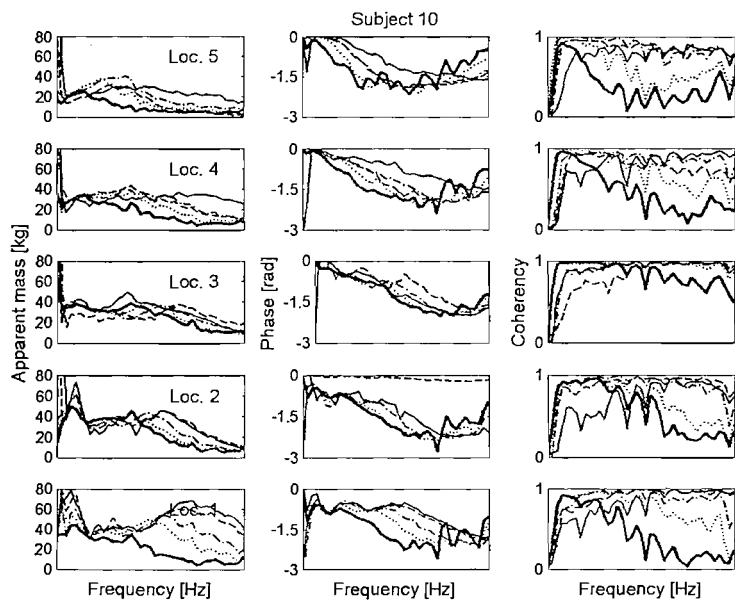


**Figure C.10:** The moduli of the apparent mass of the back and the corresponding phase and coherency at all locations for subject 10 at  $0.1 \text{ ms}^{-2}$  r.m.s. (—),  $0.2 \text{ ms}^{-2}$  r.m.s. (---),  $0.4 \text{ ms}^{-2}$  r.m.s. (-----),  $0.8 \text{ ms}^{-2}$  r.m.s. (.....) and  $1.6 \text{ ms}^{-2}$  r.m.s. (—).

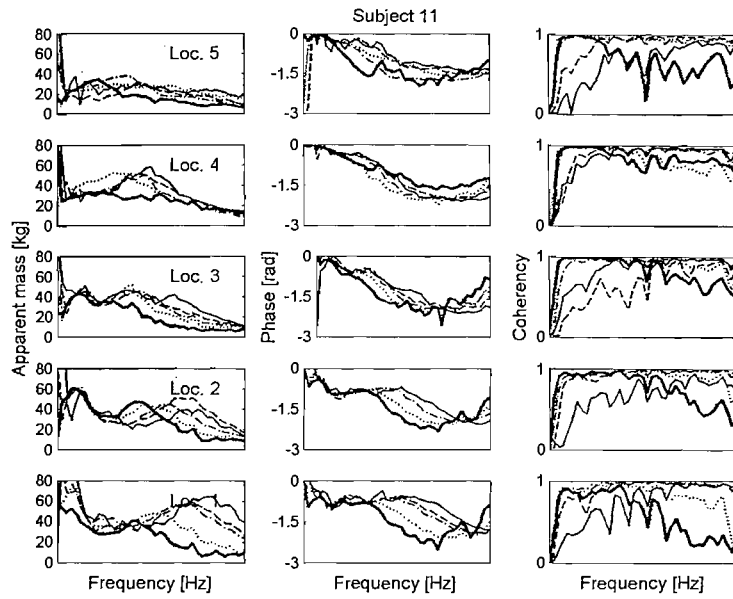


**Figure C.11:** The moduli of the apparent mass of the back and the corresponding phase and coherency at all locations for subject 11 at  $0.1 \text{ ms}^{-2}$  r.m.s. (—),  $0.2 \text{ ms}^{-2}$  r.m.s. (---),  $0.4 \text{ ms}^{-2}$  r.m.s. (—·—),  $0.8 \text{ ms}^{-2}$  r.m.s. (····) and  $1.6 \text{ ms}^{-2}$  r.m.s. (—·—).

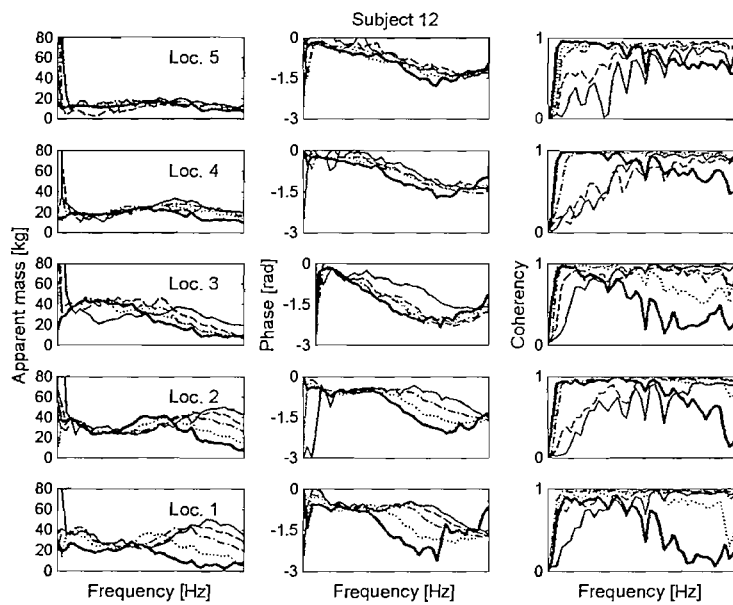


**Figure C.12:** The moduli of the apparent mass of the back and the corresponding phase and coherency at all locations for subject 12 at  $0.1 \text{ ms}^{-2}$  r.m.s. (—),  $0.2 \text{ ms}^{-2}$  r.m.s. (---),  $0.4 \text{ ms}^{-2}$  r.m.s. (—·—),  $0.8 \text{ ms}^{-2}$  r.m.s. (····) and  $1.6 \text{ ms}^{-2}$  r.m.s. (—·—).

## Appendix D

# Derivation of equations of motion (EOM) using *Lagrange's* method

### D.1 Example of derivation of EOM for Model 2

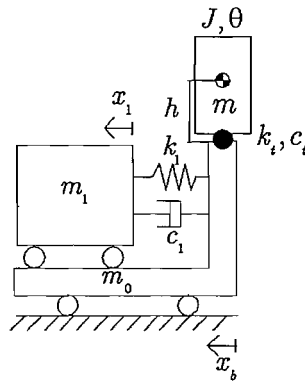


Figure D.1: Model 2, as described in Chapter 8

The *Lagrange* equation can be described as

$$\frac{d}{dt} \left( \frac{\partial L}{\partial \dot{q}_i} \right) - \frac{\partial L}{\partial q_i} + \frac{\partial P}{\partial \dot{q}_i} = Q_i \quad (D.1)$$

where

$$L = T - V \quad (D.2)$$

Kinetic energy:

$$T = \frac{1}{2} m_0 \dot{x}_b^2 + \frac{1}{2} m_1 \dot{x}_1^2 + \frac{1}{2} m_2 (\dot{x}_b + h\dot{\theta})^2 + \frac{1}{2} J\dot{\theta}^2 \quad (\text{D.3})$$

Potential energy:

$$V = \frac{1}{2} k_1 (x_1 - x_b)^2 + \frac{1}{2} k_i \theta^2 \quad (\text{D.4})$$

Power function:

$$P = \frac{1}{2} c_1 (\dot{x}_1 - \dot{x}_b)^2 + \frac{1}{2} c_i \dot{\theta}^2 \quad (\text{D.5})$$

The partial differentiation of equations D.3, D.4 and D.5 are as follows:

$$\begin{aligned} \frac{\partial L}{\partial \dot{x}_1} &= m_1 \dot{x}_1 \\ \frac{d}{dt} \left( \frac{\partial L}{\partial \dot{x}_1} \right) &= m_1 \ddot{x}_1 \\ \frac{\partial L}{\partial \dot{\theta}} &= m_2 (h\dot{x}_b + h^2\dot{\theta}) + J\dot{\theta} \\ \frac{d}{dt} \left( \frac{\partial L}{\partial \dot{\theta}} \right) &= m_2 (h\ddot{x}_b + h^2\ddot{\theta}) + J\ddot{\theta} \\ \frac{\partial L}{\partial x_1} &= k_1 (x_1 - x_b) \\ \frac{\partial L}{\partial \theta_1} &= k_i \theta \\ \frac{\partial P}{\partial \dot{x}_1} &= c_1 (\dot{x}_1 - \dot{x}_b) \\ \frac{\partial P}{\partial \dot{\theta}} &= c_i \dot{\theta} \end{aligned} \quad (\text{D.6})$$

Therefore, by substituting the derivatives into equation D.1, the equations of motion of the Model 2 can be described as:

$$\begin{aligned} m_1 \ddot{x}_1 + c_1 (\dot{x}_1 - \dot{x}_b) + k_1 (x_1 - x_b) &= 0 \\ m_2 (h\ddot{x}_b + h^2\ddot{\theta}) + J\ddot{\theta} + c_i \dot{\theta} + k_i \theta &= 0 \end{aligned} \quad (\text{D.7})$$

For more details on derivation of the equations of motion using Lagrange's method, readers are recommended to read Theory of Vibration with Application by W.T. Thomson, Chapter 7.

## D.2 EOM for Model 3 and Model 4

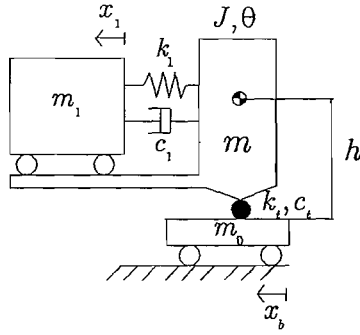


Figure D.2: Model 3

$$m_1 \ddot{x}_1 + c_1 (\dot{x}_1 - \dot{x}_b - h\dot{\theta}) + k_1 (x_1 - x_b - h\theta) = 0 \quad (D.8)$$

$$m(h\ddot{x}_b + h^2\ddot{\theta}) + J\ddot{\theta} + c_1 (\dot{x}_b h + h^2\dot{\theta} - \dot{x}_1 h) + c_t \dot{\theta} + k_t (x_b h + h^2\theta - x_1 h) + k_t \theta = 0 \quad (D.9)$$

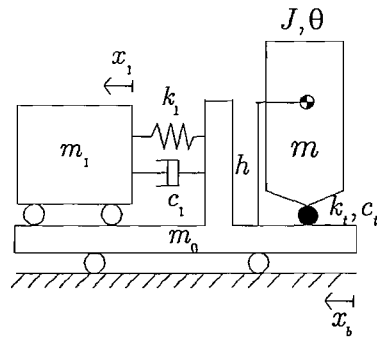


Figure D.3: Model 4

$$m_1 \ddot{x}_1 + c_1 (\dot{x}_1 - \dot{x}_b) + k_1 (x_1 - x_b) = 0 \quad (D.10)$$

$$m(h\ddot{x}_b + h^2\ddot{\theta}) + J\ddot{\theta} + c_t \dot{\theta} + k_t \theta = 0 \quad (D.11)$$

## References

- Andersson, G.B.J., Murphy, R.W., Ortengren, R. and A.L. Nachemson (1979), The influence of backrest inclination and lumbar support on lumbar lordosis. *Spine* 4, 52 – 58.
- Ashley, C. (1976), Work vehicles suspension seating. *Paper presented at the United Kingdom Informal Meeting on Human Response to Vibration*, Held at the Royal Military College of Science, Shrivenham, Swindon.
- Beards, C.F. (1983), Structural vibration analysis: modelling, analysis and damping of vibrating structures. Ellis Horwood Limited. ISBN 0-85312-325-X.
- Barlow, R.J. (1989), Statistics: A guide to the use of statistical methods in the physical sciences. ISBN 0 471 92295 1, John Wiley and Son.
- Belytschko, T. and Privitzer, E. (1978), Refinement and validation of a three-dimensional head-spine model. *Report No. AMRL-TR-78-7*. Aerospace Medical Research Laboratory, Wright-Patterson Air Force Base, Ohio.
- Boileau, P.E. and Rakheja, S. (1998), Whole-body vertical biodynamics characteristics of the seated vehicle driver-measurement and model development. *International Journal of Industrial Ergonomics*, 22, 449-472.
- British Standard Institution (1987), Measurement and evaluation of human exposure to whole-body mechanical vibration and repeated shock. *BS 6841*, London: British Standards Institution.
- Clegg, F. (1990), Simple statistics: A course book for the social science. Cambridge: Cambridge University press.
- Coermann, R.R. (1959), The mechanical impedance of the human body in sitting and standing position and its significance for the subjective tolerance to vibration. *Paper to 3<sup>rd</sup> Annual Meeting of the Biophysical Society*, Pittsburgh.

- Coermann, R.R., Ziegenruecker, G.H, Wittwer, A.L. and von Gierke, H.E. (1960), The passive dynamics mechanical properties of the human thorax-abdomen system and of the whole-body system. *Journal of Aerospace Medicine*, 31, 443-455.
- Coermann, R.R. (1962), The mechanical impedance of the human body in sitting and standing positions at low frequencies. *Human Factors*, 4(10), 227-253.
- Corbridge, C. (1981), Effect of subject weight on suspension seat vibration transmissibility: suspension in and out. *Paper presented at the United Kingdom Informal Meeting on Human Response to Vibration*, Held at Heriot-Watt University, Edinburgh, Scotland, 9-11 September.
- Corbridge, C. (1984), A comparison of the vertical and fore-and-aft dynamics performance of six suspension seats. *Paper presented at the United Kingdom Informal Meeting on Human Response to Vibration*, Held at Heriot-Watt University, Edinburgh, Scotland, 21-22 September.
- Corbridge, C. (1987), Vertical vibration transmitted through a seat: effect of vibration input, subjects' postures and subjects' physical characteristics. *Paper presented at the United Kingdom Informal Meeting on Human Response to Vibration*, Held at Royal Military College of Science, Shrivenham, 21-22 September.
- Corbridge, C., Griffin, M.J. and Harborough, P.R. (1989), Seat dynamics and passenger comfort. *Proceeding of Institution of Mechanical Engineers*, 203, 57-64.
- Cogger, M.K. (1979), The transmission of vibration to the body from seats. MSc thesis, University of Southampton.
- Dieckmann, D. (1957), A study of the influence of vibration on man. *Ergonomics*, 1, 347-355.
- Donati, P.M. and Bonthoux, C. (1983), Biodynamic response of the human body in the sitting posture when subjected to vertical vibration. *Journal of Sound and Vibration*, 90, 423-442.
- Ebe, K. (1993), Effect of composition of polyurethane foam on the vibration transmissibility of automotive seats. *Paper presented at the United Kingdom Informal Meeting on Human Response to Vibration*, Held at APRE, Ministry of Defence, Farnborough, Hampshire, GU14 6TD, UK, 20-22 September

- Ebe, K. (1994), Effect of density of polyurethane foam on vibration transmission. *Paper presented at the United Kingdom Informal Meeting on Human Response to Vibration*, Held at Institute of Naval Medicine, Alverstoke, Gosport, Hants, PO12 2DL, UK, 19-21 September.
- Ebe, K. and Griffin, M.J. (1995), Effect of foam pad construction on vibration transmission. *Paper presented at the Japan Group Meeting on Human Response to Vibration*, Held at Kurume University School of Medicine, 67 Asahi-machi, Kurume, 830, Japan 15-16 July.
- Ebe, K. (1997), Effect of thickness on static and dynamic characteristics of polyurethane foams. *Paper presented at the United Kingdom Informal Meeting on Human Response to Vibration*, Held at ISVR, University of Southampton, UK, 17-19 September.
- Ebe, K. and Griffin, M.J. (2000), Qualitative models of seat discomfort including static and dynamic factors. *Ergonomics*, 43(6), 771-790.
- Fairley, T.E. (1983), The effect of vibration input characteristics on seat transmissibility. *Paper presented at the United Kingdom Informal Meeting on Human Response to Vibration*, Held at National Institute of Agricultural Engineering, Silsoe, Bedford, 14-16 September.
- Fairley, T.E. (1986), Predicting the dynamic performance of seats, PhD thesis, University of Southampton.
- Fairley, T.E. and Griffin, M.J. (1984), Modelling a seat person system in the vertical and fore-and-aft axes, *Institute of Mechanical Engineers Conference*, C149/84, 83-89.
- Fairley, T.E. and Griffin, M.J. (1986), A test method for the prediction of seat transmissibility. *Society of Automotive Engineers*, SAE Paper 860046, International Congress and Exposition, Detroit.
- Fairley, T.E. and Griffin, M.J. (1989), The apparent mass of the seated human body: vertical vibration. *Journal of Biomechanics*, 22(2), 81-94.
- Fairley, T.E. and Griffin, M.J. (1990), The apparent mass of the seated human body in the fore-and-aft and lateral directions. *Journal of Sound and Vibration*, 139, 299-306.
- General Motors (1978), HYBRID III Exterior Body. *Proving Ground General Motors Corporation*, May 1978.

- Goldman, D.E. and von Gierke, H.E. (1960), The effects of shock and vibration on man. *Naval Medicine Research Institute*, Report no. 60-3, Bethesda.
- Griffin, M.J. (1990), Handbook of Human Vibration. Academic Press, ISBN 0-12-303040-4.
- Griffin, M.J. (2001), The validation of biodynamic models. *Clinical Biomechanics*, 16(1), S81-S92.
- Harris, C.M. and Crede, C.E. (1976), Shock and vibration handbook, 2<sup>nd</sup> Edition McGraw-Hill, Inc. ISBN 0-07-026799-5.
- Hinz, B. and Seidel, H. (1987), The nonlinearity of the human body's dynamic response during sinusoidal whole body vibration. *Industrial Health*, 25, 169-181.
- Holmlund, P. and Lundström, R (1998), Mechanical impedance of the human body in the horizontal directions. *Journal of Sound and Vibration*, 215(4), 801-812.
- Holmlund, P. and Lundström, R (2001), Mechanical impedance of the sitting human body in single-axis compared to multi-axis whole-body vibration exposure. *Clinical Biomechanics*, 16(1), S101-S110.
- Hopkins, G.R. (1971), Non-linear lumped parameter mathematical model of dynamic response of the human body. *Symposium on Biodynamic Models and their Application*, Daytona, Ohio, 26-28 October, Paper, 25, 649-669, Technical report no. 71-29. Aerospace Medical Research Laboratories.
- Houghton, T.J.C. (2003), The effect of backrest inclination on the transmission of vertical vibration through an automotive seat. *Paper presented at the 38<sup>th</sup> United Kingdom Conference on Human Responses to Vibration*, Held at Institute of Naval Medicine, Gosport, Hampshire, UK. 17-19 September.
- Huang, Y. (2004), Review of the nonlinear biodynamic responses of the seated human body during vertical whole-body vibration: the significant variable factors. *Paper presented at the 39<sup>th</sup> United Kingdom Group Meeting on Human Responses to Vibration*, Held at Ludlow, Shropshire, UK. 15-17 September.
- International Organization for Standardization, ISO 5353 (1978) – Earth-moving machinery – seat index point.
- International Organization for Standardization, ISO 10326-1 (1992), Mechanical vibration – Laboratory method for evaluating vehicle seat vibration, Part 1: Basic requirements.

- International Organization for Standardization, ISO/FDIS 5982 (2001), Mechanical vibration and shock – Range of idealized values to characterize seated-body biodynamic response under vertical vibration.
- Kitazaki, S. (1994), Modelling mechanical responses to human whole-body vibration, PhD thesis, University of Southampton.
- Kitazaki, S. and Griffin, M.J. (1997), A modal analysis of whole-body vertical vibration using a finite element model of human body. *Journal of Sound and Vibration*, 200, 83-103.
- Kitazaki, S. and Griffin, M.J. (1998), Resonance behaviour of the seated human body and effect of posture. *Journal of Biomechanics*, 31, 143-149.
- Lantham, F. (1957), A study in body ballistics; seat ejection. *Proceeding of the Royal Society, B*, 147, 121-139.
- Leatherwood, J.D. (1975), Vibrations transmitted to human subjects thorough passenger seats and considerations of passenger comfort. *NASA Technical Note*, NASA TN D-7929.
- Lewis, C.H. and Griffin, M.J. (1996), The transmission of vibration to the occupants of a car seat with a suspended back-rest. *Proceeding Institution of Mechanical Engineers*, 210, 199-207.
- Lewis, C.H. and Griffin, M.J. (2002), Evaluating the vibration isolation of soft seat cushion using an active anthropodynamic dummy. *Journal of Sound and Vibration*, 253(1), 295-311. The transmission of vibration to the occupants of a car seat with a suspended back-rest. *Proceeding Institution of Mechanical Engineers*, 210, 199-207.
- Liu, Y.K. and Wickstrom, J.K. (1973), Estimation of the inertial property distribution of the human torso from segmented cadaveric data. In: *Perspectives in Biomedical Engineering, Proceeding of a Symposium Organised in Association with the Biological Engineering Society*, Glasgow, 203-213.
- Mansfield, N.J. and Griffin, M.J. (1996), Vehicle seat dynamics measured with an anthropodynamic dummy and human subjects. *Proceeding of Internoise 96*, 1725-1730.

- Mansfield, N.J. (1997), A consideration of alternative non-linear lumped parameter models of the apparent mass of a seated person. *Paper presented at the United kingdom Group Meeting on Human Response to Vibration*; Held at ISVR, University of Southampton, 17-19 September.
- Mansfield, N.J. (1998), Non-linear dynamic response of the seated person to whole-body vibration, PhD thesis, University of Southampton.
- Mansfield, N.J., Holmlund, P. and Lundström, R (1999a), Apparent mass and absorbed power during exposure to whole-body vibration and repeated shocks, *Journal of Sound and Vibration*, 248(3), 427-440.
- Mansfield, N.J. and Lundström, R. (1999b), The apparent mass of the human body exposed to non-orthogonal horizontal vibration, *Journal of Biomechanics*, 32, 1269-1278.
- Mansfield, N.J. and Lundström, R. (1999c), Models of the apparent mass of the seated human body exposed to horizontal whole-body vibration. *Aviation, Space and Environmental Medicine*, 70(12), 1166-1172.
- Mansfield, N.J. and Griffin, M.J. (2000), Non-linearities in apparent mass and transmissibility during exposure to whole-body vertical vibration. *Journal of Biomechanics*, 33, 933-941.
- Mansfield, N.J. and Griffin, M.J. (2002), Effect of posture and vibration magnitude on apparent mass and pelvis rotation during exposure to whole-body vertical vibration. *Journal of Sound and Vibration*, 253(1), 93-107.
- Matsumoto, Y. and Griffin, M.J. (1998), Movements of the upper-body of seated subjects exposed to vertical whole-body vibration at the principal resonance frequency. *Journal of Sound and Vibration*, 215(4), 743-762.
- Matsumoto, Y. (1999), Dynamic response of standing and seated persons to whole-body vibration: principal resonance of the body, PhD thesis, University of Southampton.
- Matsumoto, Y. and Griffin, M.J. (2001), Modelling the dynamic mechanisms associated with the principal resonance of the seated human body. *Clinical Biomechanics*, 16, S31-S44.
- Matsumoto, Y. and Griffin, M.J. (2002), Effect of muscle tension on non-linearities in the apparent mass of seated subjects exposed to vertical whole-body vibration. *Journal of Sound and Vibration*, 253, 77-92.

- Matthews, J. (1964), Ride comfort for tractor operators II. Analysis of ride vibrations on pneumatic-tyred tractors. *Journal of Agricultural Engineering Research*, 9(2), 147-158.
- Matthews, J. (1966), Ride comfort for tractor operators IV. Assessment of ride quality of seats. *Journal of Agricultural Engineering Research*, 11(1), 44-57.
- Matthews, J. (1967), Progress in the application of ergonomics to agricultural engineering. *Engineering Symposium of the Institution of Agricultural Engineers*, National College of Agricultural Engineering, Silsoe, 12 September.
- Mertens, H. (1978), Nonlinear behavior of sitting humans under increasing gravity. *Aviation, Space and Environmental Medicine*, 49(1), 287-298.
- Mertens, H. and Vogt, L. (1978), The response of a realistic computer model for sitting humans to different types of shocks. *AGARD Conference Proceedings CP-253: Models and Analogues for the Evaluation of Human Biodynamic Response, Performance and Protection*, Paris, 6-10 November, (von Gierke, H.E., ed.), Paper A26, Advisory Group of Aerospace Research and Development.
- Miwa, T. and Yonekawa, Y. (1971), Evaluation methods for vibration effect, Part 10. Measurements of vibration attenuation. Effect of cushions. *Industrial Health*, 9, 81-98.
- Miwa, T. (1975), Mechanical impedance of human body in various postures. *Industrial Health*, 13, 1-22.
- Muksian, R. and Nash, C.D. (1974), A model for the response of seated humans to sinusoidal displacements of the seat. *Journal of Biomechanics*, 7, 209-215.
- National Aeronautics and Space Administration (1978), Anthropometric source book, Vol. 1, anthropometry for designers. NASA Reference Publication 1024.
- Nawayseh, N. (2002), Modelling the vertical and fore-and-aft forces caused by whole-body vertical vibration. *Paper presented at the 37<sup>th</sup> United Kingdom Conference on Human Responses to Vibration*, Held at Department of Human Sciences, Loughborough University, UK, 18-20 September.
- Nawayseh, N. and Griffin, M.J. (2003), Non-linear dual-axis biodynamic response to vertical whole-body vibration. *Journal of Sound and Vibration*, 268, 503-523.

- Nawayseh, N. (2004), Cross-axis movements of the seated human body in response to whole-body vertical and fore-and-aft vibration, Ph.D thesis, University of Southampton.
- Nawayseh, N. and Griffin, M.J. (2004), Tri-axial forces at the seat and backrest during whole-body vertical vibration. *Journal of Sound and Vibration*, 277, 309-326.
- Nawayseh, N. and Griffin, M.J. (2005a), Tri-axial forces at the seat and backrest during whole-body fore-and-aft vibration. *Journal of Sound and Vibration*, 281, 921-942.
- Nawayseh, N. and Griffin, M.J. (2005b), Non-linear dual-axis biodynamic response to fore-and-aft whole-body vibration. *Journal of Sound and Vibration*, 282, 831-862.
- Nawayseh, N. and Griffin, M.J. (2005c), Effect of seat surface angle on forces at the seat surface during whole-body vertical vibration. *Journal of Sound and Vibration*, 284 (3-5), 613-634.
- Paddan, G.S. and Griffin, M.J. (1994), Transmission of roll and pitch seat vibration to the head. *Ergonomics*, 37(9), 1513-1531.
- Paddan, G.S. and Griffin, M.J. (1998a), The transmission of translational seat vibration to the head. II. Vertical seat vibration. *Journal of Biomechanics*, 21(3), 191-197.
- Paddan, G.S. and Griffin, M.J. (1998b), The transmission of translational seat vibration to the head. II. Horizontal seat vibration. *Journal of Biomechanics*, 21(3), 199-206.
- Payne, P.R. (1969), Injury potential of ejection seat cushions. *Journal of Aircraft*, 6(3), 273-278.
- Payne, P.R. and Band, E.G. (1971), A four-degree-of-freedom lumped parameter model of the seated human body. *Report No. AMRL-TR-70-35*. Aerospace Medical Research Laboratory, Wright-Patterson Air Force Base, Ohio.
- Pheasant, S. (1996), Bodyspace: anthropometry, ergonomics and the design of work. London: Taylor & Francis Ltd; ISBN: 0-7484-0067-2.
- Pradko, F., Lee, R. and Kaluza, V. (1966), Theory of human vibration response. *ASME Paper No. 66-WA/BHF-15*.
- Price, F.A., Morioka, M. and Griffin, M.J. (2004), Effect of fore-and-aft vibration at the back, seat and feet on discomfort and the location of discomfort, Final Report, HFRU 04/16, ISVR, University of Southampton, Subjective and biodynamics studies to develop a predictive model of tip-in smoothness.

- Qiu, Y. and Griffin, M.J. (2003), Transmission of fore-aft vibration to a car seat using field tests and laboratory simulation. *Journal of Sound and Vibration*, 264, 135-155.
- Qiu, Y. and Griffin, M.J. (2004), Transmission of vibration to the backrest of a car seat evaluated with multi-input models. *Journal of Sound and Vibration*, 274, 297-321.
- Qiu, Y. and Griffin, M.J. (2005), Transmission of roll, pitch and yaw vibration to the backrest of a seat supported on a non-rigid car floor. *Journal of Sound and Vibration*, 288(4-5), 1197-1222.
- Radke, A.O. (1956), The application of human engineering data to vehicular seat design. *Bostrom Research Laboratories Report, Report No. 117*, Presented to participants in Project 335. European Productivity Agency, Purdue University, October 1.
- Rakheja, S., Stiharu, I. and Boileau, P.E. (2002), Seated occupant apparent mass characteristics under automotive postures and vertical vibration. *Journal of Sound and Vibration*, 253, 57-75.
- Richard, L. (1996), A study of the effect of gender on the transmissibility of car seats. . *Paper presented at the United Kingdom Informal Meeting on Human Response to Vibration*, Held at MIRA, 18-20 September.
- Robertson, C.D. and Griffin, M.J. (1989), Laboratory studies of the electromyographic response to whole-body vibration, ISVR Technical Report 184, University of Southampton.
- Sandover, J. (1978), Modelling human responses to vibration. *Aviation, Space and Environmental Medicine*, 49(1), 335-339.
- Siegel S. and Castellan, N.J. (1988), Nonparametric statistics for the behavioral sciences. Singapore: McGraw-Hill.
- Singley, G.T. and Haley, J.L. (1978), The use of mathematical modelling in crashworthy helicopter seating systems. *AGARD Conference Proceeding No. 253*, A22-1-21, Paris, France, 6 – 10 November.
- Smith, C.C. and Kwak, Y.K. (1978), Identification of the dynamic characteristics of a bench type automotive seat for the evaluation of ride quality. *Journal of Dynamic Systems, Measurement and Control*, 100, 42-49.

- Suggs, C.W., Abrams, C.F. and Stikeleather, L.F. (1969), Application of a damped spring-mass human vibration simulator in vibration testing of vehicle seats. *Ergonomics*, 12(1), 79-90.
- Society of Automotive Engineers (1974), Measurement of whole-body vibration of a seated operator of agricultural equipment. (the Society of Automotive Engineers recommended practice). *The Society of Automotive Engineers SAE J1013, Handbook Part II*, 1404-1407, Society of Automotive Engineers, Detroit, Michigan.
- Stayner, R.M. and Bean, A.G.M. (1971), Review of measurements of tractor suspension seats 1970/1971, *Interim Report DN/TE/214/445*. National Institute of Agricultural Engineering, Silsoe, Bedford.
- Thomson, W.T. (1988), Theory of vibration with application, Third Edition, Prentice Hall.
- Toward, M.G.R, (2000), Use of an anthropodynamic dummy to measure seat dynamics. *Paper presented at the 35<sup>th</sup> United Kingdom Meeting on Human Responses to Vibration*, Held at ISVR, University of Southampton, Southampton, UK, 13-15 September.
- Toward, M.G.R, (2001), Effect of backrest interaction on seat cushion transmissibility. *Paper presented at the 36<sup>th</sup> United Kingdom Group Conference on Human Responses to Vibration*, Held at Centre for Human Sciences, QinetiQ, Farnborough, UK. 12-14 September.
- Vogt, H.L., Coermann, R.R. and Fust, H.D. (1968), Mechanical impedance of sitting human under sustained acceleration. *Aerospace Medicine*, 39, 675-679.
- Wang, W. Rakheja, S. and Boileau, P.-É. (2004), Effect of sitting postures on biodynamic response of seated occupants under vertical vibration. *International Journal of Industrial Ergonomics*, 34, 289-306.
- Wei, L. and Griffin, M.J. (1997), The influence of contact area, vibration magnitude and static force on the dynamic stiffness of polyurethane seat foam. *Paper presented at the United Kingdom Group Meeting on Human Response to Vibration*, Held at the ISVR, University of Southampton, Southampton, UK, 17-19 September.
- Wei, L. and Griffin, M.J. (1998a), The influence of seat cushion inclination on subject apparent mass and seat transmissibility. *Paper presented at the 33<sup>rd</sup> United Kingdom Group Meeting on Human Response to Vibration*, Held at the Health and Safety Executive, Buxton, Derbyshire, UK. 16-18 September.

- Wei, L. and Griffin, M.J. (1998b), Mathematical models for the mechanical impedance of the seated human body exposed to vertical vibration. *Journal of Sound and Vibration*, 212, 855-874.
- Wei, L. and Griffin, M.J. (1998c), The prediction of seat transmissibility from measures of seat impedance. *Journal of Sound and Vibration*, 214(1), 121-137.
- Wei, L. and Griffin, M.J. (1999), Modelling the effect of backrest angle on the vertical apparent mass of seated subjects. *Paper presented at the 34<sup>th</sup> United Kingdom Group Meeting on Human Response to Vibration*, Held at Ford Motor Company, Dunton, Essex, UK, 22-24 September.
- Wei, L. and Griffin, M.J. (2000), Effect of subject weight on predictions of seat cushion transmissibility. *Paper presented at the 35<sup>th</sup> United Kingdom Group Meeting on Human Response to Vibration*, Held at ISVR, University of Southampton, Southampton, UK. 13-15 September.
- Wei, L. (2000), Predicting transmissibility of car seats from the seat impedance ad the apparent mass of the human body, PhD thesis, University of Southampton.
- Whitham, E.M. and Griffin, M.J. (1977), Measuring vibration on soft seats. *Society of Automotive Engineers*, SAE Paper 770253, International Automotive Engineering Congress and Exposition, Detroit.
- Wittman, T.J. and Phillips, N.S. (1969), Human body nonlinearity and mechanical impedance analyses. *Journal of Biomechanics*, 2, 281-288.
- Wu, X. and Griffin, M.J. (1996), Towards the standardization of a testing method for the end-stop impacts of suspension seats. *Journal of Sound and Vibration*, 192(1), 307-319.